MATHEMATICAL RECONSTRUCTION OF ACCIDENTS
ANALYTICAL AND PHYSICAL RECONSTRUCTION OF TEN SELECTED HIGHWAY ACCIDENTS

DISCLAIMER

TECHNICAL REPORT STANDARD TITLE PAGE

1. Report No.	2. Government Accession No.	3. Recipient's Catalog No.
DOT HS-801 150		PB 234 707

4. Title and Subtitle
Mathematical Reconstruction of Accidents - Analytical and Physical Reconstruction of Ten Selected Highway Accidents

5. Report Date
March 1974

6. Performing Organization Code

7. Author(s)
John A. Bartz, Raymond R. McHenry, David J. Segal

8. Performing Organization Report No.
ZQ-5341-V-1

9. Performing Organization Name and Address
Calspan Corporation
4455 Genesee Street
Buffalo, New York 14221
(Phone: 716-632-7500)

10. Work Unit No.
W11 Series

11. Contract or Grant No.
DOT-HS-053-3-658

12. Sponsoring Agency Name and Address
U. S. Department of Transportation
National Highway Traffic Safety Administration
Washington, D. C. 20590

13. Type of Report and Period Covered
Interim
June 1973 - March 1974

14. Sponsoring Agency Code

15. Supplementary Notes

16. Abstract

Ten actual highway accidents have been mathematically reconstructed in a process comprised of two parts. First, trajectories of the vehicles were reconstructed from physical evidence observed at the scene, using a computer simulation of a two-vehicle, planar collision. Next, the responses of the right front occupant of the subject vehicle were reconstructed from observed internal vehicle damage and passenger injuries, using the predicted vehicle crash history and a nonplanar mathematical model of the crash victim. The predicted vehicle trajectories are in general agreement with on-site observations for nine of the ten cases. The rest positions of the vehicles in the remaining case were strongly influenced by a secondary collision. In seven of the ten cases, the predicted occupant responses likewise agree generally with the reported evidence. Discrepancies of occupant responses in the remaining three cases are considered attributable to active responses exerted by the occupant in anticipation of crash. The effect of occupant response is demonstrated through computer simulation. Predicted values of head injury indicators in current use (head severity index and HIC number) do not correlate significantly with observed injuries as measured by the ten-point injury scale. The predicted values of the head injury indicators do, however, fall largely within the broad envelope of corresponding windshield impact test results.

Following this analytical effort, the ten accident cases were physically reconstructed on an impact sled, using a sled pulse corresponding to the predicted vehicle deceleration history and an anthropometric crash test dummy to represent the accident victim. The results of most of the sled tests agree generally with observations from the actual crash and the results from the analytical reconstructions of crash victim responses. Differences are traceable to a number of factors, including uncertainties in the vehicle crash history; uncertainties in occupant position, orientation, and muscular response; differences in size between the actual and simulated occupants; and differences in material properties and geometry between the actual and simulated vehicle interiors. Measured values of the head severity index show no distinct correlation with the observed injuries measured on the ten-point scale. However, a correlation is shown to exist between observed injury and predicted vehicle speed change.

17. Key Words	18. Distribution Statement
Accident Reconstruction Highway Accidents, Reconstruction Computer Simulation, Accidents Multiple Vehicle Accidents, Automobile Injury, Automobile Occupant	Unlimited

19. Security Classif. (of this report)	20. Security Classif. (of this page)	21. No. of Pages	22. Price
None	None	283	

Form DOT F 1700.7 (8-69)

FOREWORD

This report describes the analytical and physical reconstruction of ten selected highway accidents from evidence gathered at the accident scenes.

The research effort summarized in this report was performed by Calspan Corporation for the National Highway Traffic Safety Administration as a task under Contract No. DOT-HS-053-3-658. Mr. Raymond R. McHenry of Calspan's Transportation Safety Department serves as principal investigator, and Dr. Eugene E. Flamboe of the National Highway Traffic Safety Administration is contract technical manager for this continuing research effort.

The opinions, findings, and conclusions expressed in this publication are those of the authors and not necessarily those of the National Highway Traffic Safety Administration.

This report has been reviewed and approved by:

Edwin A. Kidd, Head
Transportation Safety Department

ACKNOWLEDGMENTS

The authors wish to acknowledge contributions of the following Calspan personnel in this phase of the research effort:

Case report selection and acquisition - Messrs. Donald L. Hendricks, Theodore E. Anderson, and John W. Garrett

Computer data processing - Mr. Robert F. Wantuck

Impact sled testing - Mr. Michael J. Walsh, operating engineer of the sled facility, and the impact sled crew

Report preparation and typing - Mrs. Maureen E. Ball.

The authors also gratefully acknowledge the assistance of Dr. Eugene E. Flamboe, contract technical manager, in case report acquisition and technical monitoring.

In two of the reported accident cases, reconstruction results from an earlier Calspan study supported by the Engineering Staff of the General Motors Corporation have been used by special permission.

ABSTRACT

Ten actual highway accidents have been mathematically reconstructed in a process comprised of two parts. First, trajectories of the vehicles were reconstructed from physical evidence observed at the scene, using a computer simulation of a two-vehicle, planar collision. Next, the responses of the right front occupant of the subject vehicle were reconstructed from observed internal vehicle damage and passenger injuries, using the predicted vehicle crash history and a nonplanar mathematical model of the crash victim. The predicted vehicle trajectories are in general agreement with on-site observations for nine of the ten cases. The rest positions of the vehicles in the remaining case were strongly influenced by a secondary collision. In seven of the ten cases, the predicted occupant responses likewise agree generally with the reported evidence. Discrepancies of occupant responses in the remaining three cases are considered attributable to active responses exerted by the occupant in anticipation of crash. The effect of occupant response is demonstrated through computer simulation. Predicted values of head injury indicators in current use (head severity index and HIC number) do not correlate significantly with observed injuries as measured by the ten-point injury scale. The predicted values of the head injury indicators do, however, fall largely within the broad envelope of corresponding windshield impact test results.

Following this analytical effort, the ten accident cases were physically reconstructed on an impact sled, using a sled pulse corresponding to the predicted vehicle deceleration history and an anthropometric crash test dummy to represent the accident victim. The results of most of the sled tests agree generally with observations from the actual crash and the results from the analytical reconstructions of crash victim responses. Differences are traceable to a number of factors, including uncertainties in the vehicle crash history; uncertainties in occupant position, orientation, and muscular response; differences in size between the actual and simulated

occupants; and differences in material properties and geometry between the actual and simulated vehicle interiors. Measured values of the head severity index show no distinct correlation with the observed injuries measured on the ten-point scale. However, a correlation is shown to exist between observed injury and predicted vehicle speed change.

SUMMARY

The purpose of this section is to present the most noteworthy findings of this research effort in a concise form, and also to provide an overview of the detailed cross-correlation that is possible for evidence gathered at an actual highway accident scene, the corresponding predictions of an analytical reconstruction of the event, and the results of a physical reconstruction of the accident in a crash test.

One of the most significant findings of this effort is that a definite correlation exists between the observed injuries to the crash victim, as measured on the ten-point injury scale, and the predicted speed changes of the subject vehicles involved in the crashes. This result is summarized in Figure S-1 for the ten accident cases of this study. There are two important points to note in connection with this figure. First, the ten-point scale is to a considerable degree both qualitative and subjective. Second, the vehicle speed change is predicted from somewhat limited evidence from the accident scene, and is therefore subject to some error. Considering these two factors, the correlation shown in Figure S-1 is considered significant. The faired curve is a first estimate of the trend of the correlation. Although the evidence shown in the figure is quite limited, the advantage of occupant restraint is also suggested by these results.

To provide an overview of the quantity of detailed information that can be extracted by correlating data from the accident case reports, the computer simulations of vehicle and occupant responses, and the crash test reconstructions, the results for one of the ten selected cases will be briefly reviewed in this section.

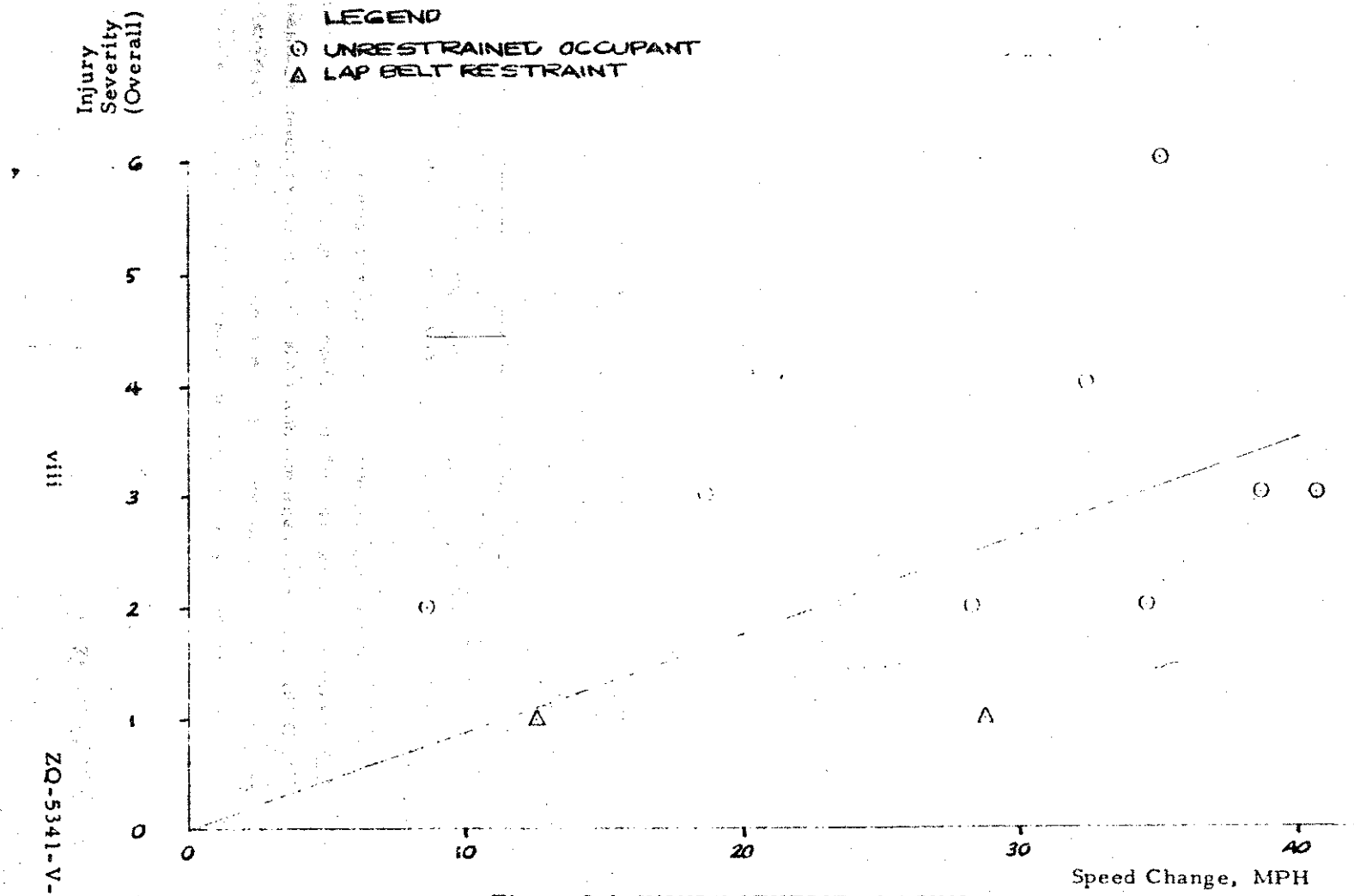

Figure S-1 INJURY SEVERITY RATING COMPARED TO PREDICTED SPEED CHANGE

Case No. TR01316 was chosen for this review because it is considered representative of the ten cases, and because it is relatively free of complexities that require detailed discussion.

Case No. TR01316

Description of the Accident

(Excerpts from the Multidisciplinary Accident Investigation case reports are presented in Section 3.3)

The case vehicle was proceeding along a dirt road at 35-40 MPH. The driver, to avoid striking a utility pole, countersteered excessively and the vehicle ran off of the road. The driver locked the wheels, leaving 32 feet of skidmarks, and impacted a fruit tree at about 10-15 MPH. The accident scene schematic is shown in Figure S-2. After impact, the vehicle came to rest against the fruit tree (Vehicle Damage Index: 12FCEW3).

The vehicle right front occupant (15 yrs., 68 in., 150 lbs.), restrained by a lap belt, moved forward and struck his head on the instrument panel. Injuries sustained included concussion, facial contusion, and head laceration (Ten-Point Abbreviated Injury Scale rating - 1 (minor)).

Analytical Reconstruction of Vehicle Responses

(The mathematical reconstructions of the vehicle responses are summarized in Section 3.2, and relevant details are discussed in Section 3.3)

Results of computer simulation of the vehicle responses are summarized in the plotter graphics display of Figure S-3. The measured Vehicle Damage Index (VDI) of 12FCEW3 and the predicted VDI, 12FCEW2, are in substantial agreement. The predicted speed change, 12.5 MPH, lies within the estimate of 10-15 MPH from the accident case report.

Figure 6-2

Accident Case Schematic

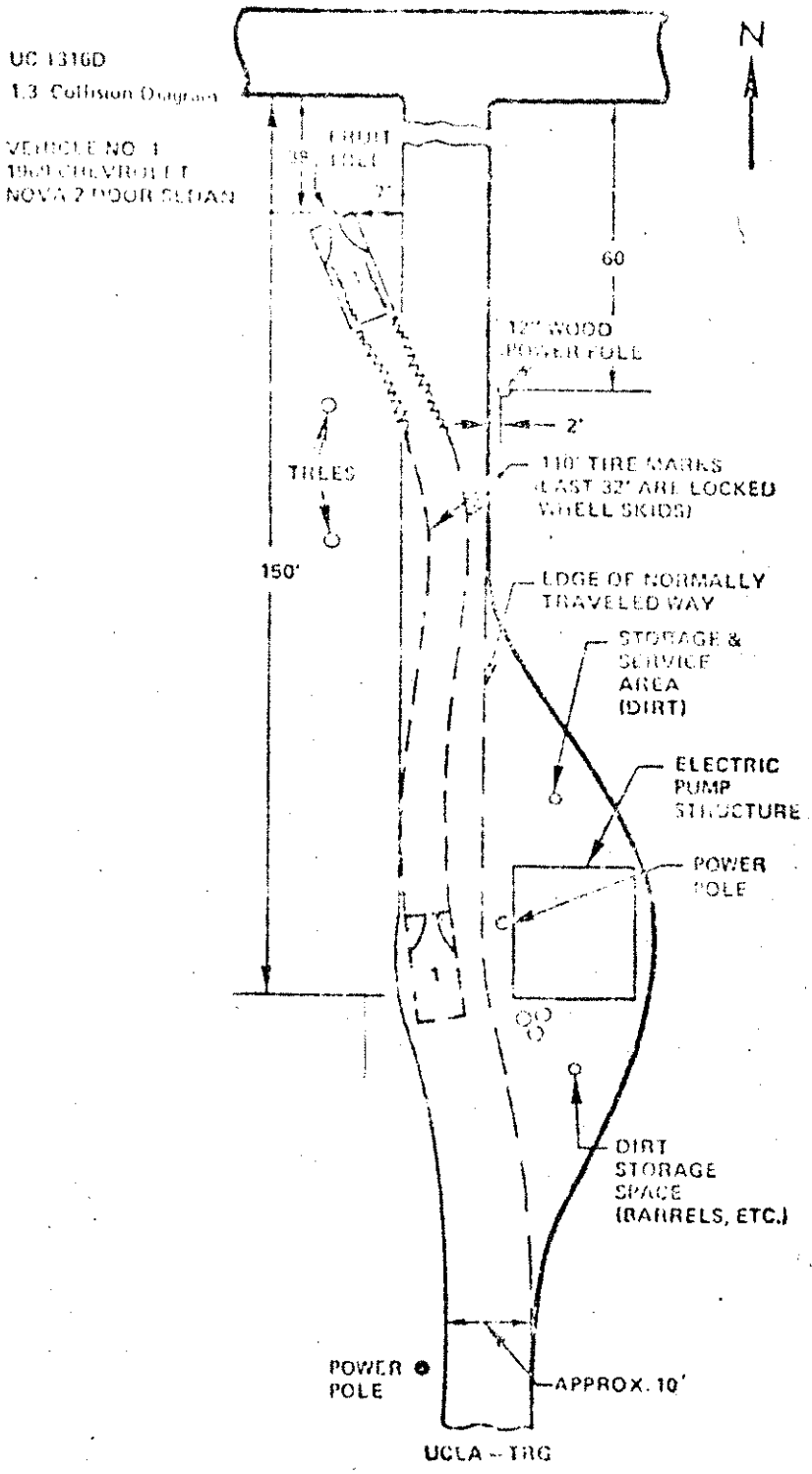

ZQ-5341-V-1

Figure S-3

Analytical Reconstruction of Vehicle Responses

GRAPHIC DISPLAY OF OUTPUTS OF ACCIDENT RECONSTRUCTION

COLLISION AND TRAJECTORY

CASE NO. 1918 A RUN NO. TH01318

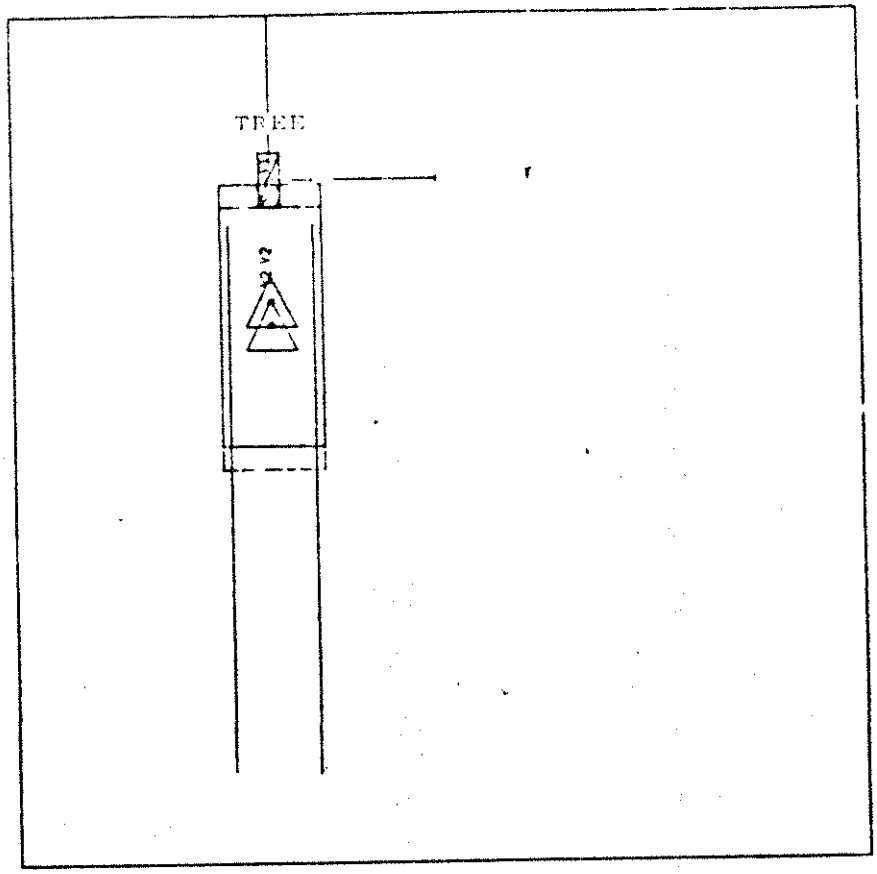

AXIS INTERVALS ARE 10. FEET

	RECONSTRUCTED POSITIONS AND VELOCITIES AT IMPACT						DISPLAYED FINAL POSITIONS				VEHICLE DAMAGE INDICES	ΔV
	C.G. POSITION		HEADING				C.G. POSITION		HEADING	REMARKS		
	XC1	YC1	PSI1	FWD	LATERAL	ANGULAR	XC1F	YC1F	PSI1F			MPH
	FT.	FT.	DEG.	MPH	MPH	DEG/SEC	FT.	FT.	DEG.			
VEHICLE # 1	0.0	0.0	0.0	0.0	0.0	0.0	0.0	0.0	-0.0	VEHICLE AT REST		0.0
VEHICLE # 2	-8.8	0.0	0.0	12.7	0.0	0.0	-7.4	-0.0	-0.0	VEHICLE AT REST	12FCEW2	12.5

Analytical Reconstruction of Occupant Responses

(The mathematical reconstructions of the occupant responses are summarized in Section 3.2, and relevant details are discussed in Sections 3.3 and 3.5)

The predicted kinematic responses of the right front occupant, summarized in the plotter graphics displays of Figure S-4, are essentially identical to the observations summarized in the accident case report. Predicted values of head injury indicators are as follows: head severity index - 1080, head injury criterion (HIC number) - 920.

Physical Reconstruction of the Accident

(The physical reconstructions are summarized in Section 3.4, and relevant test details are discussed in Section 3.5)

The accident was physically reconstructed on the Calspan impact sled using an automobile body buck to represent the subject vehicle, and a crash test dummy to represent the right front occupant in the accident, as illustrated in Figures S-5 and S-6. The sled pulse was chosen to match approximately the predicted vehicle deceleration history, as shown in Figure S-7. From the photographs of Figures S-5 and S-6, it can be seen that the dummy head struck the instrument panel in the same general manner as reported in the accident case. In contrast to the accident report and the computer simulation of occupant responses (Figure S-8), however, the dummy head grazed the windshield, as indicated in Figure S-6. The measured value of the head severity index for this test is 110.

Crash Victim -

Male
15 Years
68 in.
150 lbs.

Lap Belt In Use

Accident -

Head struck upper instrument panel - concussion, facial contusion, laceration

Injury Rating -

Face - 1 (Minor)
Brain - 1
Overall - 1

CASE NO. TR 01316

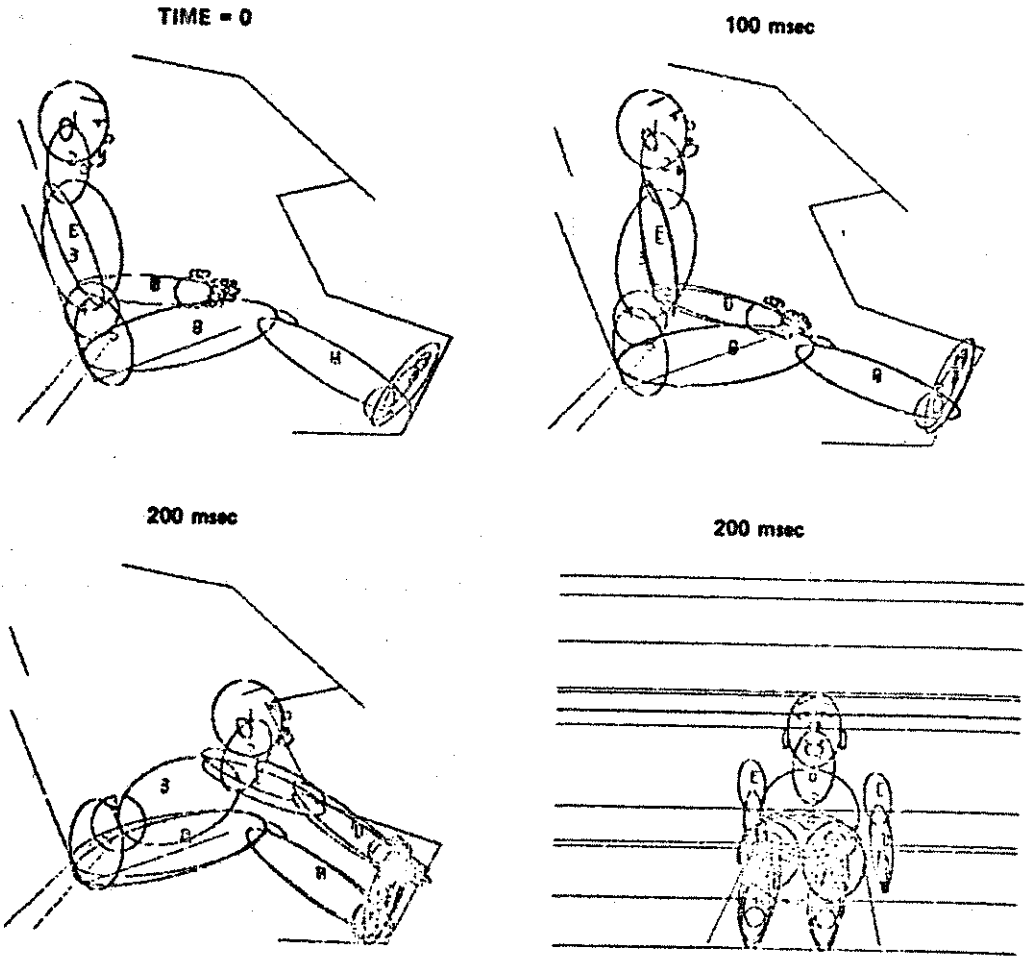

Figure S-4

CRASH VICTIM -

MALE
15 YEARS
68 in.
150 lb
LAP BELT IN USE

ACCIDENT -

HEAD STRUCK UPPER INSTRUMENT PANEL - CONCUSSION, FACIAL CONTUSION, LACERATION

INJURY RATING -

FACE - 1 (MINOR)
BRAIN - 1
OVERALL - 1

WINDSHIELD

UNBROKEN, UNCRACKED, NO CONTACT REPORTED.

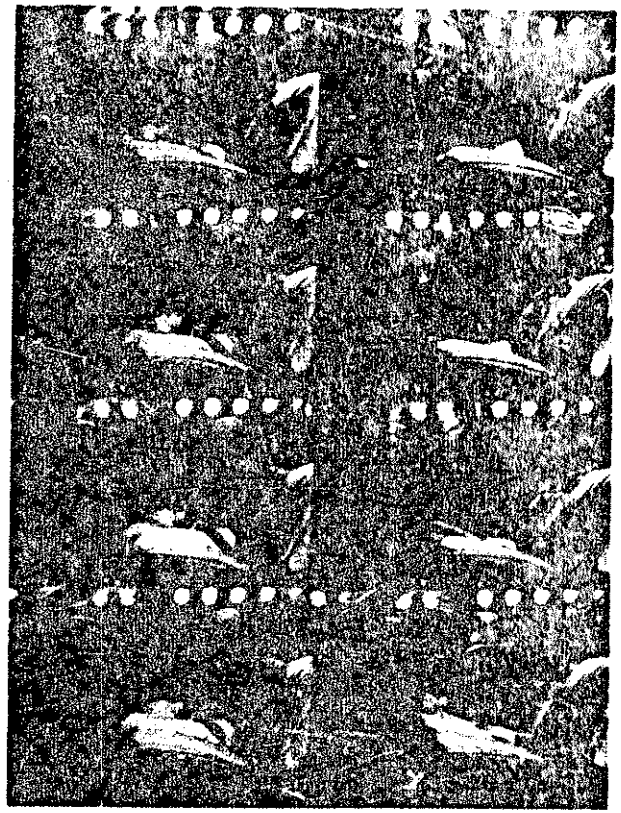

Figure S-5 PHYSICAL RECONSTRUCTION OF THE ACCIDENT

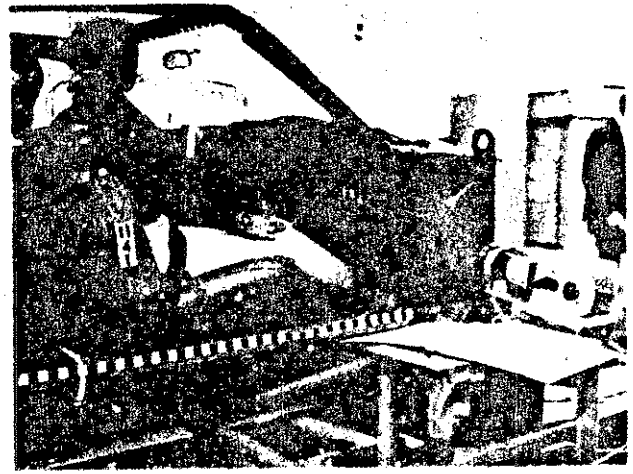

PRE-TEST

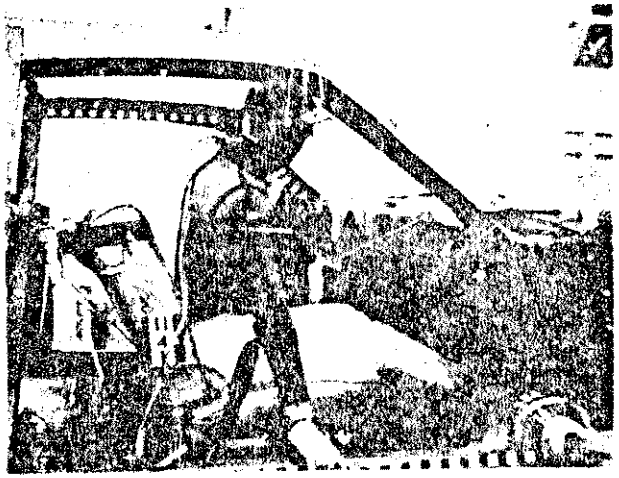

POST-TEST

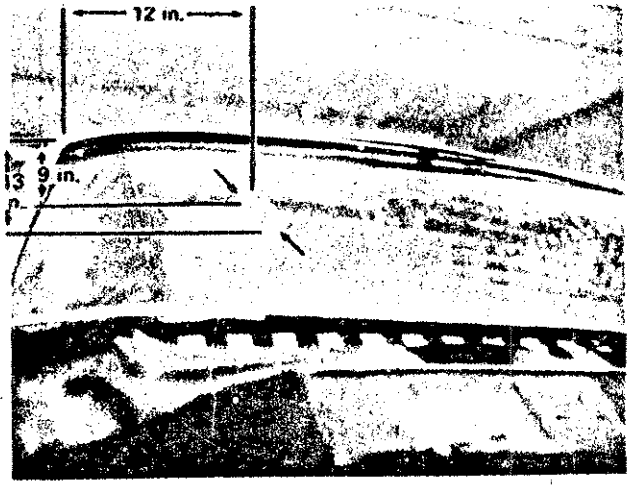

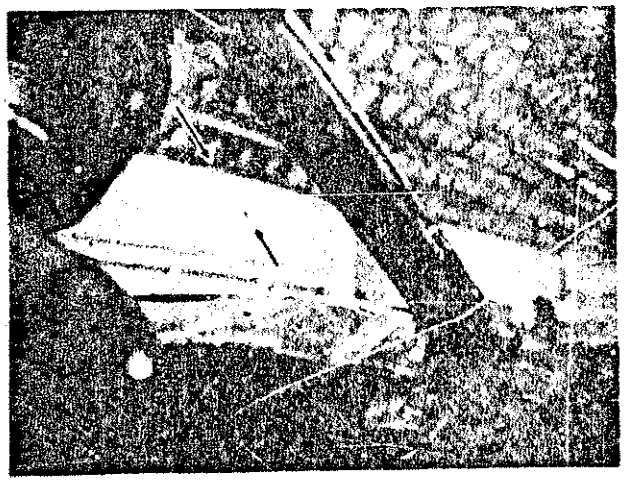

WINDSHIELD CONTACT

TR 3121G

SPEED CHANGE, mph	
TEST	SIMULATION
16.5	12.5

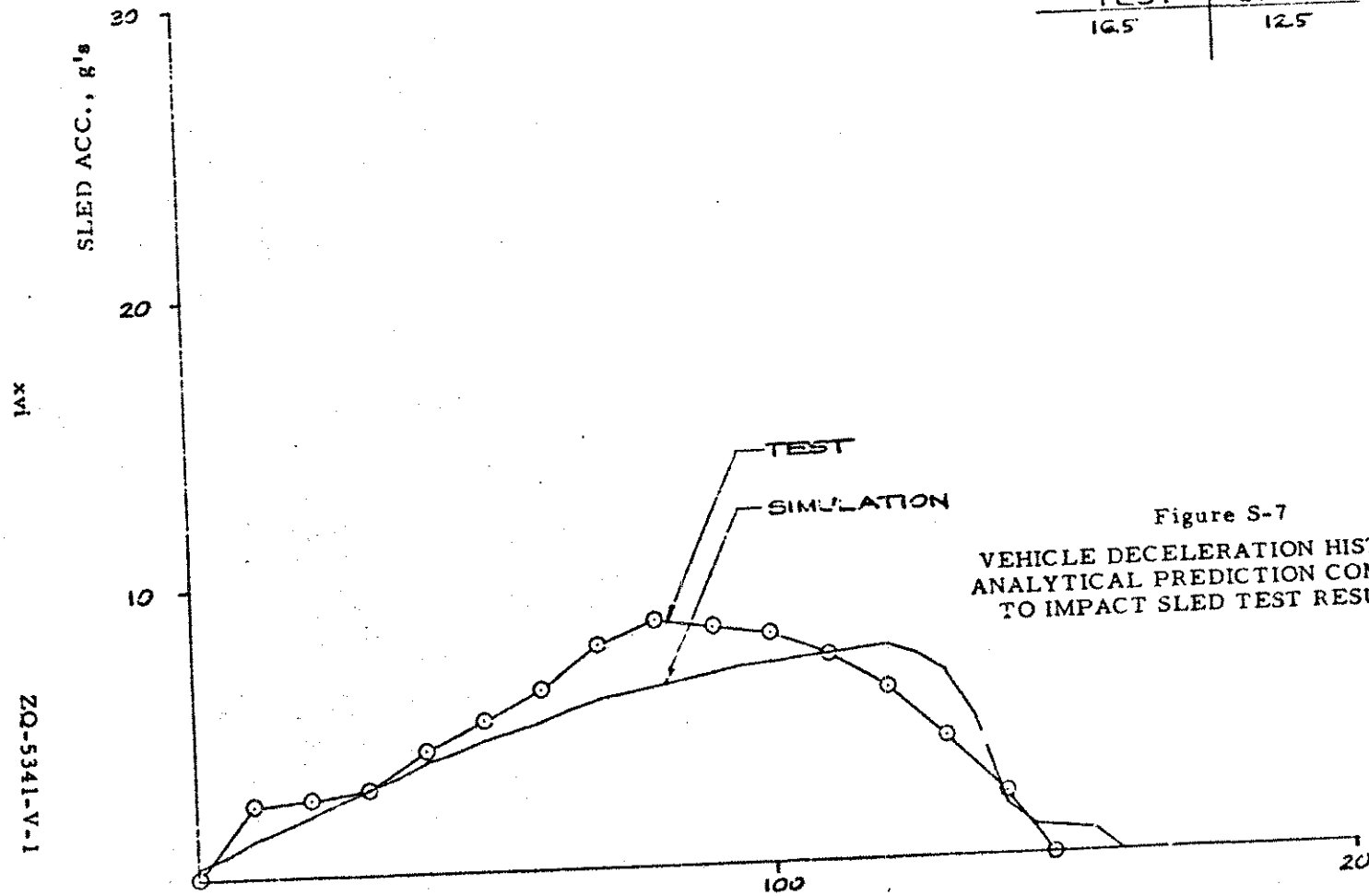

Figure S-7

VEHICLE DECELERATION HISTORY - ANALYTICAL PREDICTION COMPARED TO IMPACT SLED TEST RESULTS

ZQ-5341-V-1

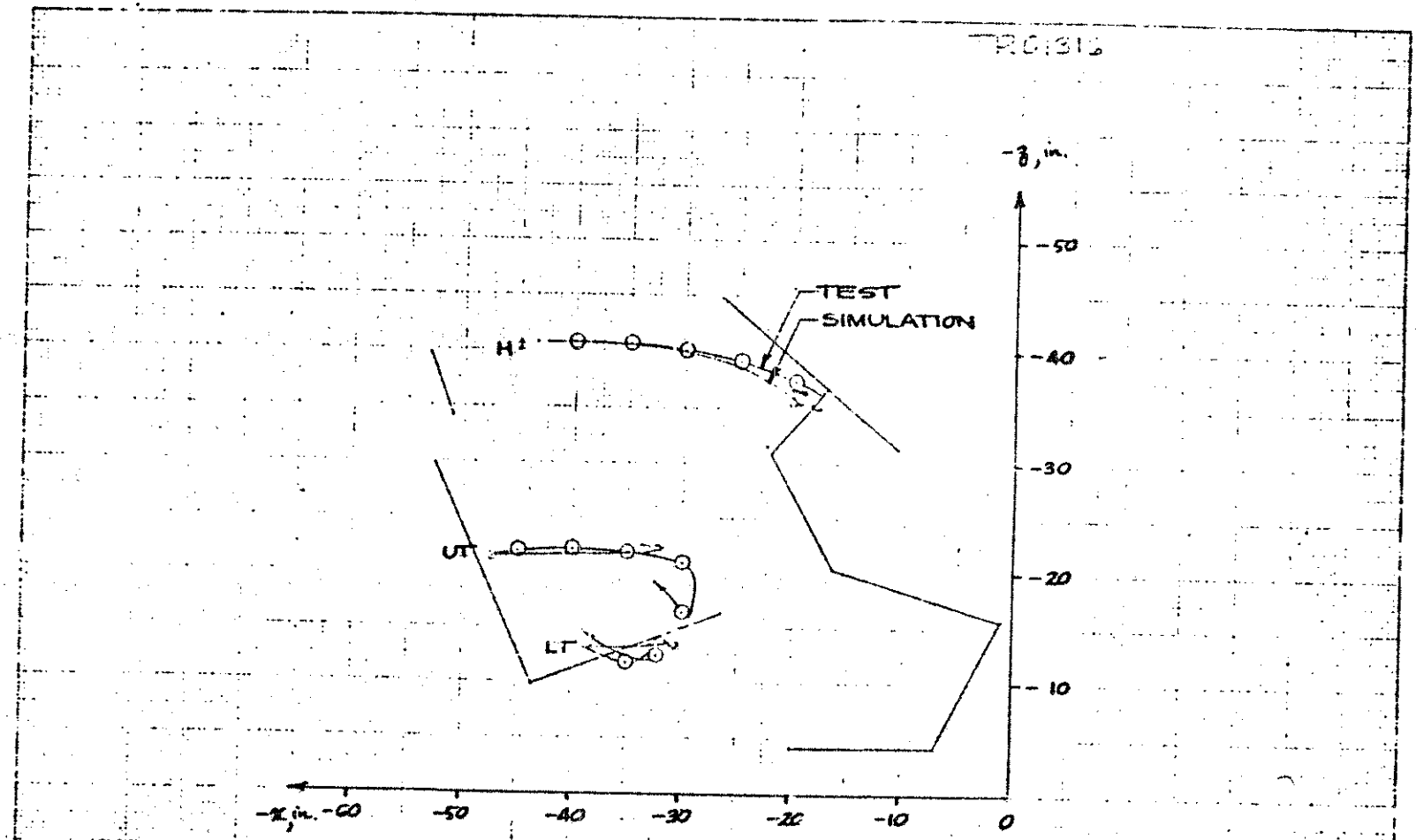

Figure S-8

OCCUPANT KINEMATICS -
ANALYTICAL PREDICTION COMPARED
TO IMPACT SLED TEST RESULTS

Conclusions

Predicted vehicle responses agree in detail with the accident case report. The kinematic responses of the simulated crash victim in the analytical and physical reconstructions are also in generally good agreement with the case report.* The observed head injury in the accident of 1 (minor) is consistent with the small value of the measured HSI of 110 in the sled test. The rather large value of the predicted HSI of 1080 in the computer simulation is considered to be primarily the result of using a "typical" force-deflection characteristic to represent the head-instrument panel contact in the simulation, because no measured properties were available.

The generally reasonable agreement between the accident case report and the analytical and physical reconstructions lends support to the reconstruction technique. This concise example also illustrates, at least partially, the detailed information discussed in subsequent sections, which is provided by the technique.

*In the sled test, the speed change was 16.5 MPH, compared to a predicted speed change of 12.5 MPH. This higher speed likely caused dummy head contact with the windshield, in contrast to no head-windshield contact in either the accident or analytical reconstruction.

TABLE OF CONTENTS

TABLE OF CONTENTS (continued)

TABLE OF CONTENTS (continued)

LIST OF FIGURES

LIST OF FIGURES (continued)

LIST OF FIGURES (continued)

LIST OF FIGURES (continued)

LIST OF FIGURES (continued)

LIST OF FIGURES (continued)

LIST OF TABLES

1.0 INTRODUCTION

The overall objective of this research is to develop techniques and equipment that will permit a general upgrading in the quality and completeness of data obtained from the scenes of accidents, so that the categorization of occupant exposures can be refined and the roles of vehicle and/or highway defects and of driver judgment in causation can be evaluated in a more uniform manner.

In research recently completed at Calspan, Reference 1, promising results have been achieved in the development of a measurement and data processing system to aid the investigation of highway accidents.

The present research effort consists of two major tasks. The first, still in progress, is a continuation of such system development and field testing, which includes the performance of field tests by police personnel. The second task is an application of mathematical reconstruction techniques to the calibration of anthropometric dummy responses for injury interpretations based on injuries that have occurred in actual highway accidents. The analytical and physical reconstruction phase of the second task is the subject of this report.

Interpretation of measured dummy responses in terms of the corresponding injury potential for humans constitutes a highly controversial aspect of MVSS 208. One source of difficulty is the lack of a "one to one" relationship between the dynamic responses of existing dummies and those of living humans. Another is the fact that differences exist between sensor mounting methods and positions, and resulting frequency response characteristics, in the cases of the specimens used in tests of impact tolerances (i.e., animals, cadavers, volunteers) and in anthropometric dummies.

A long range approach to the alleviation of this problem is to strive for a test dummy which will approach a "one to one" relationship with the responses of a living human. However, it must be recognized that, despite future improvements, dummies will continue to be test devices that require calibration.

The present research effort is aimed at defining calibration factors for existing dummies, instrumented in accordance with MVSS 208, by means of direct correlation of their measured responses with injuries that have occurred in actual highway accidents. Analytical techniques have been applied to reconstruct the vehicle and occupant dynamics in selected, actual accidents, as discussed herein. The injuries of occupants are thus related to specific acceleration exposures and conditions of restraint. Physical simulations of the injury producing conditions, by means of the Calspan HYGE impact sled, were then used subsequently to determine the corresponding measured responses of anthropometric test dummies. By this means, the measured dummy responses can be directly correlated with injuries to living humans.

With refined categorization of occupant exposures, actual highway accidents are seen as being potentially the best available source of improved information on the injury thresholds of humans in the automobile-crash type of exposure (i.e., partial or no restraint, including impact on the vehicle interior) and of measures of the effectiveness of protective devices. This viewpoint is based on the facts that experimental research with volunteers must be run substantially below injury thresholds, and that the interpretation of results obtained with cadavers and animals, in terms of corresponding results of living humans, is not a straightforward and validated procedure. Thus, there is no direct means of generating improved tolerance data for this type of exposure, and the development of improved protective devices for use in automobiles is hampered by the limited extent of applicable human tolerance information.

The problem of developing and evaluating protective devices is compounded by the use of anthropometric dummies to apply the grossly approximate, available human tolerance information. The dummies do not respond like living humans and they are instrumented differently from the various subjects used in the tolerance experimentation.

The present research is therefore aimed at the direct development of calibration factors for anthropometric dummies on the basis of injuries to living humans in actual highway accidents. By this means, the intermediate step of tolerance experimentation with animals, cadavers and volunteers and the associated problems of interpretation can be bypassed in a parallel research approach aimed at the same end objectives. It should be noted that the present research is not intended to be a replacement for tolerance experimentation but rather to serve as a supplementary technique.

The Simulation Model of Automobile Collisions (SMAC) computer program, References 2 and 3, has recently been developed by Calspan as an aid to the investigation of highway accidents. An encouraging degree of detailed correlation has been demonstrated to exist between predictions of the SMAC computer program and measured responses, including Vehicle Damage Indices (SAE J224a), in staged collisions. Using this program in an iterative manner, vehicle responses in actual collisions can be reconstructed with a higher degree of confidence than that provided by other available techniques. In parallel with the final iterations of collision conditions in the SMAC reconstruction of vehicle responses, the Calspan 3-D simulation of the crash victim, References 4-6, has been used to reconstruct the responses of the injured occupants. In this manner, both the interior and the exterior physical evidence have been used to achieve a detailed reconstruction of the collision event.

In subsequent research, the Calspan HYGE impact sled has been used to physically simulate the direction and time history of the reconstructed acceleration exposure. Anthropometric dummies, instrumented in accordance with MVSS 208, were used to determine measured dummy responses corresponding to the known injuries of the actual crash victims.

In view of the exploratory nature of this research, this study was limited to ten accident cases. These ten cases involved right front passengers with injuries over a range of severities from minor to fatal.

The experience gained in an earlier pilot study* of three accident cases, Reference 7, was most valuable in performing this research. In that study, the overall correlation of actual and reconstructed evidence was considered to be quite good. However, the predicted values of head severity index for the occupants did not correlate well with the reported injury severities as measured by the 10-point injury scale. It was not possible at that point in that research effort to determine whether the lack of correlation reflected deficiencies in the reconstructed occupant responses or shortcomings in the severity index as an indicator of injury potential. Subsequent tests, to aid in reaching a firm conclusion, have not yet been performed as part of that research effort.

Two cases from the exploratory three-case study have been included in the present ten-case investigation, as will be subsequently discussed.

The purely analytical reconstruction of accidents offers several distinct advantages over corresponding experimental methods. First, parameters may be varied in a rapid and cost-effective manner to achieve

*Sponsored by General Motors Corporation. Permission to publish results from this Calspan Commercial Confidential Report was granted to Calspan by General Motors.

a best fit to on-site observations. Second, results from the computer simulations are not clouded by experimental nonrepeatability. Third, the analytical methods provide detailed quantitative results from which additional insight into the complex vehicle-occupant interaction may be gained. It should be emphasized, however, that the analytical techniques are intended as a compliment to physical testing, and not a substitute. An obvious limitation as a substitute technique is the fact that in some cases computer program inputs cannot be defined with a high degree of confidence because of limited experimental data on required system characteristics.

In the case of the SMAC program, development has been aimed not so much at producing a very complex, large computer program that will predict vehicle responses at a state-of-the-art level of vehicle and collision dynamics, but rather to achieve a state-of-the-art advance in accident reconstruction technology. The intent is to provide a uniform measurement and reporting format for accident investigation and to provide the investigator with a time-sharing computer-based reconstruction tool that will be within the capabilities of a person not trained in vehicle and collision dynamics and computer programming.

Consequently, the SMAC program contains simplifying assumptions in order to achieve that goal. The inevitable trade-offs involved in applying simplifying assumptions to analyses result in a degradation in the predictive capability for some types of events. In the present case, the lack of consideration of vehicle pitch (during severe collisions) and the simulation of the peripheral vehicle structure by a single, homogenous material property tends to result in low predicted values of vehicle yaw during high-speed offset frontal collisions. A concern for the validity of SMAC in these situations is evident since case selection for the current application has resulted in just this type of collision. However, while it is felt that a more detailed analytical treatment would improve the vehicle trajectory predictions with respect to yaw angles observed, most of the vehicle yaw takes place after initial longitudinal deceleration and thus after the occupant has contacted

the vehicle interior. Consequently, it is felt that the predictive capability of SMAC is adequate for the current application.

In the present application of the 3-D crash victim program, the material (force-deflection) properties of the vehicle interior are based upon representative values, rather than direct measurement. Because the inputted windshield properties in most cases strongly affect predicted values of the head injury indicators, the experimental variability of windshield failure properties will be discussed in some detail in this section.

This variability of characteristics is perhaps best illustrated by the summary of representative windshield data presented in Figures 1.1 and 1.2. In Figure 1.1, the conventional head severity (Gadd) index is plotted versus impact speed, and in Figure 1.2, the head injury criterion (HIC number) is plotted against the same abscissa.

There are several important items to be noted in connection with these two figures. First, the plots are a summary of published experimental data on conventional* high-penetration-resistant (HPR) windshields of the type installed in U. S. automobiles since 1966. This summary, however, is not intended to be all-inclusive. In fact, some of the anomalous results of the cited investigators have been excluded from these plots, to avoid possible confusion. Second, the testing facilities and techniques, glass sample size and mounting, impactor, impact angle, glass composition, and glass exterior surface condition differed in the tests, as can be seen from the legend of Figure 1.1. (Only the ambient temperature, approximately 70-75°, was common for the test data shown in Figure 1.1 and 1.2.)

*1/8 in. glass outer layer - 0.030 in. polyvinyl butyral liner - 1/8 in. glass inner layer.

Figure 1.1

IMPACT DATA ON CONVENTIONAL WINDSHIELDS -
HEAD SEVERITY INDEX MEASUREMENTS
LEGEND

	INVESTIGATOR(S)	TEST	IMPACT ANGLE, deg.	GLASS	TEMP.
○	BLIZARD & HOWITT (Ref. 8)	HEADFORM IMPACT (17 lbs., 6½ in. dia.)	45	ABRADED FLOAT	75°F.
△	PATRICK, TROSIEN, & DUPONT (Ref. 9)	50th pct. DUMMY/ IMPACT SLED	~45	-	ROOM
□	ALEXANDER, MATT-IMOE, & HOFMANN (Ref. 10)	HEADFORM DROP (22 lbs.)	90	PLATE	ROOM
◇	"	"	90	FLOAT	ROOM
⊏	KAY, PICKARD, & PATRICK (Ref. 11)	HEADFORM DROP (22 lbs.)	90	FLOAT	20°C.
◈	"	50th pct. DUMMY/ IMPACT SLED	~45	FLOAT (0.1 in.)	21-23 °C
▽	KRAMER (Ref. 12)	50th pct. DUMMY/ CATAPAULT	~45	-	23°C.
◆	HODGSON, THOMAS, & BRINN (Ref. 13)	CADAVERS/ IMPACT SLED	~45	ABRADED	ROOM

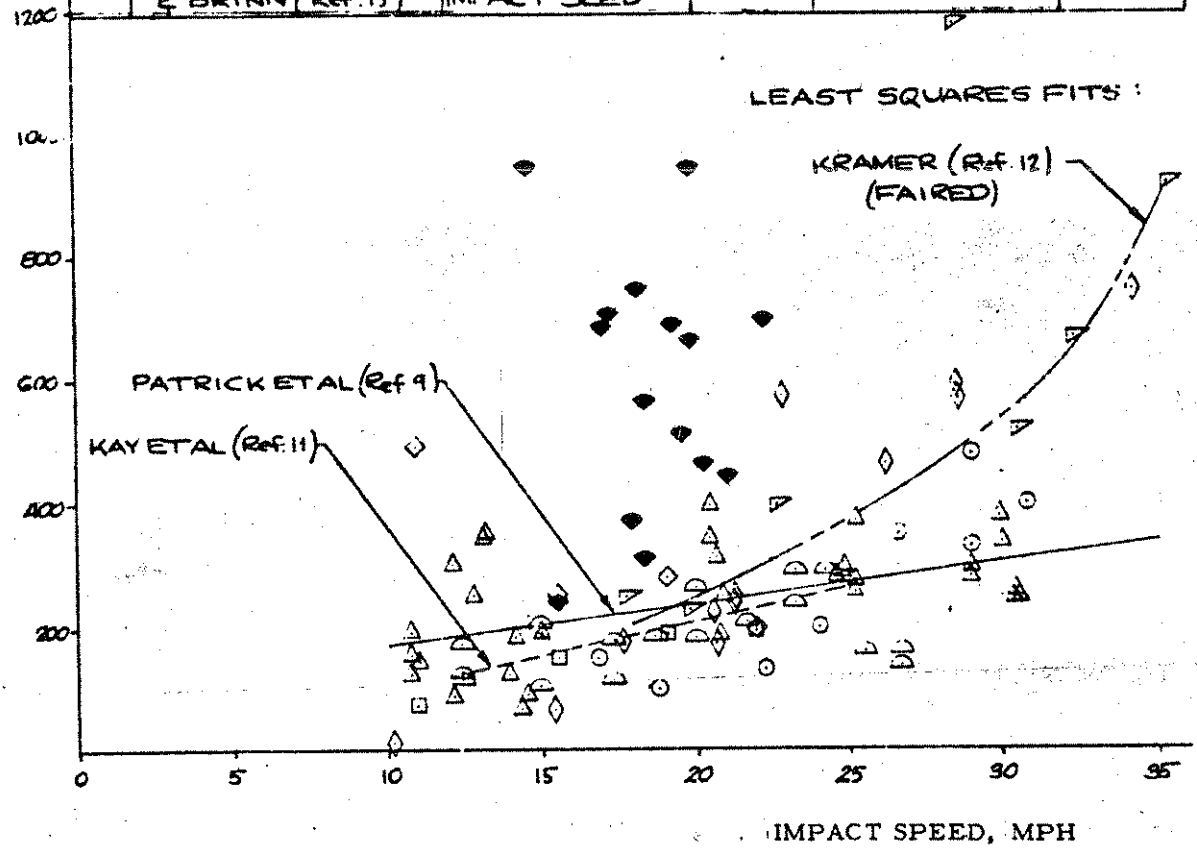

Figure 1.2

IMPACT DATA ON CONVENTIONAL WINDSHIELDS -
HEAD INJURY CRITERION MEASUREMENTS
LEGEND - SEE FIG. 1.1

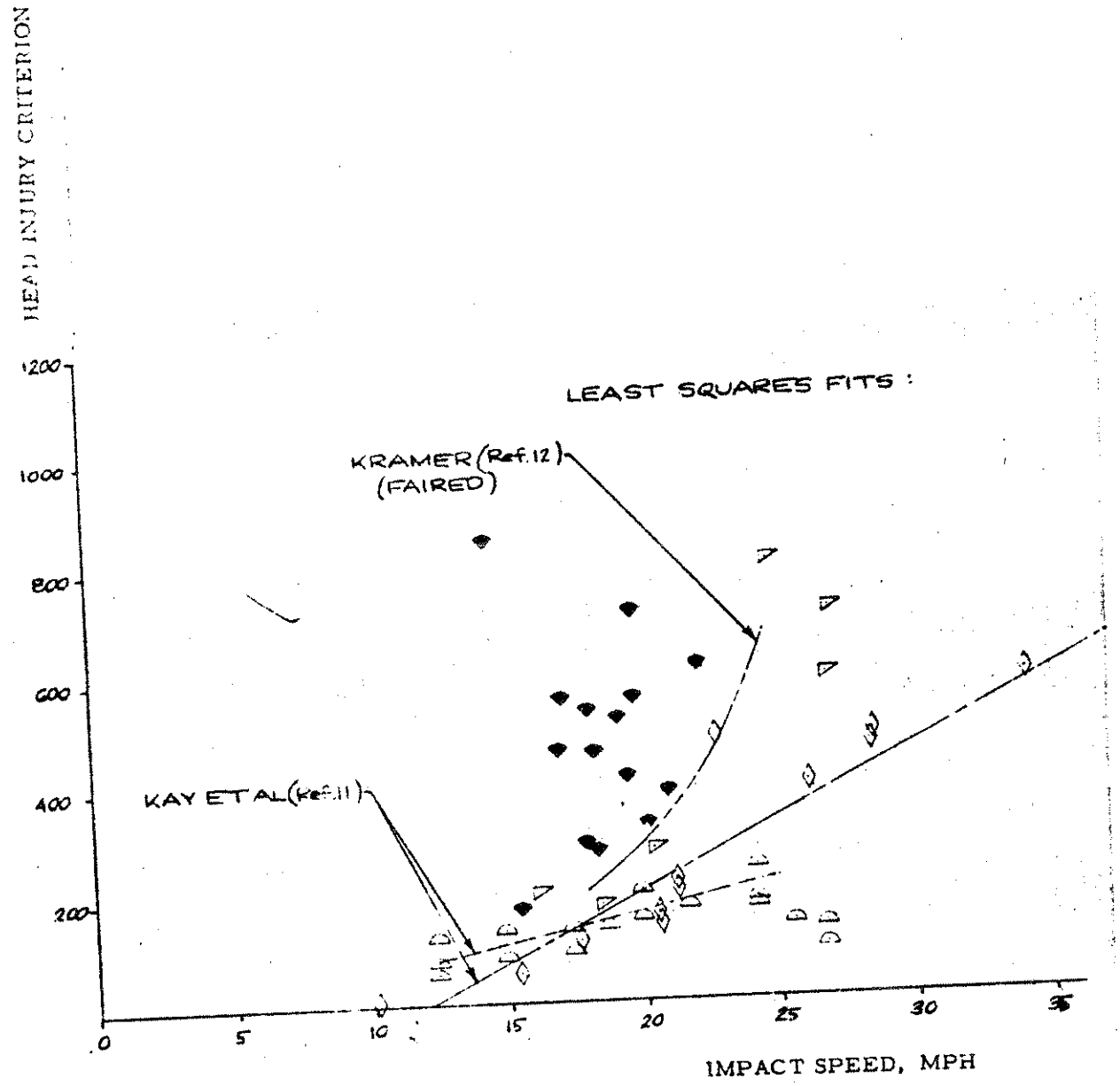

ZQ-5341-V-1

It is apparent from Figures 1.1 and 1.2 that the results reported by various investigators for conventional windshields differ appreciably. This is not surprising, considering the differences in test conditions that have been noted. Of more significance for the present purposes, however, is the considerable scatter within each set of data. As discussed by the cited researchers, References 8 to 14, such scatter is at least partially the result of variations in initial impact location on the glass, glass mounting, glass exterior surface condition, etc., within any given set of tests. Figures 1.1 and 1.2 therefore clearly illustrate the variability of windshield failure characteristics that is inherent in the problem of accident reconstruction, for cases in which the windshield is struck.

For the physical reconstruction of the ten accident cases, an automobile body buck mounted on a turn table and fastened to the Calspan HYGE impact sled, Figure 1.3, was used to simulate the subject vehicles. The planar deceleration history of the accident vehicle predicted by the SMAC program was approximated by a unidirectional sled pulse, with the direction of buck rotation selected to correspond to the predicted vehicle yaw during peak deceleration. It should be noted that all existing accelerator sleds are limited to unidirectional pulses. However, exploratory applications of the computer simulation of occupant responses, in which the SMAC predicted vehicle yaw responses were included, have indicated that occupant behavior and interior contact points are not significantly affected. This finding stems from the facts that the occupant is not strongly coupled to rotational motions and that the short duration of the collision event limits the extent of rotation that can occur prior to occupant contact with the interior.

Because of the limited scope of the experimental program, only one automobile body buck, fabricated from a 1969 Ford sedan, was used in the sled test series. To simulate approximately the differing interiors of the ten accident vehicles, seat types and seat locations were varied, with minor modifications in the instrument panel location also made to approximate the actual vehicle geometry. Most of the tests were performed with an HSRI 50th percentile male crash test dummy representing the crash victim.

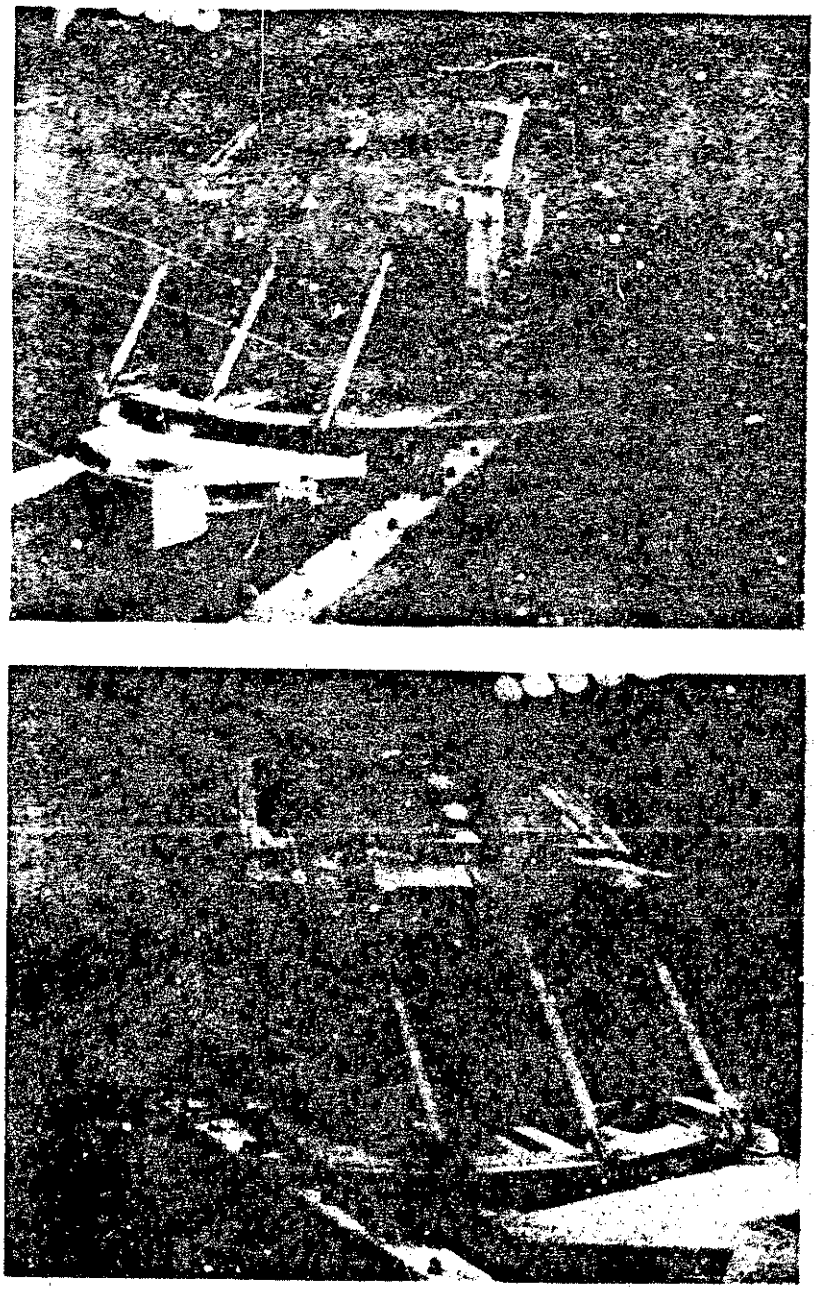

Figure 1.3 IMPACT SLED TEST SETUP

In the next section, conclusions and recommendations stemming from this research are reviewed. Following that, the techniques that were utilized in the reconstruction process are reviewed, beginning with the basis and methods of case selection. Then, concise summaries of results of the reconstruction procedure are presented for each of the ten cases. The SMAC input format and vehicle parameters are summarized in Appendix A, followed by corresponding information on the 3-D crash victim program in Appendix B, vehicle stiffness properties in Appendix C, and details of the impact sled tests in Appendix D.

2.0 CONCLUSIONS AND RECOMMENDATIONS

2.1 Conclusions

2.1.1 The feasibility of using a mathematical reconstruction technique to define exposures in which the responses of anthropometric dummies can be calibrated in terms of injuries to living humans has been successfully demonstrated.

While needs for a number of refinements in accident reporting and in reconstruction and testing procedures are indicated by the achieved results, the demonstrated technique is believed to be the most direct method available for correlating the responses of test dummies with injuries to living humans.

2.1.2 Variability in the size, position, muscular reactions and tolerance levels of individual crash victims, combined with the generall subjective nature of injury severity ratings, will require the use of a numbe of cases with similar exposures to establish a basis for tests to calibrate dummy responses.

This statistical aspect of interpreting results of the reconstruction technique is, of course, also a requirement in alternative approaches to dummy calibration.

2.1.3 The multi-disciplinary case reports are generally inadequate for purposes of a detailed accident reconstruction.

The costs of adding essential details, such as dimensions, would appear to be negligible in view of the fact that professional investigators are available at the accident scenes to obtain such data.

2.1.4 Generally good agreement has been achieved between the accident reconstructions and available details in the ten reported cases.

In nine of the ten cases, the vehicle responses were successfully reconstructed by the analytical methods. In seven of the ten cases, the predicted crash victim responses are in reasonably good agreement with the accident case reports. Furthermore, the physical reconstructions of the ten cases, in impact sled tests, generally substantiate the analytical predictions and are consistent with the accident case reports.

In the present exploratory effort, a number of factors contributed to differences between evidence from the accident and the analytical and physical reconstructions. The primary factors are believed to be:

- Variations between the interior geometry and material properties of the simulated vehicle and the case vehicle.
- The unknown initial position, orientation, and muscular state of the crash victim.
- Differences between the crash victim size and the size of the simulated occupant.
- The lack of a rigorously established relationship between the predicted vehicle crash deceleration history and the (unknown) actual crash history.
- Differences between the sled test deceleration pulse and the predicted vehicle crash deceleration history.

2.2 Recommendations

2.2.1 The demonstrated technique should be refined, as required, and applied more extensively to fully exploit its capability of directly correlating dummy responses with injuries to living humans.

This approach to dummy calibration is considered to be an attractive supplement to the ongoing tolerance experimentation with animals, cadavers and volunteers which has served to establish existing response criteria. The cited difficulties are seen as being less formidable than those associated

with the interpretation and application to living humans of the results of tolerance experiments.

2.2.2 The format of multi-disciplinary accident case repor should be modified to include more detailed quantitative results from the accident investigations.

Such details should include sketches drawn to scale of the accident scenes with relevant dimensions indicated, and additional dimensional sketches and/or photographs of the vehicle interior, particularly the region of occupant contact.

2.2.3 Subsequent to the planned development of an automate iteration capability in the SMAC computer program, levels of confidence should be established for reconstructions of different collision configuration by means of applications to staged collisions that are adequately reported. In future applications of the present type, the levels of confidence which can be achieved in reconstructing a given case should serve as a basis for case selection.

In the current mode of SMAC applications, the user selects iterative adjustments of the unknown collision conditions and formal criteria for the acceptability of the overall evidence "fit" have not yet been established. Thus, some minor variations in the detailed results obtained by individual users are likely. While extensive evidence of detailed correlation with collision data has been established in the present operating mode (References 1, 2, 3), it is obvious that further investigation of the accuracy of reconstructions would be desirable. With the user "in the iterative loop" staged collisions for which the reconstruction is completed without knowledg of the actual collision conditions are essential to achieve realistic measures of accuracy. With the planned automation of iterative adjustments, it will be possible to test the program with any adequately defined staged collisions and to establish ranges of impact conditions that will produce equally acceptable matches of the available evidence.

2.2.4 In future studies of this type, a dummy that meets the specifications of MVSS 208 should be used in the sled tests.

In the present exploratory study, constraints on budget and schedule made it necessary to use an HSRI dummy, rather than a Hybrid II (i.e., a dummy meeting the specifications of MVSS 208). Also, because of the nature of the injury type investigated, the head responses to windshield impact played a major role in the presented comparisons. Obviously such comparisons would be made more meaningful by the use of a dummy meeting the specifications of MVSS 208.

Because of the various factors cited in Section 2.1.4 that resulted in differences between the accident observations, the computer simulation, and the sled test reconstruction, no attempt was made to judge the dummy responses in light of the actual observed injuries, except on a case-to-case basis. The potential for a calibration procedure, however, is indicated by the degree of correlation obtained in this research effort. It should be noted here that lack of correlation of either analytical or experimental injury indicators with reported injuries may reflect shortcomings in either the indicators or the linear scale that has been used to quantify the injuries.

3.0 DISCUSSION OF RESULTS

3.1 Reconstruction

3.1.1 Accident Case Selection

In the initial accident case selection, to establish an efficient method for eliminating hundreds of case reports which would not be usable in this study, the following requirements were specified:

(1) the crash victim, a vehicle right front occupant, must have sustained a head (head, face, or brain) injury

(2) the crash victim, either male or female, was approximately the weight and stature of a 50th percentile male (152 to 182 lbs. and 66 to 72 inches, respectively

(3) the occupant was not ejected from the vehicle

(4) the primary vehicle did not roll over or sustain a rear-end collision.

Using these criteria, the Multidisciplinary Accident Investigation (MDAI) automated report file of the Highway Safety Research Institute, Reference 15, was searched with a digital computer code designed for information retrieval from the file, and yielded 66 cases satisfying these four requirements. The distribution of these 66 cases as a function of injury (both specific and overall) is illustrated in Figure 3.1.1. It is apparent that the distribution is markedly skewed, with most of the injuries falling in the minor and moderate categories.

Figure 3.1.1

INJURY SEVERITY OF THE RIGHT FRONT OCCUPANT IN SIXTY-SIX ACCIDENT CASES

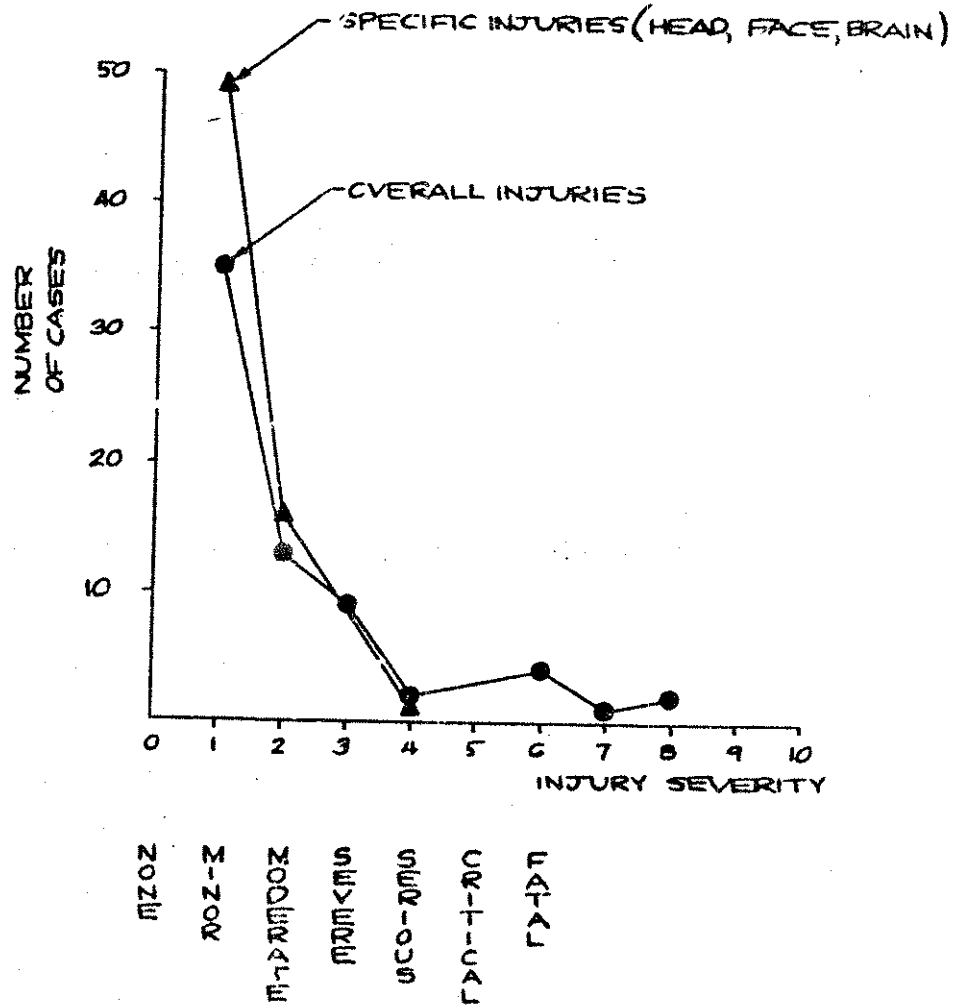

To obtain a more even distribution of injuries in the 10 cases to be reconstructed, criterion (2), relating to occupant size, was eliminated and the file search repeated. This relaxation of the occupant size requirement resulted in about 30 additional cases in which the specific (i.e., head, face, or brain) injury equalled or exceeded the Abbreviated Injury Scale (AIS) injury rating of 3 (severe).

Following this initial selection process, the cases satisfying the stated requirements were reviewed in detail, and a number of cases were excluded for a variety of reasons, e.g.,

(1) complex vehicle dynamics, such as multiple vehicle collisions

(2) complications in simulating occupant responses, such as an unknown initial position and orientation of the occupant in the vehicle.

Pertinent data on these cases are summarized in Table 3.2.1 of the next section. Note in that table the fairly even distribution of specific injuries (i.e., head, face, and brain), as well as overall injury, which was obtained by relaxing the crash victim height and weight requirements.

3.1.2 SMAC Program

3.1.2.1 Summary

Detailed documentation and validation of the SMAC program has been reported in the literature (References 1, 2, and 3). Therefore, only a summary of the approach and assumptions are presented here for the unfamiliar reader.

For the purpose of approximating trajectories preceding and following collisions, the vehicle representation is limited to the three degrees of freedom associated with plane motions. The "friction circle" concept (Reference 18) is used to approximate interactions between circumferential forces (i.e., braking or tractive) and side forces of the tires. The cornering stiffnesses of the individual tires are entered separately to permit simulation of damaged tires. A vehicle tread dimension is included to provide realistic effects of individual tire forces (e.g., locked wheels or flat tires) on yaw behavior and to permit detailed transitions across a boundary defining terrain zones with different friction coefficients.

Tabular inputs, as functions of time, are used for individual wheel torques and for steer angles of the individual front wheels and the rear axle (i.e., control inputs and/or effects of damage). Provision is included for a linear decrement of the effective tire-ground friction coefficient with speed.

Predictions of tire tracks and skid marks are generated as a part of the output information.

The original (undeformed) boundaries of the vehicles are defined in the form of rectangles. Discrete points defining the body outlines in contacted regions are generated and displaced during the impact calculations. These points serve to define the deformed boundaries. The distance between a displaced point and the initial boundary of the deflected surface is used to determine the dynamic pressure at that point during any time increment in which the point is displaced. An iterative procedure is used to achieve equal pressures from the two mutually deformed bodies.

The specific analytical assumptions employed in treatment of car-to-car collisions are:

(1) The vehicles are treated as rigid bodies surrounded by a layer of isotropic, homogeneous material that exhibits elastic-plastic behavior.

(2) The dynamic pressure in the peripheral layer increases linearly with the depth of penetration relative to the initial boundary of the deflected surface.

(3) The adjustable, nonlinear coefficient of restitution varies as a function of maximum deflection.

(4) Plane motion is assumed. The effects of pitch and roll are neglected.

A post-processing routine for interpretation of damage predictions in terms of a standard collision deformation classification, or "vehicle damage index" (VDI), based on SAE J224a is also included in the program.

3.1.2.2 SMAC Program Input

Input requirements for the SMAC program fall into four general categories:

(1) Vehicle properties (excluding structural properties),

(2) Vehicle structural (crush) properties,

(3) Control inputs (steer, braking), and

(4) Initial conditions.

The first category, vehicle properties, includes dimensional, inertial and tire cornering stiffness data. Values used for these program inputs were the best available data obtained from the accident case reports, typical or average data compiled in Reference 1, or from empirical relationships given in Reference 19.

The vehicle crush properties used in reconstruction of the ten selected cases were also obtained from Reference 1, with the exception of those cases where the collision occurred with narrow obstacles. While the value of 50 lb/in^2 used to represent the crushable layer has been shown to be adequate for wide area engagements of the vehicle structure, data from Reference 20 indicate that the effective stiffness per unit engagement area increases for narrow obstacles. Appendix C documents a derivation of the narrow obstacle crush characteristic for a sample case from this study using the data reported in Reference 20.

The control inputs and initial conditions used in this study were based on the individual accident cases as reported and are described in Section 3.3.

3.1.3 3-D Crash Victim Simulation Program

3.1.3.1 Summary

Development and validation of the Three-Dimensional Crash Victim Simulation computer program has been described in some detail in the literature, References 4-6. Consequently, only features of this program that are pertinent to the present study are summarized in this section.

The crash victim simulation program, Reference 4, is a fifteen-segment model of the human body, plus a model of the crash environment, in three dimensions. The simulated victim responds to crash decelerations through forces produced by vehicle contact surfaces, inflatable and belt restraints, and contacts between body segments.

Program input consists of the crash victim properties (dimensional and inertial data and joint torque characteristics), the vehicle deceleration time history, material (force-deflection) and geometrical properties of the contact surfaces and restraints, plus a matrix of allowed contacts between the victim and the crash environment. Sample input data are summarized in Table B-1 of Appendix B. To simplify preparation of input data sets, a preprocesser program,* References 16 and 17, was developed to calculate dimensional and inertial properties of the human body from inputs of sex, height, and weight of the victim.

*"GOOD" Program - Generator Of Occupant Data, developed under the sponsorship of the Motor Vehicle Manufacturers Association.

Output from the crash victim simulation includes tabular time histories of segment linear and angular accelerations, velocities, and displacements, joint motions and torques, contact forces and associated deformations, and restraint system forces and related restraint data. In addition, printer plot displays of selected time histories and crash victim kinematics are produced as part of the printed output.

Post processer options include a plotter graphics display and an injury criteria routine, which computes head and chest severity indices and the HIC (head injury criterion) number.

This crash victim simulator, together with its preprocesser input data generator and the post processing options, was found to be naturally suited to analytical reconstruction of the responses of the crash victim in this study.

3.1.3.2 Program Input

Inputs to the 3-D Crash Victim Simulation computer program for these analytical reconstructions were as follows:

(1) Crash victim inputs, in most cases, were based on measurements on a Sierra 292-1050 (50th percentile male) dummy, reported in References 4, 6. To study the effect of occupant size, dimensional and inertial inputs for a small female occupant in one of the cases were generated using the "GOOD" program previously mentioned. Effect of occupant size on crash responses is discussed in some detail in connection with Case No. CB71055.

(2) Vehicle deceleration inputs were obtained as tabular acceleration time histories from the SMAC program, as previously discussed. In addition, the vehicle yaw time history obtained from the SMAC program was used to assign an effective direction to the unidirectional* deceleration history inputted to the crash victim simulation by selecting a mean value of yaw from the plotted yaw time history. (This value differed at most by only a few degrees from the value of yaw corresponding to the peak resultant acceleration.)

(3) Plane inputs (vehicle interior geometry) were obtained from measurements on vehicles closely corresponding to the case vehicles.

(4) Function inputs (material properties of contact surfaces) were typical values, based upon available experimental data.

As an example, consider the inputted windshield force-deflection characteristic, illustrated in Figure 3.1.2, which is based upon typical test results from a conventional HPR windshield at a 30 MPH impact speed.** Following glass fracture at $\sim$ 0.5 in. deflection with a resulting "inertial" spike, the plastic interlayer bulges at a reduced force level. The effect of the windshield failure on resultant head acceleration that is predicted in the simulation is illustrated by the typical result shown in Figure 3.1.3.

---

* Nonrotating vehicle deceleration histories were inputted to the program to correspond to unidirectional decelerations in the subsequent impact sled tests.

** Published windshield impact data are not sufficiently detailed to define such a characteristic as a function of impact speed.

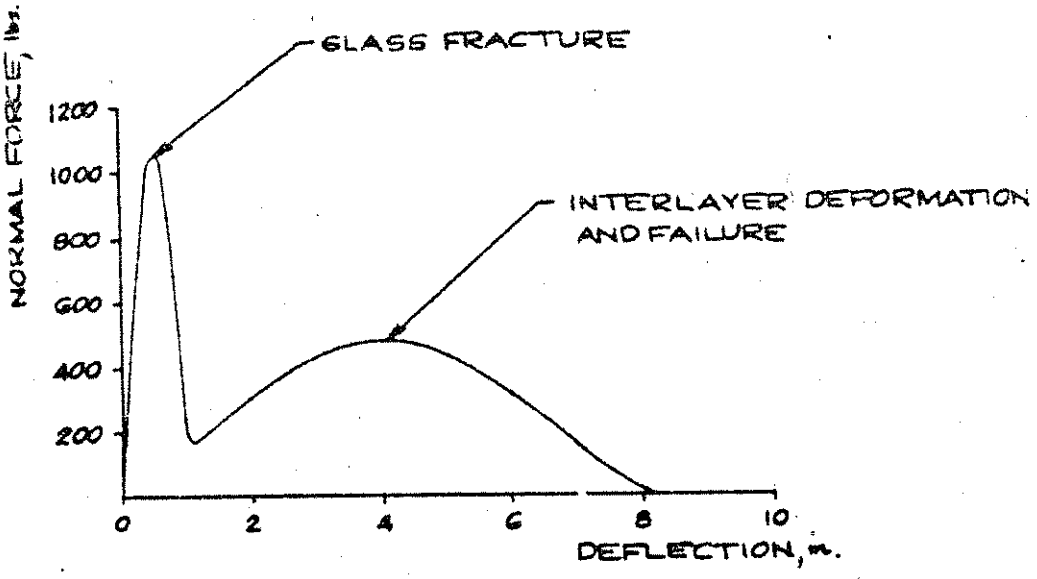

Figure 3.1.2 WINDSHIELD FAILURE CHARACTERISTIC

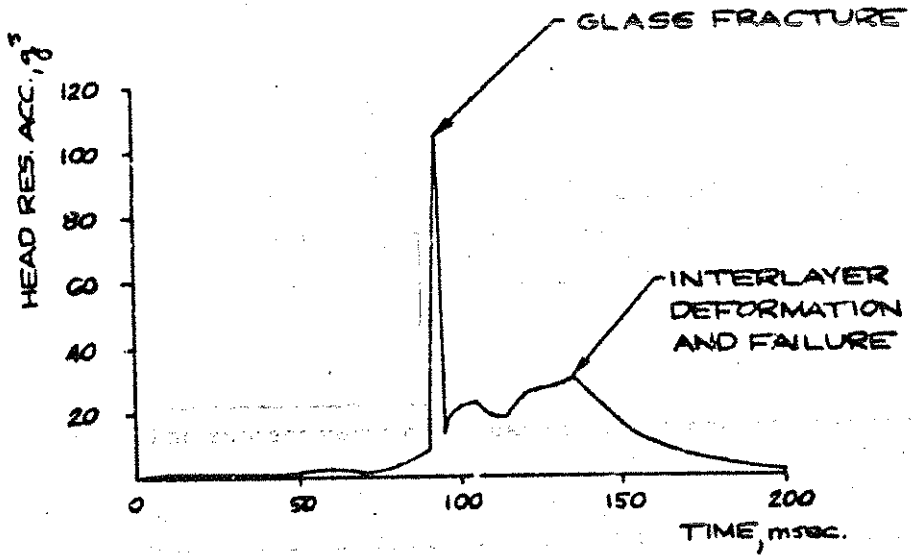

Figure 3.1.3 TYPICAL PREDICTED HEAD ACCELERATION RESPONSE

The predicted response is similar in form and magnitude to that experimentally observed, for example, References 9, 11.

(5) Allowed contacts were based upon anticipated occupant responses during crash.

(6) Initial body positions (initial position and orientation of the crash victim) were based in most cases upon a relaxed seated posture consistent with the vehicle interior geometry. To study the effect of an active response by the occupant to the anticipated collision, crash victim inputs corresponding to a rigid, braced position were used in Case No. AA00145, as will be subsequently discussed.

3.1.4 Impact Sled Tests

3.1.4.1 Summary

The ten accident cases were physically reconstructed on the Calspan HYGE impact sled, using an automobile body buck fabricated from a 1969 Ford Torino sedan*, Figure 3.1.4, to represent the ten subject vehicles. To insure adequate structural strength for the more severe crash conditions (41 MPH predicted maximum speed change, 32 g predicted peak resultant acceleration), the buck was reinforced with steel plates and struts as shown in Figure 3.1.4. The buck was mounted on the sled by means of a circular turn table or jig containing mounting

*The subject vehicle in a case that was originally anticipated to be one of the ten final selected accident cases was a 1969 Ford Torino sedan. That case was later excluded because of the complexity of the multiple vehicle dynamics in the accident. The 1969 Ford Torino buck, however, was considered to be a representative vehicle interior for the ten cases.

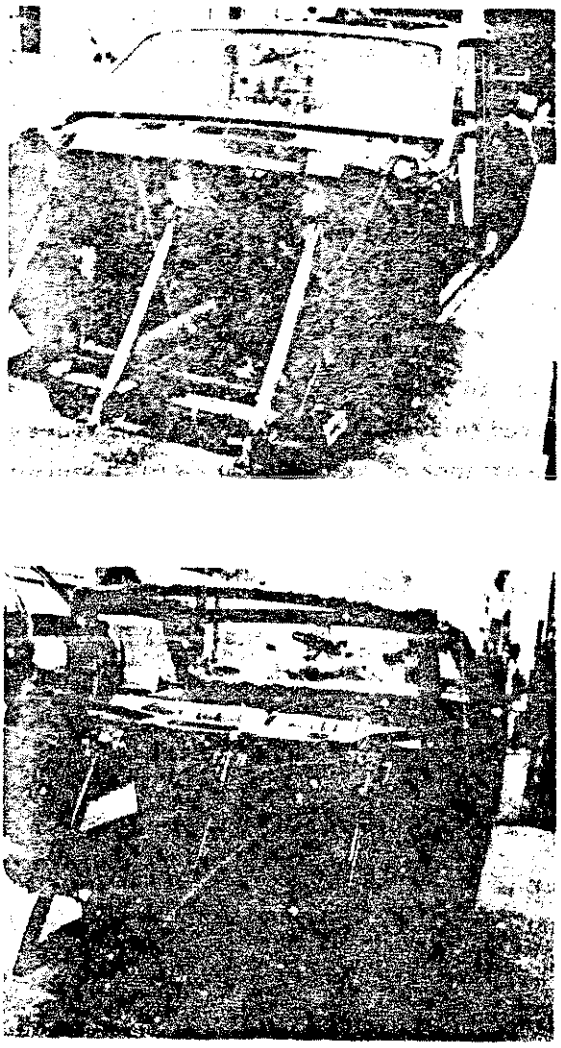

Figure 3.1.4 BODY BUCK FOR IMPACT SLED TESTS

holes spaced at 2 degree angular increments. This jig, Figure 1.3, provides a rapid means to set the desired buck rotation angle for each test.

The basic impact sled test schedule consisted of one test for each of the ten accident cases, plus three additional runs to vary parameters as follows:

- variation in stiffness of the dummy joints, to study the effect of muscular reaction by the crash victim in anticipation of collision

- variation in dummy size (5th percentile female, compared to 50th percentile male) to assess the importance of matching the crash victim stature and weight with that of the dummy

- variation in vehicle interior geometry (seat location relative to the windshield) to obtain an indication of the results of a mismatch between the occupant position and/or vehicle interior in the actual vehicle and that in the reconstruction sled test.

For each run in this series, the sled test conditions were chosen to duplicate approximately the corresponding vehicle resultant deceleration history predicted by the SMAC program. Because of the limited scope of the experimental program, the required sled conditions were analytically estimated rather than determined through additional facility calibration. In attempting to duplicate the predicted deceleration history, emphasis was placed first on matching speed change, second on peak deceleration, and third on acceleration waveform. In addition, the predicted vehicle yaw time history was used to select an effective direction (turn table rotation angle) for the unidirectional sled pulse.

The different interiors of the ten accident vehicles were approximated in the test mock-up by varying the seat types (two different split bench seats and one bucket seat), and by varying seat position relative to the windshield location, which was fixed in the buck/sled reference. In addition, the instrument panel location was altered slightly for some tests to match the geometry of the subject vehicle interiors more closely.

Any damage to the instrument panels and seats was repaired after each test to restore the original geometry and material properties of the interior as much as possible. After each test in which windshield failure occurred, the glass was replaced from a supply of duplicate HPR windshields (standard replacements for the 1969 Ford sedan). Care was taken to match the windshield installation procedure as closely as possible for each run.*

For tests involving lap belt restraint, standard nylon webbing was used to fabricate the belts.

In all of the sled tests except one, an HSRI 50th percentile male crash test dummy** was used to simulate the crash victim. In one test a 5th percentile female (Sierra 592-805) crash test dummy was used to study the effect of dummy size. Both dummies were clothed for testing, and except as otherwise noted, dummy joints were set at a nominal "1g" torque adjustment.

The initial position and orientation of the dummy for each test were selected to match the corresponding geometry of the computer simulation as closely as possible. An exact match could not be accomplished,

* The windshields were secured with 3-M brand Windo-Weld Ribbon Sealer Auto Glass Replacement Kits (3/8 in. size), using procedures routinely followed by the Calspan impact sled crew for windshield installations.

** HSRI 50th percentile male crash test dummy (no serial or identification number), provided by Mr. Stanley Backaitis of NHTSA.

however, for several reasons. As an example, the stiff rubber neck of the HSRI dummy prevented adjusting the dummy head position after the torso position and orientation were fixed. Comparisons of initial conditions between the computer simulations and the corresponding sled tests can be made by referring to Sections 3.3 and 3.4,* respectively.

Sled instrumentation conforming to MVSS 208 provided the following time history records on magnetic tape:

- sled acceleration
- dummy head and chest accelerations (x, y, and z components and resultant)
- dummy head and chest severity indices (based on resultant accelerations
- dummy femur loads
- restraint belt loop load (where applicable), measured with a Lebow gauge.

In addition, two high-speed motion picture cameras and an eight-frame sequence camera mounted on the sled provided photographic coverage of the dummy responses.

*In some cases, the pre-test orientation of the dummy was altered slightly to conform more closely to the desired initial conditions immediately prior to the sled test. The first photograph in the sequence camera series shows that final pre-test orientation.

Following each test, the data channels were plotted on a direct-writing (Brush) recorder. No subsequent processing of the analog data was performed. Copies of some of these data traces are presented in Appendix D.

3.2 Summary of Analytical Results

A concise description of the ten highway accident cases is presented in the summary tabulation of Table 3.2.1. Items worth noting in the table are:

(1) the wide range of vehicle sizes

(2) vehicle frontal damage of varying degrees

(3) many accident types over a broad speed range

(4) differing occupant sizes

(5) minimal use of restraints (belts)

(6) varying types of head contacts

(7) assorted head injuries

(8) overall injury ratings rather evenly distributed from 1 (minor) to 6 (fatal) on the 10-point injury scale.

Table 3.2.1

SUMMARY OF TEN ACCIDENT CASES

CASE IDENTIFICATION NUMBER	VEHICLE	VEHICLE DAMAGE INDEX	ACCIDENT TYPE	CRASH VICTIM				RESTRAINTS[1]		HEAD CONTACTS	INJURIES	INJURY RATING (19-POINT CODE)			
				SEX	AGE YEARS	HEIGHT IN	WEIGHT LBS	LAP	SHOULDER			HEAD	FACE	BRAIN	OVERALL[2]
AA69146	1972 MERCURY COMET	12 FDLW 2	CAR-CAR FRONTAL 20 MPH/15 MPH*	M	19	70	150	1	0	HEAD INSTRUMENT PANEL	FACIAL ABRASIONS/ LACERATIONS	1	1		1 (MINOR)
TR01316	1968 CHEVROLET NOVA	12 FCEW 3	HEAD ON TREE 10-15 MPH	M	15	68	140	1	0	HEAD UPPER INSTRUMENT PANEL	CONCUSSION, FACIAL CONTUSION AND LACERATION		1	1	1
CA71831	1970 PLYMOUTH BARRACUDA	12 FCEW 7	OFF ROAD TREE FRONTAL 35 MPH	M	19	70	160	0	0	FACE INSTRUMENT PANEL (PROBABLE)	CONCUSSION, FACIAL CONTUSIONS		2	1	2 (MODERATE)
CB00872	1970 CHEVROLET CAMARO	12 FDEW 4	OFF ROAD TREE FRONTAL 35 MPH	M	18	71	165	0	0	HEAD SURVISOR, WIND SHIELD, INSTRUMENT PANEL	CONTUSIONS/ABRASIONS TO FOREHEAD AND CHIN		2		2
BR71F14	1965 FORD CUSTOM	12 FZEW 3	OFFSET FRONTAL PARKED CAR 30 MPH	M	18	71	160	0	0	FACE WINDSHIELD (BROKEN)	FACIAL LACERATION		2		2
CB00853	1970 CHEVROLET NOVA	12 FYEW 7	OFFSET FRONTAL 4 DR MPH	F	52	66	130	0	0	HEAD WINDSHIELD, KNEES INSTRUMENT PANEL	FACIAL ABRASIONS/ LACERATIONS, BROKEN TEETH	1	2	2	2 (SEVERE)
CS71886	1971 FORD MUSTANG	11 FLEE 2	OFFSET OBLIQUE FRONTAL 6 MPH/28 MPH	F	49	60	130	0	0	HEAD REAR VIEW MIRROR UPPER INSTRUMENT PANEL	FACIAL LACERATIONS, FRACTURED TEETH	1	2		2
TR01101	1968 AMERICAN AMX	12 FZEW 7	HEAD ON TREE 30 MPH	M	22	—[2]	—[2]	0	0	HEAD WINDSHIELD/HOOD	FACIAL LACERATIONS		2		2
GA87096	1968 PONTIAC LEMANS	12 FCEN 6	HEAD-ON TREE 50 MPH	M	16	—[2]	—[2]	0	0	HEAD INSTRUMENT PANEL	CONCUSSION	3	3	2	4 (SERIOUS)
TR00872	1965 FORD GALAXIE	12 FLEW 5	MULTIPLE CAR OFFSET FRONTAL-NO SPEED ESTIMATE	M	52	71	196	0	0	FACE WINDSHIELD (BROKEN)	FACIAL ABRASIONS/ LACERATIONS, SEVERE THORACIC INJURIES		1		6 (FATAL)

*SPEED ESTIMATES FROM CASE REPORTS

1 - 0 NO RESTRAINT, 1 RESTRAINT IN USE

2 - UNKNOWN

Briefly, these analytical reconstructions, when compared with the case reports, indicate:

(1) For nine of the ten cases, analytically reconstructed vehicle responses are in general agreement with on-site observations.

In the only remaining reconstructed vehicle response, discrepancies in the vehicle rest positions were believed to result from a secondary collision involving a third vehicle.

(2) In seven of the ten cases, the predicted responses of the occupant agree generally with evidence summarized in the accident case reports.

Discrepancies of occupant responses in the remaining three cases, considered to be attributable to active occupant responses in anticipation of the crash, are discussed in a subsequent section.

Comparisons of actual occupant injuries (as measured by overall injury severity on the 10-point scale) with values of predicted head injury indicators* (head severity index (HSI) and the head injury criterion (HIC)) are shown in Figures 3.2.1 and 3.2.2, respectively.

*Throughout this report, all values of head injury indicators are based upon the time from start of vehicle deceleration to the time at which significant loadings in rebound are applied to the crash victim.

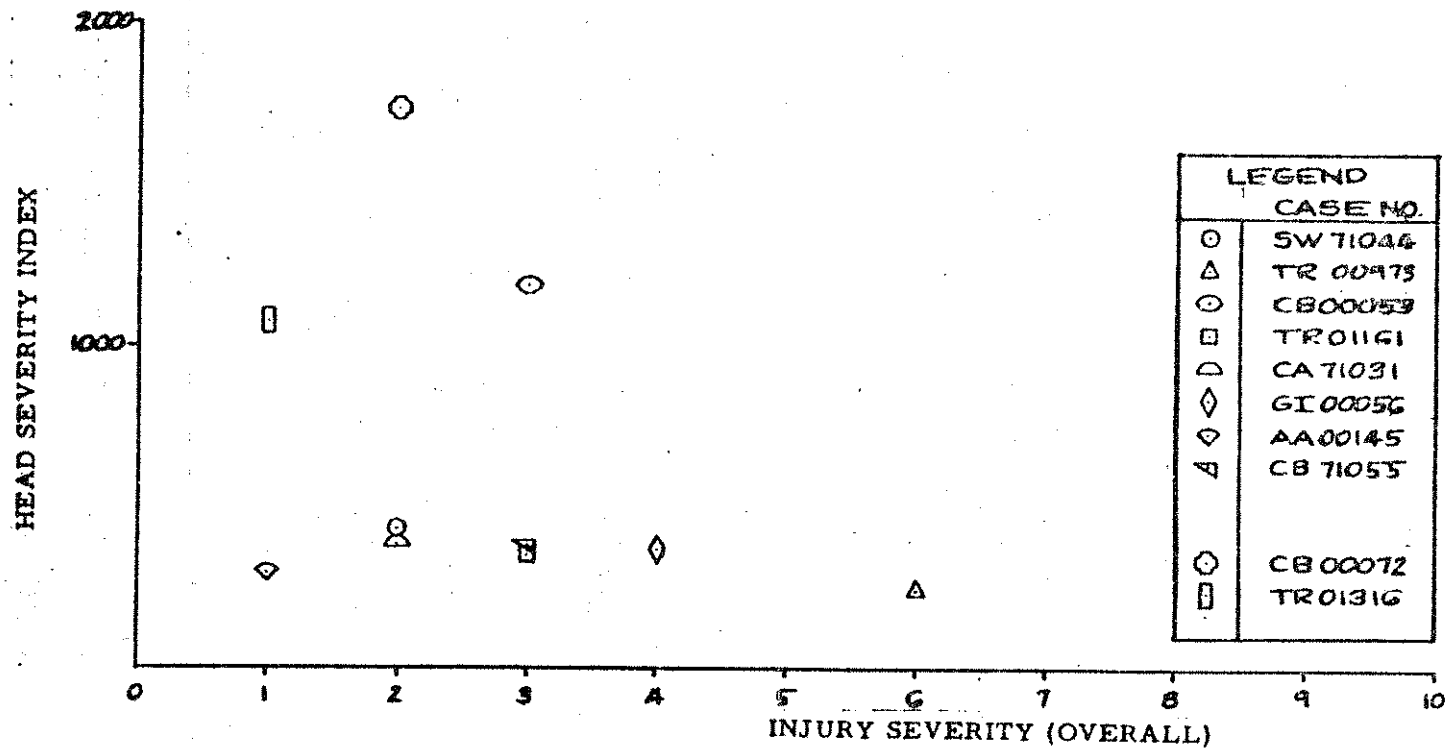

Figure 3.2.1 PREDICTED HEAD SEVERITY INDEX COMPARED TO ACTUAL INJURY SEVERITY

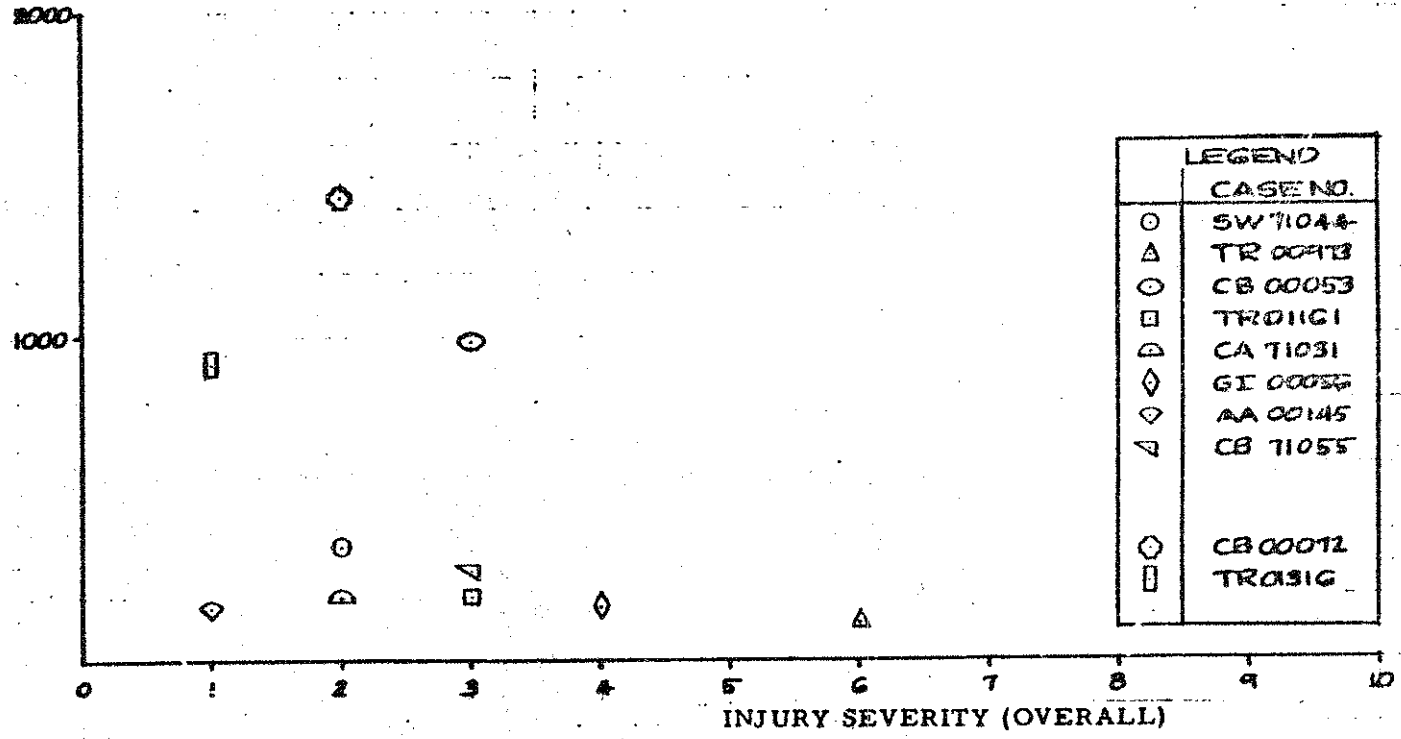

Figure 3.2.2 PREDICTED HEAD INJURY CRITERION COMPARED TO ACTUAL INJURY SEVERITY

Points to note in these comparisons are:

(1) No significant correlation is indicated between overall injury severity and either HSI or HIC.

No significantly better correlation occurs if specific (head, face, or brain) injury severity is used rather than overall* injury severity (see Table 3.2.1).

(2) Most of the HSI or HIC numbers cluster near constant values of 400 and 300, respectively.

This is a result of the assigned force-deflection characteristic for the windshield, Figure 3.1.2. In most occupant simulations the peak head resultant acceleration, Figure 3.1.3, was essentially a function only of the peak force of the inputted force-deflection characteristic. Consequently, in these cases, the predicted HSI and HIC values varied only slightly. In the other cases, contact loadings on other surfaces produced the observed variations in predicted HSI and HIC values.

In Figures 3.2.3 and 3.2.4, those predicted head injury indicators, HSI and HIC, respectively, are compared to envelopes of experimental results from windshield impact tests that were previously discussed (see Figures 1.1 and 1.2).

*Only overall injury severity was listed for all ten cases in the accident reports.

LEGEND - SEE FIG. 3.2.1

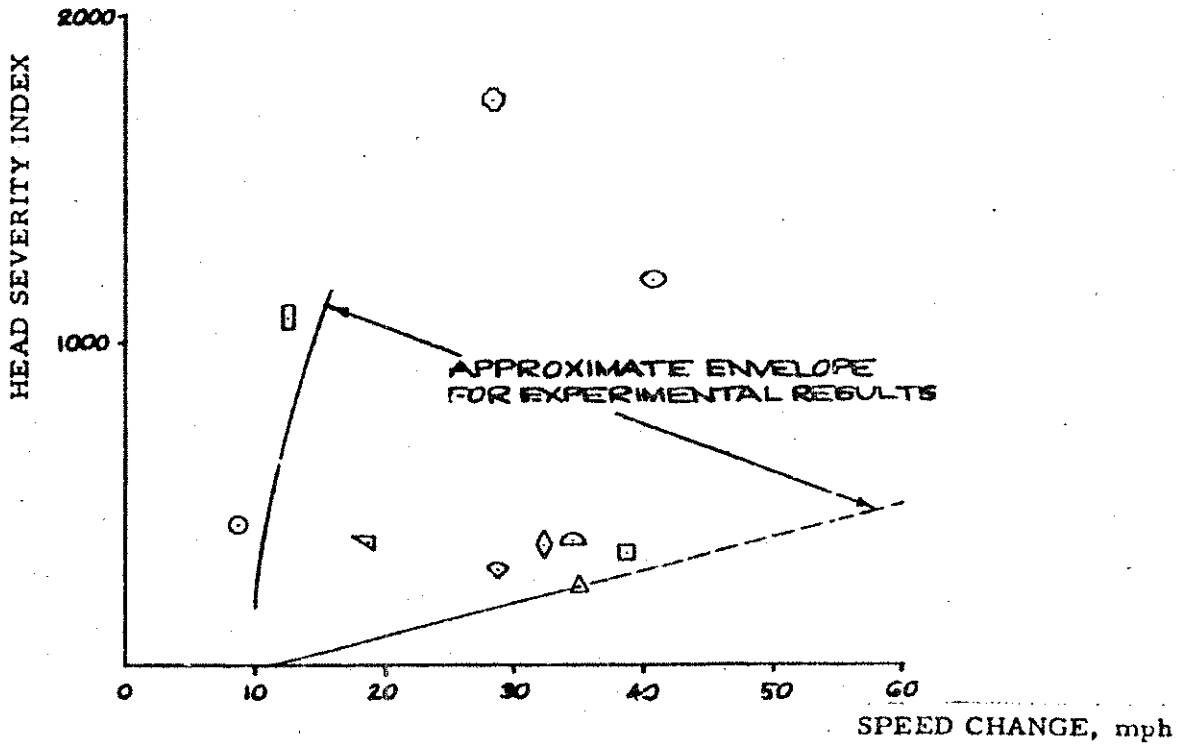

Figure 3.2.3 PREDICTED HEAD SEVERITY INDEX COMPARED TO WINDSHIELD TEST DATA

LEGEND - SEE FIG. 3.2.2

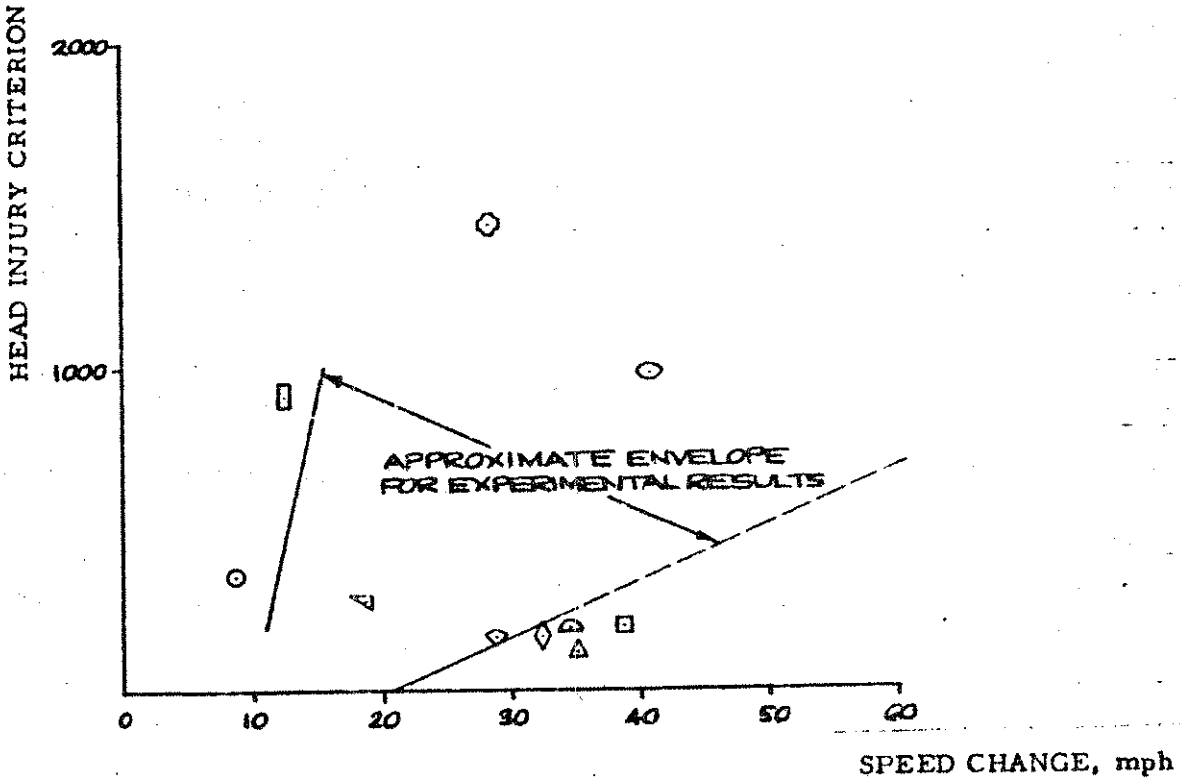

Figure 3.2.4 PREDICTED HEAD INJURY CRITERION COMPARED TO WINDSHIELD TEST DATA

It should be noted that, in the literature surveyed, both HSI and HIC are plotted versus impact speed, which is essentially equal to the speed change in the reported tests (see Figures 1.1 and 1.2). In Figures 3.2.3 and 3.2.4, however, speed change is used as the abscissa. This is because speed change, not impact speed, is the more meaningful parameter for collisions between two vehicles (see Figure S-1).

From Figures 3.2.3 and 3.2.4, it is noted that:

(1) No significant correlation is indicated between speed and either HSI or HIC.

(2) The predicted results fall largely within the envelope of experimental results.*

*Some cases did not involve head-windshield contact (observed and/or simulated) and therefore should not be included in the plots of Figures 3.2.3 and 3.2.4 in the strictest sense. Data from all ten cases were included, however, for the sake of uniformity.

3.3 Analytical Reconstruction of Ten Accident Cases

3.3.1 Summary

In this section, the analytical reconstructions of each of the ten accident cases are discussed in some detail, with primary emphasis placed on the observations of the accident case report and corresponding reconstruction of the vehicular collision. The analytical reconstruction of occupant responses is also discussed, but additional details are presented in Section 3.5, in which the impact sled test results are compared to the corresponding analytical predictions of the occupant responses.

3.3.2 Detailed Discussion of the Ten Accident Cases

CASE NO. AA145 (Case Identification No. AA00145)

1. Case Report Summary

Primary Vehicle - 1972 Mercury Comet
Secondary Vehicle - 1957 Chevrolet station wagon

1.1 Description of Accident

Pre-crash:

The driver of the secondary vehicle had just previously been involved in a rear-end collision immediately south of the site of the subject case. He had been drinking heavily and was apparently confused after the first collision. After leaving the scene of that accident, he drove north in the opposing lane. The driver of the primary vehicle braked when he saw the secondary vehicle approaching him in his lane. The case report schematic is shown in Figure 3.3.1.

Crash:

The vehicles collided very nearly head-on with approximately 90% overlap of the front ends. The impact speeds were estimated at 25 MPH for the primary vehicle and 15 MPH for the secondary vehicle.

Post-crash:

There was little or no motion after impact. The investigator-determined VDI's were 12FDEW3 for the Comet and 12FDEW2 for the Chevrolet.

Figure 3.3.1

Accident Schematic - Case No. AA145

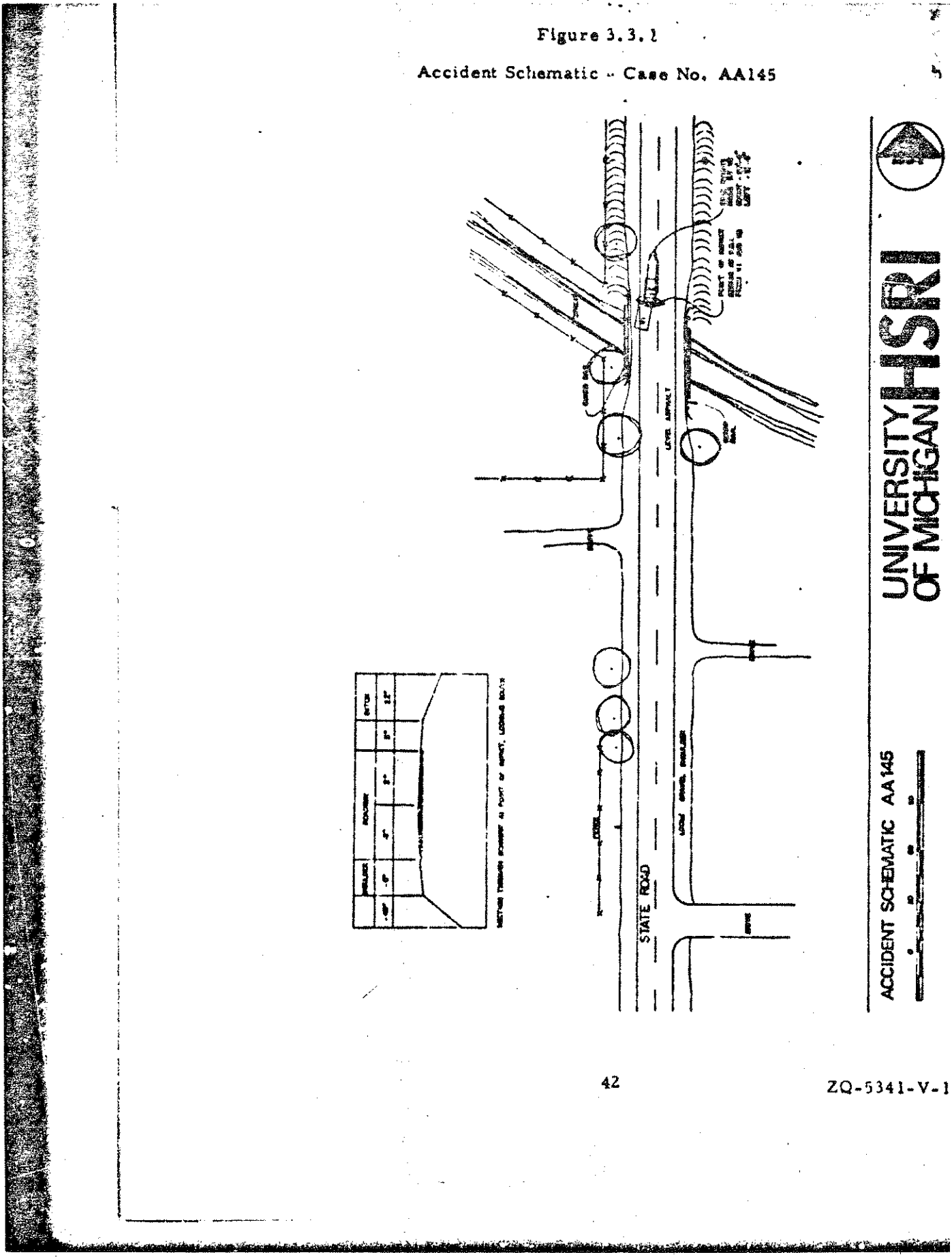

1.2 Primary Vehicle Right Front Occupant

19 year old male, 5'10" tall, 150 lbs.

This occupant was loosely wearing a lap belt. On impact he was thrown forward striking his head on the instrument panel. He suffered lacerations to the chin and lower lip, minor abrasions from the seat belt webbing and other minor injuries. He complained of soreness to the neck and pain in the lumbar region of the spine. Injury rating: Minor, AIS-1.

2. Analytical Reconstructions

2.1 SMAC Reconstruction

The input parameters used in the final reconstruction run of this case are shown in Table A-2.1. With these values, excellent agreement with the physical evidence was obtained with the SMAC program. It should be noted that the speed listed for the subject vehicle, the 1972 Comet, is the pre-braking speed. The application of locked wheel braking to produce the measured skidmarks resulted in an impact speed of 26.2 MPH for the Comet and 17 MPH for the Chevrolet.

The predicted VDI's match those measured identically, being 12FDEW3 for the Comet and 12FDEW2 for the Chevrolet.

The resultant acceleration and angle for the case vehicle and the damage patterns for both vehicles are shown in Figure 3.3.2. The reconstruction summary is presented in Figure 3.3.3.

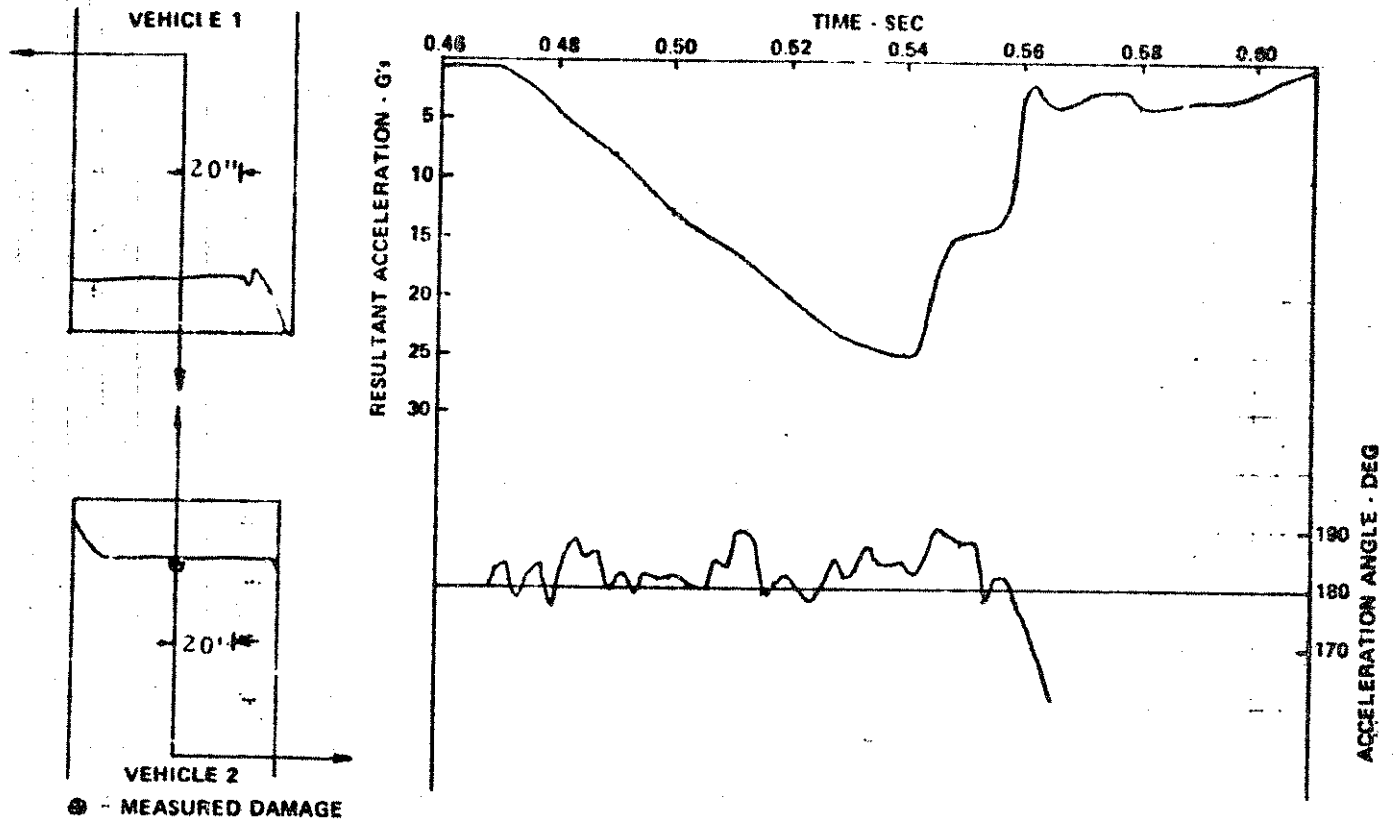

Figure 3.3.2 - ACCELERATION AND DAMAGE - CASE NO. AA145

Figure 3.3.3

Accident Reconstruction Summary - Case No. AA145

GRAPHIC DISPLAY OF OUTPUTS OF ACCIDENT RECONSTRUCTION

COLLISION AND TRAJECTORY

CASE NO. AA 145 RUN NO. AA0145

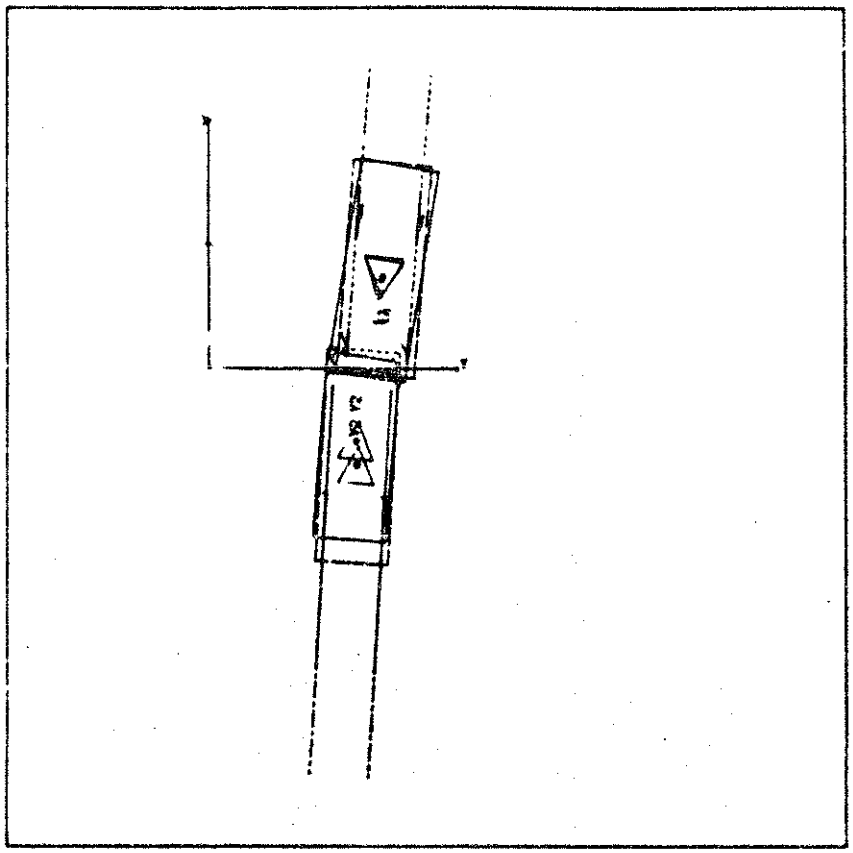

AXIS INTERVALS ARE 10. FEET

RECONSTRUCTED POSITIONS AND VELOCITIES AT IMPACT							DISPLAYED FINAL POSITIONS				VEHICLE DAMAGE INDICES	ΔV
	C.G. POSITION		HEADING				C.G. POSITION		HEADING	REMARKS		
	XC1	YC1	PSI1	FMB	LATERAL	ANGULAR	XC1F	YC1F	PSI1F			
	FT.	FT.	DEG.	MPH	MPH	DEG/SEC	FT.	FT.	DEG.			MPH
VEHICLE # 1	7.5	14.0	185.0	17.0	0.0	0.0	7.2	13.6	188.7	VEHICLE AT REST	12FLEW2	21.6
VEHICLE # 2	-7.7	11.0	5.5	28.9	0.0	0.0	-5.6	11.0	4.6	VEHICLE AT REST	12FREW3	28.7

In Figure 3.3.4, the predicted kinematic responses of the right front occupant are compared to a concise description of actual contacts and injuries sustained by the crash victim, as obtained from the case report. Note from the figure that in the accident, the occupant struck the instrument panel, resulting in facial abrasions and lacerations. In contrast, the simulation predicts head contact with the windshield for the computer run in which a normal seated posture and a relaxed muscular condition were inputted (labeled "PASSIVE RESPONSE" in Figure 3.3.4). It is rather apparent from Figure 3.3.4 that for a broad range of near-frontal vehicle crash conditions, head contact with the windshield would likely occur unless the occupant braced against the vehicle interior in anticipation of crash. To illustrate this point, the simulation was repeated, with the initial occupant orientation altered to represent a braced position (see "ACTIVE RESPONSE" in Figure 3.3.4), with the coulomb component of joint torque at the elbows and shoulders increased by a factor of 10* to simulate muscular flexure in response to the impending crash. The marked effect on crash victim kinematics is apparent from the plotter graphics displays of Figure 3.3.4. Note that the two predicted responses tend to bracket the actual victim responses reported in the accident investigation. No attempt was made to obtain a closer correspondence of predicted and observed results through a "tuning" process, however.

It is apparent that a degree of uncertainty exists in the initial orientation, position, and condition of muscular flexure of the crash victim. This degree of uncertainty is naturally reflected as a range of tolerance in reliability of the predicted results.

*A value approximately corresponding to the maximum static muscular strength of the human arm that is reported in the literature.

Crash Victim -

Male
19 Years
70 in.
150 lbs.

Lap Belt In Use

Accident -

Head struck instrument panel - facial abrasions/ lacerations

Injury Rating -

Head - 1 (Minor)
Face - 1
Overall - 1

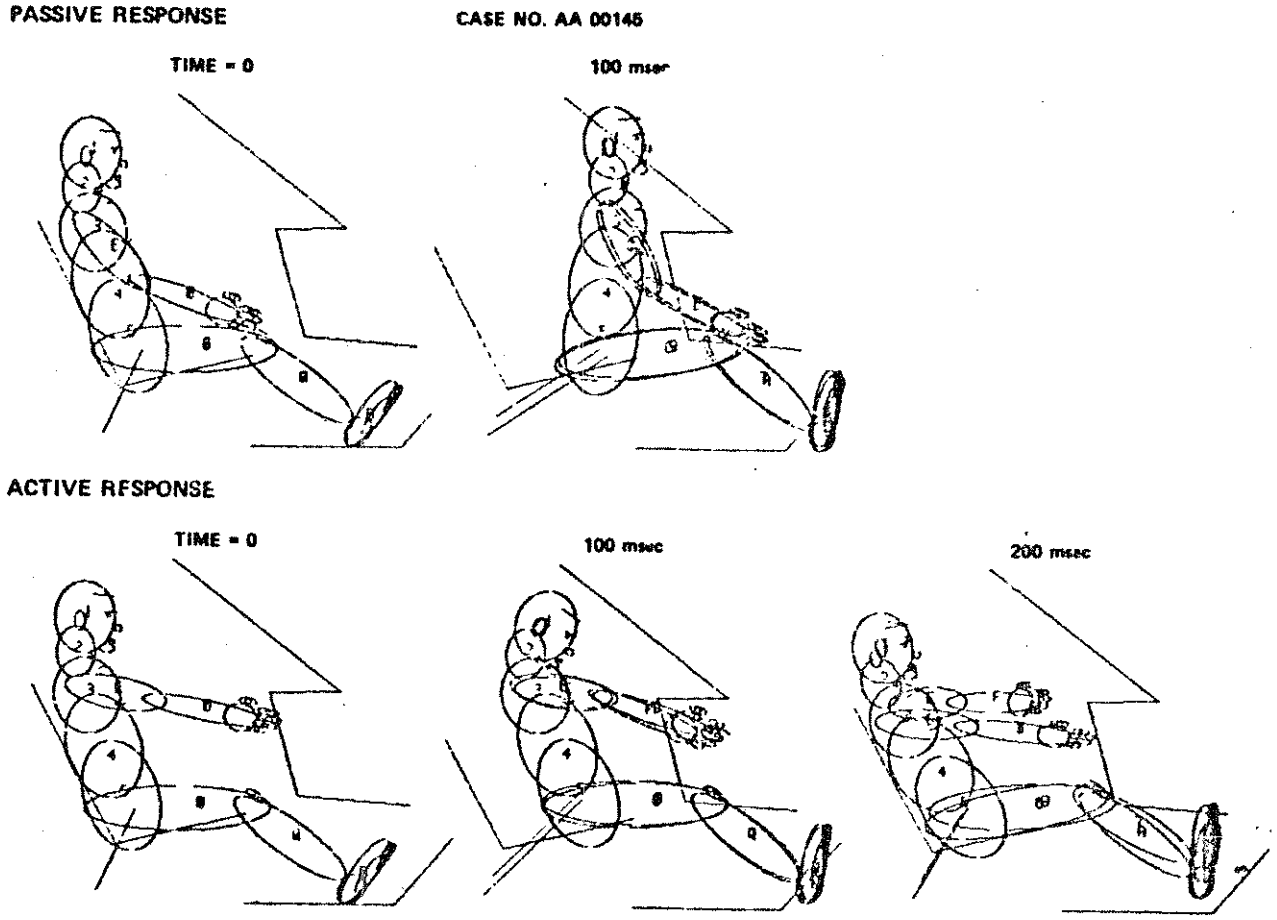

Figure 3.3.4
Accident Reconstruction Summary -
Case No. AA145

CASE NO. 1316D (Case Identification No. TR01316)

1. Case Report Summary

Primary Vehicle - 1969 Chevrolet Nova
Secondary Vehicle - None

1.1 Description of Accident

Pre-crash:

The Nova was proceeding along a dirt road at 35-45 MPH. The driver negotiated several curves and found himself on the left edge of the road. He steered to the right, crossed the road, and then counter-steered to avoid a utility pole. The counter-steer was excessive and the vehicle ran off the road to the left. The driver locked the wheels leaving about 32 ft. of skidmarks leading up to impact with a fruit tree. The accident scene schematic is shown in Figure S-2.

Crash:

The vehicle was traveling at about 10-15 MPH when it struck the fruit tree head-on.

Post-crash:

The vehicle came to rest at its point of impact still against the fruit tree with no apparent rotation. The Vehicle Damage Index was 12FCEW3.

1.2 Primary Vehicle Right Front Occupant

15 year old male, 68" tall, 150 lbs.

This occupant was restrained by a lap belt, and on impact moved forward striking his knees on the lower instrument panel. His torso continued forward with his head and chest striking the instrument panel. Injuries sustained included concussion, facial contusion and laceration, pain to chest and abdomen. Severity was rated as Minor, AIS-1.

2. Analytical Reconstructions

2.1 SMAC Reconstruction

The inputs used for the SMAC reconstruction of this case are shown in Table A-2.2. The measured VDI, 12FCEW3, and the predicted VDI, 12FCEW2, are in agreement with the exception of the last digit which is a measure of the extent of the permanent deformation. This difference is primarily attributed to a change in the procedure for coding this column of the VDI.

Since this was a purely longitudinal collision, the resultant and longitudinal accelerations are identical and are shown with the vehicle damage pattern in Figure 3.3.5. The reconstruction summary is shown in Figure S-3.

2.2 3-D Crash Victim Reconstruction

This analytical reconstruction, excerpted from an earlier study at Calspan, Reference 7, used a crash victim input description based largely on the measured properties of a GM Hybrid II dummy, and supplemented with more extensive Calspan measurements on a Sierra 292-1050 dummy. The plotter graphics displays of Figure S-4 (compared to Figure 3.3.4) reflect some of the differences in computer program inputs.

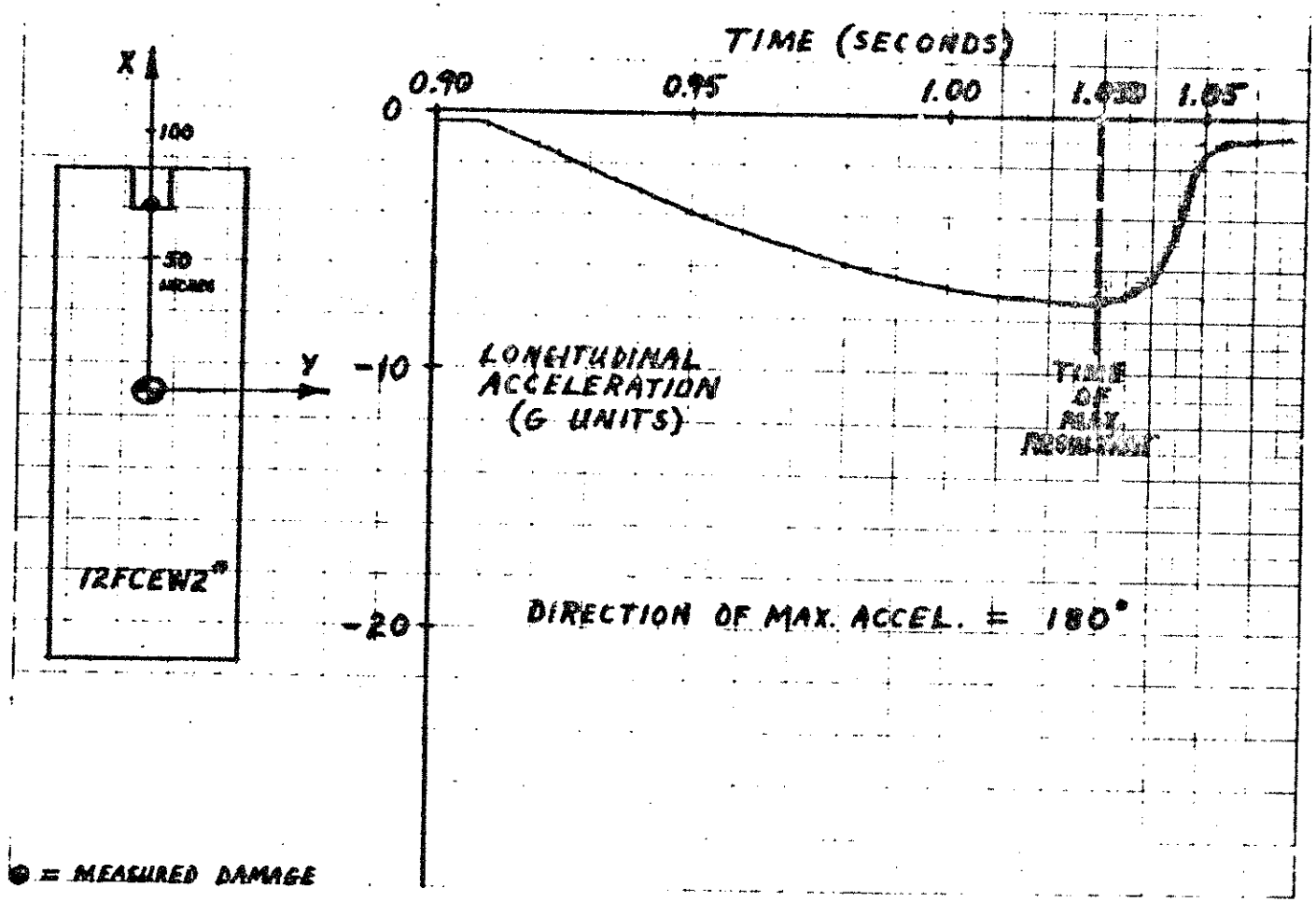

Figure 3.3.5

Acceleration and Damage
Case No. 1316D

In this case, the predicted kinematic responses of the right front occupant, Figure S-4, are essentially identical to the observations summarized in the accident case report. The slightly nonplanar predicted kinematic response of the occupant in this frontal crash case is a result of the nonsymmetrical restraint belt geometry. Figure S-4 graphically illustrates the potential of the analytical reconstruction technique.

CASE NO. 71-31A (Case Identification No. CA71031)

1. Case Report Summary

Primary Vehicle - 1970 Plymouth Barracuda
Secondary Vehicle - None

1.1 Description of Accident

Pre-crash:

The case vehicle was traveling westbound on a two lane rural roadway. The roadway was wet and visibility was obscured by rain and fog. As the vehicle entered into a shallow right curve, the driver turned the vehicle sharply to the right and the vehicle left the roadway at the north edge.

Crash:

The center front of the vehicle struck a tree located near the roadway. At impact, both doors opened but the occupants remained in the vehicle. The estimated impact speed was 35 MPH and the VDI was 12FCEW7.

Post-crash:

The vehicle rotated clockwise slightly and came to rest against the tree. The case report schematic is shown in Figure 3.3.6.

Figure 3.3.6

Accident Schematic - Case No. 71-31A

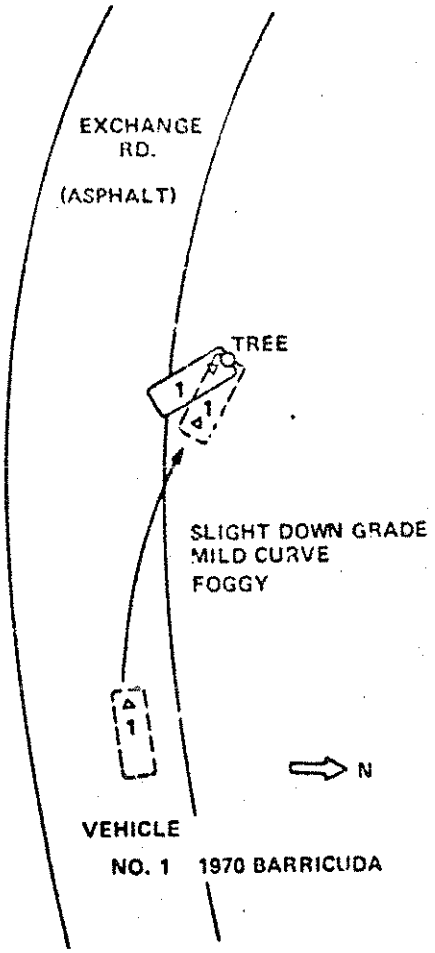

1.2 Primary Vehicle Right Front Occupant

19 year old male, 5'10" tall, 180 lbs.

This occupant was not wearing available restraint belts. On impact, he moved forward, striking the instrument panel and components located below the instrument panel suffering severe facial contusions and injuries to the extremities. Injury rating: Moderate, AIS No. 02.

2. Analytical Reconstructions

2.1 SMAC Reconstruction

The SMAC input parameters used in the final iteration in reconstructing this case are illustrated in Table A-2.3. It should be noted that the value for the load-deflection characteristic of the vehicle structure of 73.8 lb/in^2 was calculated based on data accumulated on vehicle impacts with narrow rigid obstacles. The calculation is shown in Appendix C

With this value of structural stiffness, an impact velocity of 35 MPH produced excellent agreement with the measured maximum deformation. The VDI comparison, 12FCEW7 measured and 12FCEW4 predicted, also agrees, with the exception of the extent of damage, which reflects a change in coding procedure.

The predicted vehicle yaw during impact was only 0.55 degrees. No value is given in the case report but the accident schematic appears to indicate 5 to 10 degrees of yaw. In view of the fact that the roadway was wet, values of tire-ground friction coefficient of 0.6 and 0.3 were tried with no significant differences in vehicle yaw. The case report indicates that the driver veered sharply off the roadway and therefore the vehicle may have had an initial angular and lateral velocity at impact. This would tend to increase the clockwise yaw of the vehicle. Unfortunately, the case

.eport is not detailed enough to make any ertimate of these velocities, so they were assumed to be zero in the predictions.

The resultant acceleration and angle for the SMAC reconstruction are shown in Figure 3.3.7, and the reconstruction summary is shown in Figure 3.3.8.

2.2 3-D Crash Victim Reconstruction

The predicted crash victim responses are compared to a summary of reported crash results in Figure 3.3.9. For this case, the computer simulation predicted head contact with the windshield for the condition of passive response by the occupant (that is, normal seated posture with no bracing against the vehicle interior). The accident report, however, indicates no head-windshield contact, with head-instrument panel contact listed as probable. As with Case No. AA145, it appears that occupant bracing against the instrument panel would likely have produced the head-instrument panel contact. Although simulation of occupant bracing was not attempted* for this accident case, it is anticipated that such bracing would have resulted in reasonable agreement between computer prediction and actual crash victim kinematics. It is recognized that a degree of uncertainty of occupant position, orientation, and the state of muscular condition is inherent in the problem of accident reconstruction.

*Only the orientation of the legs (knees raised) was selected to correspond to some degree to the case report observation that head-windshield contact did not occur.

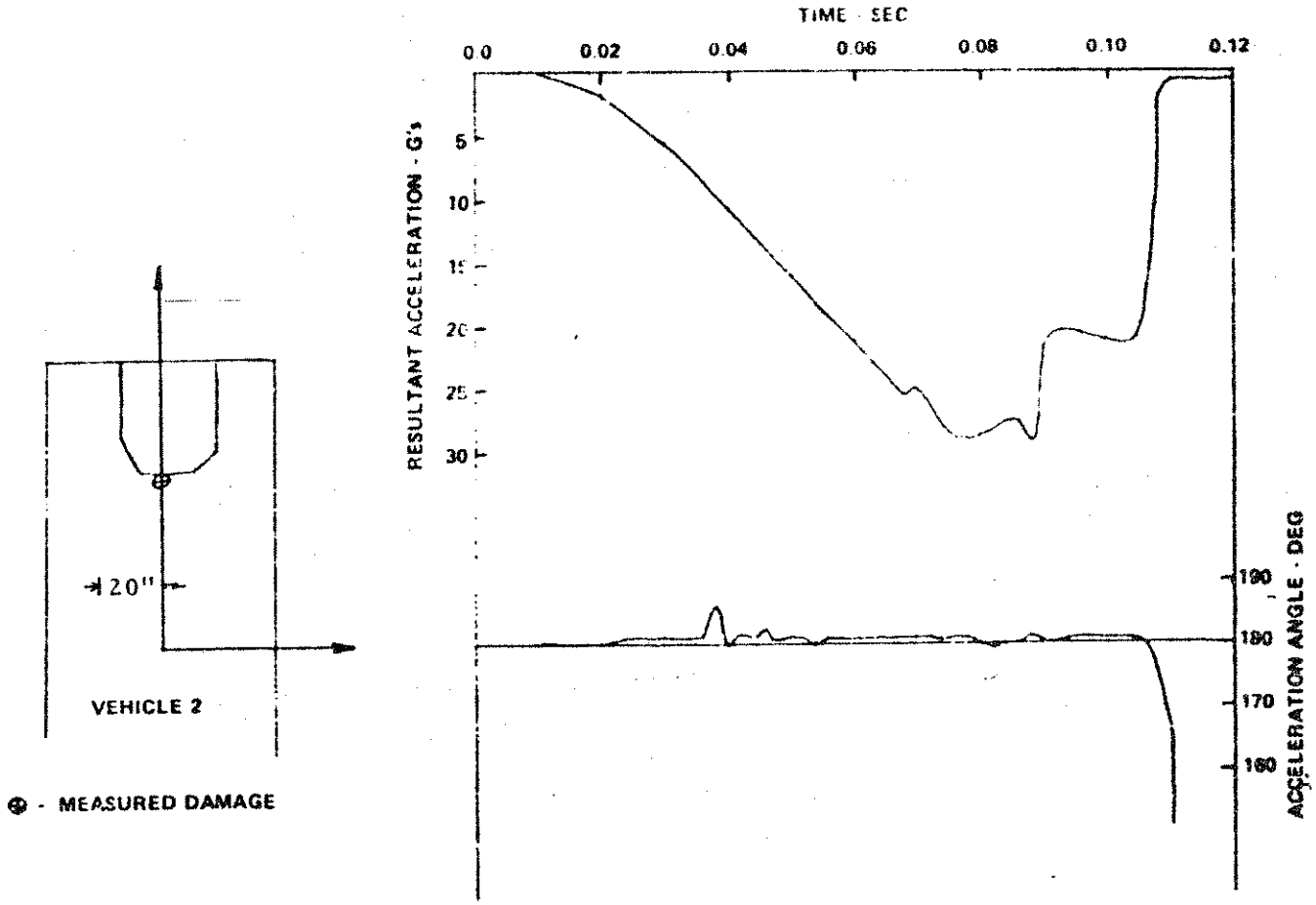

Figure 3.3.7 ACCELERATION AND DAMAGE - CASE NO. 71-31A

Figure 3.3.8

Accident Reconstruction Summary - Case No. 71-31A

GRAPHIC DISPLAY OF OUTPUTS OF ACCIDENT RECONSTRUCTION

COLLISION AND TRAJECTORY

CASE NO. 71-31A AGNY NO. 3471331

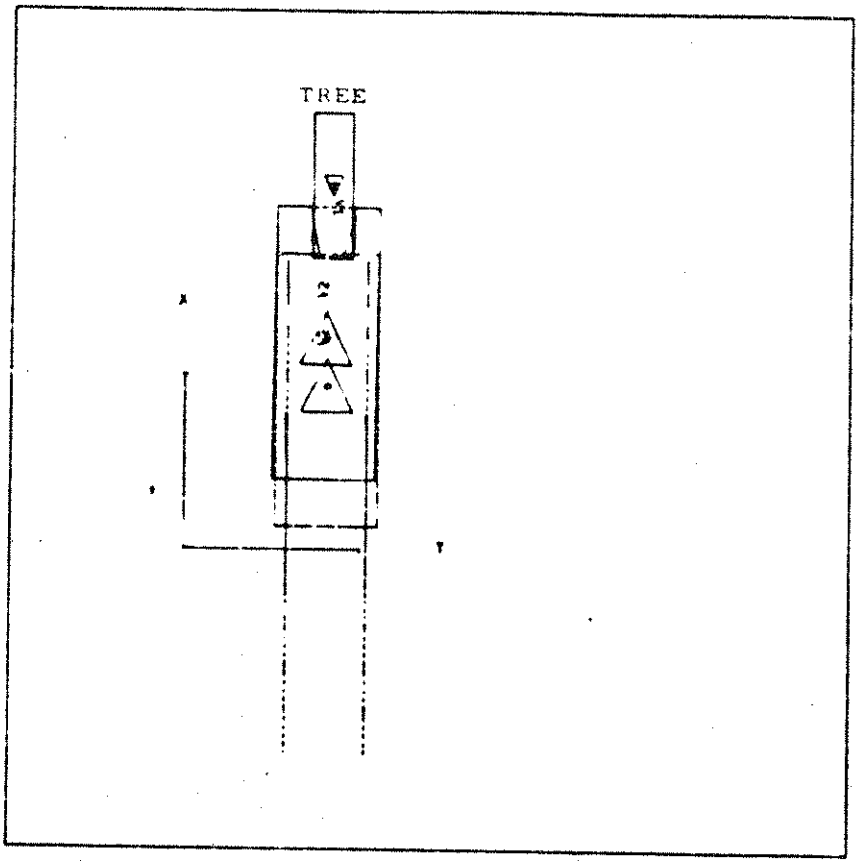

UNIT INTERVALS ARE 10. FEET

	RECONSTRUCTED POSITIONS AND VELOCITIES AT IMPACT						DISPLAYED FINAL POSITIONS				VEHICLE DAMAGE INDICES	ΔV
	C.G. POSITION		HEADING				C.G. POSITION		HEADING	REMARKS		
	XCI	YCI	PSII	FNS	LATERAL	ANGULAR	XCIF	YCIF	PSIIF			
	FT.	FT.	DEG.	MPH	MPH	DEG/SEC	FT.	FT.	DEG			MPH
VEHICLE # 1	20.8	8.3	180.3	0.0	0.0	0.0	20.9	8.3	180.0	VEHICLE AT REST	[redacted]	0.0
VEHICLE # 2	9.4	5.1	0.0	35.0	0.0	0.0	12.1	8.0	0.7	VEHICLE AT REST	12FCEW4	34.5

CASE NO. CA 71031

Crash Victim -

Male
19 Years
70 in.
180 lbs.

Accident -

Face struck instrument panel (probable) - concussion, facial contusion

Injury Rating -

Face - 2 (Moderate)
Brain - 1 (Minor)
Overall - 2

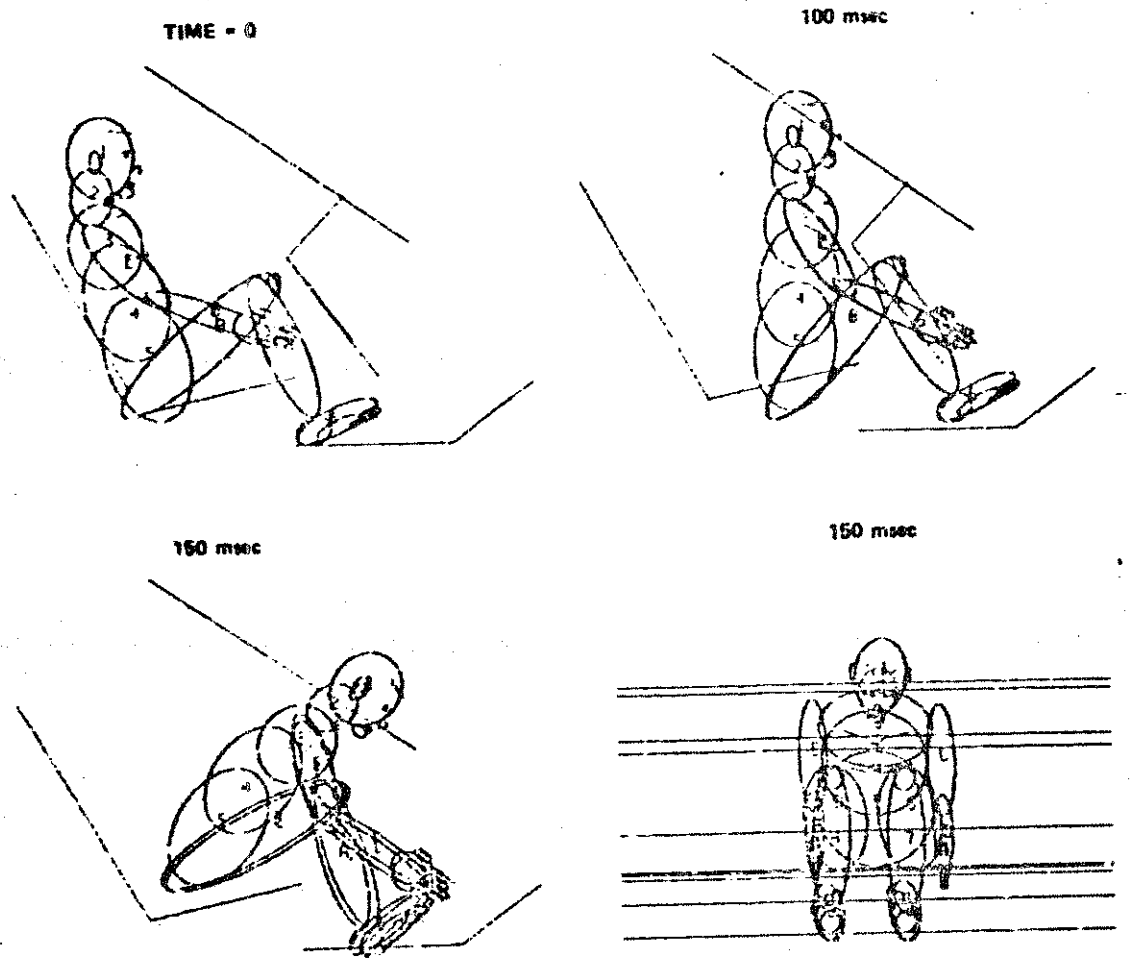

Figure 3.3.9

Accident Reconstruction Summary -
Case No. 71-31A

CASE NO. 72 (Case Identification No. CB00072)

1. Case Report Summary

Primary Vehicle - 1970 Camaro
Secondary Vehicle - None

1.1 Description of Accident

Pre-crash:

The Camaro was proceeding behind a vehicle which was not involved in the impact. The driver of the Camaro pulled abreast of the other vehicle and both drivers started an impromptu "drag race". The Camaro passed the other vehicle but did not attempt to return to the right lane. He approached an upcoming curve high and a short distance before the curve applied light brake pressure. The left front tire marked the pavement for 125 feet. At this point the driver applied heavy pedal pressure and locked all four wheels. The Camaro skidded 7 feet before leaving the left side of the road.

Crash:

After leaving the road, the Camaro continued to skid for 51 feet before striking a 43 inch diameter tree with the center front of the vehicle. The estimated impact speed was 33 MPH.

Post-crash:

The vehicle rebounded from the tree approximately 10 inches to the final rest position. The investigator VDI rating was 12FDEW4. The case report schematic is shown in Figure 3.3.10.

Figure 3.3.10

Accident Schematic - Case No. 72

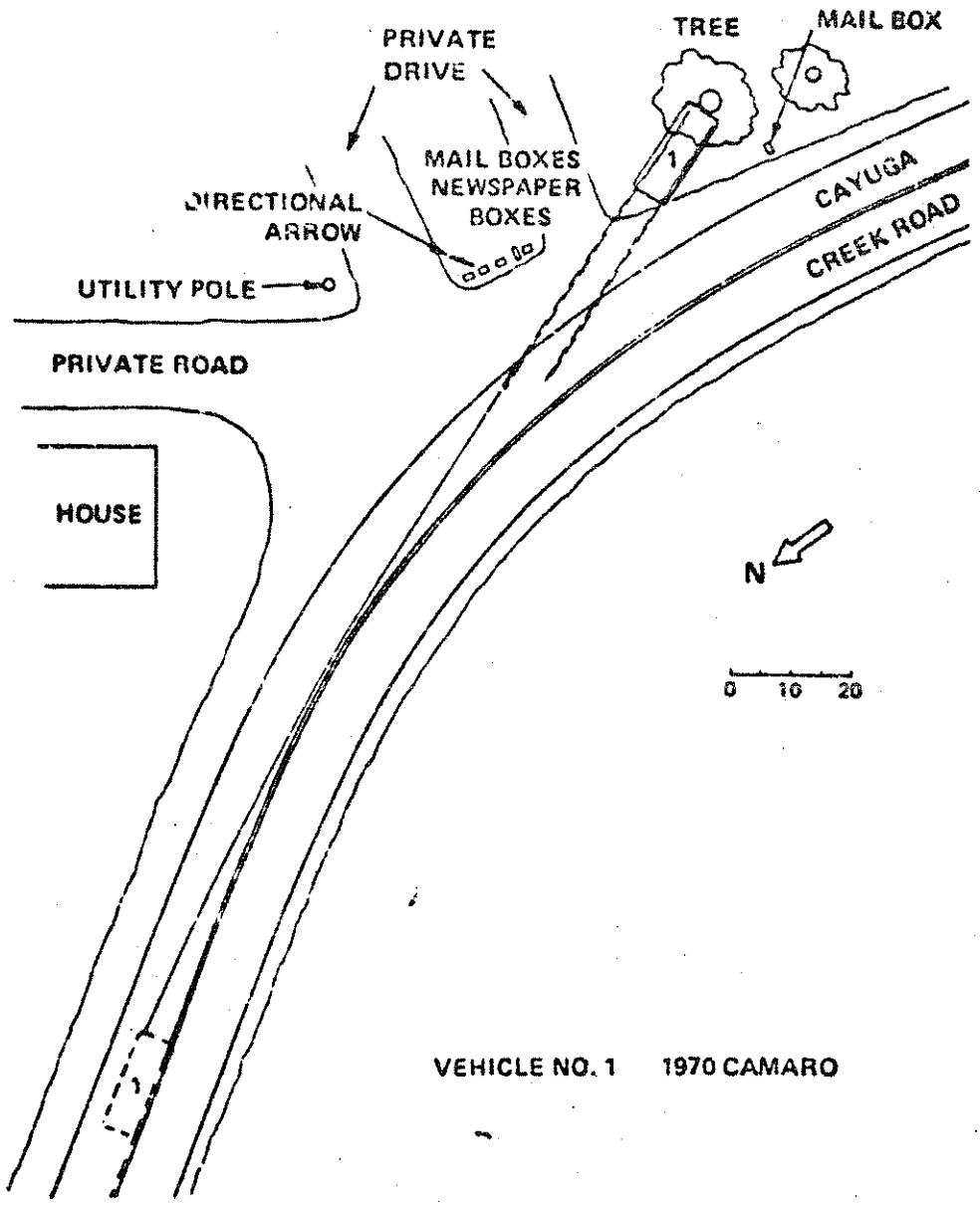

ZQ-5341-V-1

1.2 Primary Vehicle Right Front Occupant

18 year old male, 70" tall, 160 lbs.

This occupant did not use the available restraint. On impact he moved forward, striking his head on the sunvisor, windshield, and top of the instrument panel and his right knee on the lower instrument panel. He sustained injuries of a laceration of the right eyelid, contusions and abrasions of the forehead and chin, fracture of the jawbone, and fractures of two fingers on the left hand. The rated AIS severity index was moderate (02).

2. Analytical Reconstructions

2.1 SMAC Reconstruction

The SMAC program inputs for the final iteration of this case are shown in Table A-2.4. The measured VDI (12FDEW4) and the predicted VDI (12FDEW3) agree, with the exception of the measure of the extent of deformation, column 7. The resultant acceleration, angle and the damage pattern for the vehicle are shown in Figure 3.3.11. The reconstruction summary is displayed in Figure 3.3.12.

2.2 3-D Crash Victim Reconstruction

This analytical reconstruction, excerpted from an earlier study, Reference 7, used a crash victim description based largely on the measured properties of a GM Hybrid II dummy, as in Case No. 1316D. For Case No. 72, no plotter graphics displays were produced in that earlier study, in the interests of program economy. Consequently, printer graphics displays obtained from the line printer output of the computer program are used to illustrate the predicted victim responses in Figure 3.3.13. Note that these predicted responses are in good agreement with the observed occupant contacts in the accident. Because of unknown force-deflection properties, the head-sunvisor contact was not simulated.

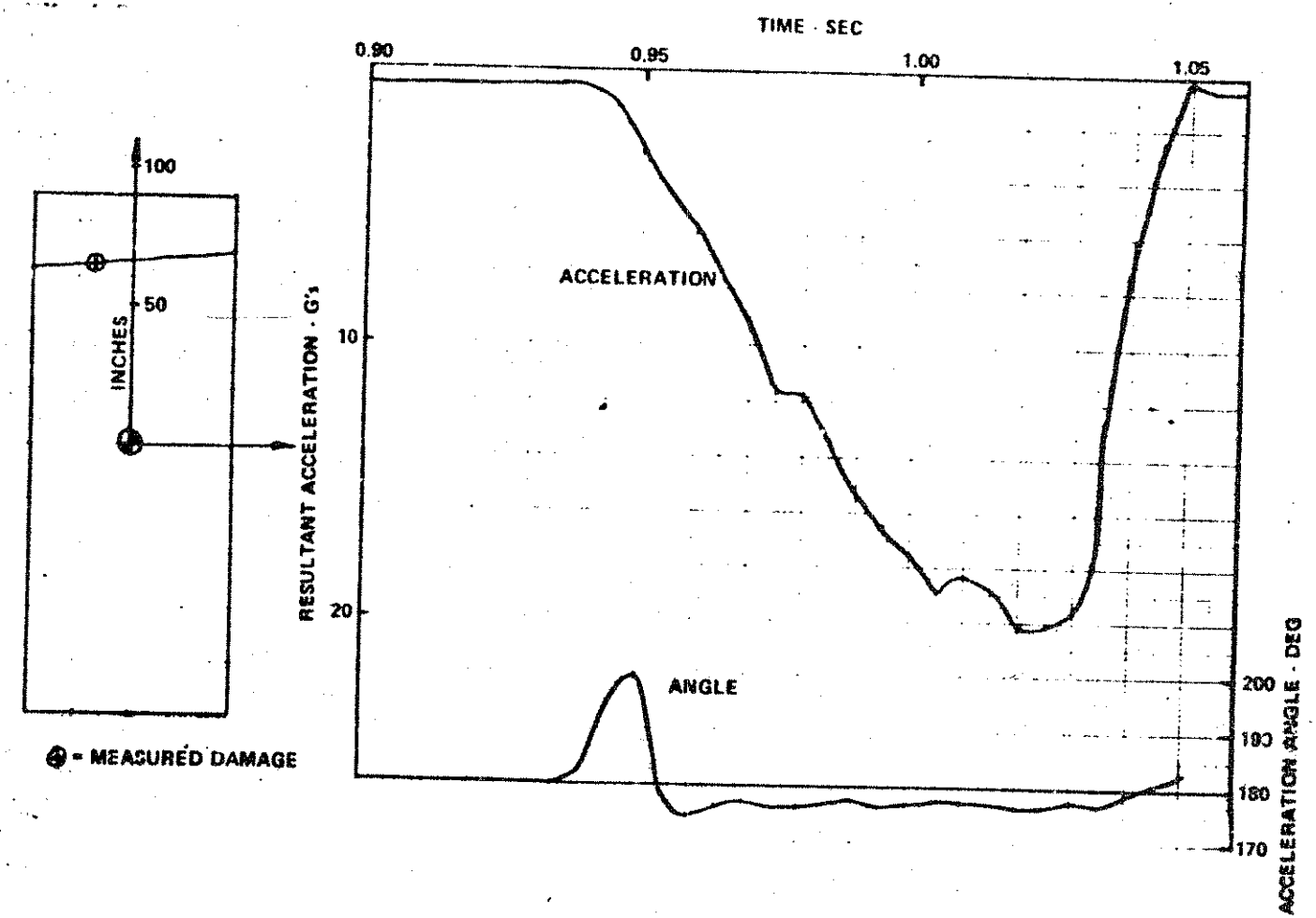

Figure 3.3.11 ACCELERATION AND DAMAGE - CASE NO. 72

Figure 3.3.12

Accident Reconstruction Summary - Case No. 72

GRAPHIC DISPLAY OF OUTPUTS OF ACCIDENT RECONSTRUCTION

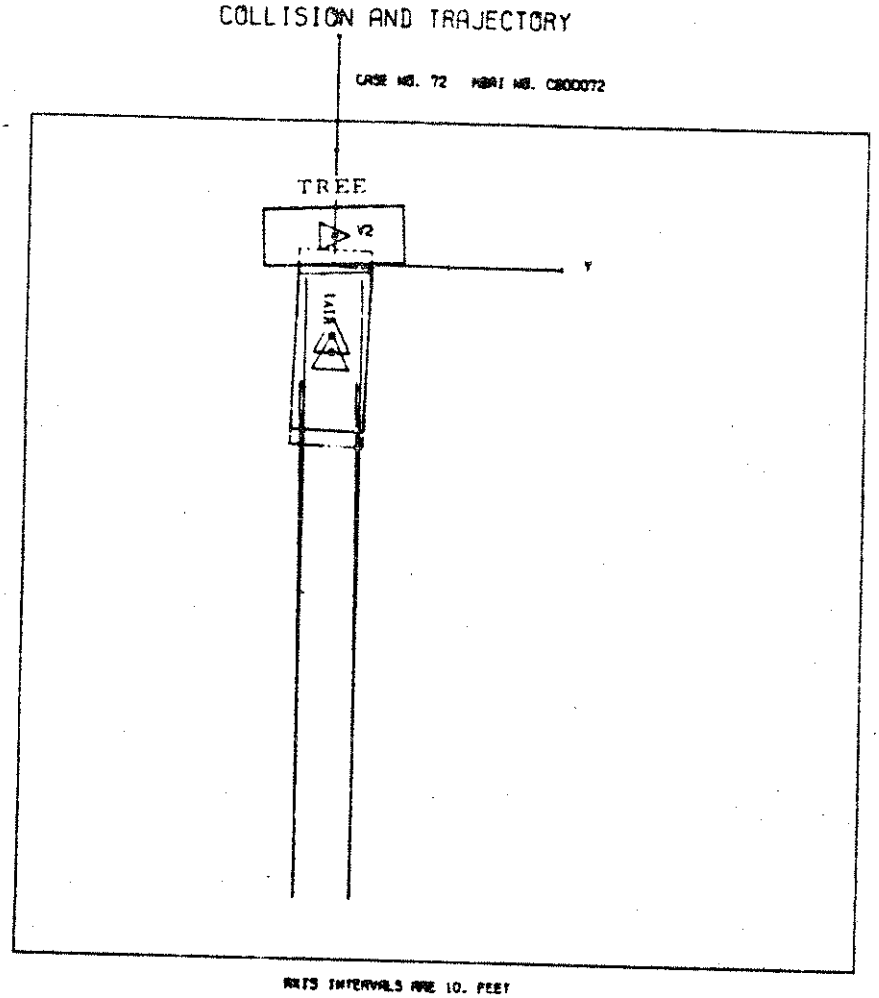

RECONSTRUCTED POSITIONS AND VELOCITIES AT IMPACT							DISPLAYED FINAL POSITIONS				VEHICLE DAMAGE INDICES	ΔV
	C.G. POSITION		HEADING				C.G. POSITION		HEADING	REMARKS		
	XC1	YC1	PSI1	PHD	LATERAL	ANGULAR	XC1F	YC1F	PSI1F			
	FT.	FT.	DEG.	MPH	MPH	DEG/SEC	FT.	FT.	DEG.			MPH
VEHICLE # 1	-7.8	-0.1	2.2	25.2	-1.2	2.9	-6.2	-0.0	1.5	VEHICLE AT REST	12FDEW3	28.2
VEHICLE # 2	2.5	0.0	87.5	0.0	0.0	0.0	2.5	0.0	87.5	VEHICLE AT REST		0.0

CASE NO CB 00072

Crash Victim -

Male
18 Years
70 in.
165 lbs.

Accident -

Head struck sunvisor, windshield, instrument panel - contusions/ abrasions to forehead and chin

Injury Rating -

Face - 2 (Moderate)
Overall - 2

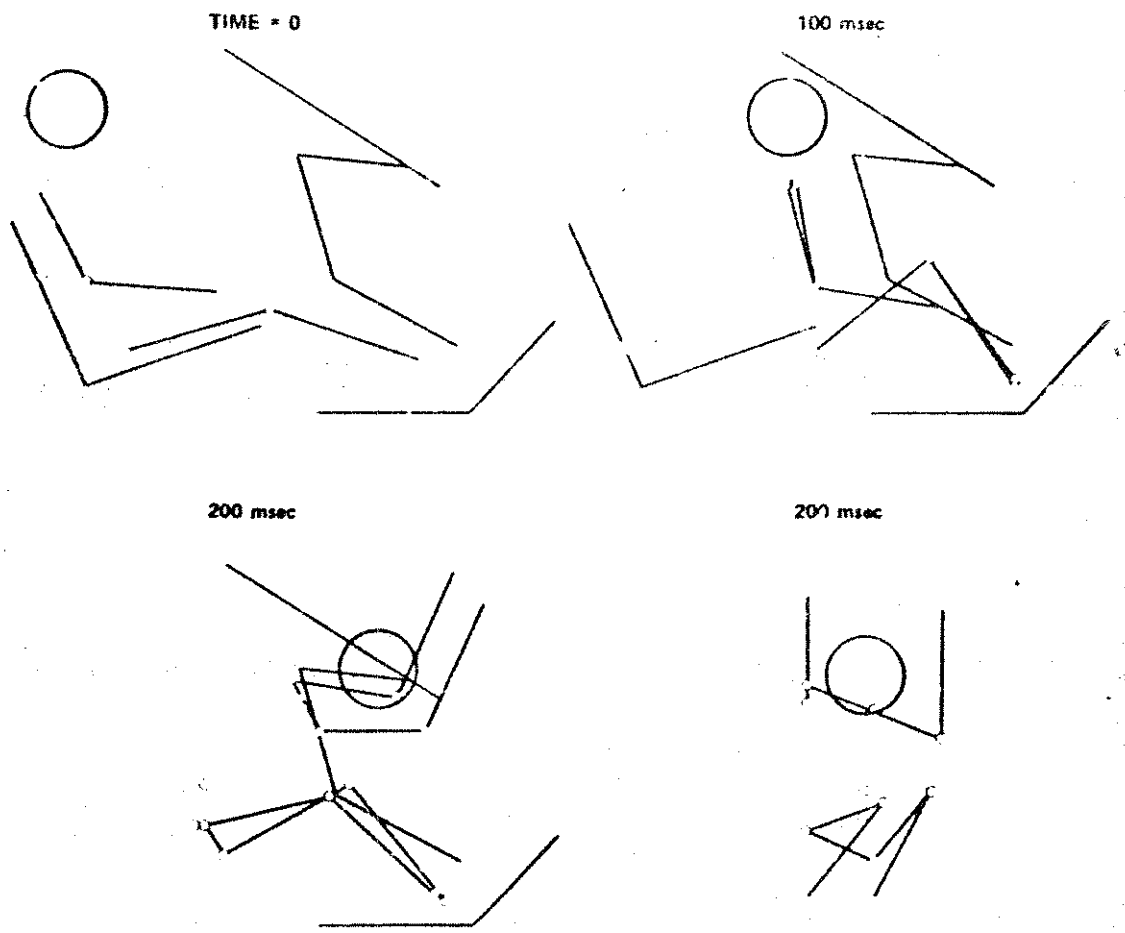

Figure 3.3.13
Accident Reconstruction Summary -
Case No. 72

CASE NO. 7144 (Case Identification No. SW71044)

1. Case Report Summary

Primary Vehicle - 1965 Ford Custom
Secondary Vehicle - 1969 Oldsmobile Royale Delta 88

1.1 Description of Accident

Pre-crash:

The secondary vehicle was parked facing east, on the wrong side of an urban/residential street, as shown in the collision scene schematic from the case report, Figure 3.3.14. The primary vehicle was traveling west on the street at a speed estimated to be between 25 and 30 MPH. The driver was familiar with both the route and vehicle, but was inattentive as she passed a soft drink to the center front passenger. During this brief period of inattention, the primary vehicle veered to the right into the secondary vehicle, leaving no skidmarks prior to impact.

Crash:

The right front corner of the primary vehicle struck the right front corner of the parked vehicle. On impact the three front seat occupants of vehicle 1 were thrown against the steering wheel, instrument panel and windshield. The vehicle yawed 5 to 10 degrees clockwise and came to rest within 2 to 3 feet. The secondary vehicle similarly yawed 5 to 10 degrees clockwise and traveled 2 to 3 feet to final rest. The VDI's were 12FZEW3 for vehicle 1 and 12FZEW1 for vehicle 2.

Figure 3.3.14

Collision Scene Schematic - Case No. 7144

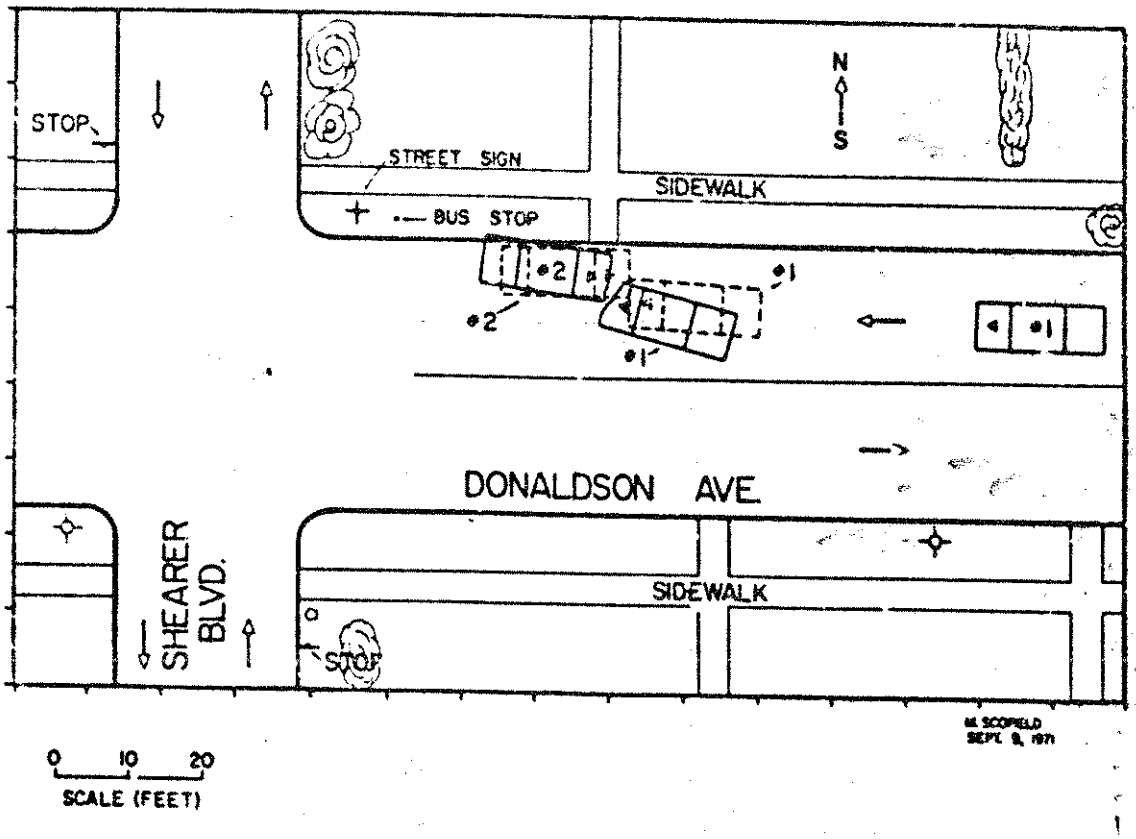

1.2 Primary Vehicle Right Front Occupant

18 year old male, 71" tall, 160 lbs.

This occupant was not wearing an available lap belt restraint and on impact was thrown forward, breaking the windshield with his face, which resulted in a laceration extending from the lower aspect of the right ear to the anterior medial aspect of the chin. Tooth number 29 was totally dislocated. He also struck the upper and lower instrument panel with his right arm and left knee, respectively, resulting in no injuries. Overall injury rating: Moderate - AIS Severity Code No. 2.

2. Analytical Reconstructions

2.1 SMAC Reconstruction

The case report approximates the impact speed as having been between 25 and 30 MPH, the translations from impact positions to final rest as 2 to 3 feet and the rotations as 5 to 10 degrees for both vehicles. There was no reporting of skidmarks left by the vehicles.

Inputs to the SMAC program were based on best available data from a number of sources including References 1 and 19 and the case report. These inputs are summarized in the required SMAC format in Table A-2.5. For the purposes of this reconstruction, it was assumed that the parking brake was engaged on the parked vehicle resulting in rear wheel lockup during the post-impact translation. It was also assumed that the impact-induced damage produced locking of the right front wheels of both vehicles during the collision.

The initial SMAC runs were made using an estimated speed for vehicle 1 based on the case report. This speed resulted in both excessive damage sustained by both vehicles and excessive translations to the final rest positions. As a result, in subsequent runs the initial velocity of vehicle 1 was reduced until good correlations with damage and translations were obtained. The final estimate of the impact speed from the SMAC program was 12.5 MPH. A comparison of predicted and measured VDI's is shown below.

	Measured	Predicted
vehicle 1	12FZEW3	12FZEW2
vehicle 2	12FZEW1	12FZEW2

Note that the predicted values are identical to those measured with the exception of the distribution of the extent of damage between the two vehicles (column 7). The case report indicates that the maximum deformations sustained by the two vehicles were approximately 28 and 12 inches for the primary and secondary vehicles. respectively, whereas the SMAC program predicted corresponding deformations of 19 and 21 inches. It is therefore seen that the maximum total system deformation is 40 inches for both measurement and prediction. The difference in distribution of the total deformation between the two vehicles undoubtedly results from the use of a single, general structural stiffness parameter to represent the entire vehicle population and all areas on a given vehicle within a given size classification.

Although the predicted vehicle translations are in good agreement with measurements, the predicted final vehicle yaw angles are less than the estimates given in the case report. In the SMAC reconstruction, the primary and secondary vehicles yawed 1.4 and 0.7 degrees, respectively.

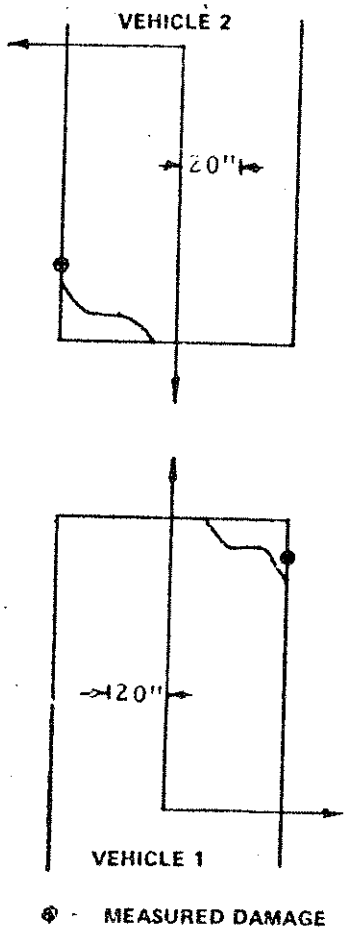

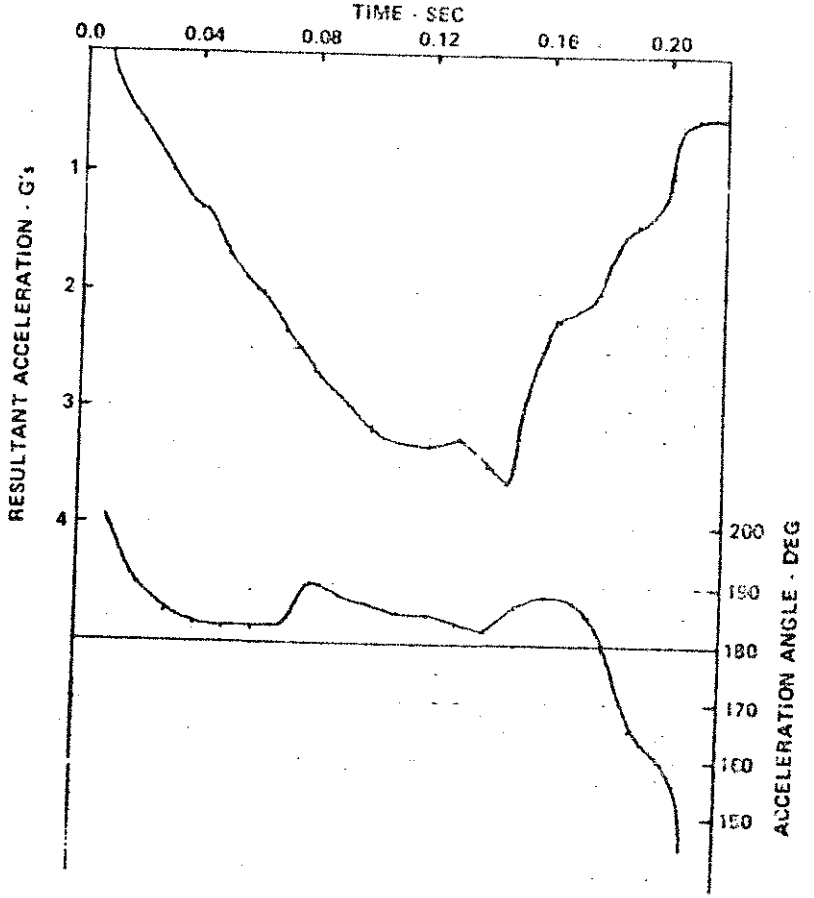

Figure 3.3.15 ACCELERATION AND DAMAGE - CASE NO. 7144

Figure 3.3.16

Accident Reconstruction Summary - Case No. 7144

GRAPHIC DISPLAY OF OUTPUTS OF ACCIDENT RECONSTRUCTION

COLLISION AND TRAJECTORY

CASE NO. 7144 HSRI NO. 8871044

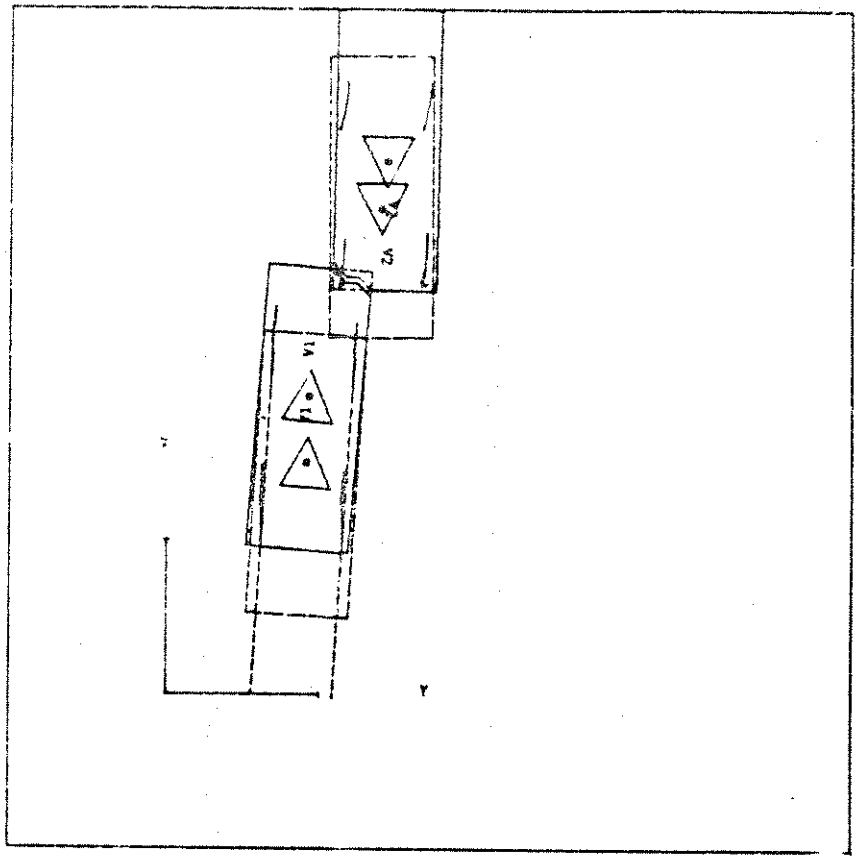

AXIS INTERVALS ARE 10. FEET

RECONSTRUCTED POSITIONS AND VELOCITIES AT IMPACT							DISPLAYED FINAL POSITIONS				VEHICLE DAMAGE INDICES	
	C.G. POSITION		HEADING				C.G. POSITION		HEADING	REMARKS		
	YC1	YC1	PSI1	FWD	LATERAL	ANGULAR	XC1F	YC1F	PSI1F			ΔV
	FT.	FT.	DEG.	MPH	MPH	DEG/SEC	FT.	FT.	DEG.			MPH
VEHICLE # 1	15.0	9.1	9.5	12.5	0.0	0.0	18.3	8.3	4.6	VEHICLE AT REST	12FZEW2	8.8
VEHICLE # 2	31.5	13.8	180.0	0.0	0.0	0.0	36.8	14.2	180.9	VEHICLE AT REST	12FZEW2	5.4

The underestimation of vehicle yaw in this case may result from a number of assumptions inherent in the SMAC program or from the lack of adequate reporting of the physical evidence. The effects of dynamic fore-aft weight transfer are not included in SMAC. For the case considered here, such weight transfer should increase the tendency for both vehicles to yaw. Another possible explanation is that, based on the damage patterns, substantial impact forces may have been transmitted through the suspensions of both vehicles to the sprung masses. These relatively "hard" points in the vehicle structure are not considered in SMAC.

The results of the SMAC reconstruction for this case are summarized in Figures 3.3.15 and 3.3.16.

2.2 3-D Crash Victim Reconstruction

The predicted kinematic responses of the crash victim are illustrated in the plotter graphics display of Figure 3.3.17. It can be seen from the display that the right front occupant, according to the simulation, moved forward and struck the windshield with his forehead near the windshield header. Note also that several inches of lateral displacement of the head is predicted, a result of the oblique crash angle (about 5 degrees to the right)*. The predicted location of initial head contact on the windshield is within about two inches of the observed location of contact (as evidenced by the windshield fracture pattern from a photograph in the case report). (It should be noted that the initial location of the right front occupant on the seat is not known to this degree of accuracy.) Furthermore, the degree of windshield fracture is quite consistent with the predicted head-windshield contact. (In the simulation, the head penetrates the windshield plane about 1 1/2 inches, and dynamic windshield failure is predicted.)

*The plotter graphics displays are right and rear orthogonal views of the crash victim.

Crash Victim -

Male
18 Years
71 in.
160 lbs.

Accident -

Face struck windshield (broken) - facial laceration

Injury Rating -

Face - 2 (Moderate)
Overall - 2

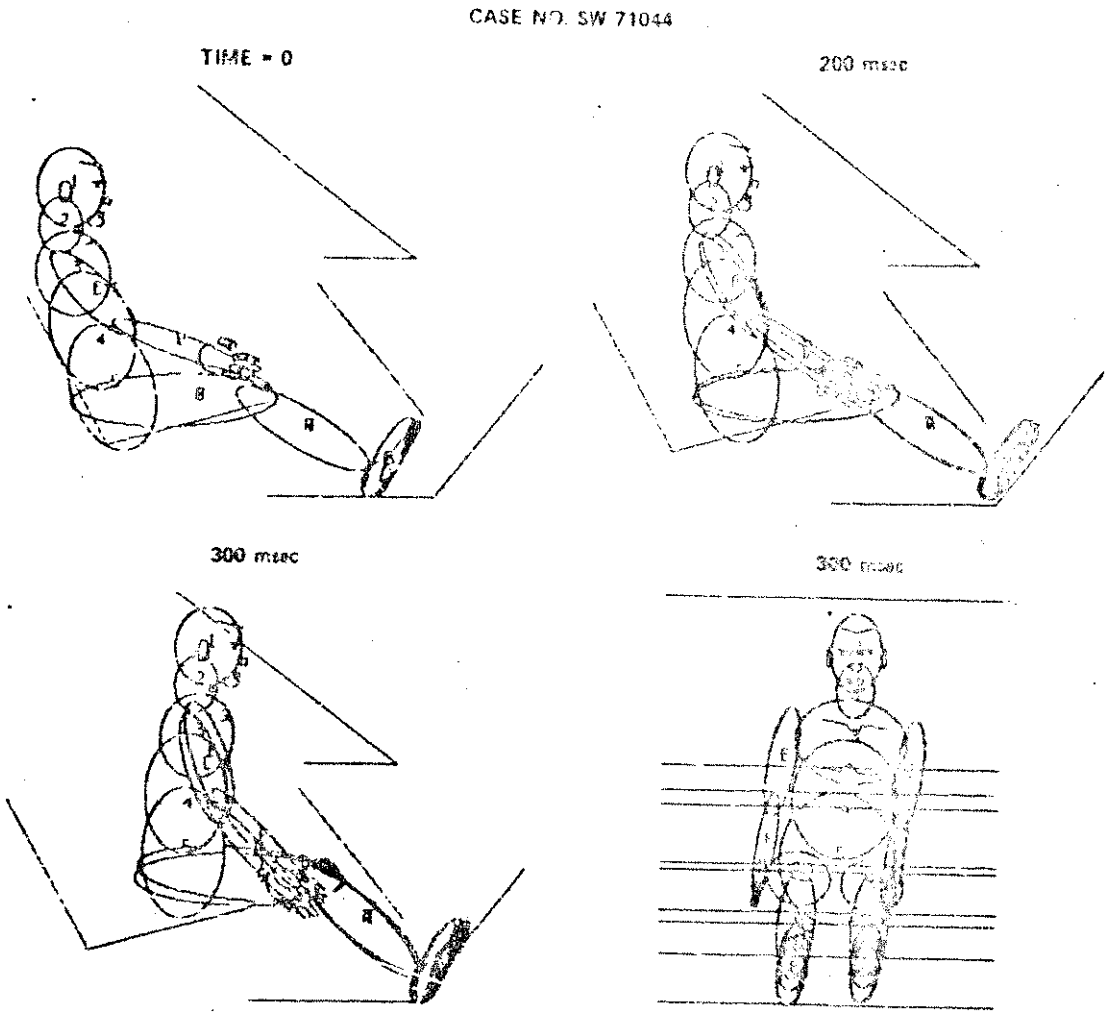

Figure 3.3.17
Accident Reconstruction Summary -
Case No. 7144

CASE NO. 53 (Case Identification No. CB00053)

1. Case Report Summary

Primary Vehicle - 1970 Chevrolet Nova
Secondary Vehicle - 1964 Mercury Comet Caliente

1.1 Description of Accident

Pre-crash:

The primary and secondary vehicles were traveling in opposite directions on a straight and level two lane asphalt highway. The secondary vehicle (Comet) was left of the center line. Speeds were believed to be less than the 50 MPH limit. No evidence of pre-impact braking was found. The case report schematic is shown in Figure 3.3.18.

Crash:

The left fronts of the two vehicles collided. The Comet rotated 80-85 degrees and came to rest facing across its lane. The Nova rotated nearly 180 degrees and came to rest along its shoulder. The VDI's were 12FYEW7 for the primary vehicle and 11FYEW8 for the secondary vehicle.

1.2 Primary Vehicle Right Front Occupant

52 year old female, 5'6" tall, 130 lbs.

This occupant was not wearing the available restraints. On impact, she moved forward and upward, contacting the windshield with her head and face, causing a loss of consciousness. She incurred multiple lacerations and abrasions of the face and broke several teeth. Her knees

Figure 3.3.18

Accident Schematic - Case No. 53

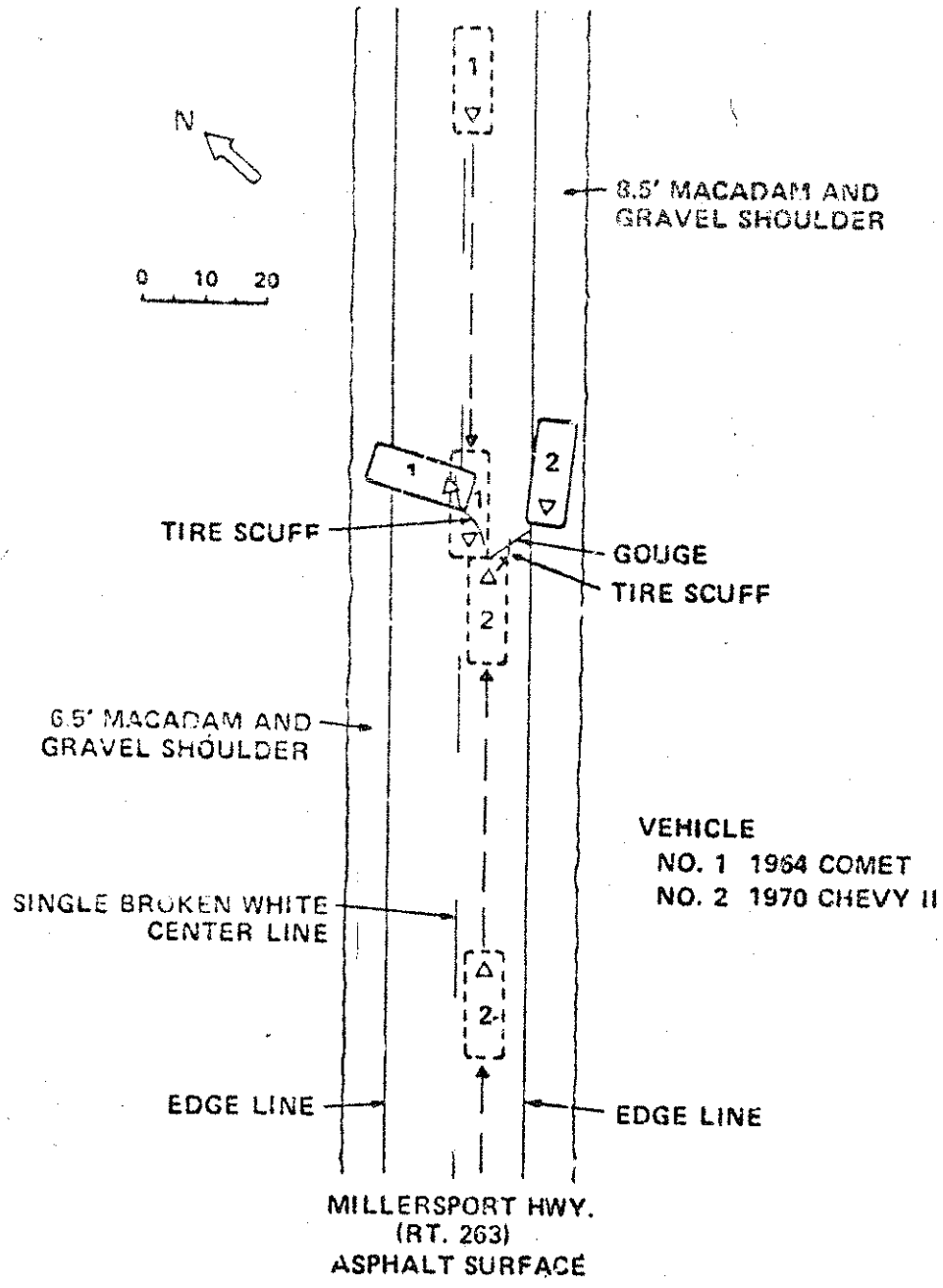

ZQ-5341-V-1

contacted the instrument panel, the left knee receiving a severe laceration and tear into the capsule from contact with an open ashtray. Her right pelvis and left femur were fractured. She also incurred an impacted fractur of the left distal radius. Her head also contacted the instrument panel as she fell. Injury ratings to various body regions varied from AIS-1 (chest) to AIS-3 (brain).

2. Analytical Reconstruction

2.1 SMAC Reconstruction

The SMAC inputs used in the final reconstruction run for this case are shown in Table A-2.6. The reconstructed impact speeds were found to be 53 MPH for vehicle 1 and 42 MPH for vehicle 2. The measured and predicted VDI's for the two vehicles are compared below.

	Measured	Predicted
Vehicle 1	12FYEW7	12FLEW5
Vehicle 2	11FYEW8	11FLEW5

Differences in column 7 reflect a different coding procedure used to determine the extent of deformation. The differences in the code for the specific horizontal location of the damage (column 4) are not considered to be significant.

The deformation of the two vehicles is shown in Figure 3.3.19. It should be noted that the somewhat greater penetration of the reconstruction was accepted as a compromise between damage and rest position agreement (see Figure 3.3.18) with the case report. That is, at lower impact speeds the damage match was improved, but at the expense of a significant degradation in the rest position match. It should further be noted that, as indicated in Appendix C, the effective vehicle crush characteristic is stiffer for narrow, pole impacts than for wide, barrier impacts. Since there was

Figure 3.3.19 ACCELERATION AND DAMAGE - CASE NO. 53

GRAPHIC DISPLAY OF OUTPUTS OF ACCIDENT RECONSTRUCTION

COLLISION AND TRAJECTORY

CASE NO. 53 MDAI NO. 85-0063

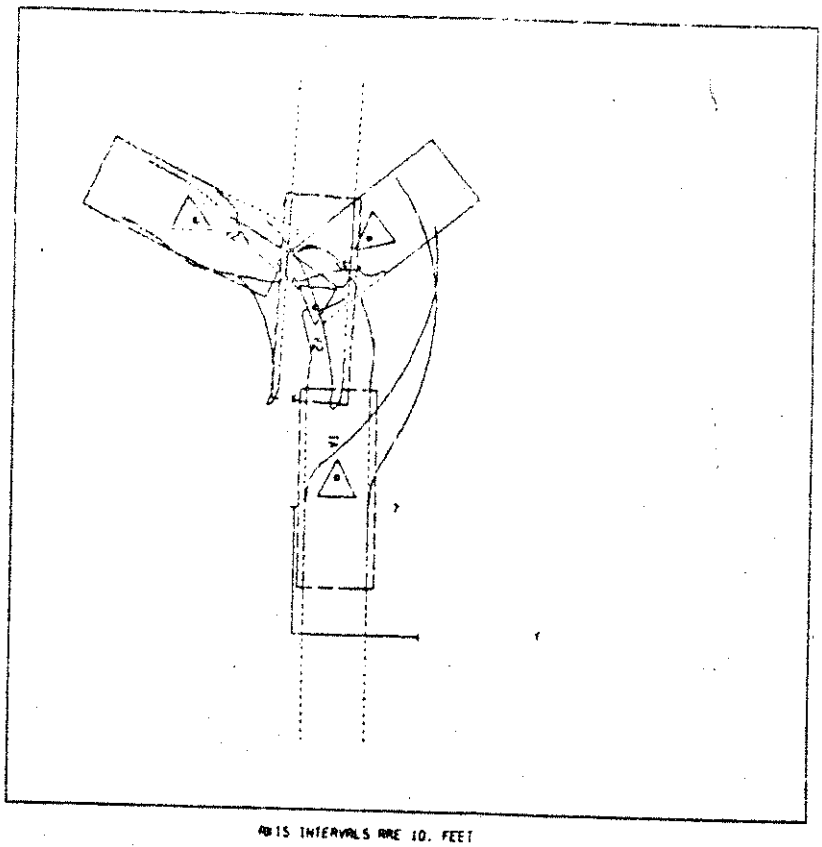

AXIS INTERVALS ARE 10. FEET

RECONSTRUCTED POSITIONS AND VELOCITIES AT IMPACT							DISPLAYED FINAL POSITIONS				VEHICLE DAMAGE INDICES	ΔV
	C.G. POSITION		HEADING				C.G. POSITION		HEADING	REMARKS		
	XCI	YCI	PSII	FWD	LATERAL	ANGULAR	XCIF	YCIF	PSIIF			
	FT.	FT.	DEG.	MPH	MPH	DEG/SEC	FT.	FT.	DEG.			MPH
VEHICLE # 1	12.4	3.3	-0.0	53.0	0.0	-0.1	31.0	5.0	-179.5	VEHICLE AT REST	12FYEW5	40.6
VEHICLE # 2	28.0	1.5	183.0	45.0	0.0	0.0	32.0	-8.1	115.8	VEHICLE AT REST	11FYEW5	48.3

Figure 3.3.20 ACCIDENT RECONSTRUCTION SUMMARY - CASE NO. 53

no evidence to extend this behavior to narrow, offset frontal impacts between cars, the barrier equivalent stiffness was used for this case. However, it seems likely that this type of impact is analogous to a pole impact and that had a stiffer value of the crush characteristic been used the penetrations would have been reduced while maintaining acceptable agreement with the rest positions.

The resultant acceleration and angle time histories for the vehicle of interest are shown in Figure 3.3.19, and the accident reconstruction summary is presented in Figure 3.3.20.

2.4 3-D Crash Victim Reconstruction

In this case, the predicted victim kinematics, Figure 3.3.21, agree well with the observations of the accident investigator. It is worth noting, however, that head-windshield contact for this vehicle geometry-passenger orientation appears highly probable for a broad range of near-frontal crash conditions. Simulation of the secondary collision of the head on the instrument panel was not attempted (the simulation was terminated before this possible contact), because the secondary contact was regarded as of relatively minor importance compared to the windshield impact.

Crash Victim -

Female
52 Years
66 in.
130 lbs.

Accident -

Head struck windshield - facial abrasions/ lacerations, broken teeth (loss of consciousness)

Injury Rating -

Head - 1 (Minor)
Face - 2 (Moderate)
Brain - 3 (Severe)
Overall - 3

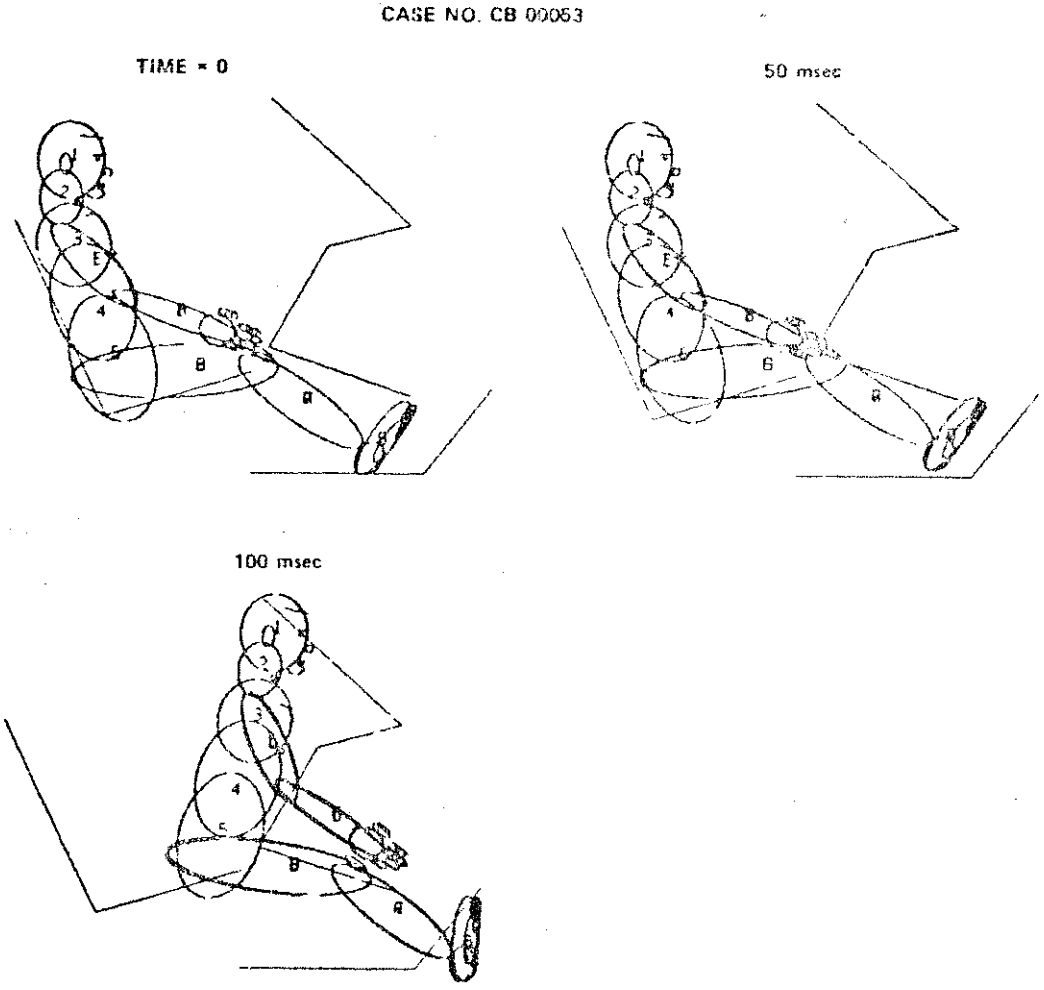

Figure 3.3.21
Accident Reconstruction Summary - Case No. 53

CASE NO. 71-55B (Case Identification No. CB71055)

1. Case Report Summary

Primary Vehicle - 1971 Ford Mustang
Secondary Vehicle - 1971 Ford Torino GT

2. Description of Accident

Pre-crash:

The Torino was proceeding north in lane #2 preparing to make a left turn. As the intersection signal light changed from red to green, the driver noticed the lead vehicle in southbound lane #2 was signaling to turn left. The driver of the Torino initiated a shallow left hand turn and applied the brakes when she saw the primary vehicle, the Mustang, approaching in southbound lane #1. The Torino skidded 24 ft. to impact. The case report schematic is shown in Figure 3.3.22.

Crash:

The center front of the Torino struck the left front corner of the Mustang. The Torino rotated counterclockwise and was forced backward due to the impact. The Mustang was deflected 21° to the left.

Post-crash:

The Torino left 11 ft. of front wheel skidmarks before coming to rest at approximately a right angle to the roadway. The Mustang translated approximately 10 ft. to its rest position facing south-southwest. The VDI's were 02FDEW2 for vehicle 1 and 11FLEE2 for vehicle 2.

Figure 3.3.22

Accident Schematic - Case No. 71-55B

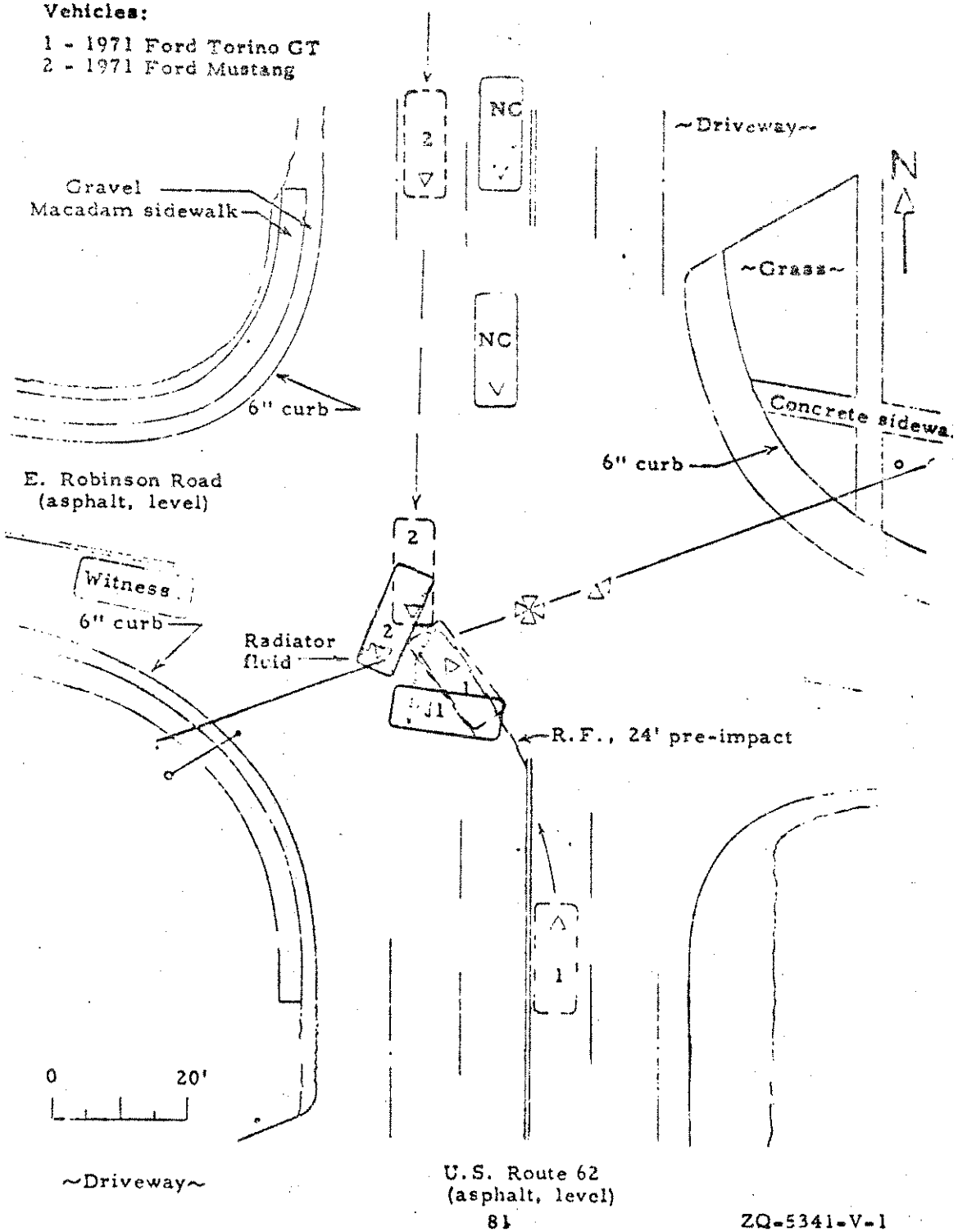

ZQ-5341-V-1

1.2 Primary Vehicle Right Front Occupant

49 year old female, 60" tall, 130 lbs.

This occupant was not wearing available restraints. At impact, she moved forward and to the left, contacting the rearview mirror (head), upper instrument panel (face), center instrument panel (chest). Injuries sustained included minor lacerations to scalp (rearview mirror), laceration to lower lip (upper instrument panel), fracture of four central incisors (upper instrument panel), displaced fracture of alveolar ridge (upper instrument panel), contusions to chest (instrument panel), and minor injuries to the extremities. The injury rating was AIS-3, Severe.

2. Analytical Reconstruction

2.1 SMAC Reconstruction

The inputs used in the final reconstruction run of this case are shown in Table A-2.7. The reconstructed impact speeds were 25 MPH for vehicle 2 (the primary vehicle) and 10.8 MPH for vehicle 1 (the secondary vehicle). The predicted and measured VDI's are compared below.

	Measured	Predicted
Vehicle 1	02FDEW2	12FDEW2
Vehicle 2	11FLEE2	11LFEW2

While it is apparent that significant lateral impact forces relative to vehicle 1 must be developed from the orientations of the two vehicles, the time history of forces for vehicle 1 calculated by SMAC indicate that the direction of the maximum force is nearly twelve o'clock. Both before and after the peak force occurs, sizeable lateral forces are developed which produce the rotation to the rest orientation. Therefore, while the average clock

direction of the impact force may be around two o'clock the peak force is nearly longitudinal. The discrepancies in VDI's for vehicle 2 result from minor differences in the damage patterns that result primarily from more damage across the front of the vehicle than was observed in the case report. This probably results from the lack of simulated hard suspension "points". The damage patterns of the two vehicles are shown in Figure 3.3.23.

The resultant acceleration and angle time histories for the vehicle of interest (vehicle 2) are also shown in Figure 3.3.23, and the reconstruction is summarized in Figure 3.3.24.

2.2 3-D Crash Victim Reconstruction

This case was selected to at least partially investigate the effect of occupant size on predicted crash victim responses. This effect of size is particularly significant in comparing responses of the actual crash victim to anthropometric dummy responses, because of the inherent mismatch in both stature and weight between the human victim and the dummy. The computer simulation provides an ideal means to perform the required parameter variation to study the effect of size on responses.

Case No. 71-55B was chosen for this study because of the rather large difference in weight and stature between the right front occupant in the accident case and the basic reference occupant size selected for this effort, the 50th percentile male. That difference is apparent in the summary of occupant sizes for the ten cases that is presented in Table 3.3.1.

The effect of occupant size on predicted kinematic responses is shown in Figure 3.3.25, together with a concise summary of observations from the case report. In Figure 3.3.25, the predicted responses of a 50th percentile male (defined by measurements on a Sierra 292-1050, 50th percentile dummy) are compared to those of a 60 in., 130 lb. female (defined by data generated from the "GOOD" program, References 16, 17).

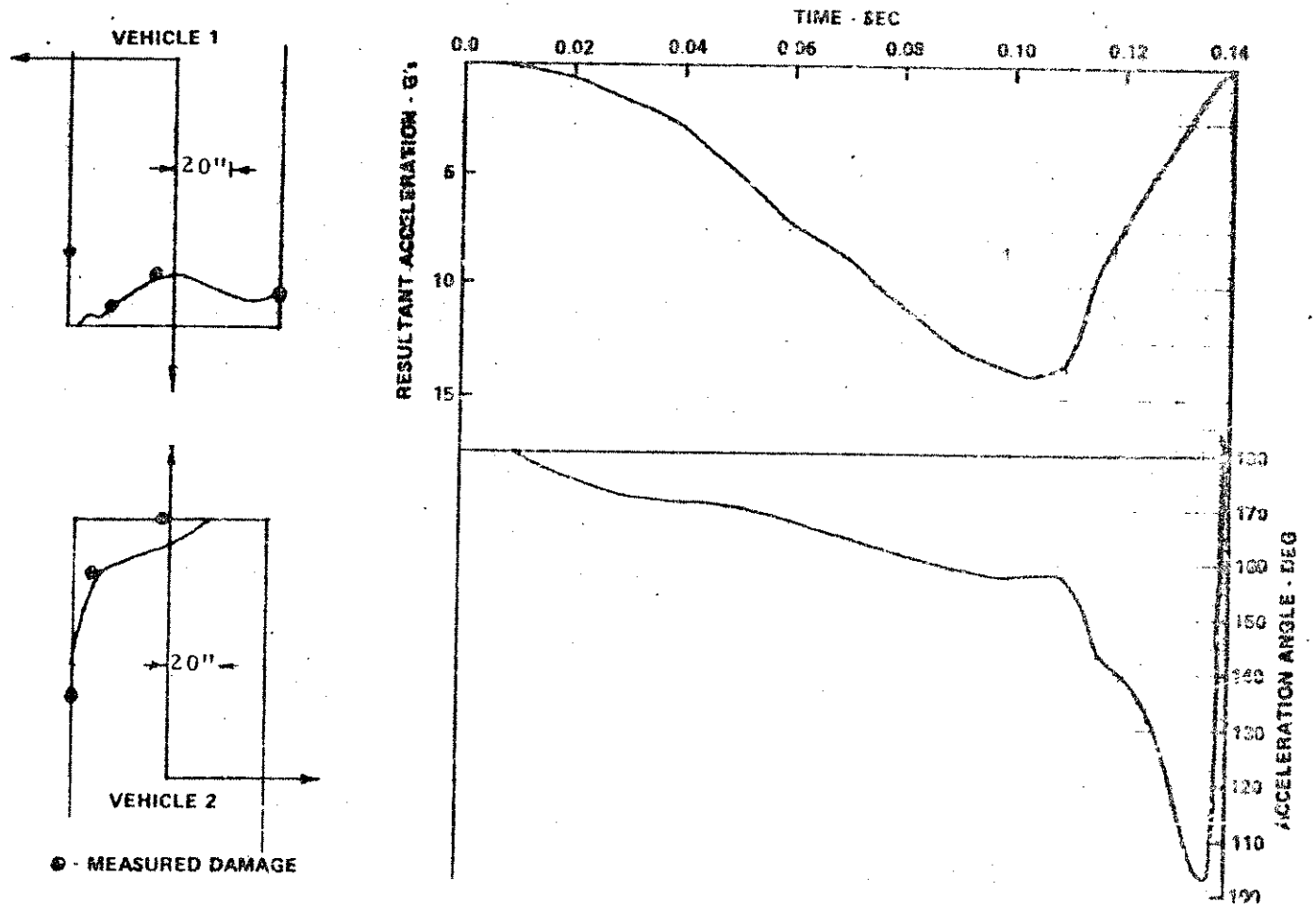

Figure 3.3.23 ACCELERATION AND DAMAGE - CASE NO. 71-55B

Figure 3.3.24

Accident Reconstruction Summary - Case No. 71-55B

GRAPHIC DISPLAY OF OUTPUTS OF ACCIDENT RECONSTRUCTION

COLLISION AND TRAJECTORY

CASE NO. 71-55B NDAI NO. C071095

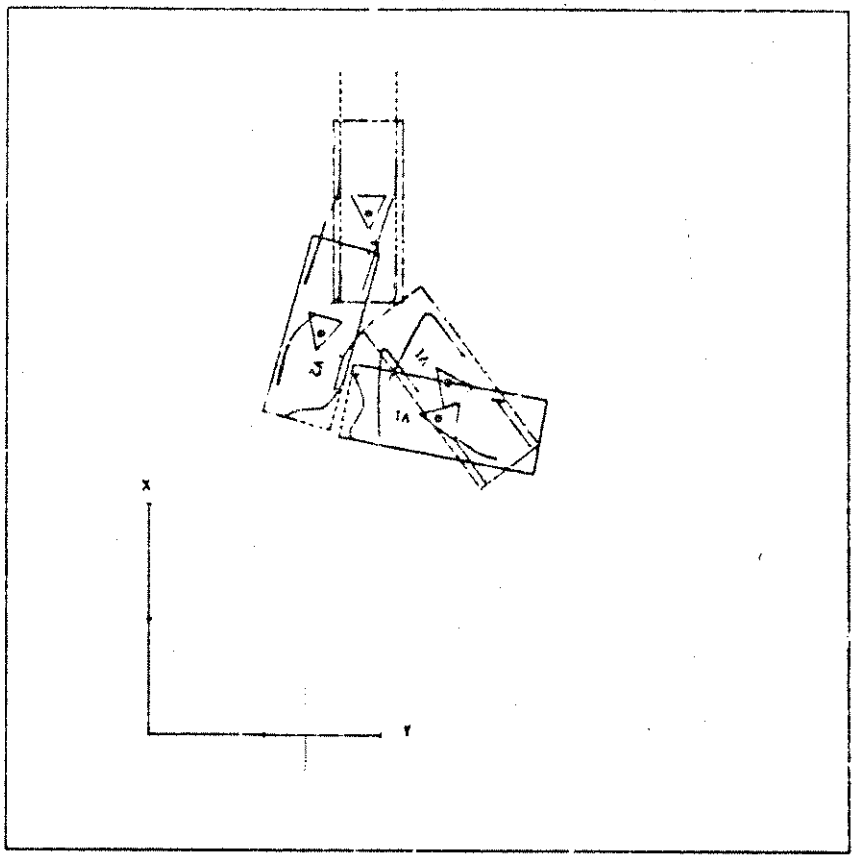

AXIS INTERVALS ARE 10. FEET

RECONSTRUCTED POSITIONS AND VELOCITIES AT IMPACT							DISPLAYED FINAL POSITIONS				VEHICLE DAMAGE INDICES	ΔV
	C.G. POSITION		HEADING				C.G. POSITION		HEADING	REMARKS		
	XC1	YC1	PSI1	FWD	LATERAL	ANGULAR	XC1F	YC1F	PSI1F			
	FT.	FT.	DEG.	MPH	MPH	DEG/SEC	FT.	FT.	DEG.			MPH
VEHICLE # 1	30.6	25.6	-97.0	10.3	0.0	0.0	27.6	25.0	-79.5	VEHICLE AT REST	12FBEN2	16.9
VEHICLE # 2	46.4	18.9	180.0	25.0	0.0	-0.1	34.9	14.9	185.5	VEHICLE AT REST	11LFEN2	16.6

Table 3.3.1

Summary of Right Front Occupant Sizes in the Ten Accident Cases

Case Identification Number	Right Front Occupant Sex	Age, Years	Height Inches	Height Percentile*	Weight Pounds	Weight Percentile*
AA00145	M	19	70	74	150	27
TR01316	M	15	68	47	150	27
CA71031	M	19	70	74	180	69
CB00072	M	18	70	74	165	49
SW71044	M	18	71	84	160	41
CB00053	F	52	66	21	130	7
CB71055	F	49	60	0.6	130	7
TR01161	M	22	+/—	-	+/—	-
GI00056	M	16	+/—	-	+/—	-
TR00973	M	52	71	84	155	35

*Based on percentile tables for adult males.

Note: 50th percentile adult male height is approximately 68 in.
50th percentile adult male weight is approximately 166 lbs.

+Not reported in accident case report.

Crash Victim -

Female
49 Years
60 in.
130 lbs.

Accident -

Head struck rear view mirror, upper instrument panel - facial lacerations, fractured teeth

Injury Rating -

Head - 1 (Minor)
Face - 3 (Severe)
Overall - 3

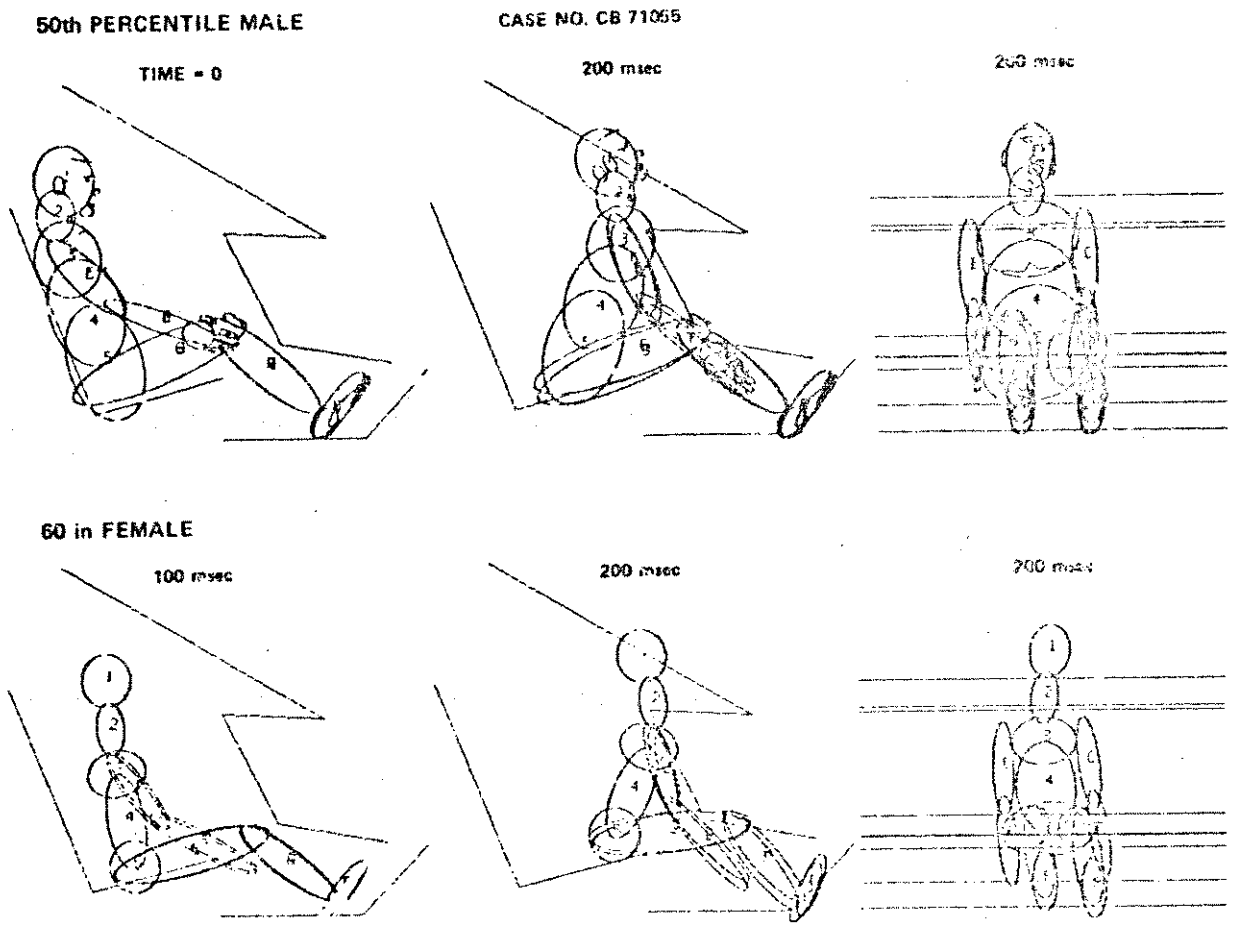

Figure 3.3.25
Accident Reconstruction Summary -
Case 71-55B

The effect of size on predicted kinematics, at least for this configuration, is very small. Although not presented in this section, the predicted peak head resultant acceleration is affected notably, however (about 20%), approximately in the ratio of the head masses for the 50th percentile male and 60 in. female victims.

For this case, the head-rearview mirror contact that occurred in the accident was not simulated, because of the unknown force-deflection characteristic for that contact. The kinematic response of the head, however, indicates that contact with the rearview mirror would have been predicted if a contact surface corresponding to the mirror had been inputted to the computer program.

CASE NO. 1161D (Case Identification No. TR01161)

1. Case Report Summary

Primary Vehicle - 1968 American AMX
Secondary Vehicle - None

1.1 Description of Accident

Pre-crash:

The AMX was traveling at an estimated speed of 40-45 MPH. Upon entrance to a curve around a raised elliptical island, the driver apparently realized he was traveling at an excessive speed, and applied the brakes, leaving 15 ft. of four wheel locked skidmarks. The AMX then struck the curb and traveled along it for 40 ft. leaving brush type skidmarks in the roadway. The case schematic is shown in Figure 3.3.26.

Crash:

After traveling along the curb, the AMX jumped the curb and struck a 4 ft. diameter palm tree that was located 3 ft. from the pavement. The estimated speed at impact was 35-40 MPH. The reported VDI was 12FZEW7.

Post-crash:

After the initial impact, the AMX rotated approximately 70° clockwise and came to rest at the side of the road.

Figure 3.3.26

Accident Schematic - Case No. 1161D

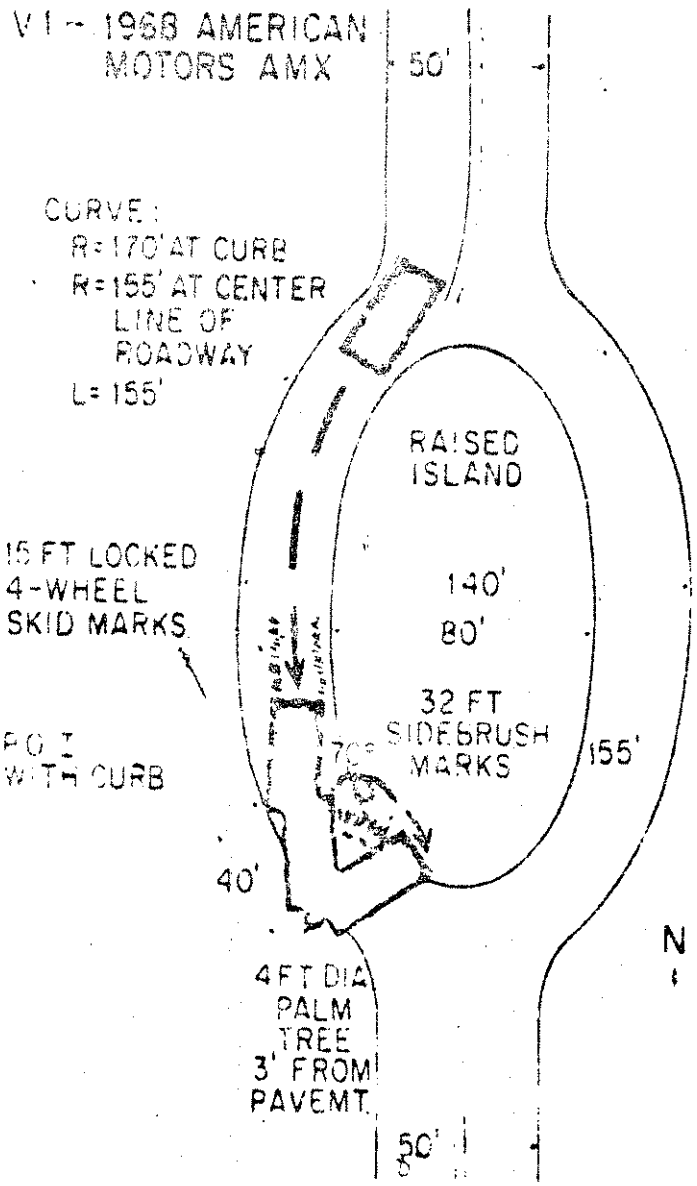

ZQ-5341-V-1

1.2 Primary Vehicle Right Front Occupant

22 year old male, unknown height and weight

The available restraint was not in use. Upon impact with the tree, the occupant moved straight ahead in a seated posture with his knees striking the instrument panel. His upper torso continued forward with his shoulder striking the right A-pillar and his face striking the windshield producing facial lacerations. Note that the hood was displaced rearward as a result of the impact, fracturing the glass before the occupant contacted it. This resulted in a decrease in energy absorbing capabilities and probably increased the severity of facial lacerations. The occupant's face may have also struck the hood, but this was not confirmed. Injury rating: Severe, AIS Severity Code No. 3.

2. Analytical Reconstructions

2.1 SMAC Reconstruction

Since this case involves vehicle path constraints that the current SMAC program cannot simulate, namely the vehicle travel along the curb, it was decided to forego reconstruction of the pre-crash phase and attempt to reconstruct the event from the time of the initial tree impact.

The program inputs used in the final reconstruction run for this case are shown in Table A-2.8. The reconstructed impact speed was 40 MPH. The predicted VDI of 12RFEW4 and the investigator-determined VDI of 12FZEW7 are in noticeable disagreement in columns 3, 4 and 7. The difference in column 7 is due to a change in the procedure for coding the extent of damage. The difference between RF and FZ are not in this case considered significant. As has been shown in Reference 7, very small changes in the distribution of the damage in corner damage cases such as this may shift the damage location code (column 3) from front to side or

vica-versa in the SMAC program. Similar situations are believed to exist in the ratings produced by the investigators. The predicted damage pattern is shown in Figure 3.3.27.

The resultant acceleration and angle are also shown in Figure 3.3.27, and the reconstructed scene is displayed in Figure 3.3.28. Note that the rotation of the simulated vehicle is not as great as indicated in the case report. As discussed previously, this is believed to be primarily due to assumptions in the SMAC program.

3.2 3-D Crash Victim Reconstruction

In this case, the predicted occupant kinematic responses, including deep penetration of the windshield by the head and possible head contact with the displaced hood (Figure 3.3.29), agree well with the accident case report. No attempt was made to simulate shoulder contact with the A-pillar, as noted in the case report, because of its anticipated minor effect on simulated head responses.

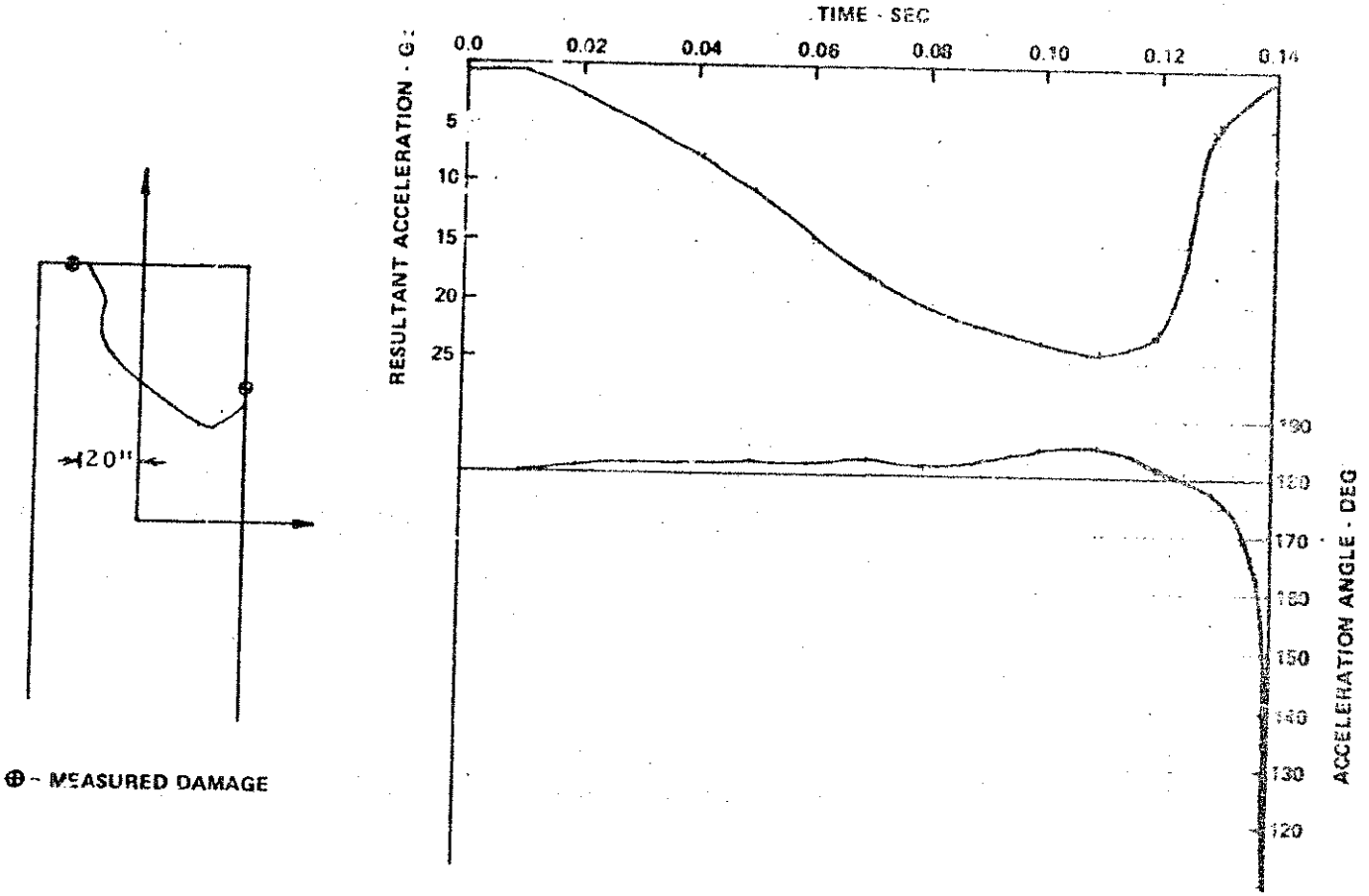

Figure 3.3.27 ACCELERATION AND DAMAGE - CASE NO. 1161

Figure 3.3.28

Accident Reconstruction Summary - Case No. 1161D

GRAPHIC DISPLAY OF OUTPUTS OF ACCIDENT RECONSTRUCTION

COLLISION AND TRAJECTORY

CASE NO. 1161 D RUN NO. PRO1161

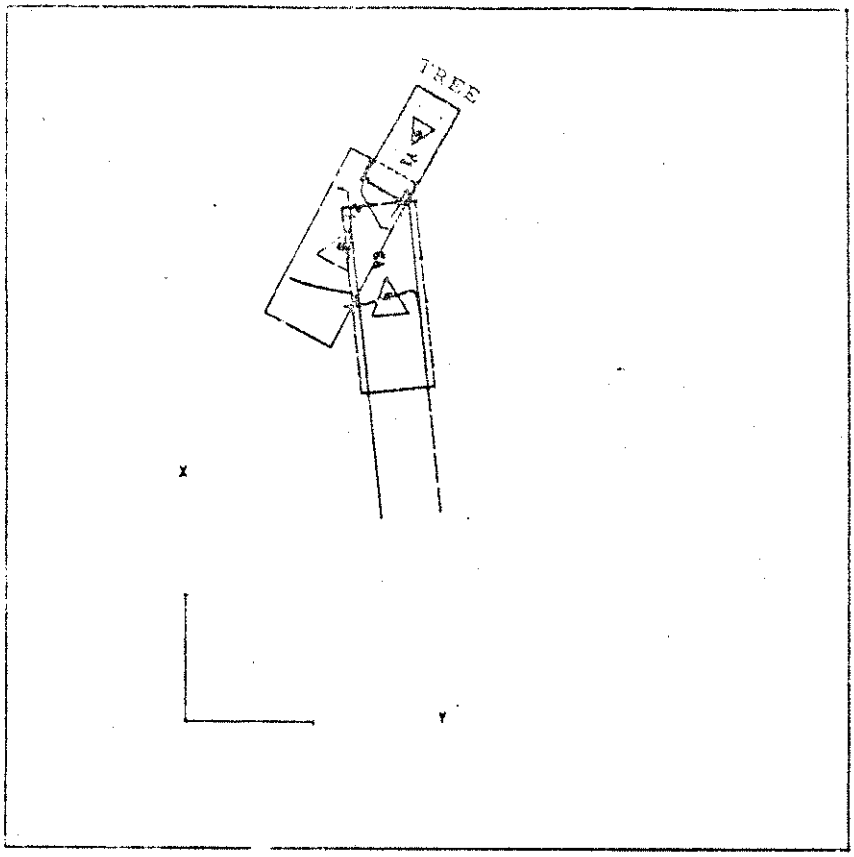

AXIS INTERVALS ARE 10. FEET

	RECONSTRUCTED POSITIONS AND VELOCITIES AT IMPACT						DISPLAYED FINAL POSITIONS				VEHICLE	
	C.G. POSITION		HEADING				C.G. POSITION		HEADING			
	XC1	YC1	PSI1	FWD	LATERAL	ANGULAR	XC1F	YC1F	PSI1F	REMARKS	INDICES	ΔV
	FT.	FT.	DEG.	MPH	MPH	DEG/SEC	FT.	FT.	DEG.			MPH
VEHICLE # 1	46.6	18.3	210.0	0.0	0.0	0.0	46.6	18.3	210.0	VEHICLE AT REST	[illegible]	0.0
VEHICLE # 2	73.7	16.0	-6.0	38.7	0.0	0.0	37.8	12.2	27.7	VEHICLE AT REST	12RFEW4	38.6

CASE NO. TR 01161

Crash Victim -

Male
22 Years
Height Unknown
Weight Unknown

Accident -

Head struck windshield/
hood - facial lacerations

Injury Rating -

Face - 3 (Severe)
Overall - 3

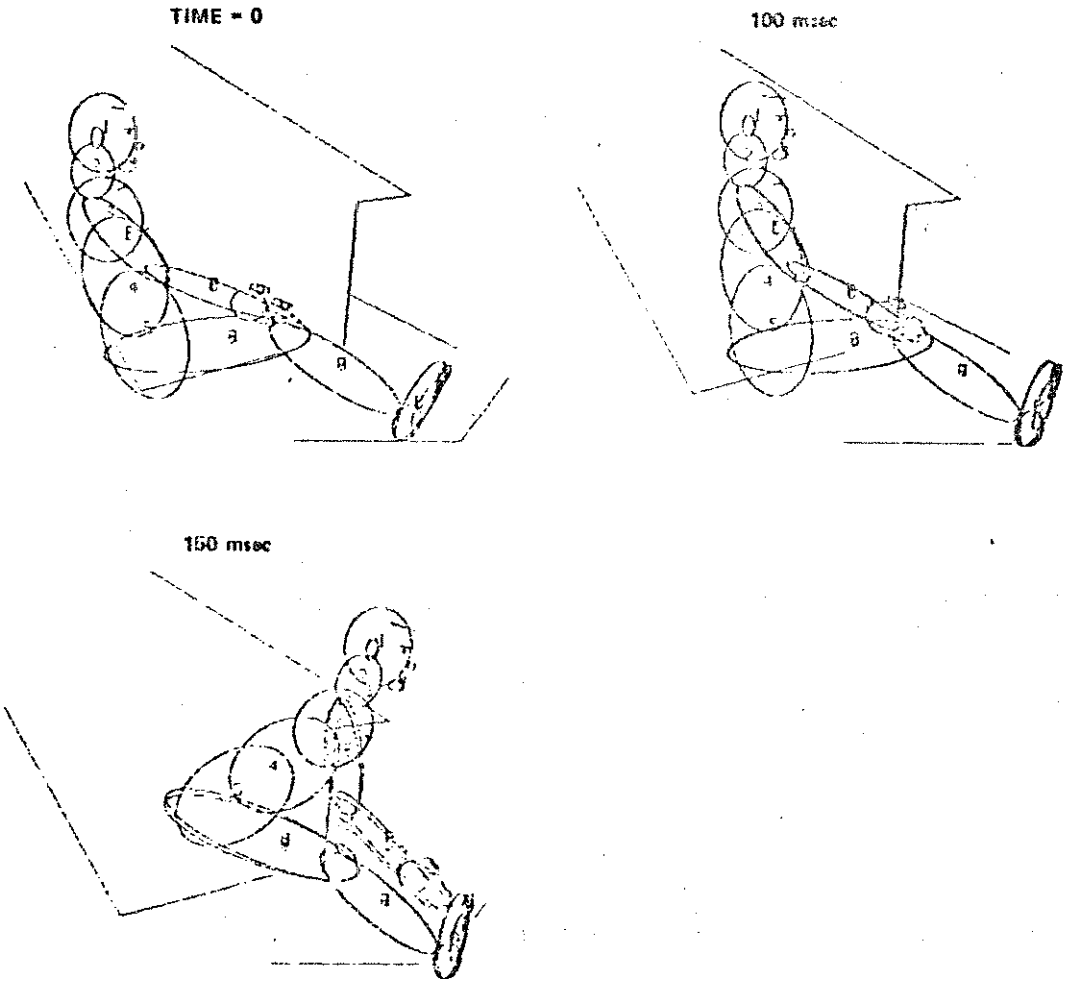

Figure 3.3.29
Accident Reconstruction Summary -
Case No. 1161D

CASE NO. 56 (Case Identification No. GI00056)

1. Case Report Summary

Primary Vehicle - 1969 Pontiac LeMans
Secondary Vehicle - None

1.1 Description of Accident

Crash:

The vehicle was traveling in a southerly direction at an estimated speed of 60-70 MPH. Upon entering a 9.5 degree curve, the driver lost control and skidded off the road for 205 feet, striking a tree with the right rear fender. The vehicle continued an additional 15 feet where it struck another tree with the right rear fender area. The vehicle then rotated clockwise and skidded 45 feet more and struck another tree head-on at an estimated speed of 45-55 MPH. The case report gives no indication of post-impact movement of the vehicle. The case report schematic is shown in Figure 3.3.30. The primary VDI was 12FCEN6.

1.2 Primary Vehicle Right Front Occupant

16 year old male, height and weight unknown

The minor sideswipe impacts with the first two trees did not result in any injury. Upon impact with the third tree, this unrestrained occupant moved forward into the instrument panel, causing injuries principally to the head. His injuries may have been increased by loading of the seat back by the right rear occupant. There was no evidence that this passenger's head struck the windshield.

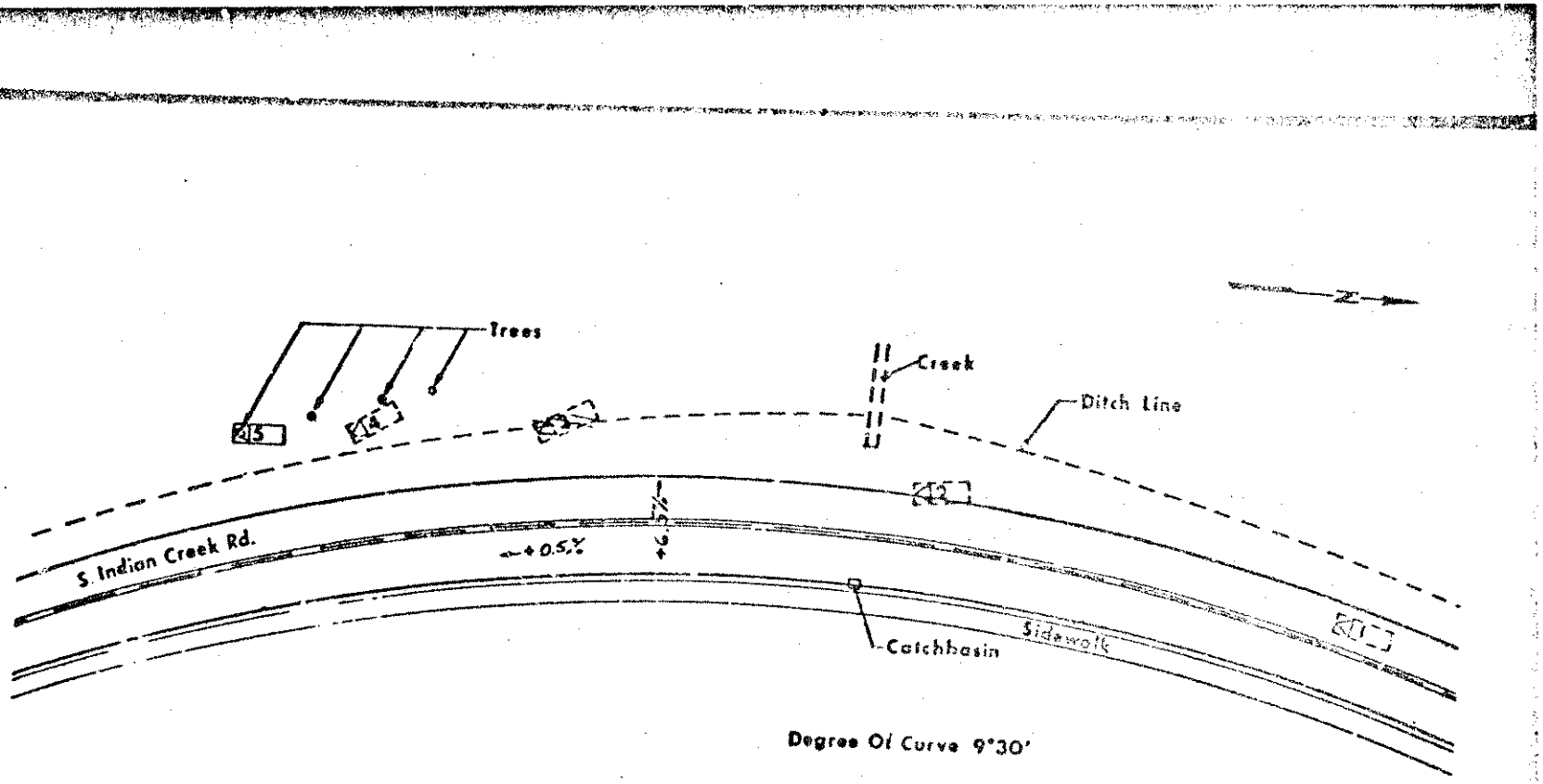

Figure 3.3.30

Accident Schematic - Case No. 56

Impact with the instrument panel resulted in a concussion, contusions to both eyes, a fractured nose and a right infra condylar fracture of the maxilla. Other minor injuries were sustained by the extremities. Overall injury severity index: Serious (AIS-4).

2. Analytical Reconstructions

2.1 SMAC Reconstruction

Because impacts with the first two trees were not injury-producing and the SMAC program can simulate impact only between two bodies, only the final head-on impact with the third tree was reconstructed. The SMAC input parameters used in the final iteration of this reconstruction are shown in Table A-2.9. The load-deflection characteristic of the vehicle structure for impact with the assumed 20 inch wide tree was 95 lb/in^2.

With these input parameters, an impact velocity of 32 MPH produced excellent agreement between the measured and predicted maximum deformation. The case report indicates a maximum deformation of approximately 29 inches, whereas the SMAC program predicted a value of slightly over 30 inches.

A comparison of the measured and predicted VDI's indicate discrepancies in the last two columns, 12FCEN5 measured versus 12FCEW3 predicted. As mentioned previously, the extent of damage discrepancy, column 7, is due to a change in the manner of coding. The discrepancy in column 6, narrow versus wide impact area, is a result of insufficient detail in the case report. The report did not indicate the size of the tree that was struck. Consequently, a rough estimate was made from the photograph of vehicle damage.

The resultant acceleration and angle of the acceleration vector from the SMAC program for this case are shown in Figure 3.3.31. The predicted damage pattern is also shown in Figure 3.3.31. The reconstruction summary is presented in Figure 3.3.32.

2.2 3-D Crash Victim Reconstruction

In this case, there is a noticeable difference between the reported head contact (on the instrument panel) and the prediction of head-windshield impact (see Figure 3.3.33). Considering the two collisions prior to the main impact event, it is likely that the accident victim braced himself prior to the final impact, rather than maintaining the passive posture inputted to the program*. As demonstrated in connection with Case No. AA145, such bracing would likely have prevented the windshield impact and quite possibly would have resulted in the observed head-instrument panel contact instead.

*Only the orientation of the legs (knees raised) was selected to correspond to some degree to the observation in the case report that head-instrument panel contact occurred. The initial crash victim position, orientation, and muscle condition must be regarded as uncertain to some degree.

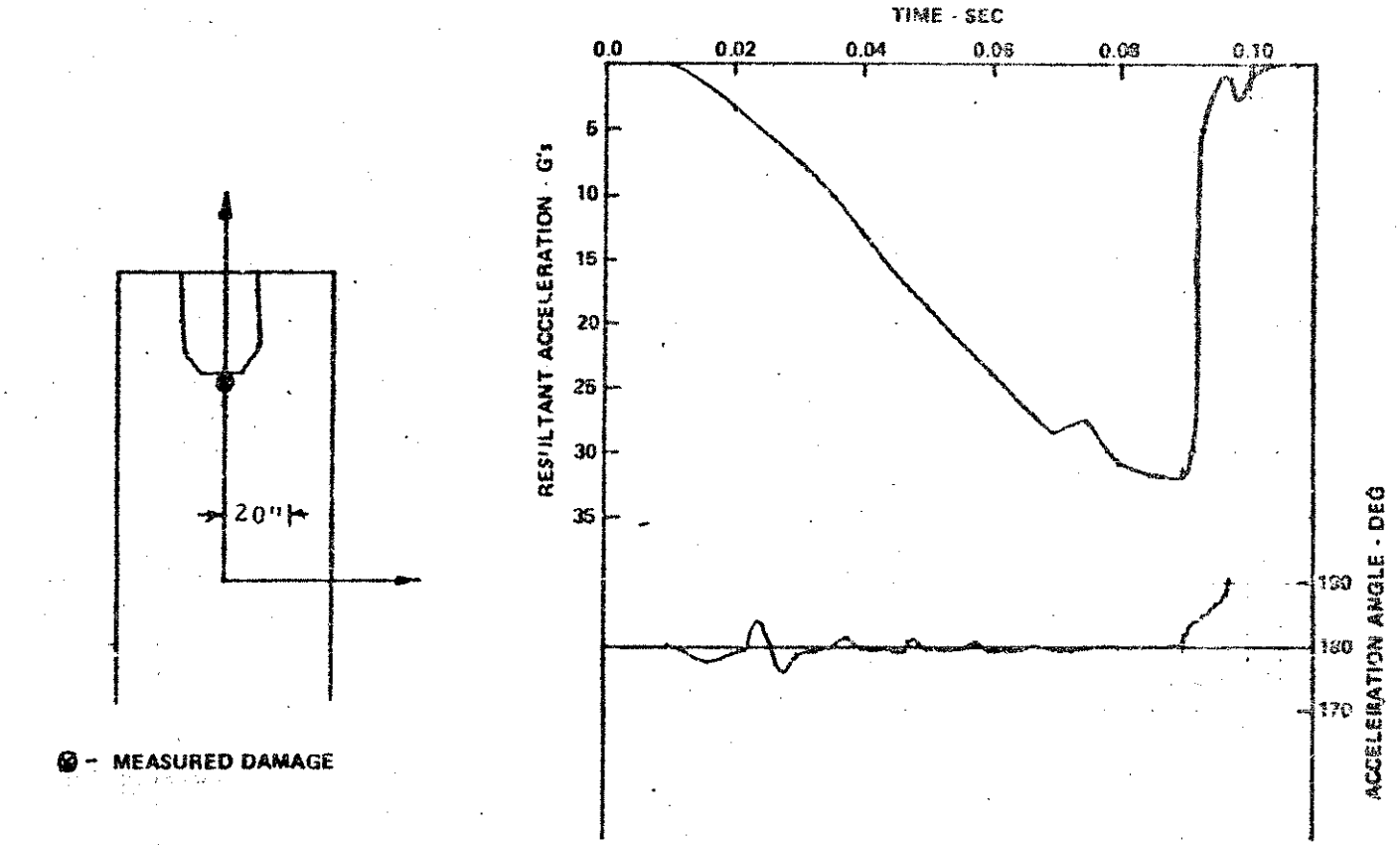

100

ZQ-5341-V-1

Figure 3.3.31 ACCELERATION AND DAMAGE - CASE NO. 56

Figure 3.3.32

Accident Reconstruction Summary - Case No. 56

GRAPHIC DISPLAY OF OUTPUTS OF ACCIDENT RECONSTRUCTION

COLLISION AND TRAJECTORY

CASE NO. 56 RUN NO. 010[illegible]

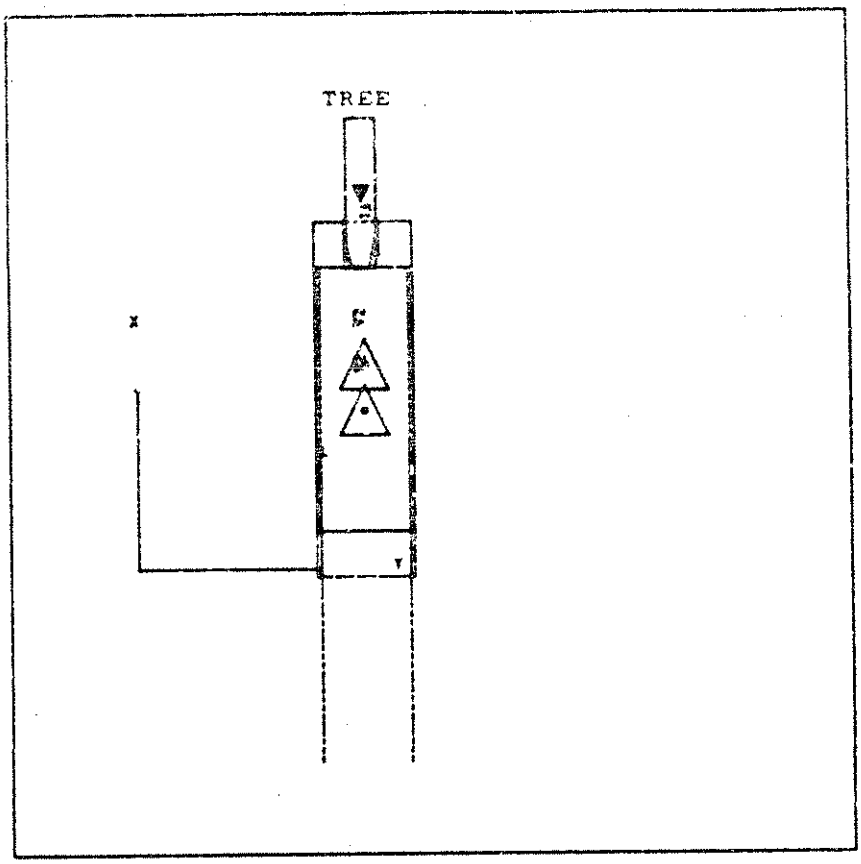

AXIS INTERVALS ARE 10. FEET

RECONSTRUCTED POSITIONS AND VELOCITIES AT IMPACT							DISPLAYED FINAL POSITIONS				VEHICLE DAMAGE INDICES	ΔV
	C.G. POSITION		HEADING				C.G. POSITION		HEADING	REMARKS		
	XC1	YC1	PSI1	FWD	LATERAL	ANGULAR	XC1F	YC1F	PSI1F			
	FT.	FT.	DEG.	MPH	MPH	DEG/SEC	FT.	FT.	DEG.			MPH
VEHICLE # 1	20.8	12.4	180.0	0.0	0.0	0.0	20.8	12.4	180.0	VEHICLE AT REST	[illegible]	0.0
VEHICLE # 2	8.8	12.5	0.0	32.0	0.0	0.0	11.5	42.5	0.0	VEHICLE AT REST	12FCYW5	32.5

CASE NO. GI 00056

Crash Victim -

Male
16 Years
Height Unknown
Weight Unknown

Accident -

Head struck instrument panel - concussion

Injury Rating -

Head - 3 (Severe)
Face - 3
Brain - 2 (Moderate)
Overall - 4 (Serious)

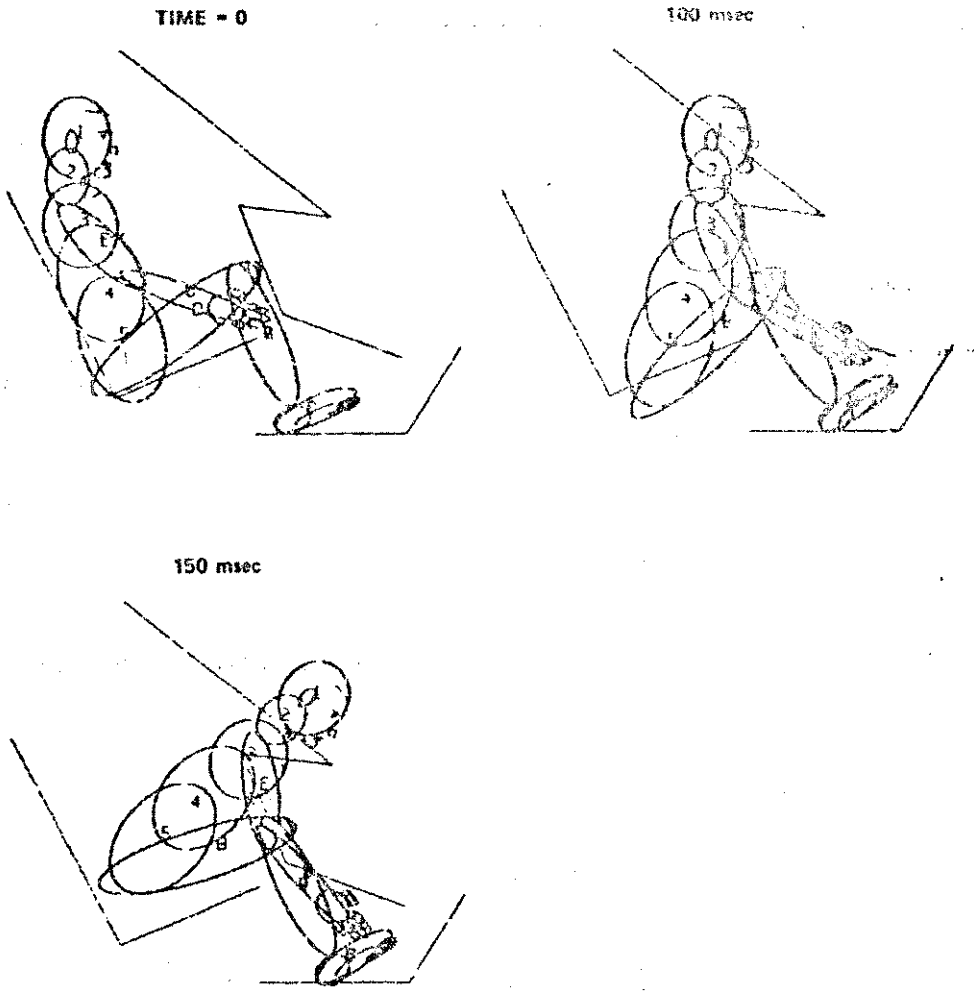

Figure 3.3.33
Accident Reconstruction Summary -
Case No. 56

CASE NO. 973D (Case Identification No. TR00973)

1. Case Report Summary

Primary Vehicle - 1965 Ford Galaxie
Secondary Vehicle - 1968 Pontiac Ventura
Additional Vehicles - 1965 Chevrolet
1968 Opel Kadett

1.1 Description of Accident

Pre-crash:

The primary vehicle was traveling the wrong way on a divided freeway resulting in a head-on collision between the primary and secondary vehicles. The secondary vehicle (Pontiac) was being followed by the third (Chevrolet) and fourth (Opel) vehicles in the same lane. There was no reported evidence of attempted evasive maneuvers for vehicles 1 and 2 during the pre-crash phase. The case report schematic is shown in Figure 3.3.34. No speed estimates were reported.

Crash:

Vehicles 1 and 2 collided in an offset frontal orientation. Vehicle 3, in attempting an evasive maneuver, struck vehicle 2 in the left rear imparting an additional yaw impulse. Subsequent collisions occurred which had no influence on the primary collision. The Ford rebounded a short distance and came to rest on the median strip. The Pontiac spun approximately 100° counterclockwise due to a combination of the primary impact and a secondary impact on the left rear quarter from the Chevrolet. The reported VDI's were 12FLEW5 for vehicle 1 and 12FLEW3 for vehicle 2.

Figure 3.3.34

Accident Schematic - Case No. 973D

V1 - 1965 FORD GALAXIE 2 DOOR HARDTOP
V2 - 1966 PONTIAC VENTURA 4 DOOR SEDAN
V3 - 1965 CHEVROLET 2-DOOR
V4 - 1968 OPEL KADETT 2-DOOR STA. WAG.

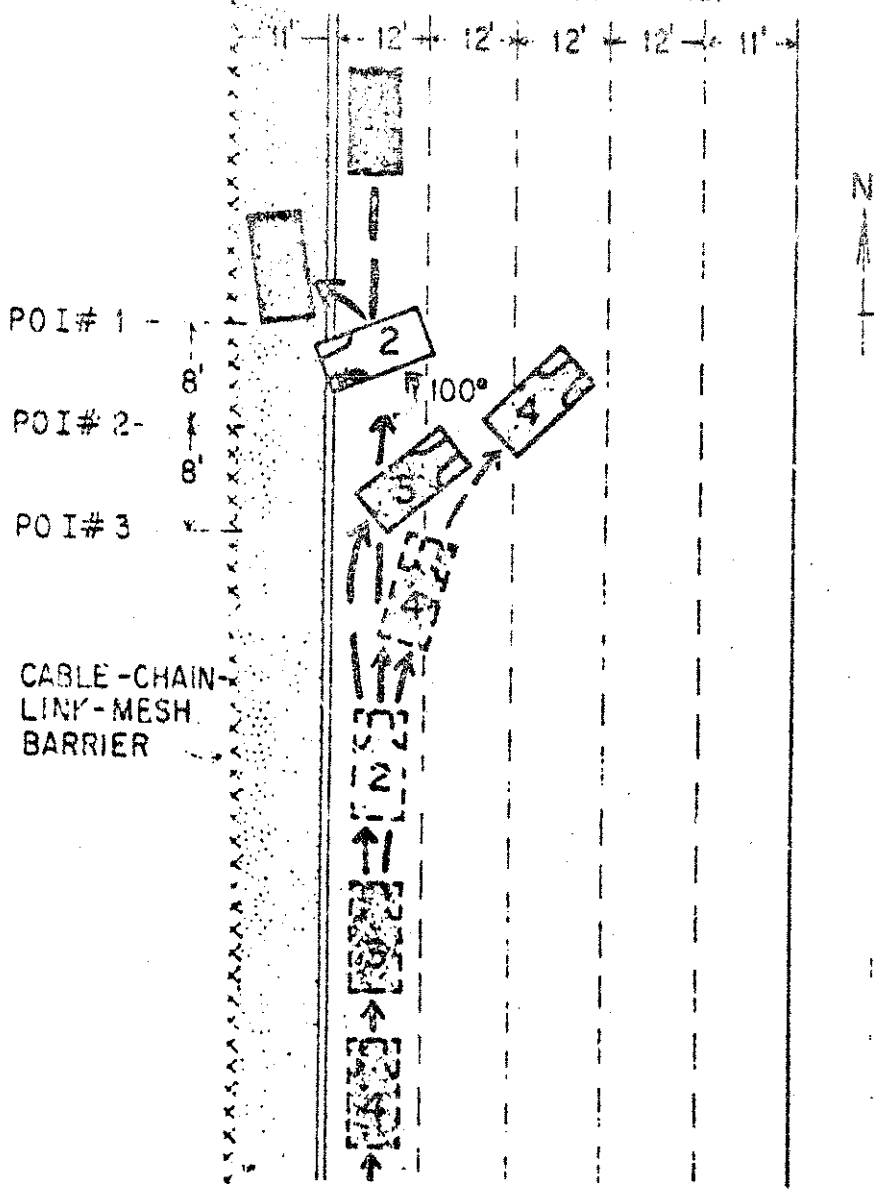

ZQ-5341-V-1

1.2 Primary Vehicle Right Front Occupant

52 year old male, 71" tall, 155 lbs.

On impact, this unrestrained occupant moved forward in a seated posture, striking his knees on the lower instrument panel. He continued forward and to the left, striking the instrument panel at the corner of the eyebrow over the instrument cluster and sustaining fractures of the rib cage. His face then struck the windshield fracturing the glass and rupturing the interlayer, sustaining abrasions and lacerations to the face and head. In addition, he sustained abrasions to the legs and a fractured sternum. Injury severity index: Fatal (AIS-6). The fatal injuries were incurred by the thorax. The facial injuries were rated as Minor (AIS-1).

2. Analytical Reconstruction

2.1 SMAC Reconstruction

The inputs for the SMAC program used in the reconstruction of this case are shown in Table A-2.10. The reconstructed pre-impact speeds were determined to be 37 MPH for vehicle 1 and 34 MPH for vehicle 2. Note that collision-induced braking of the left front wheel of both vehicles was assumed to start at impact

A comparison of the predicted and measured VDI's for both vehicles is shown below.

	Measured	Predicted
Vehicle 1	12FLEW5	11FYEW4
Vehicle 2	12FLEW3	11FYEW4

Disparities in the predicted and measured VDI's resulted from an attempt to maximize agreement with all physical evidence. In this case somewhat greater overlap was accepted in the reconstruction than was evidenced at the scene because it resulted in closer agreement with other evidence. As a result column 4 contains Y rather than L. The differences in clock direction are attributed to intervehicular friction during the collision. The damage patterns from the SMAC runs are shown in Figure 3.3.35, and the resultant acceleration and angle for the primary vehicle are also shown in Figure 3.3.35.

The reconstructed rest positions and orientations for this case (Figure 3.3.36) are not in good agreement with the investigator's report. This is believed to result from a secondary collision involving vehicle 2. During the primary collision (involving vehicles 1 and 2), a third vehicle struck the left rear of vehicle 2 while attempting an evasive maneuver. This impact imparted an additional yaw impulse to vehicle 2 which resulted in an additional lateral displacement of vehicle 1 as shown in the case report schematic, Figure 3.3.34. While this additional impact had a substantial effect on the rest positions and orientations, it is not believed to have affected greatly the primary deceleration impulse of vehicle 1 since it most likely occurred late in time.

2.2 3-D Crash Victim Reconstruction

As illustrated in Figure 3.3.37, the predicted kinematic responses of the right front occupant are in excellent agreement with the observations of the accident case report. In addition to total penetration of the windshield by the head, severe thoracic crushing is indicated by the plotter graphics displays. Furthermore, the initial knee contact with the lower instrument panel is also in agreement with the findings of the case report.

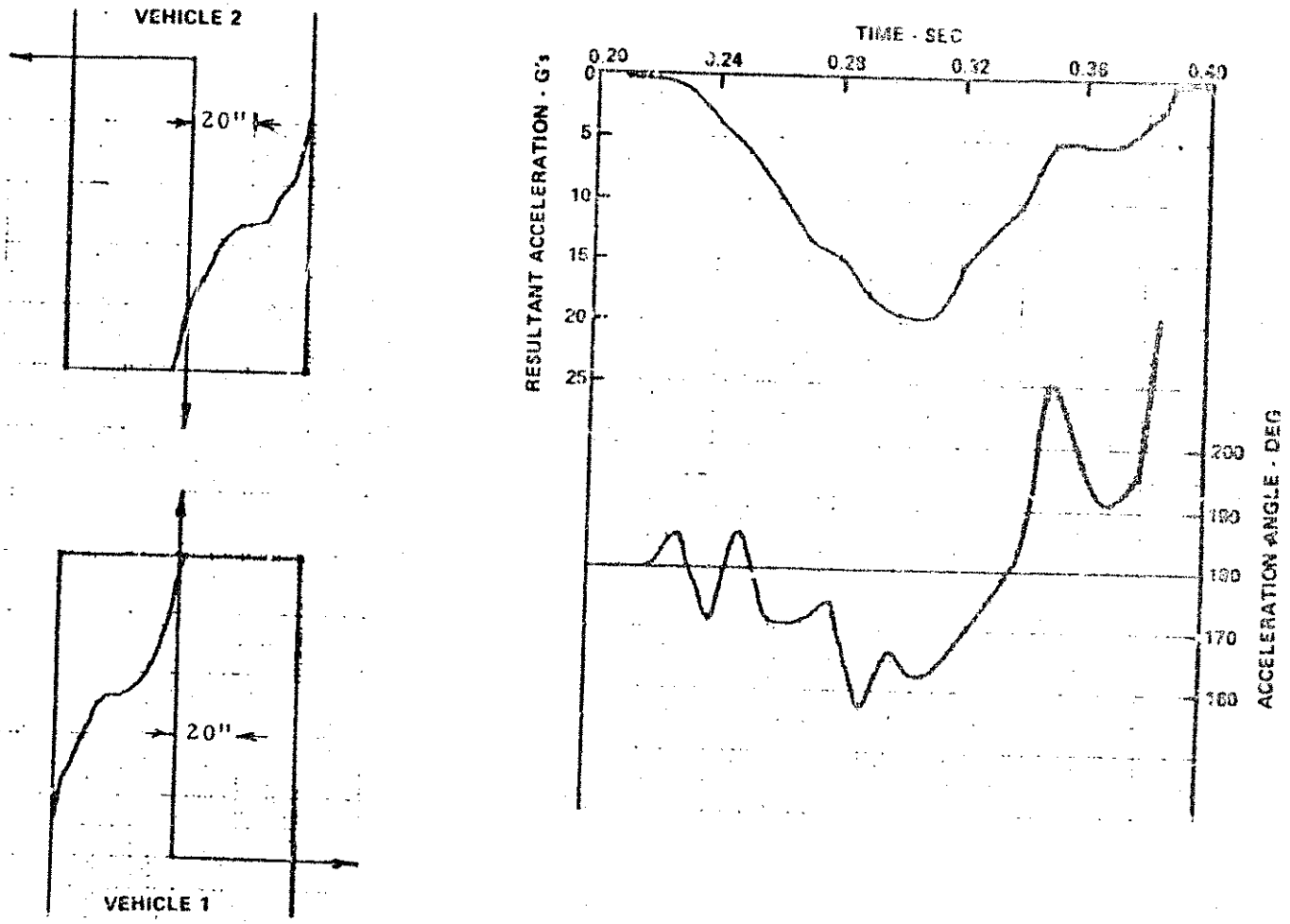

Figure 3.3.35 ACCELERATION AND DAMAGE - CASE NO. 973D

ZQ-5341-V-1

GRAPHIC DISPLAY OF OUTPUTS OF ACCIDENT RECONSTRUCTION

COLLISION AND TRAJECTORY

CASE NO. 973D RUN NO. TR030973

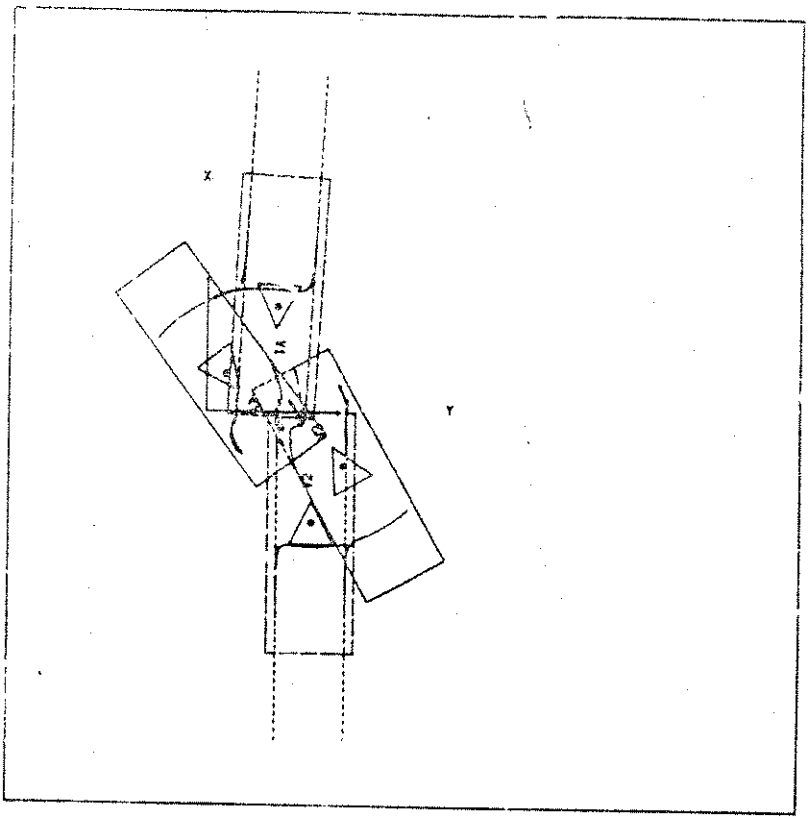

AXIS INTERVALS ARE 10. FEET

	RECONSTRUCTED POSITIONS AND VELOCITIES AT IMPACT						DISPLAYED FINAL POSITIONS				VEHICLE SAMPLE INDICES	ΔV
	C.G. POSITION		HEADING				C.G. POSITION		HEADING	REMARKS		
	XC1	YC1	PSI1	SPD	LATERAL	ANGULAR	XC1F	YC1F	PSI1F			
	FT.	FT.	DEG.	MPH	MPH	DEG/SEC	FT.	FT.	DEG.			MPH
VEHICLE # 1	8.0	5.4	183.0	38.9	0.0	-0.3	2.9	1.5	149.0	VEHICLE AT REST	1 1 F Y E N 4	35.0
VEHICLE # 2	-8.4	8.1	-0.0	34.1	0.0	-0.3	-4.1	10.5	-29.<	VEHICLE AT RES.	1 1 F Y E N 4	32.9

Figure 3.3.36 ACCIDENT RECONSTRUCTION SUMMARY - CASE NO. 973D

Crash Victim -

Male
52 Years
71 in.
155 lbs.

Accident -

Face struck windshield (broken) - facial abrasions/lacerations, severe thoracic injuries

Injury Rating -

Face - 1 (Minor)
Overall - 6 (Fatal)

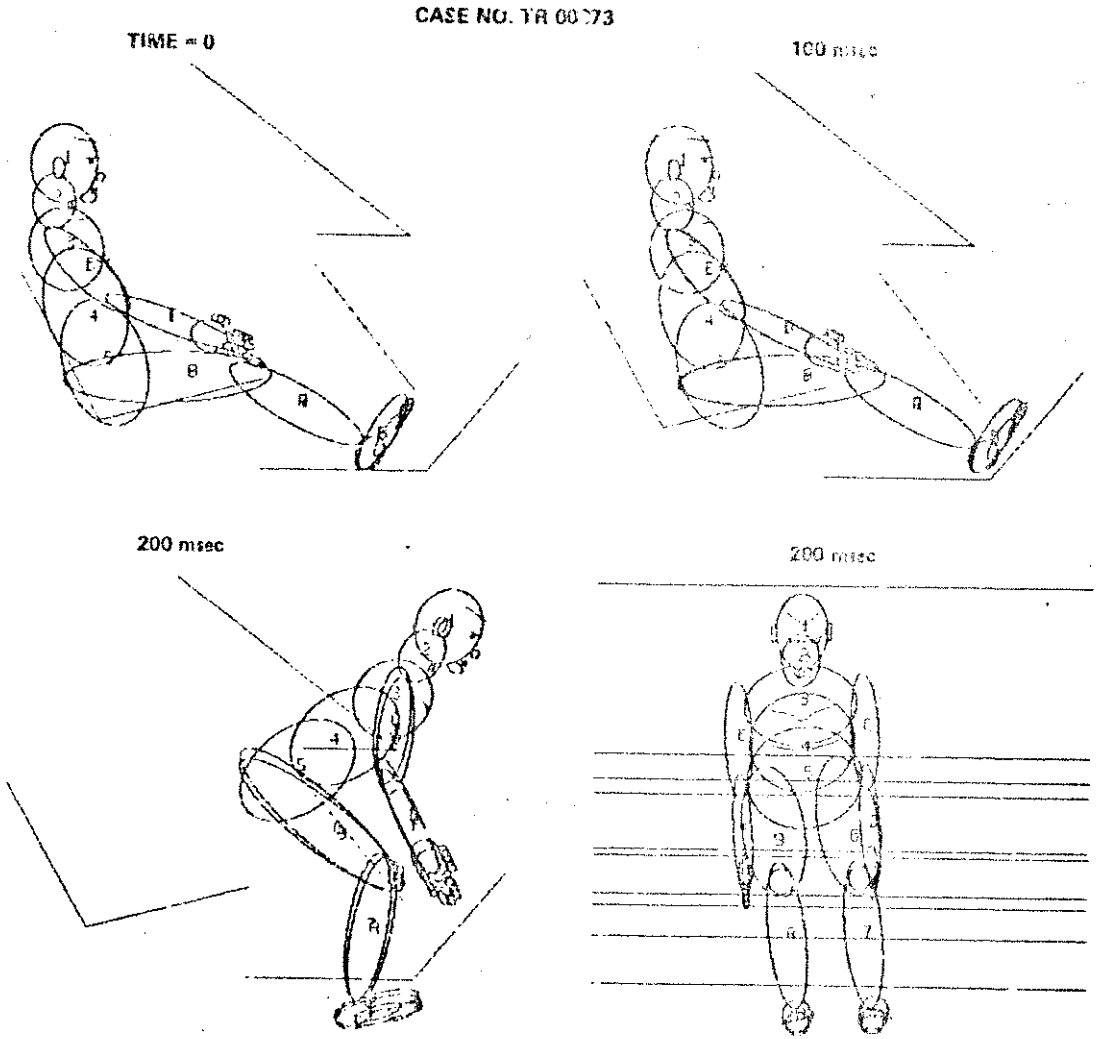

Figure 3.3.37
Accident Reconstruction Summary -
Case No. 973D

3.4 Summary of Impact Sled Test Results

A concise summary of the impact sled tests that were performed is presented in Table 3.4.1. In addition to one test corresponding to each of the ten accidents, three additional sled runs were performed to vary parameters as follows:

- variation in stiffness of the dummy joints, to study the effect of muscular reaction by the crash victim in anticipation of collision (sled run nos. 1139 and 1140)

- variation in dummy size (5th percentile female, compared to 50th percentile male), to assess the importance of matching the crash victim stature and weight with that of the dummy (sled run nos. 1134 and 1135)

- variation in vehicle interior geometry (seat location relative to the windshield) to obtain an indication of the results of a mismatch between the occupant position and/or vehicle interior in the actual vehicle and that in the reconstruction sled test (sled run nos. 1142 and 1143).

Items worth noting in Table 3.4.1 are:

(1) the wide range of accident vehicle sizes

(2) frontal or near-frontal vehicle impacts in all cases

(3) a broad range of predicted vehicle speed changes

(4) only 2 dummy sizes (50th percentile male and 5th percentile female) to represent the ten different crash victim sizes*

(5) minimal use of restraints (belts).

*See Table 3.3.1 for a summary of the crash victim sizes and weights.

Table 3.4.1

Summary of Impact Sled Test Conditions

	Sled Run Number	Case Identification Number	Predicted (SMAC) Speed Change, mph	Buck Rotation Angle, deg.	Accident Vehicle	Dummy (Right Front Occupant)	Restraint	Remarks
1.	1139	AA00145	28.7	2	1972 Mercury Comet	50th Pct. Male	Lap Belt	
2.	1140	AA00145	28.7	2	1972 Mercury Comet	50th Pct. Male (stiff joints)	Lap Belt	Joint Stiffness Varied
3.	1141	TR01316	12.5	0	1969 Chevrolet Nova	50th Pct. Male	Lap Belt	
4.	1138	CA71031	34.5	2	1970 Plymouth Barracuda	50th Pct. Male	None	
5.	1136	CB00072	28.2	4	1970 Chevrolet Camaro	50th Pct. Male	None	
6.	1144	SW71044	8.6	6	1965 Ford Custom	50th Pct. Male	None	
7.	1145	CB00053	40.6	6	1970 Chevrolet Nova	50th Pct. Male	None	
8.	1135	CB71055	18.6	-12	1971 Ford Mustang	50th Pct. Male	None	
9.	1134	CB71055	18.6	-12	1971 Ford Mustang	5th Pct. Female	None	Dummy Size Varied
10.	1137	TR01161	38.6	4	1968 American AMX	50th Pct. Male	None	
11.	1142	GI00056	32.3	0	1969 Pontiac LeMans	50th Pct. Male	None	
12.	1143	GI00056	32.3	0	1969 Pontiac LeMans (seat location varied)	50th Pct. Male	None	Vehicle Interior Geometry Varied
13.	1146	TR00973	35.0	-6	1965 Ford Galaxie	50th Pct. Male	None	

In Figures 3.4.1 to 3.4.13, succinct summaries of the physical reconstructions are presented for the thirteen impact sled tests.

Briefly, these summaries, when compared with the case reports, indicate:

(1) For seven of the ten accident cases, the physically reconstructed responses of the occupants agree generally with the evidence summarized in the accident case reports.*

Discrepancies of occupant responses are considered to be primarily attributable to active occupant responses in anticipation of crash, plus various other factors discussed in the next section.

A comparison of actual occupant injuries (as measured by overall injury severity on the 10-point scale) with values of the measured head severity index (HSI) is shown in Figure 3.4.14. From this comparison, it can be seen that there is no distinct correlation with the observed injuries measured on the ten-point scale.

In Figure 3.4.15, the measured values of HSI are compared to an envelope of experimental results from windshield impact tests that were previously discussed (see Figures 1.1 and 1.2).** From Figure 3.4.15, it is noted that:

(1) No distinct correlation is indicated between speed and HSI, although a general trend is evident.

---

* For both the actual accidents and the sled tests, the dimensions relating to windshield failure are the values from the right upper corner of the windshield (as viewed from inside) to the indicated contact location, in the (local) plane of the windshield.

** As discussed in Section 3.2, speed change rather than impact speed is the more meaningful parameter for the abscissa of Figure 3.4.15.

CRASH VICTIM -

MALE
19 YEARS
70 in.
150 lb
LAP BELT IN USE

ACCIDENT -

HEAD STRUCK INSTRUMENT PANEL - FACIAL ABRASIONS/ LACERATIONS

INJURY RATING -

HEAD - 1 (MINOR)
FACE - 1
OVERALL - 1

WINDSHIELD -

UNBROKEN, UNCRACKED, NO CONTACT REPORTED.

Figure 3.4.1 CASE NO. AA00145
SLED RUN NO. 1139

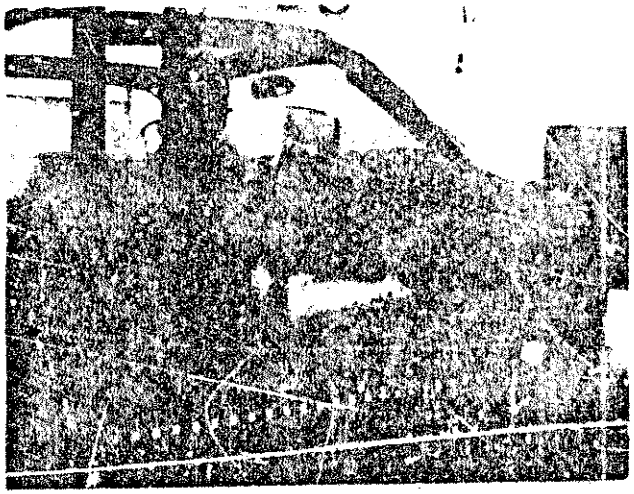

PRE-TEST

POST-TEST

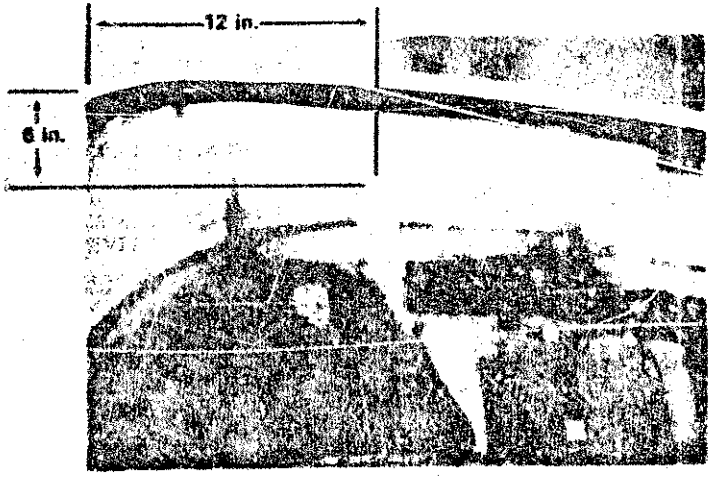

WINDSHIELD CONTACT

CRASH VICTIM -

MALE
19 YEARS
70 in.
150 lb
LAP BELT IN USE

ACCIDENT -

HEAD STRUCK INSTRUMENT PANEL - FACIAL ABRASIONS/ LACERATIONS

INJURY RATING -

HEAD - 1 (MINOR)
FACE - 1
OVERALL - 1

WINDSHIELD

UNBROKEN, UNCRACKED, NO CONTACT REPORTED.

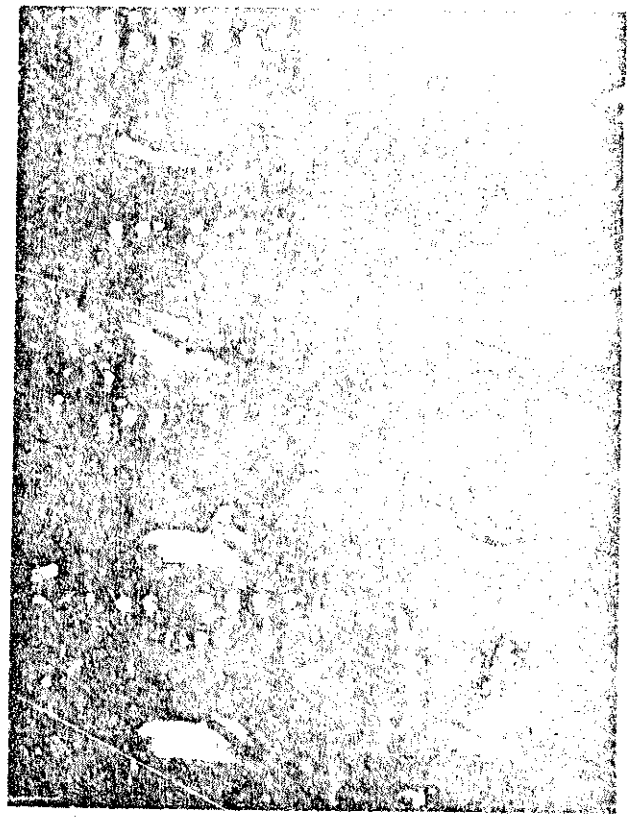

Figure 3.4.2 CASE NO. AA00145
SLED RUN NO. 1140

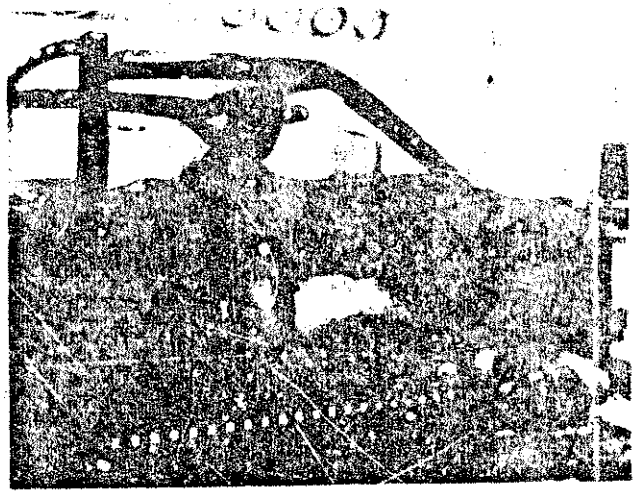

PRE-TEST

POST-TEST

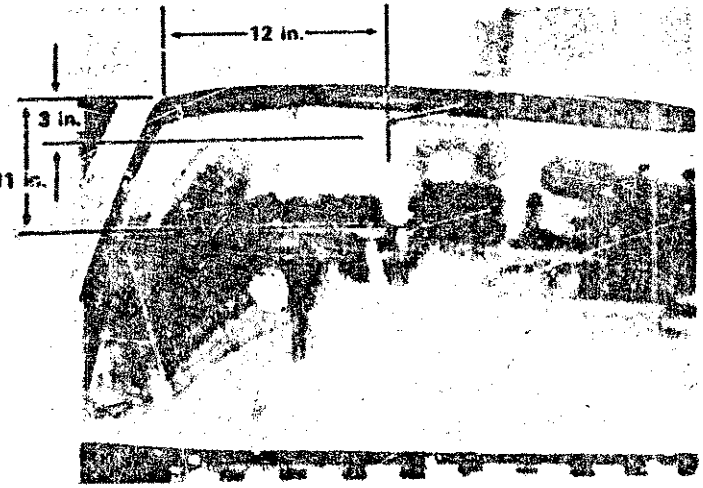

WINDSHIELD CONTACT

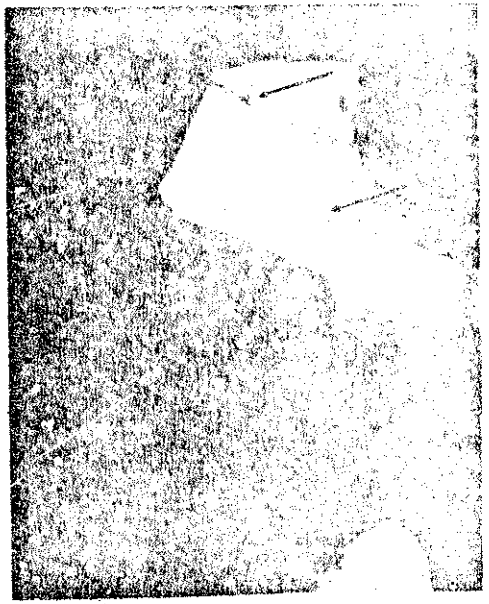

Figure 3.4.2 (Cont'd.)

CRASH VICTIM -

MALE
15 YEARS
68 in.
150 lb
LAP BELT IN USE

ACCIDENT -

HEAD STRUCK UPPER INSTRUMENT PANEL - CONCUSSION, FACIAL CONTUSION, LACERATION

INJURY RATING -

FACE - 1 (MINOR)
BRAIN - 1
OVERALL - 1

WINDSHIELD

UNBROKEN, UNCRACKED, NO CONTACT REPORTED.

Figure 3.4.3 CASE NO. TR01316
SLED RUN NO. 1141

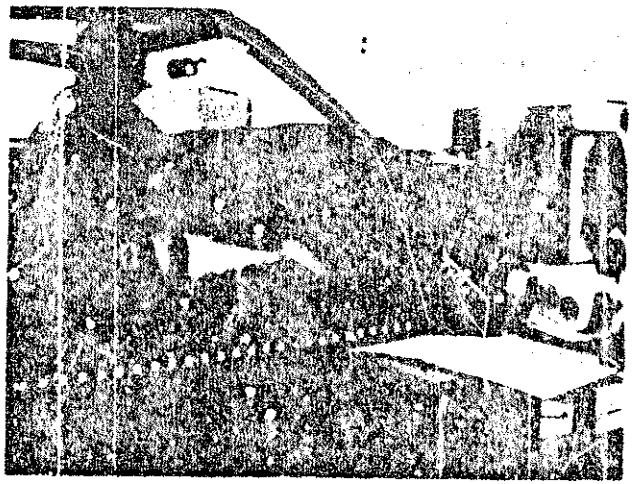

PRE-TEST

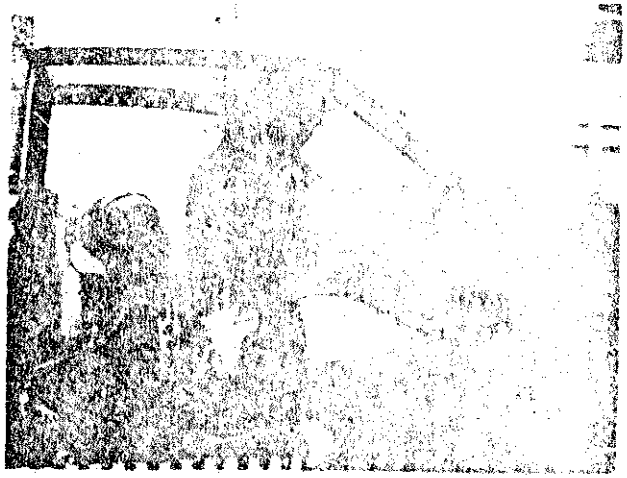

POST-TEST

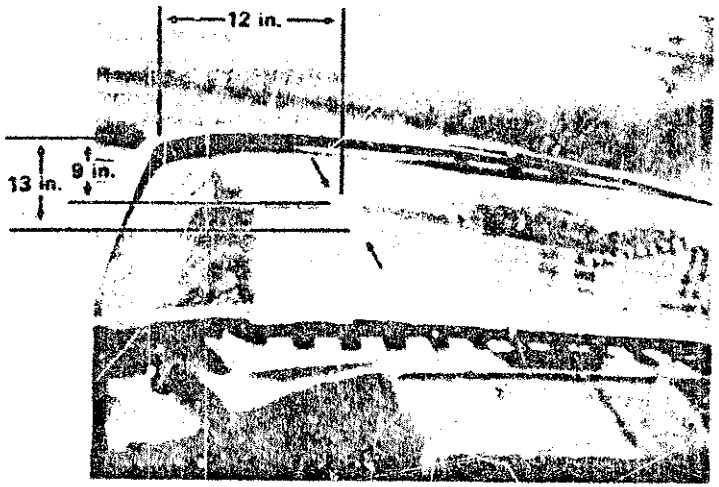

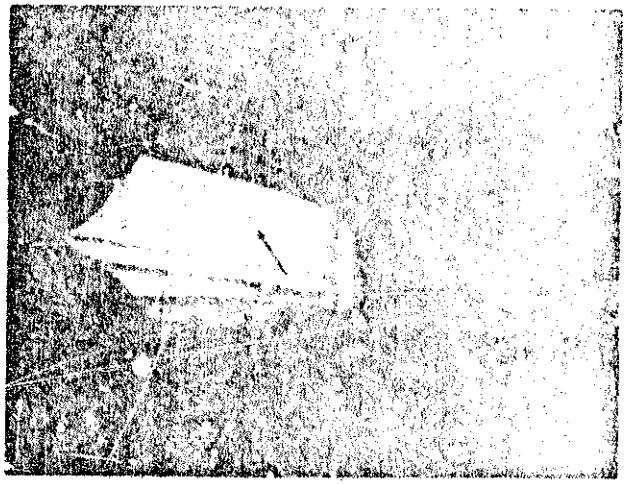

WINDSHIELD CONTACT

Figure 3.4.3 (Cont'd.)

CRASH VICTIM

MALE
13 YEARS
70 in.
180 lb

ACCIDENT -

FACE STRUCK INSTRUMENT PANEL (PROBABLE) - CONCUSSION, FACIAL CONTUSION

INJURY RATING -

FACE - 2 (MODERATE)
BRAIN - 1 (MINOR)
OVERALL - 2

WINDSHIELD -

CRACKED AND BROKEN, NO CONTACT REPORTED.

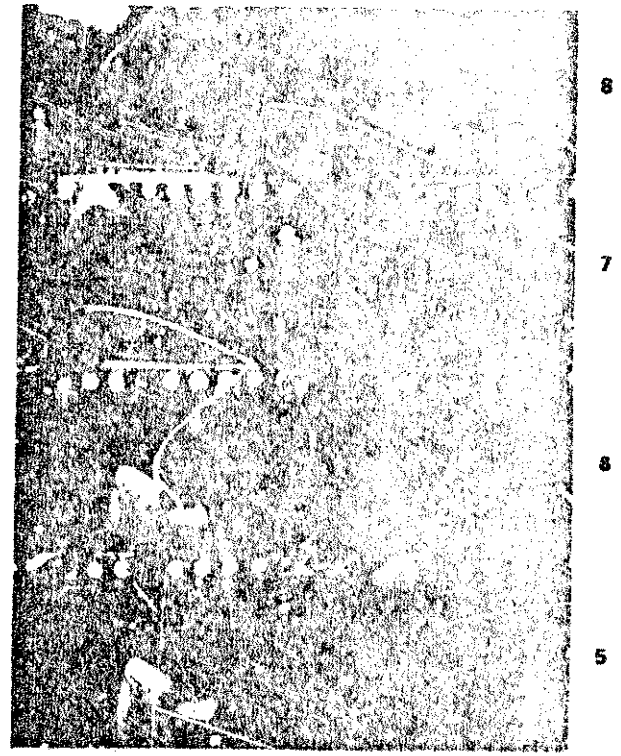

Figure 3.4.4 CASE NO. CA71031
SLED RUN NO. 1138

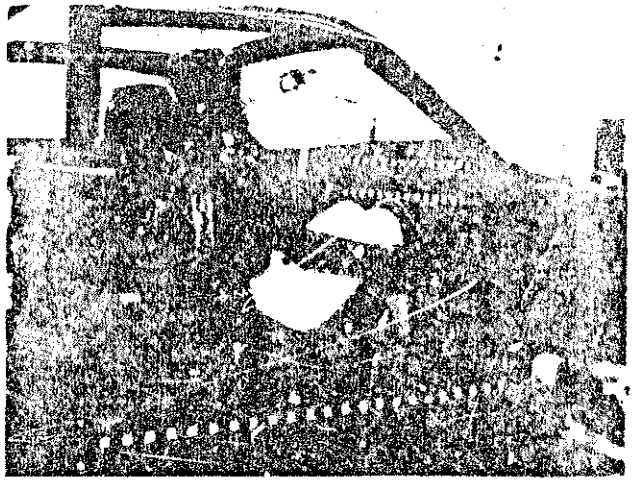

PRE-TEST

POST-TEST

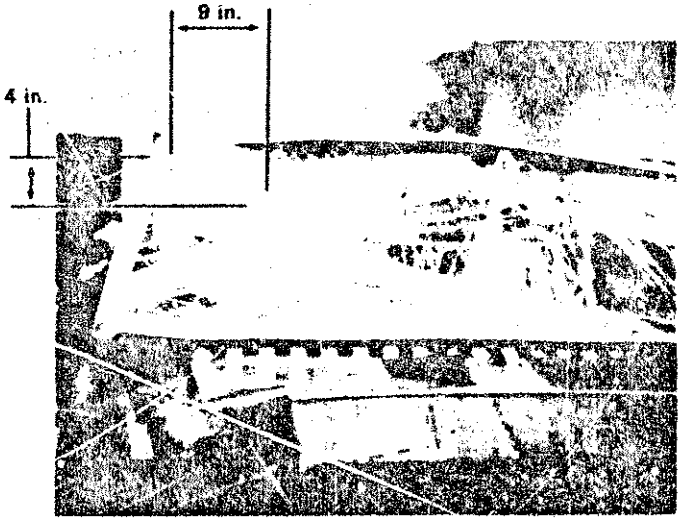

WINDSHIELD CONTACT

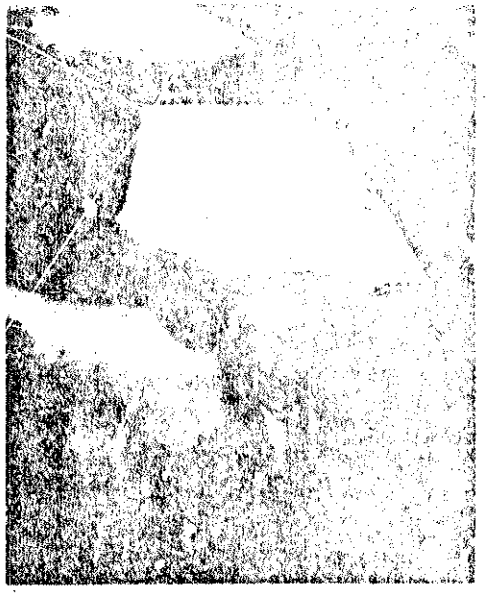

Figure 3.4.4 (Cont'd.)

CRASH VICTIM -

MALE
18 YEARS
70 in.
165 lb

ACCIDENT -

HEAD STRUCK SUNVISOR, WINDSHIELD, INSTRUMENT PANEL - CONTUSIONS/ ABRASIONS TO FOREHEAD AND CHIN

INJURY RATING -

FACE - 2 (MODERATE)
OVERALL - 2

WINDSHIELD -

CRACKED AND BROKEN, HOLES THROUGH INTERLAYER.

AS VIEWED FROM INSIDE:

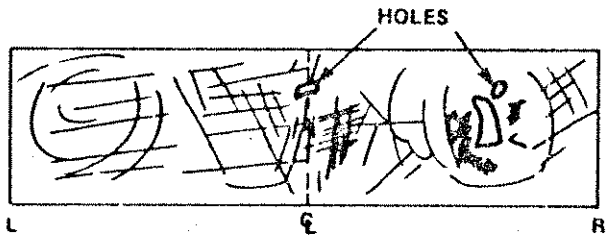

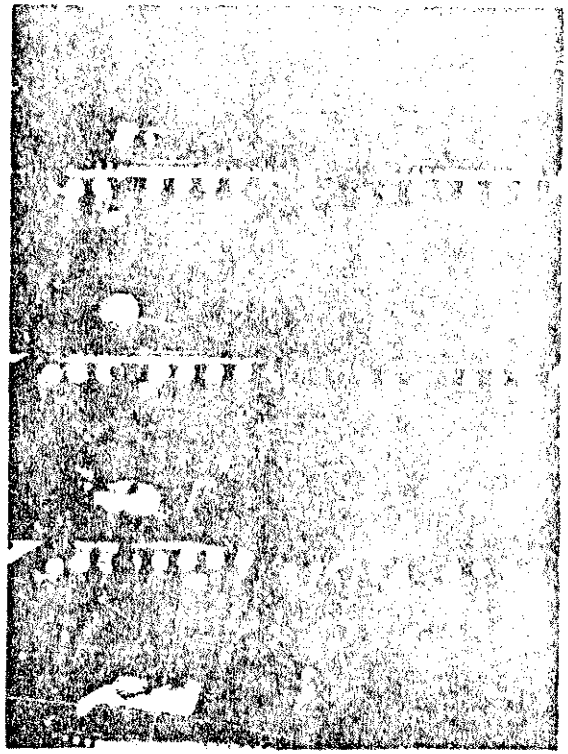

Figure 3.4.5 CASE NO. CB00072
SLED RUN NO. 1136

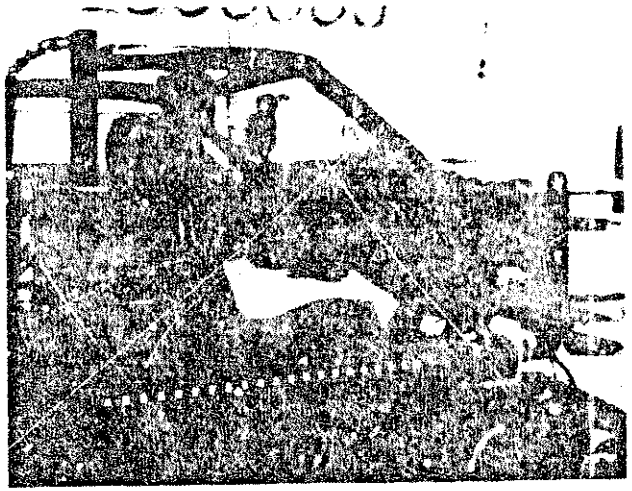

PRE-TEST

POST TEST

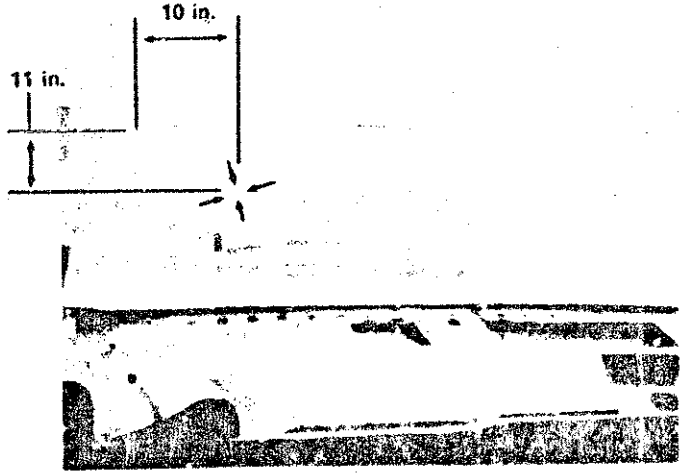

WINDSHIELD CONTACT

122

ZO-5341-V-1

CRASH VICTIM -

MALE
18 YEARS
71 in.
160 lb

ACCIDENT -

FACE STRUCK WINDSHIELD (BROKEN) - FACIAL LACERATION

INJURY RATING -

FACE - 2 (MODERATE)
OVERALL - 2

WINDSHIELD -

CRACKED AND BROKEN, HOLES THROUGH INTERLAYER.

AS VIEWED FROM INSIDE:

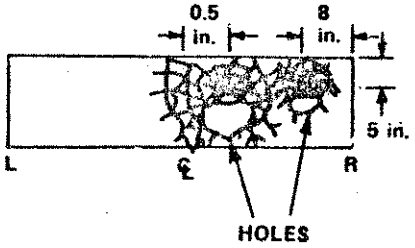

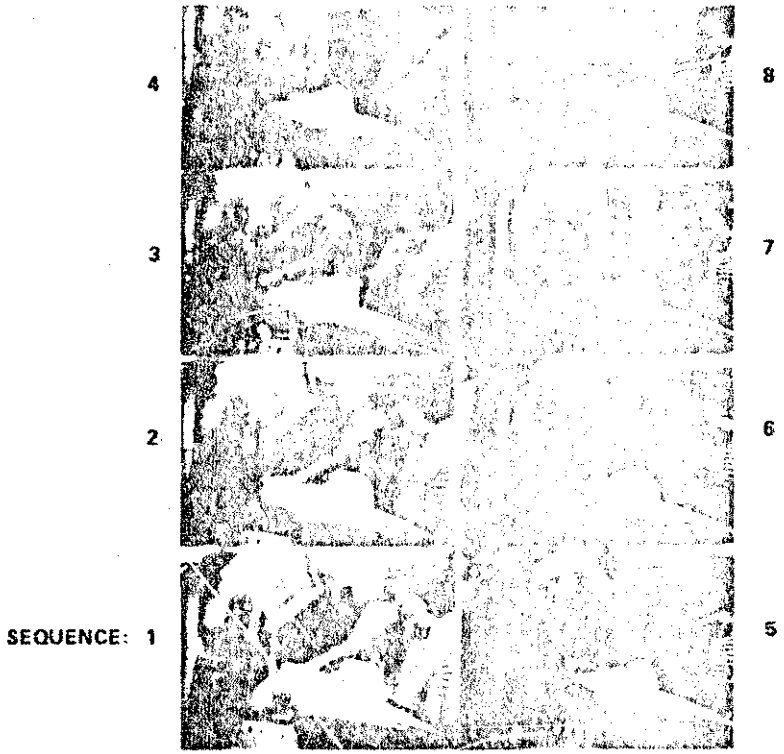

Figure 3.4.6 CASE NO. SW71044
SLED RUN NO. 1144

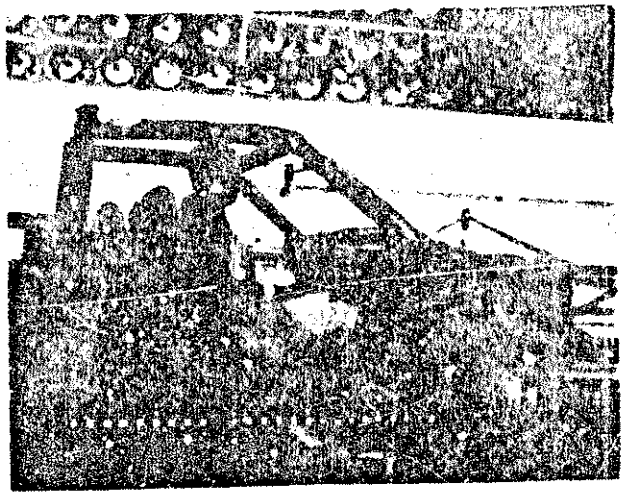

PRE-TEST

POST-TEST

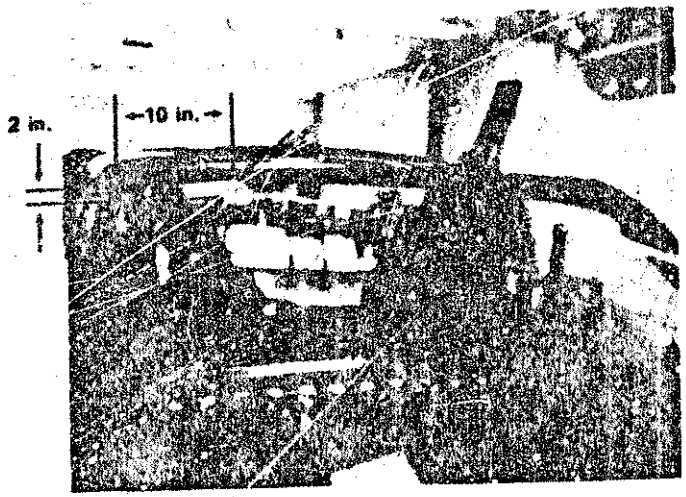

WINDSHIELD CONTACT

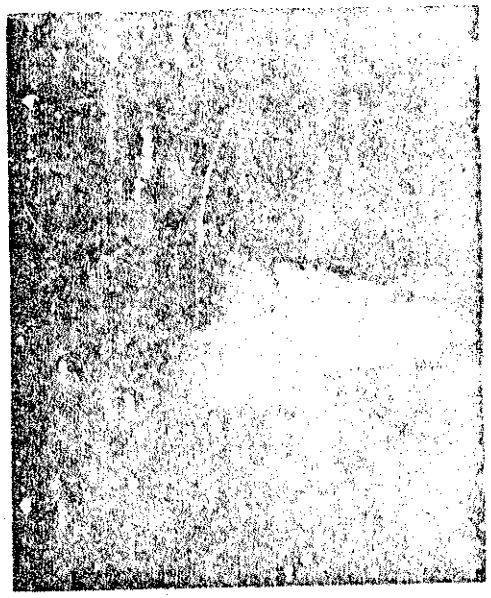

CRASH VICTIM -

FEMALE
52 YEARS
60 in.
130 lb

ACCIDENT -

HEAD STRUCK WINDSHIELD - FACIAL ABRASIONS/ LACERATIONS, BROKEN TEETH (LOSS OF CONSCIOUSNESS)

INJURY RATING -

HEAD - 1 (MINOR)
FACE - 2 (MODERATE)
BRAIN - 3 (SEVERE)
OVERALL - 3

WINDSHIELD -

CRACKED AND BROKEN.
AS VIEWED FROM INSIDE:

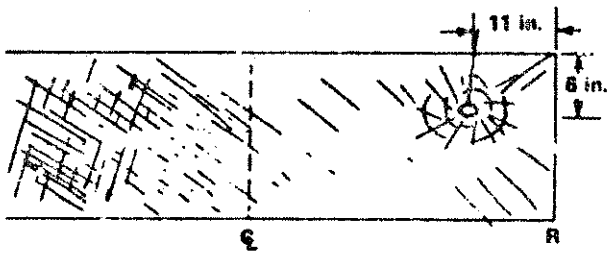

Figure 3.4.7 CASE NO. CB00053
SLED RUN NO. 1145

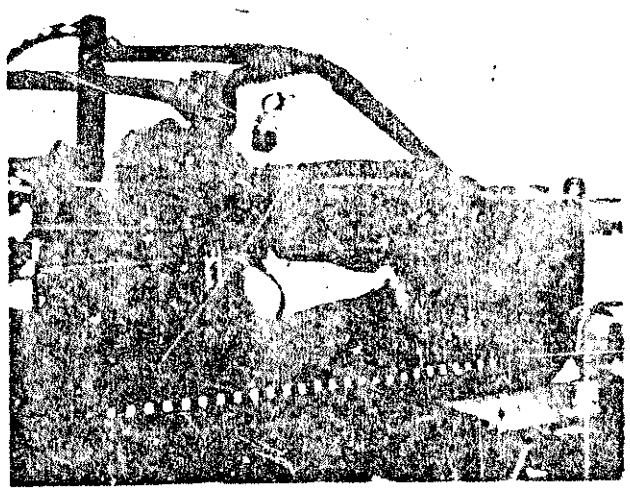

PRE-TEST

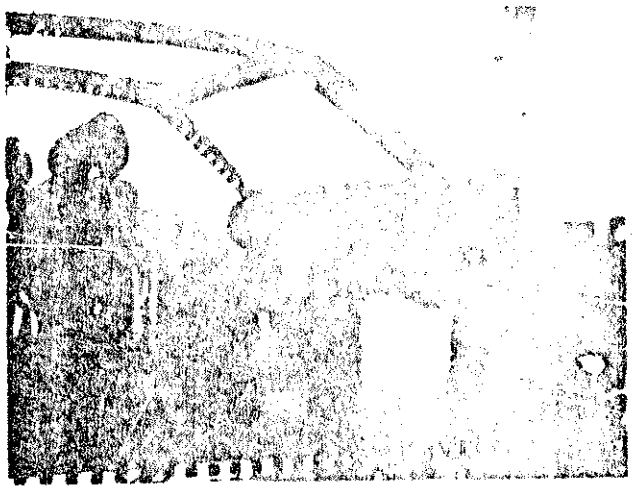

POST-TEST

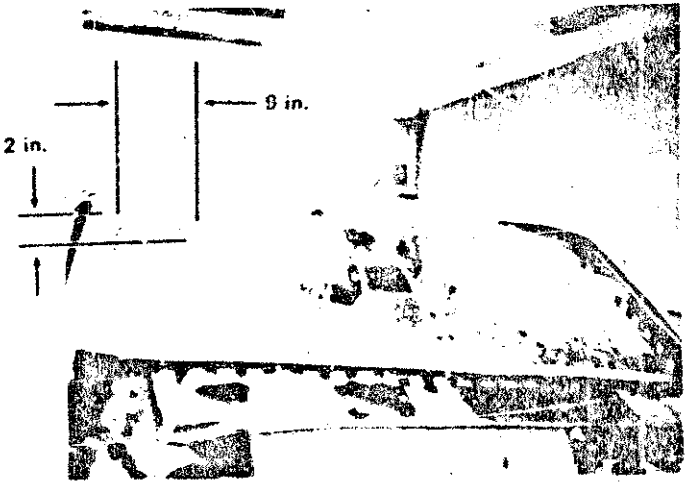

WINDSHIELD CONTACT

ZQ-5341-V-1

Figure 3.4.7 (Cont'd.)

CRASH VICTIM -

FEMALE
49 YEARS
60 in.
130 lb

ACCIDENT -

HEAD STRUCK REAR VIEW MIRROR, UPPER INSTRUMENT PANEL - FACIAL LACERATIONS, FRACTURED TEETH

INJURY RATING -

HEAD - 1 (MINOR)
FACE - 3 (SEVERE)
OVERALL - 3

WINDSHIELD -

UNBROKEN, UNCRACKED, NO CONTACT REPORTED.

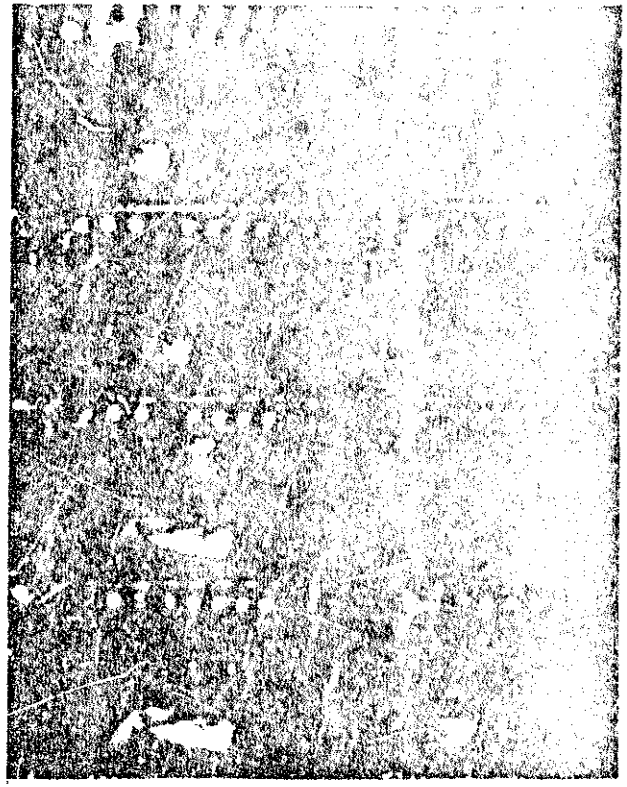

Figure 3.4.8 CASE NO. CB71065
SLED RUN NO. 1135

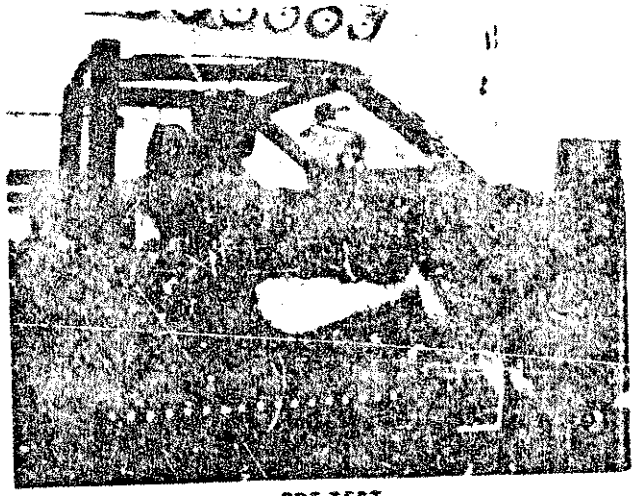

PRE-TEST

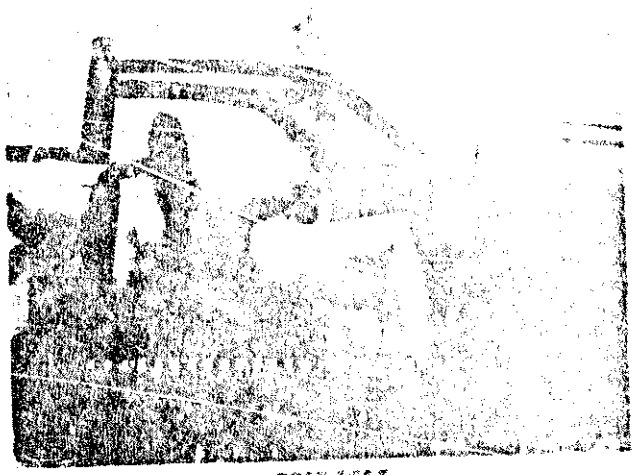

POST TEST

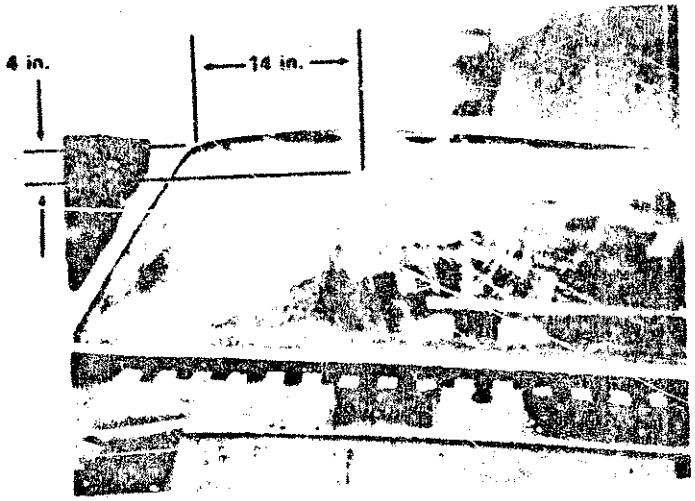

WINDSHIELD CONTACT

Figure 3.4.8 (Cont'd.)

CRASH VICTIM -

FEMALE
49 YEARS
60 in.
130 lb

ACCIDENT -

HEAD STRUCK REAR VIEW MIRROR, UPPER INSTRUMENT PANEL - FACIAL LACERATIONS, FRACTURED TEETH

INJURY RATING -

HEAD - 1 (MINOR)
FACE - 3 (SEVERE)
OVERALL - 3

WINDSHIELD -

UNBROKEN, UNCRACKED, NO CONTACT REPORTED.

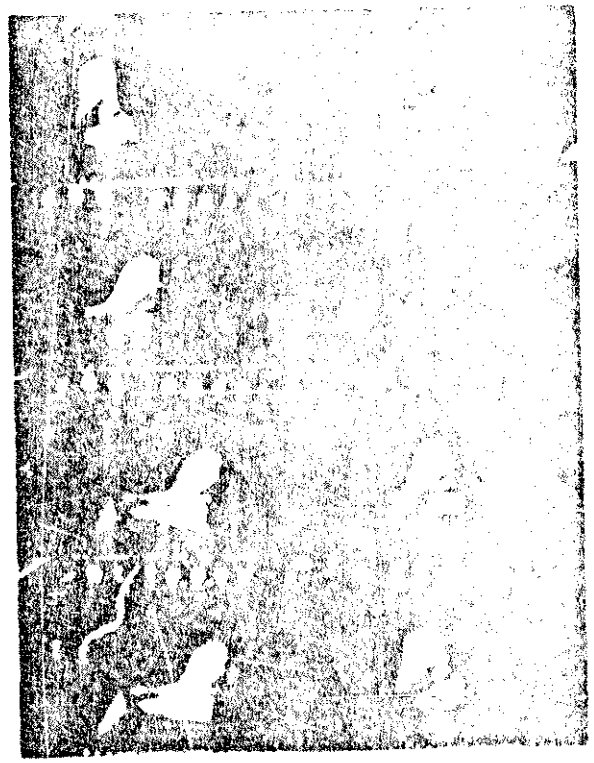

Figure 3.4.9 CASE NO. C871065
SLED RUN NO. 1134

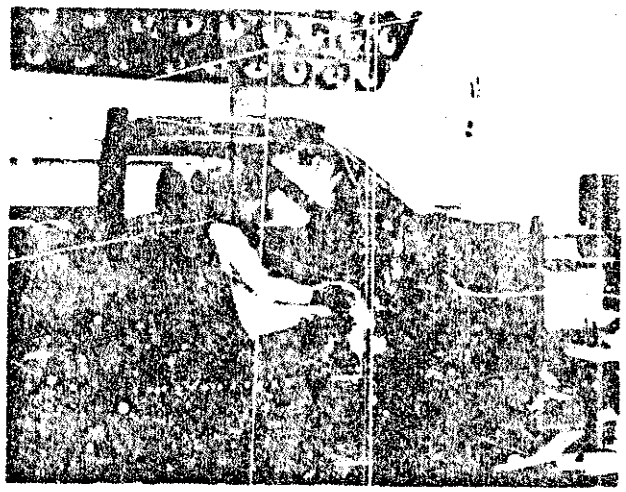

PRE-TEST

POST TEST

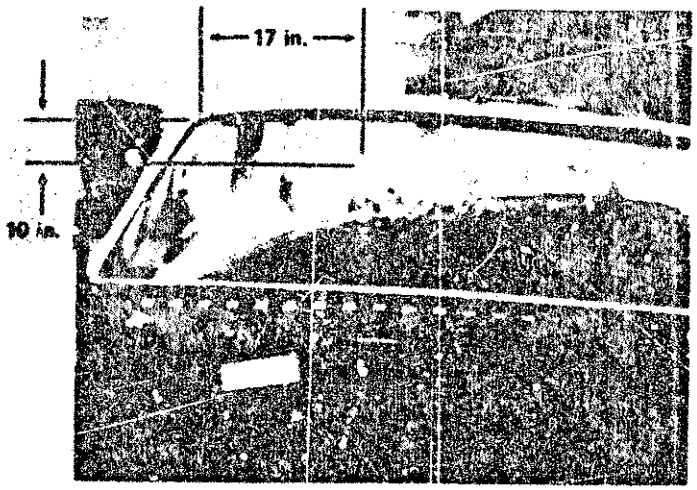

WINDSHIELD CONTACT

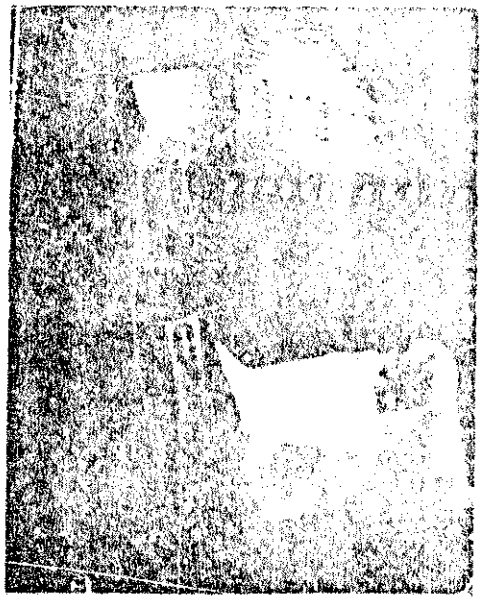

Figure 3.4.9 (Cont'd.)

CRASH VICTIM -

MALE
22 YEARS
HEIGHT UNKNOWN
WEIGHT UNKNOWN

ACCIDENT -

HEAD STRUCK WINDSHIELD/
HOOD - FACIAL LACERATIONS

INJURY RATING -

FACE - 3 (SEVERE)
OVERALL - 3

WINDSHIELD -

CRACKED AND BROKEN.
AS VIEWED FROM INSIDE:

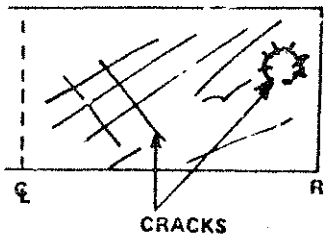

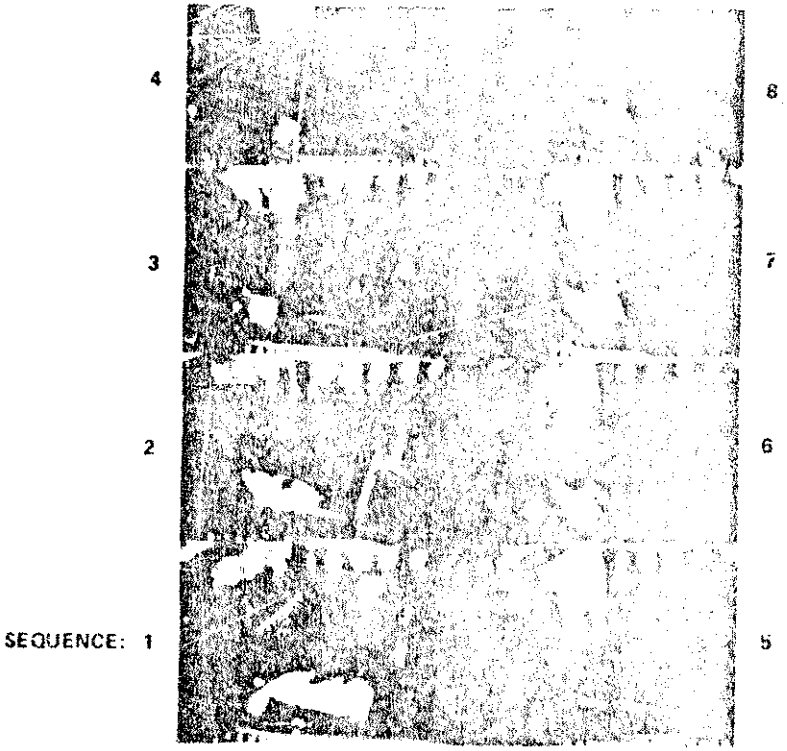

Figure 3.4.10 CASE NO. TR01161
SLED RUN NO. 1137

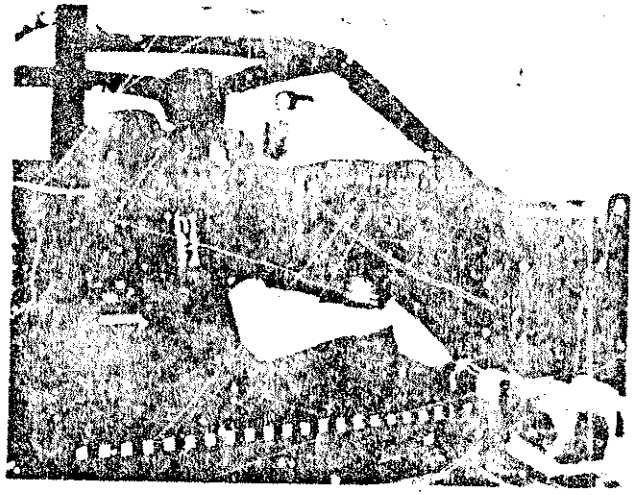

PRE-TEST

POST TEST

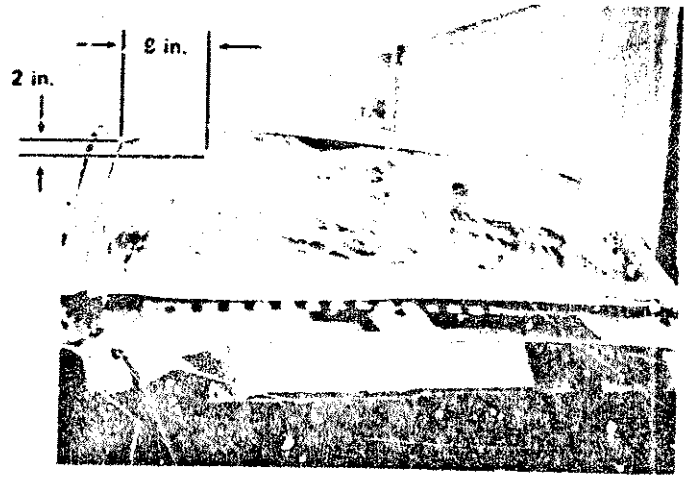

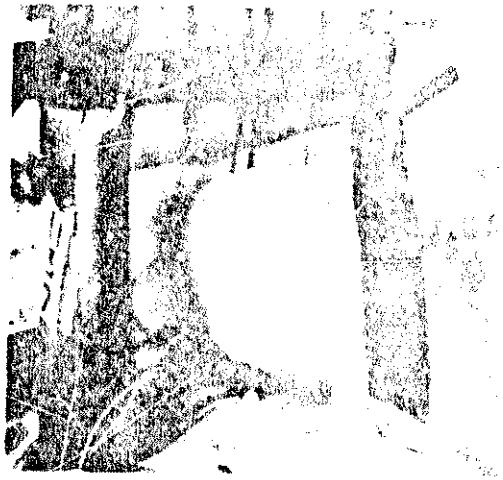

WINDSHIELD CONTACT

ZQ-5341-V-1

Figure 3.4.10 (Cont'd.)

CRASH VICTIM -

MALE
16 YEARS
HEIGHT UNKNOWN
WEIGHT UNKNOWN

ACCIDENT -

HEAD STRUCK INSTRUMENT
PANEL - CONCUSSION

INJURY RATING -

HEAD - 3 (SEVERE)
FACE - 3
BRAIN - 2 (MODERATE)
OVERALL - 4 (SERIOUS)

WINDSHIELD -

UNCRACKED, UNBROKEN, NO
CONTACT REPORTED.

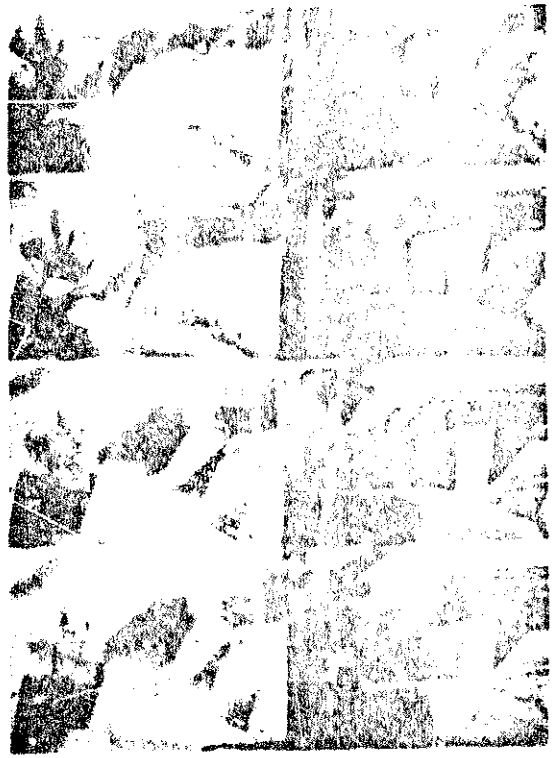

Figure 3.4.11 CASE NO. GI00056
SLED RUN NO. 1142

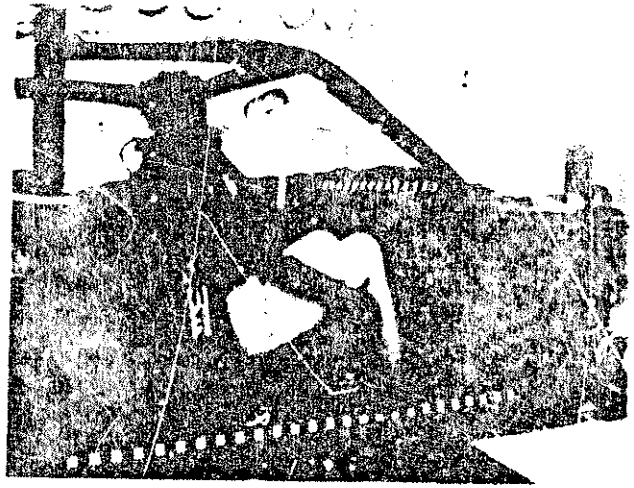

PRE-TEST

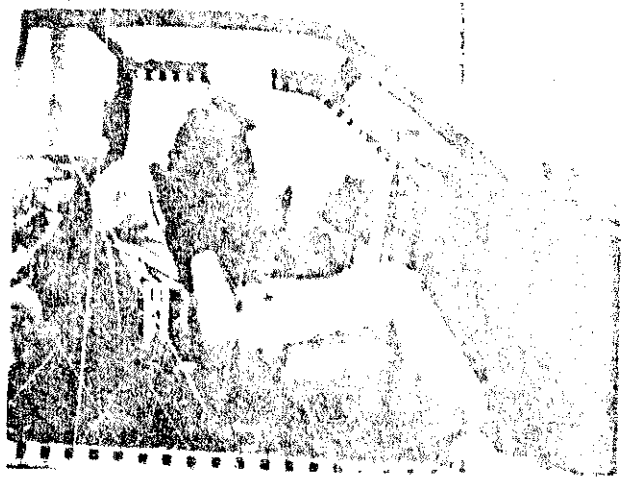

POST-TEST

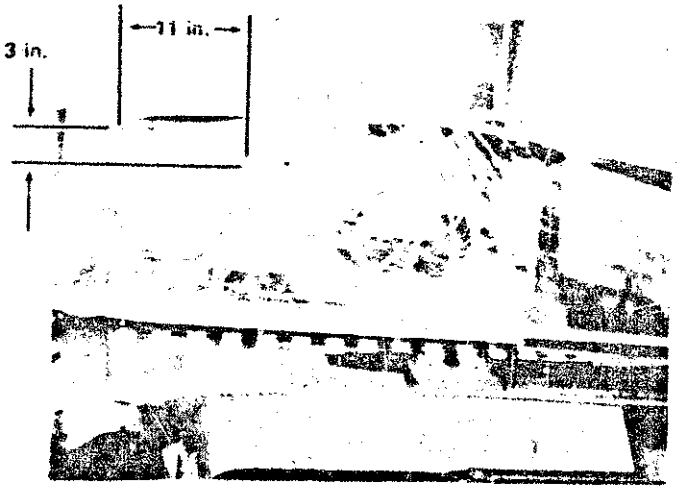

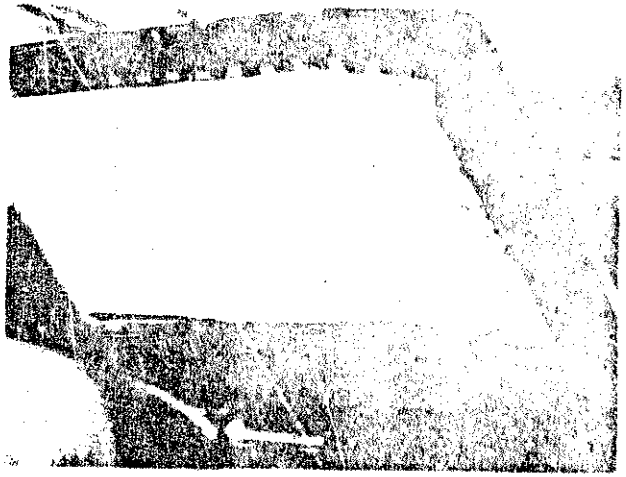

WINDSHIELD CONTACT

Figure 3.4.11 (Cont'd.)

CRASH VICTIM -

MALE
16 YEARS
HEIGHT UNKNOWN
WEIGHT UNKNOWN

ACCIDENT -

HEAD STRUCK INSTRUMENT
PANEL - CONCUSSION

INJURY RATING -

HEAD - 3 (SEVERE)
FACE - 3
BRAIN - 2 (MODERATE)
OVERALL - 4 (SERIOUS)

WINDSHIELD -

UNCRACKED, UNBROKEN, NO
CONTACT REPORTED.

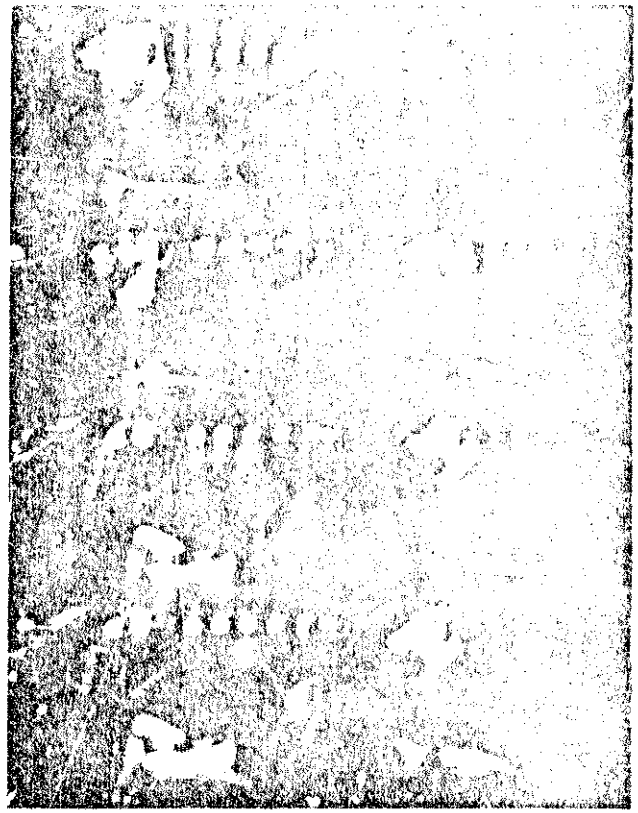

Figure 3.4.12 CASE NO. GI00056
SLED RUN NO. 1143

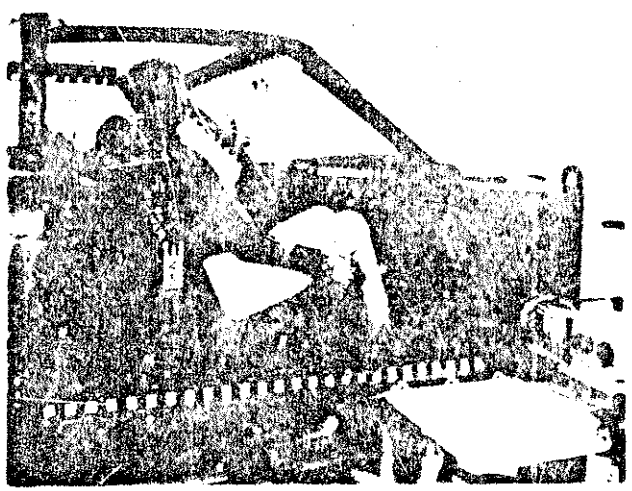

PRE-TEST

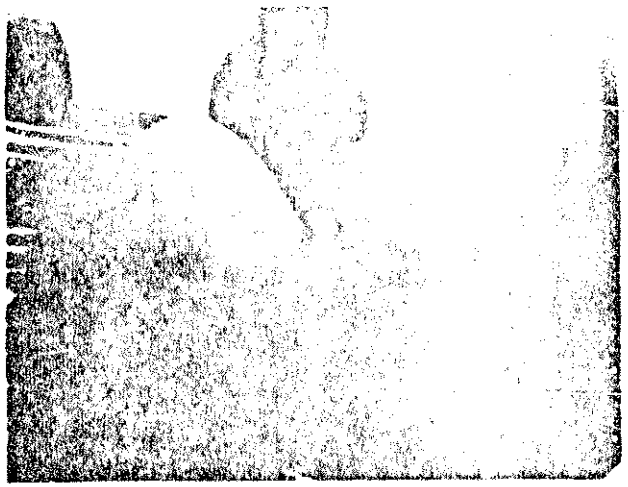

POST TEST

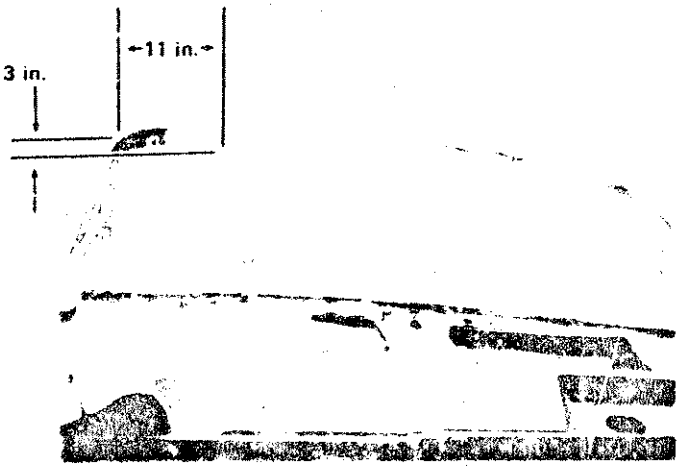

WINDSHIELD CONTACT

Figure 3.4.12 (Cont'd.)

CRASH VICTIM -

MALE
52 YEARS
71 in.
155 lb

ACCIDENT -

FACE STRUCK WINDSHIELD (BROKEN) - FACIAL ABRASIONS/LACERATIONS, SEVERE THORACIC INJURIES

INJURY RATING -

FACE - 1 (MINOR)
OVERALL - 6 (FATAL)

WINDSHIELD -

CRACKED AND BROKEN.
AS VIEWED FROM INSIDE:

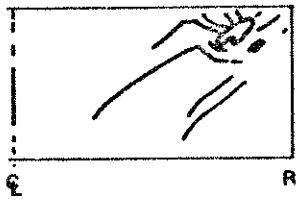

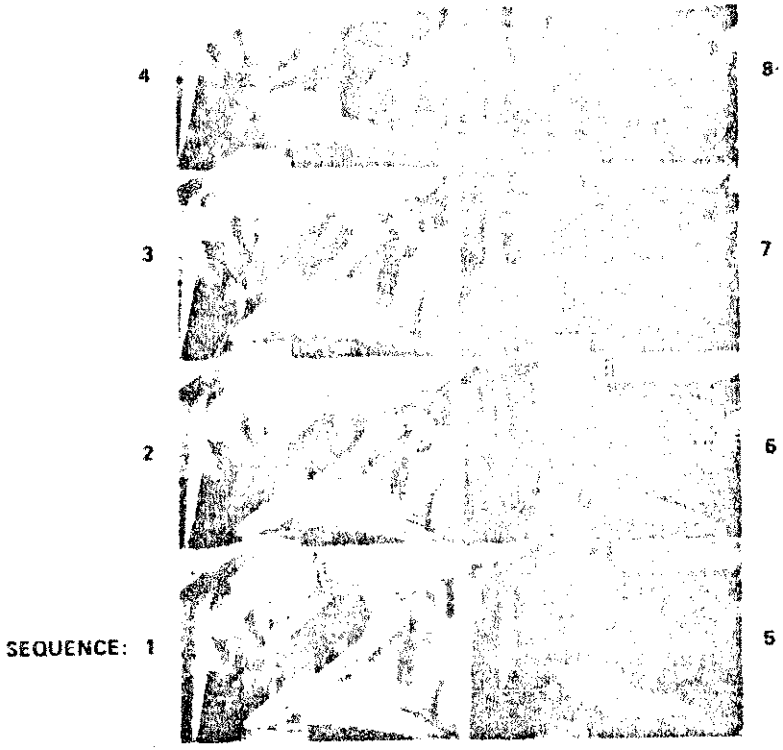

Figure 3.4.13 CASE NO. TR00973
SLED RUN NO. 1146

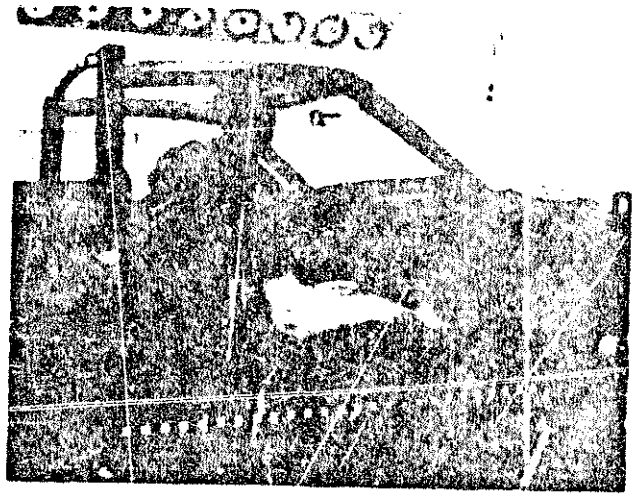

PRE-TEST

POST-TEST

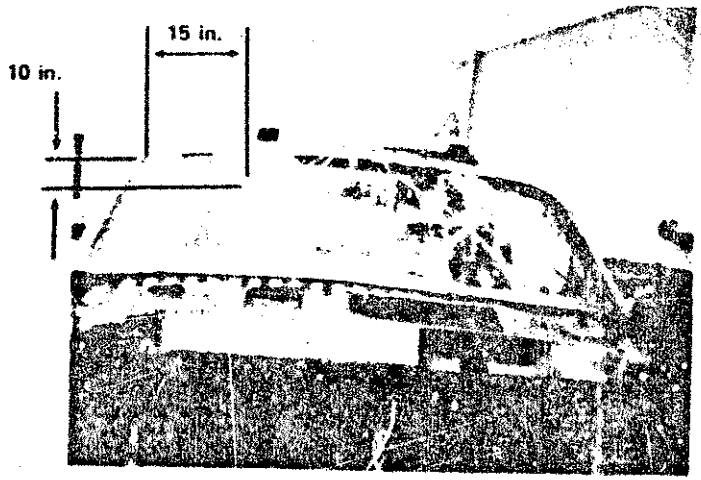

WINDSHIELD CONTACT

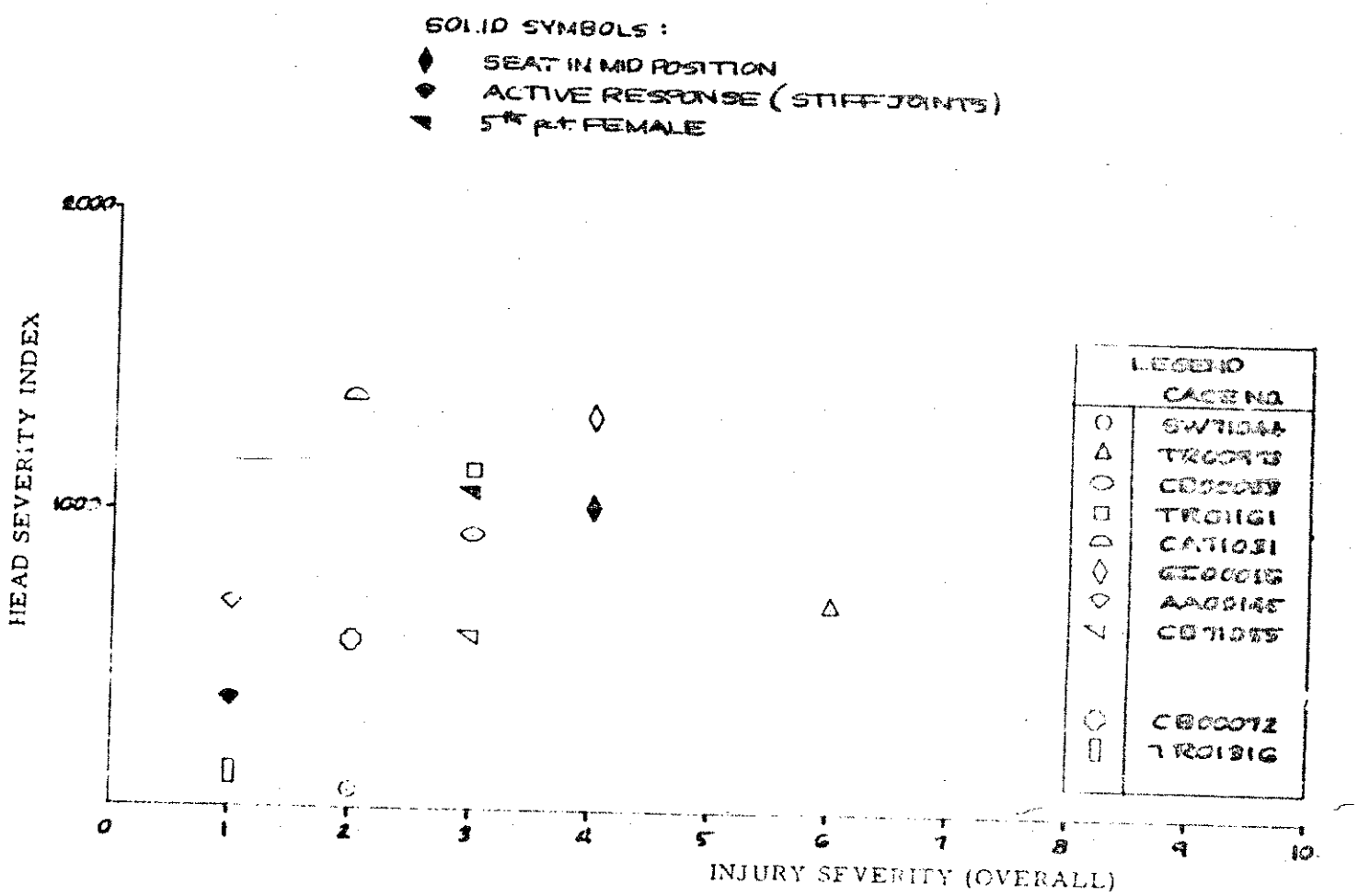

Figure 3.4.14 MEASURED HEAD SEVERITY INDEX COMPARED TO ACTUAL INJURY SEVERITY

LEGEND - SEE FIG. 3.4.14

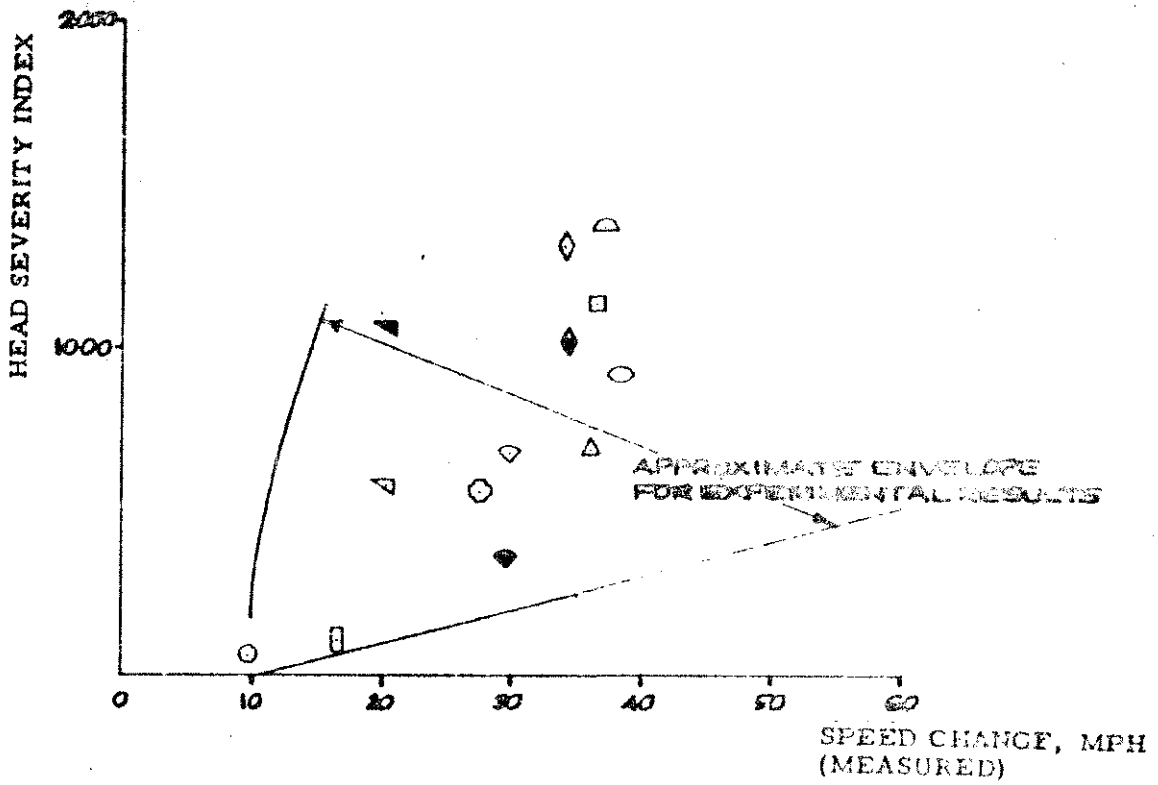

Figure 3.4.15 MEASURED HEAD SEVERITY INDEX COMPARED TO WINDSHIELD TEST DATA

(2) The measured results fall near the middle of the envelope of published HPR windshield data.*

For the sake of completeness, injuries to the crash victim lower extremities are included in this section in Table 3.4.2. This summary is included because the magnitude of applied femur load is one of the few quantitative measures of severity of loading to the occupant in crashes, and because dummy femur loads were recorded in the impact sled tests. Table 3.4.2 also contains the predicted peak knee loads** from the corresponding computer simulations. It should be emphasized that these predicted loads depend strongly on the inputted force-deflection characteristics, which were based upon "typical" values for the simulations, rather than specific measurements.

From Table 3.4.2, a general correlation of measured peak load and observed specific injury rating can be seen. This table further demonstrates the detailed information produced by the reconstruction technique.

---

* Some cases did not involve head-windshield contact (observed and/or simulated) and therefore should not be included in the plot of Figure 3.4.15, in the strictest sense. Data from all ten cases were included, however, for the sake of uniformity.

** Normal component of applied force, not the value exactly corresponding to femur load.

Table 3.4.2

Injuries to Crash Victim Lower Extremities

	Accident			Sled Test			Simulation		
Case Identification Number	Observed Injuries to Knees/Lower Legs	Injury Rating (10-point code)	Sled Run No.	Measured Peak Femur Loads, lbs. right	left	Predicted Peak Knee Loads, lbs. right	left	Remarks
AA00145	lacerations/contusions to right and left knees	1	1139	930	430	970	450	
			1140	530	580	630	630	Joint Stiffness Varied
TR01316	none	0	1141	310	310	880	780	
CA71031	lacerations to anterior left lower leg	1	1138	470	760	1500	1500	
CB00072	none	0	1136	620	750	1580	1580	
SW71044	none	0	1144	100	140	0	0	
CB00053	fracture of left femur, laceration and tear into capsule of left knee	2	1145	760	1040	1140	1160	
CB71055	contusions to anterior right and left lower legs	1	1134	630	510	840	810	Dummy Size Varied
			1135	470	350	1010	960	
TR01161	none	0	1137	700	1070	1570	1560	
GI00056	none	0	1142	700	870	1560	1560	
			1143	670	840			Vehicle Interior Geometry Varied
TR00973	abrasions to right and left legs	2	1146	710	610	960	960	

3.5 Physical Reconstruction of Ten Accident Cases

3.5.1 Summary

In this section, the physical reconstructions on the impact sled of each of the ten accident cases are discussed in some detail. In addition, the time history responses measured in the impact sled tests are compared with results from corresponding computer simulations of each case. These comparisons include vehicle acceleration history and speed change, occupant kinematic responses (displacement in the side view of the head (H), chest or upper torso (UT), and pelvis or lower torso (LT))*, head resultant acceleration history, chest resultant acceleration history, and, where applicable, lap belt load histories. The relevant sled data traces are summarized in Appendix D.

Note in the comparisons that each of these various parameters is plotted on a common scale, to emphasize the wide range of parametric variation encountered in the reconstruction of these ten cases. It should be emphasized here that these comparisons should not be used to assess directly the validity of the mathematical modeling, for several reasons. First, the sled decelerations differed measureably from the predicted (SMAC) vehicle decelerations in a number of cases, as will be subsequently discussed. Second, crash victim inputs were based (in most cases) on measurements on a 50th percentile dummy different from that used in the sled tests. Third, vehicle interior material properties were based upon "typical" values rather than based on actual measurements. For these reasons, predictions of the mathematical models should be expected to correspond to the sled test results only in a general sense.

---

*The measured kinematic responses, obtained from the high-speed motion pictures of the sled tests, have been corrected for parallax in an approximate manner. Estimated accuracy of the measured kinematic response data presented in this section is ± 20%.

3.5.2 Detailed Discussion of the Ten Accident Cases

Case No. AA00145

Sled Runs Nos. 1139 and 1140

As discussed in Section 3.3, the crash victim struck the upper instrument panel without any reported head-windshield contact. From the overall geometry of the configuration (Figure 3.3.4), however, head-windshield contact in a frontal crash appears inevitable unless prevented by occupant bracing in anticipation of crash. For this case, the effects of an active response by the occupant compared to a passive response were studied both through computer simulations (see Figure 3.3.4) and through the sled reconstructions (see Figure 3.4.1 for the case of "passive response" (sled run no. 1139) and Figure 3.4.2 for the case of "active response" (sled run no. 1140).

It was not possible to simulate bracing in the sled test by increasing the torque setting of the dummy shoulder and elbow joints, as was done in the corresponding computer simulation. These dummy joints were found to be adjustable over too limited a range. Instead, the required stiffness was achieved by strapping lightweight metal braces to the arms, and by strapping the arms together, separated at the elbows by a spacer, in the manner depicted in Figure 3.4.2. Although this arrangement proved generally satisfactory, there was not an exact correspondence between the computer simulation of the active response and the corresponding sled reconstruction.

For this case, the sled acceleration history agrees rather well with the predicted (SMAC) response, Figure 3.5.1(a). In addition, the sled pulse was found to be highly repeatable in the replicate sled runs nos. 1139 and 1140.

AA00145

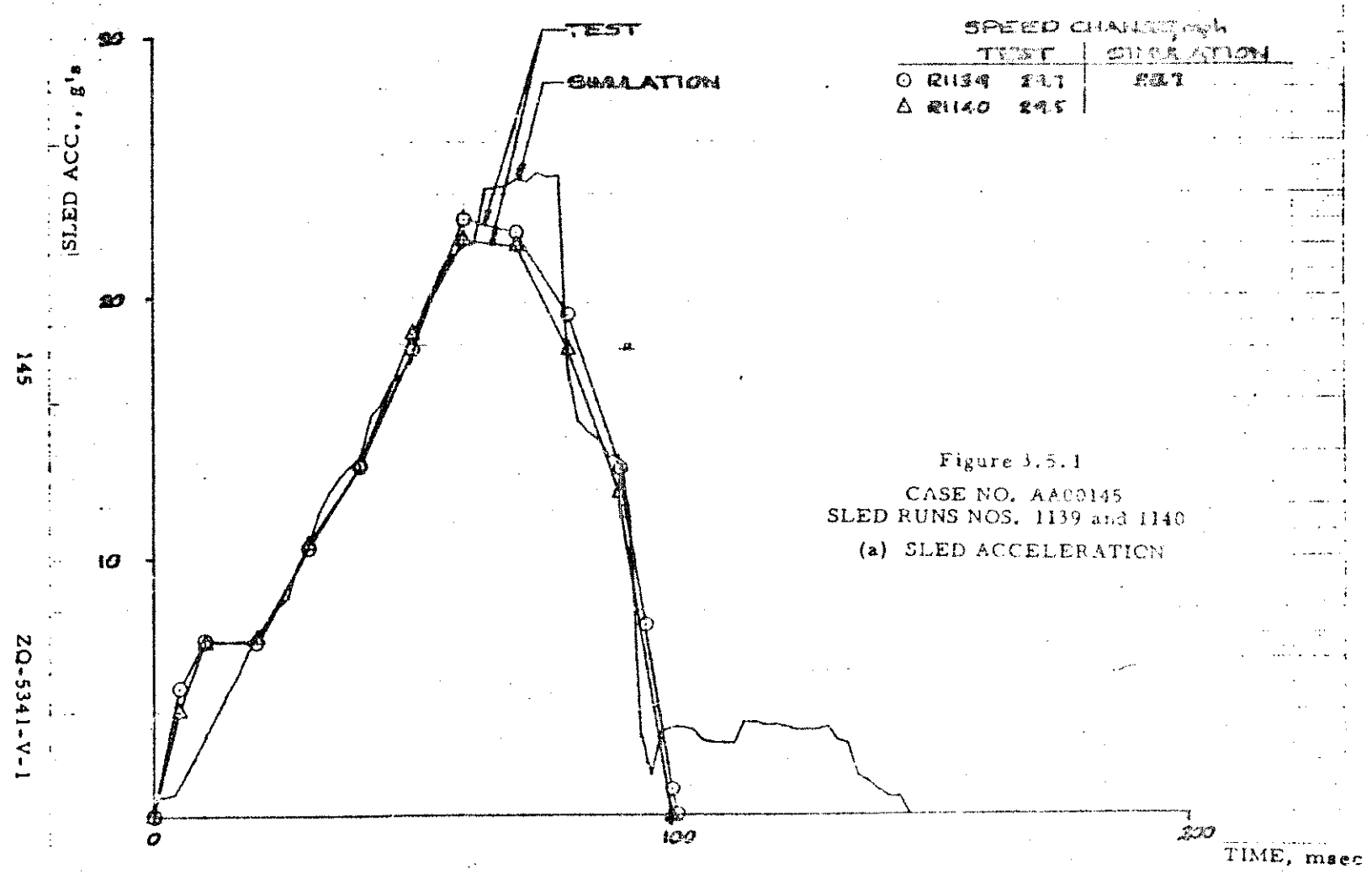

Figure 3.5.1
CASE NO. AA00145
SLED RUNS NOS. 1139 and 1140
(a) SLED ACCELERATION

Predicted and measured kinematic responses for the "active" and "passive" cases are summarized in Figure 3.5.1(b). Both the test and simulation results without active bracing indicate head-windshield contact, although the simulation predicts greater forward motion of the head.

With active bracing, head-windshield contact is prevented in the simulation, and only a grazing contact occurred in the test, insufficient to cause windshield failure (see Figure 3.4.2). A more refined method of dummy arm bracing in the test may have prevented this contact. These results, both test and simulation, illustrate the potential importance of the effect of active occupant responses in anticipation of crash.

The peak head resultant accelerations were reduced by bracing in both the sled test and the computer simulation, as can be seen in Figure 3.5.1(c). The measured peak accelerations for both cases are predicted with reasonable accuracy by the simulation.

The computer simulation predicts a somewhat higher peak chest resultant acceleration as the result of bracing, Figure 3.5.1(d). The test results agree with the simulation only in terms of general magnitude.

In Figure 3.5.1(e), it can be seen that the measured lap belt loads are significantly higher than the simulation results, although the general trends of the load curve are predicted.* Note that lower belt loads in the simulation are consistent with the larger predicted kinematic displacements, Figure 3.5.1(a). Again, it is emphasized that the belt material properties were based on "typical" properties, rather than values measured in this effort. This appears to be the likely source of the differences noted in Figure 3.5.1(e).

*In both the sled test and the simulation, 2 inches of belt slack was used (2 inches of belt length added to that belt length corresponding to a snug belt condition).

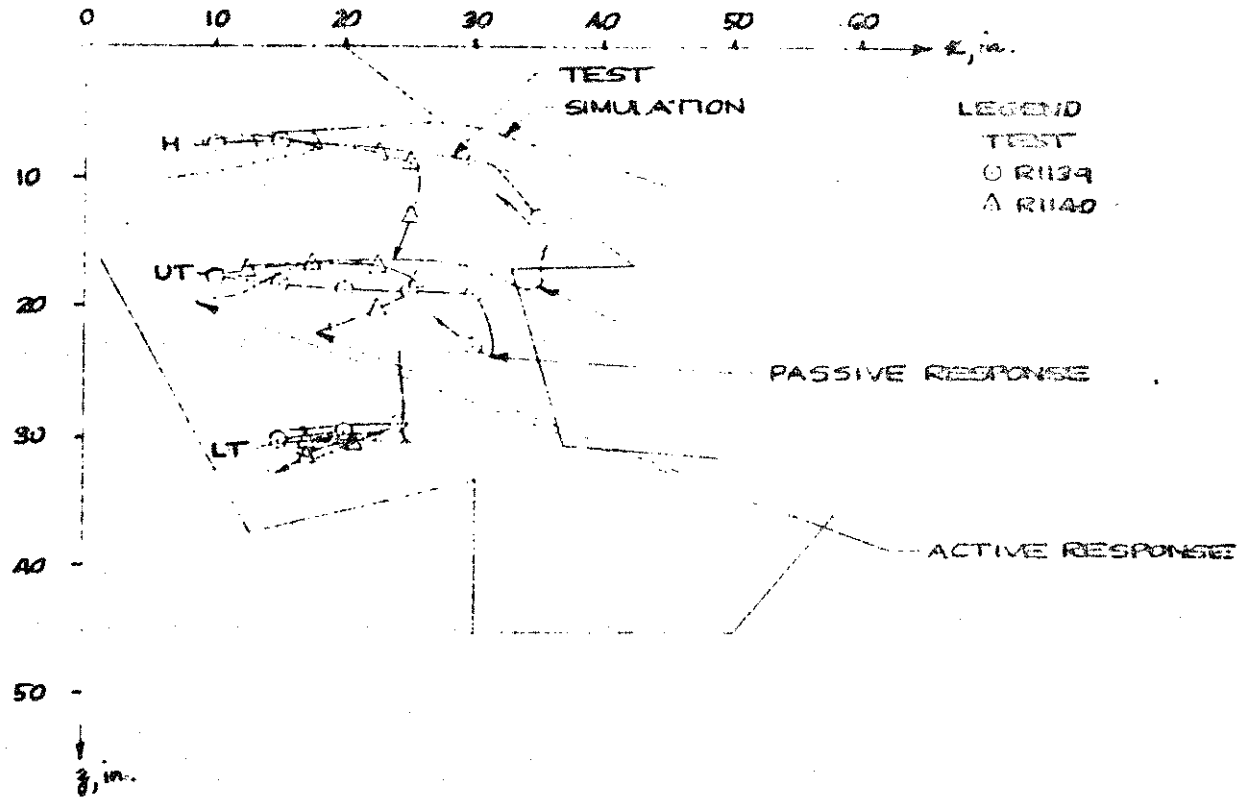

Figure 3.5.1 (cont'd)
(b) KINEMATICS

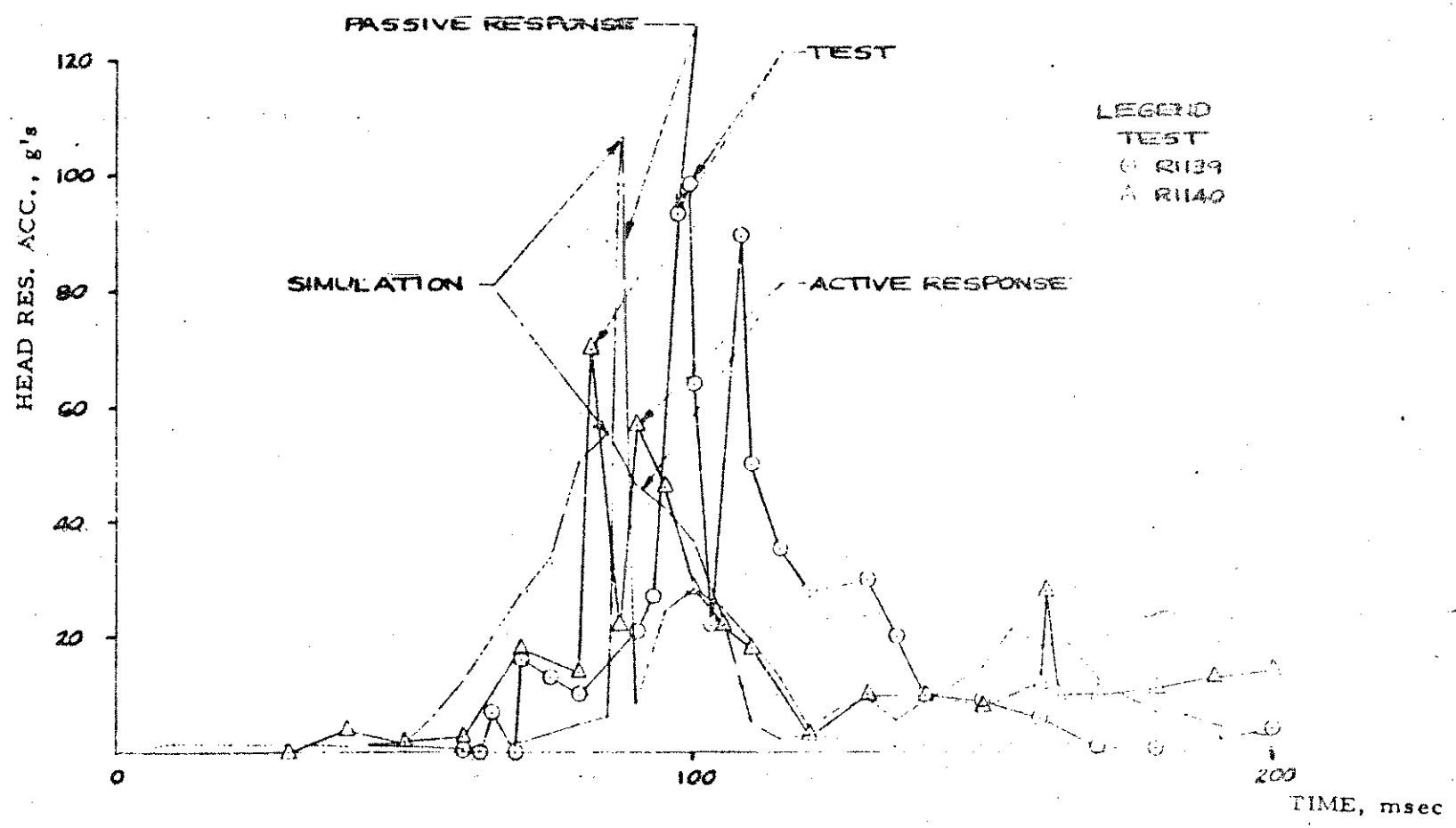

Figure 3.5.1 (cont'd)
(c) HEAD RESULTANT ACCELERATION

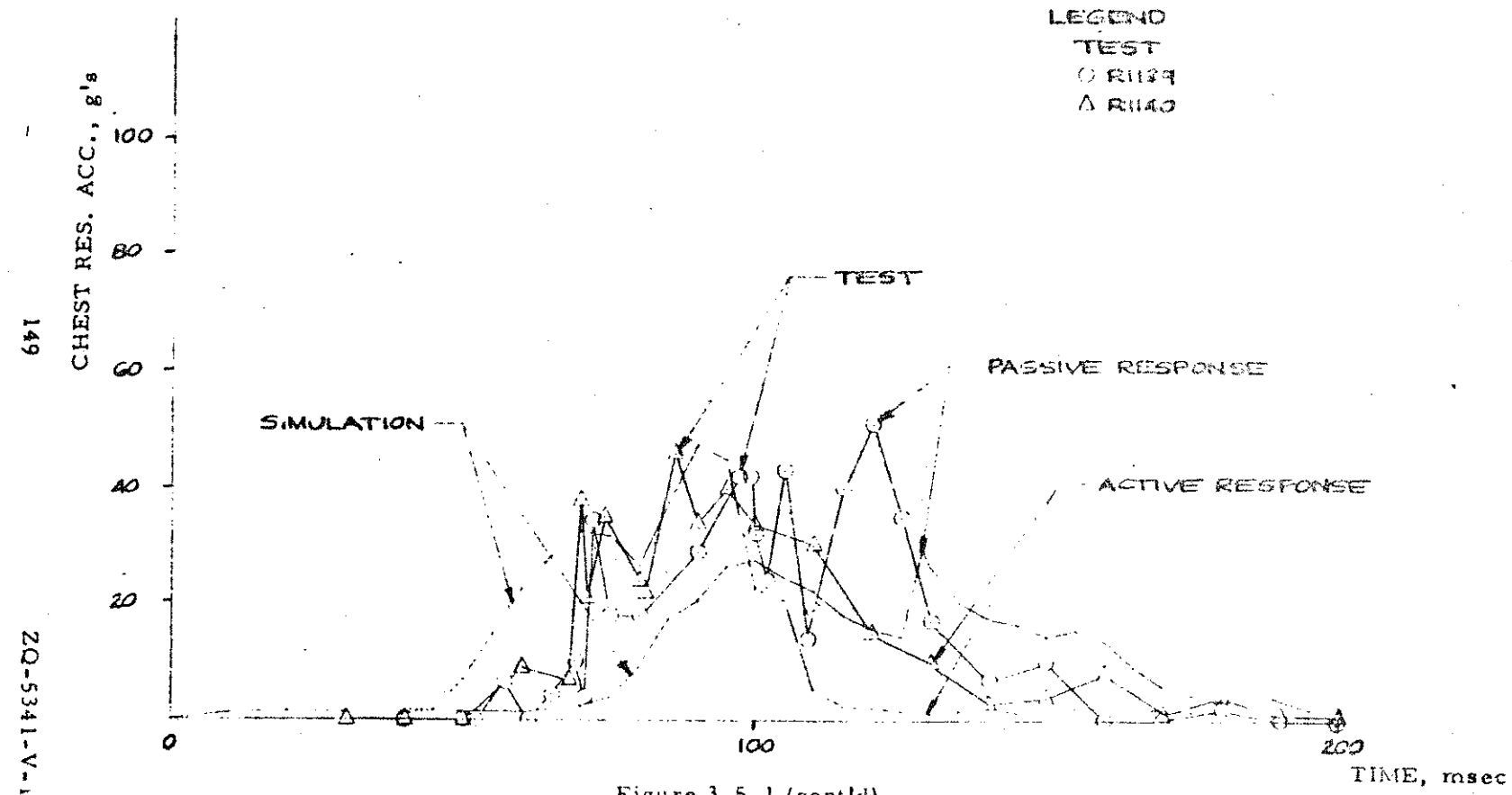

Figure 3.5.1 (cont'd)

(d) CHEST RESULTANT ACCELERATION

Figure 3.5.1 (cont'd)
(e) LAP BELT LOADS

Considering the wide difference between the "active" and "passive" cases as reconstructed both analytically and physically, it is concluded that bracing exerted by the crash victim likely prevented his head from contacting the windshield in the accident vehicle.

Case No. TR01316

Sled Run No. 1141

As noted in Section 3.4, the crash victim struck the upper instrument panel (Figure 3.4.3), resulting in facial injuries, without reported head-windshield contact. This general kinematic behavior was also observed in the corresponding computer simulation, Figure S-4. In contrast, in the sled test, the dummy head grazed and contacted the windshield for 4 inches, without the windshield being cracked or broken, before head contact with the upper instrument panel occurred, Figure 3.4.3. It is believed that the primary reason for this difference in kinematic responses is the result of the relatively large difference between the speed change measured in the sled test and the predicted speed change from the SMAC program (see Figure 3.5.2(a). The sled pulse produced a speed change in the test that was 32 per cent too high, and apparently caused the dummy head-windshield contact noted in the impact sled test results (Figure 3.4.3). In spite of this difference, the measured kinematic responses, Figure 3.5.2(b) are rather closely predicted by the computer simulation, and agree substantially with the accident case report. The predicted head resultant acceleration, Figure 3.5.2(c) differs markedly from the measured result, but this is believed to be primarily attributable to the use of a "typical" force-deflection characteristic for the head-instrument panel contact in the computer simulation. The general magnitude of the chest resultant acceleration corresponds approximately to the measured result, Figure 3.5.2(d), but the measured and predicted lap belt loads differ appreciably, as can be seen in Figure 3.5.2(e). The difference in lap belt load is considered to be mainly the effect of belt slack: in the test, 2 inches

SPEED CHANGE, mph	
TEST	SIMULATION
165	125

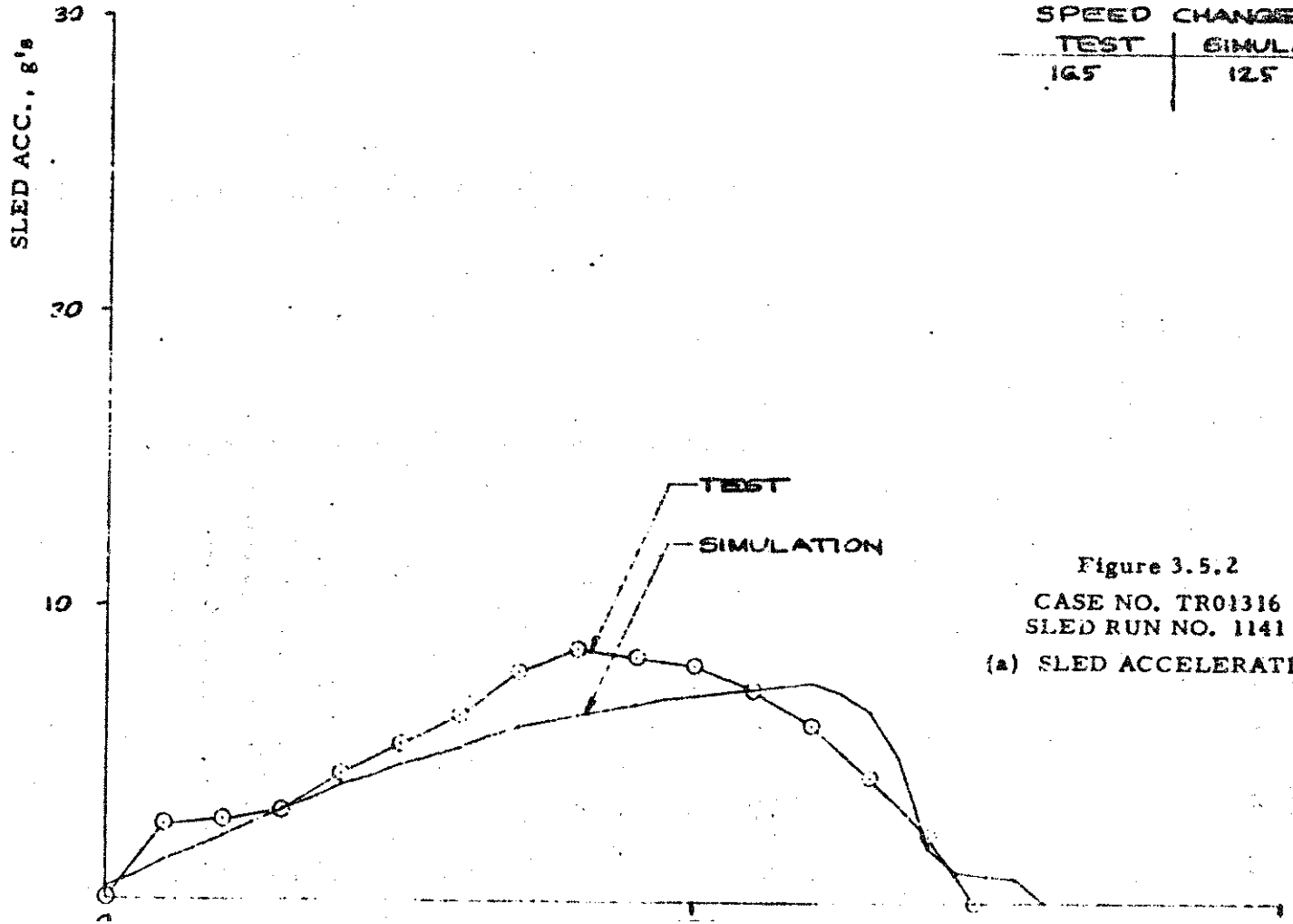

Figure 3.5.2
CASE NO. TR01316
SLED RUN NO. 1141
(a) SLED ACCELERATION

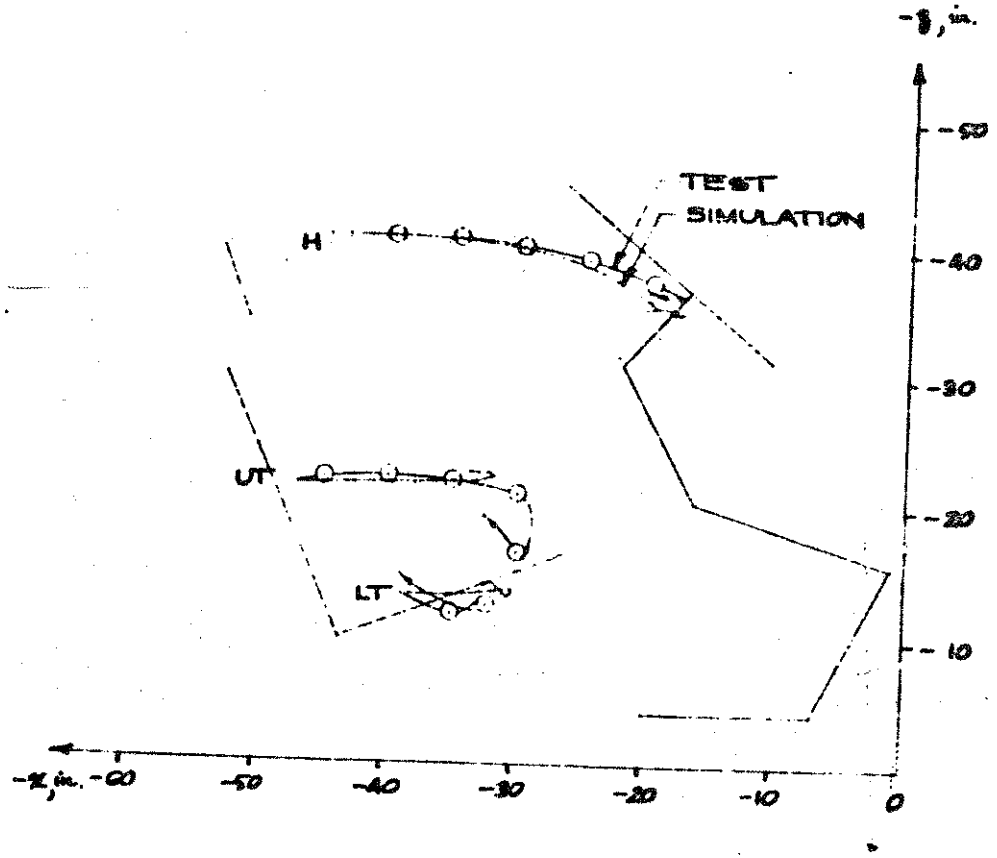

Figure 3.5.2 (cont'd)
(b) KINEMATICS

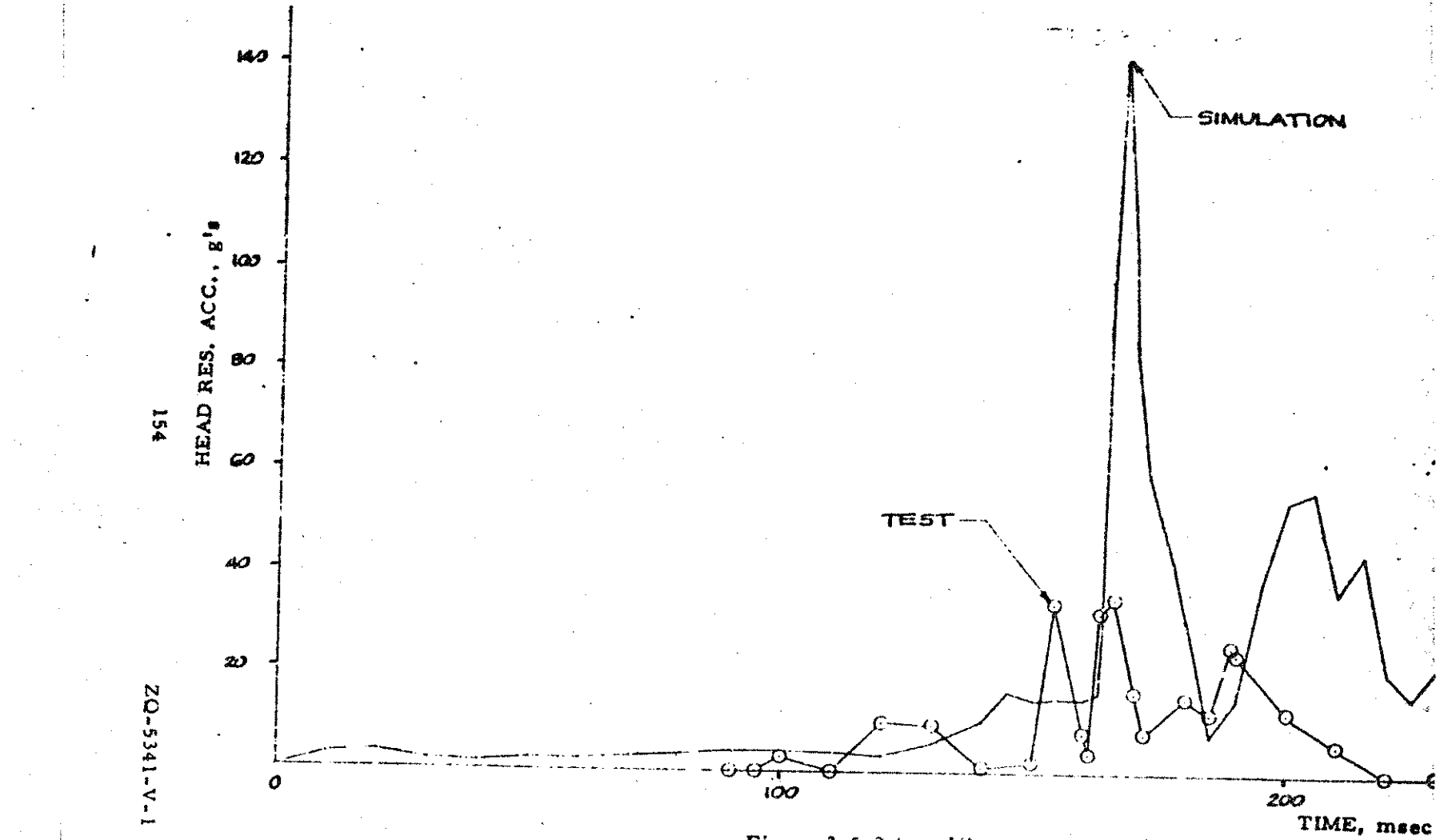

ZQ-5341-V-1

Figure 3.5.2 (cont'd)
(c) HEAD RESULTANT ACCELERATION

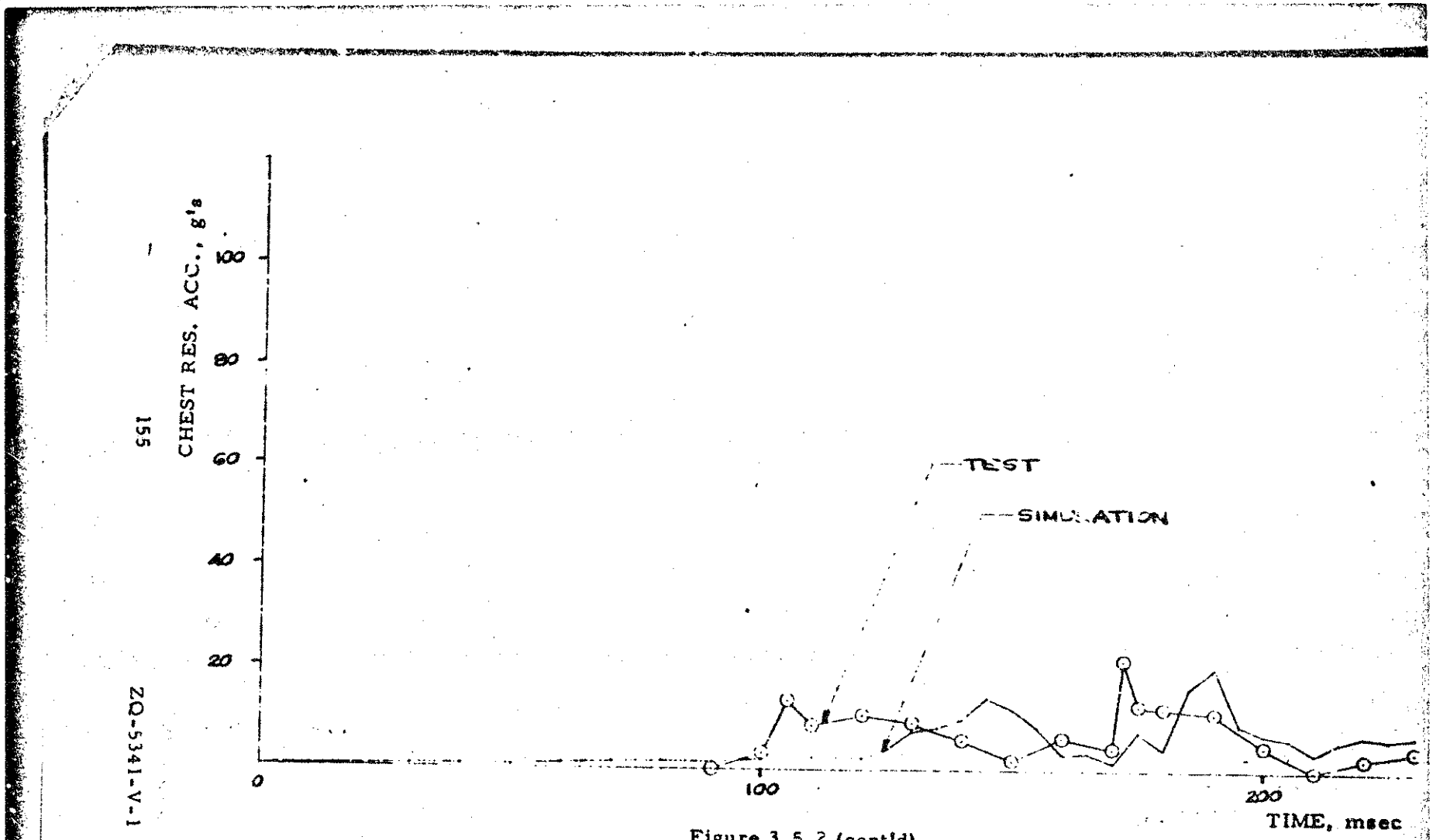

Figure 3.5.2 (cont'd)
(d) CHEST RESULTANT ACCELERATION

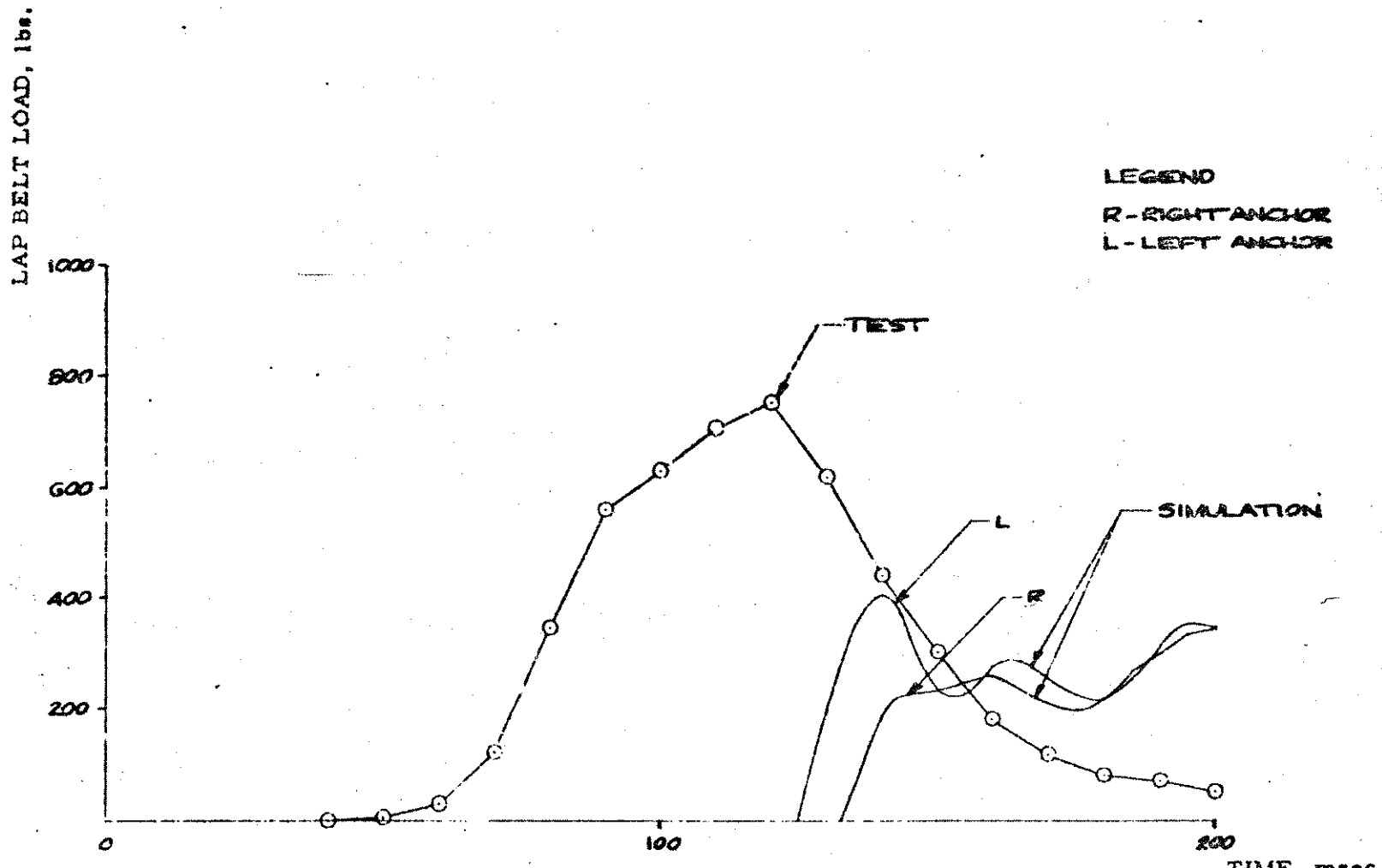

Figure 3.5.2 (cont'd)
(e) LAP BELT LOADS

of slack* was used, but in the simulation (performed as part of the previous pilot study described in this report), 6 inches of additional slack was inputted to account for deformation of the bench seat by the lap belt under load. This additional slack delays the time at which belt load is first applied in the simulation, compared to the test result (see Figure 3.5.2(e)).

Case No. CA71031

Sled Run No. 1138

In this case, the face of the crash victim struck the instrument panel without reported head-windshield contact. As with Case No. AA00145, the initial geometry (Figure 3.3.9) was such that head-windshield contact in a frontal crash appears unavoidable unless the occupant actively braced during the crash. Reconstruction of this active response, either analytically or physically, was not attempted for this case, however. The marked effect of bracing is discussed in some detail in connection with Case No. AA00145. As with other cases, the initial conditions for the sled test, Figure 3.4.4, were selected to match the corresponding computer simulation, Figure 3.3.9.

The sled acceleration pulse, Figure 3.5.3(a), is in good overall agreement with the predicted vehicle deceleration history for this case. Similarly, the head-windshield contact observed in the test, Figure 3.5.3(b), is predicted quite accurately by the computer program. The overall crash victim kinematics, however, differ considerably, as can be seen by examination of this figure. A comparison of the kinematic predictions, Figure 3.3.9 with the sequence camera photographs, Figure 3.4.4, also illustrates this point. The source of the difference in kinematics is probably attributable to the inputted force-deflection characteristics in

*Two inches of belt length added to that belt length (zero slack) which first produced an output on the Lebow gauge.

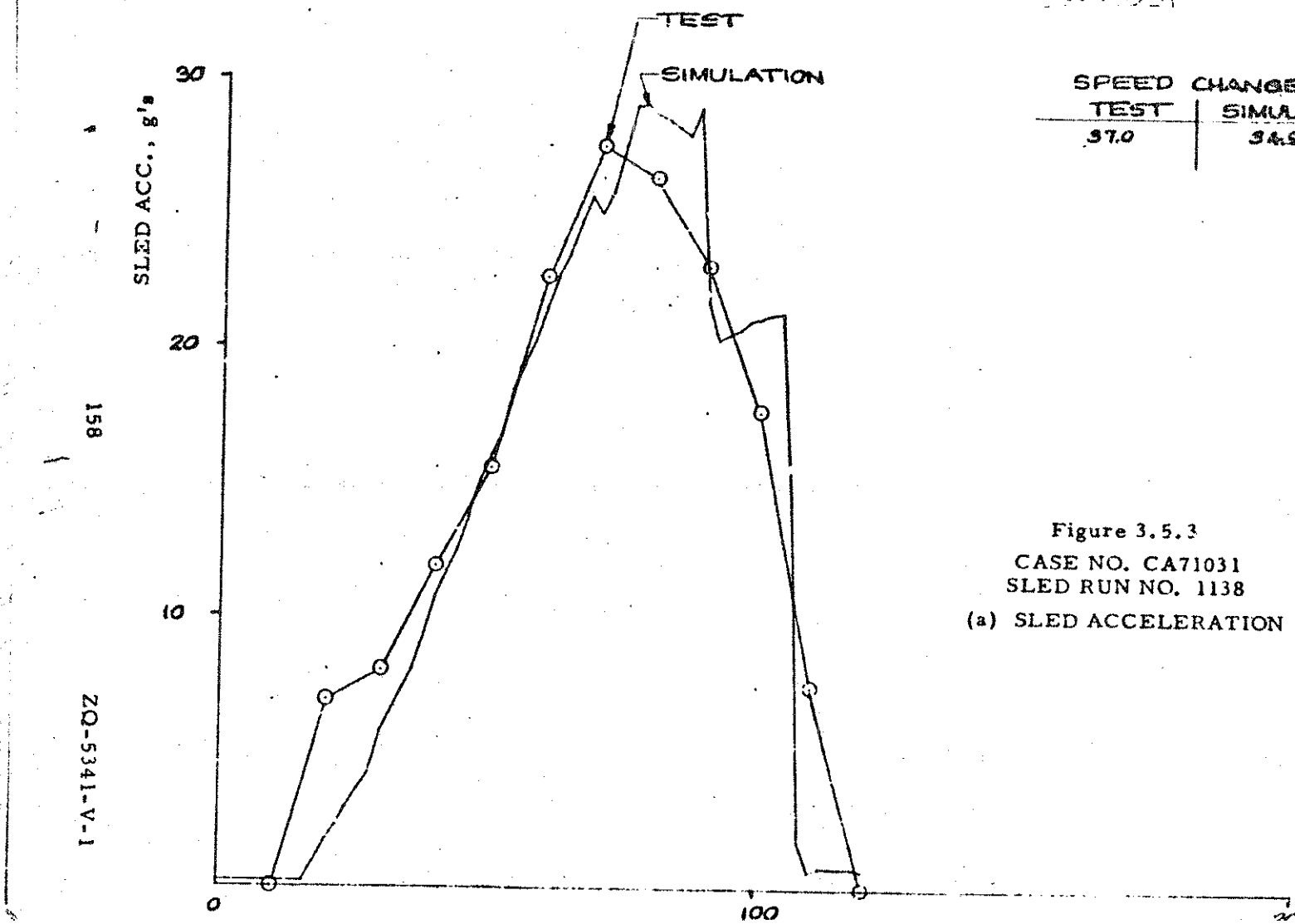

SPEED CHANGE, mph	
TEST	SIMULATION
37.0	34.5

Figure 3.5.3
CASE NO. CA71031
SLED RUN NO. 1138
(a) SLED ACCELERATION

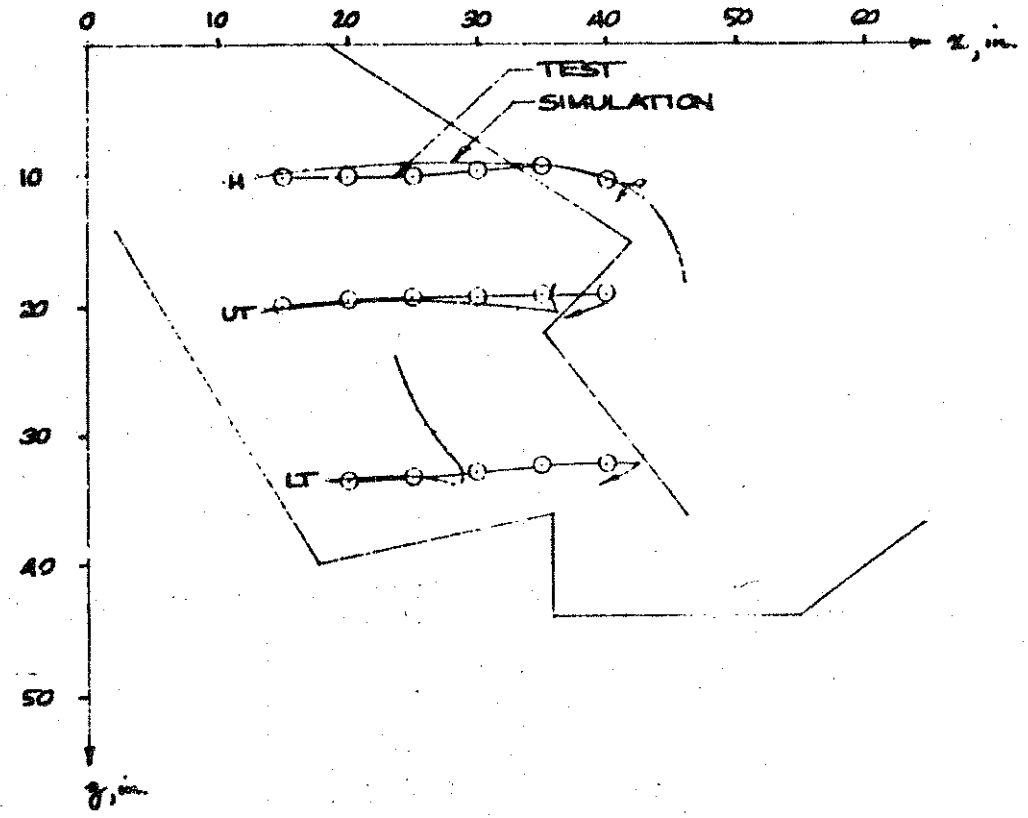

Figure 3.5.3 (cont'd)
(b) KINEMATICS

the simulation, and possibly to the contacts that were allowed in the computer program inputs. The initial head-windshield contact, however, is predicted with reasonable accuracy.

Measured and predicted head resultant accelerations are compared in Figure 3.5.3(c). The time of occurrence of head-windshield contact, evidenced by the spike in head acceleration, is predicted with good accuracy, and the predicted head acceleration level following that contact is the correct general magnitude. The difference between the predicted and measured peak head acceleration, however, is significant. An examiniation of the data traces for this sled run (No. 1138) in Appendix D indicates a considerable high-frequency content*, which may be the source of the observed difference.

In similar manner, the time of occurrence of the peak chest resultant acceleration, Figure 3.5.3(d), is predicted with reasonable accuracy, but the measured magnitude is over 100% higher than predicted. This difference, attributable to the assumed force-deflection characteristics of the instrument panel in the simulation, is probably the cause for the observed difference in kinematic responses, Figure 3.5.3(a).

Case No. CB00072

Sled Run No. 1136

In this case, the head of the right front occupant struck the sunvisor, then the windshield, causing it to break, and finally the instrument panel, as summarized in Figure 3.3.13. The predicted

*Experience gained at General Motors indicates that impacts of the HSRI dummy head on HPR windshields in drop tests have produced head acceleration traces with a considerable high-frequency content, apparently caused by the dummy head construction. Reference: Private communication, H. Mertz of General Motors Corporation; based on General Motors evaluation of the HSRI dummy for the Motor Vehicle Manufacturers Association.

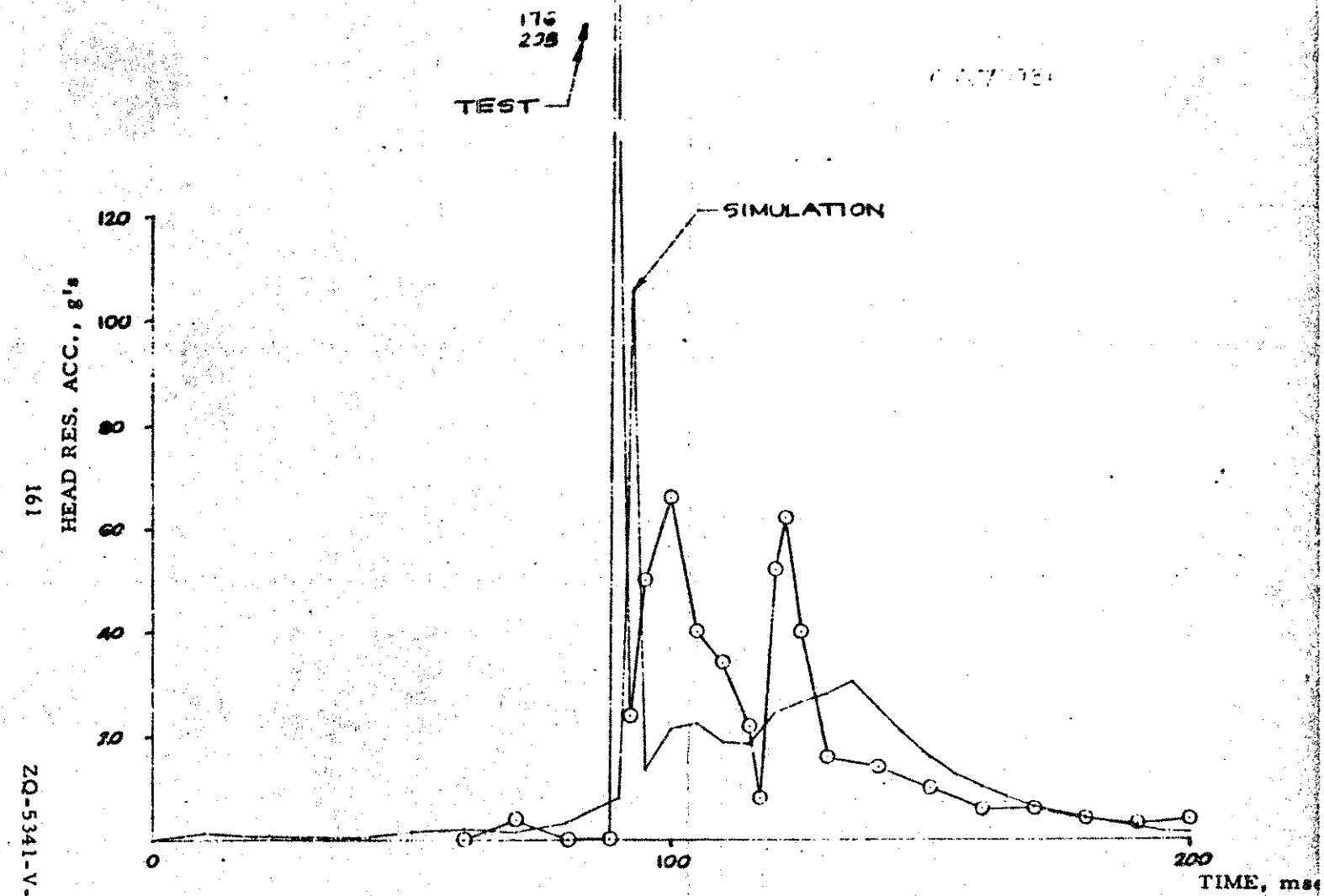

Figure 3.5.3 (cont'd)
(c) HEAD RESULTANT ACCELERATION

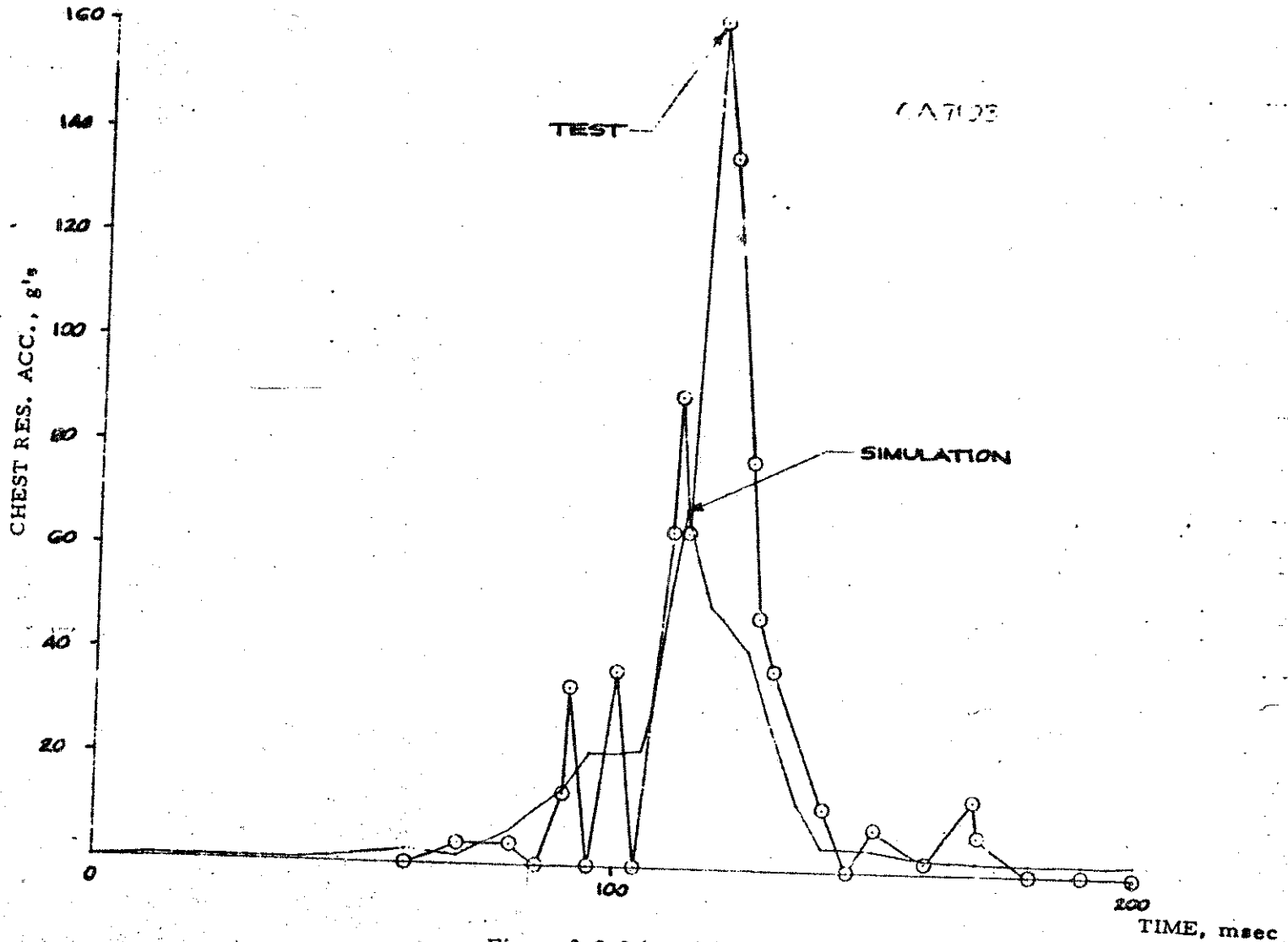

Figure 3.5.3 (cont'd)
(d) CHEST RESULTANT ACCELERATION

kinematic responses displayed in that figure are in good agreement with the accident case report. Head-sunvisor contact, however, was not simulated. The sled test summary, Figure 3.4.5, shows a similar kinematic response, except that windshield failure did not occur. In the sled test, the dummy head struck the rigid windshield header (as evidenced by damage to the header observed after the test) in the location of the sunvisor,* and apparently dissipated enough energy to prevent windshield failure. It does not appear likely that the small difference between the sled pulse and predicted vehicle deceleration, Figure 3.5.4(a), could account for the lack of windshield failure in the test.

The simulated kinematic responses, Figure 3.5.4(b), therefore show a greater forward head motion than the test results, and a corresponding effect on the kinematics of the lower torso.

The head resultant acceleration measured in the test, Figure 3.5.4(c), differs markedly from the corresponding computer prediction. This is caused partially by the head-windshield header contact in the test which was not simulated and partially by the head-instrument panel contact in the simulation, which was again based on "typical" force-deflection properties inputted to the program.

The general magnitude of the measured chest resultant acceleration, Figure 3.5.4(d) is predicted to a reasonable degree by the model.

*The sunvisors and other similar loose accessory equipment were removed from the body buck prior to the sled test series as a safety precaution.

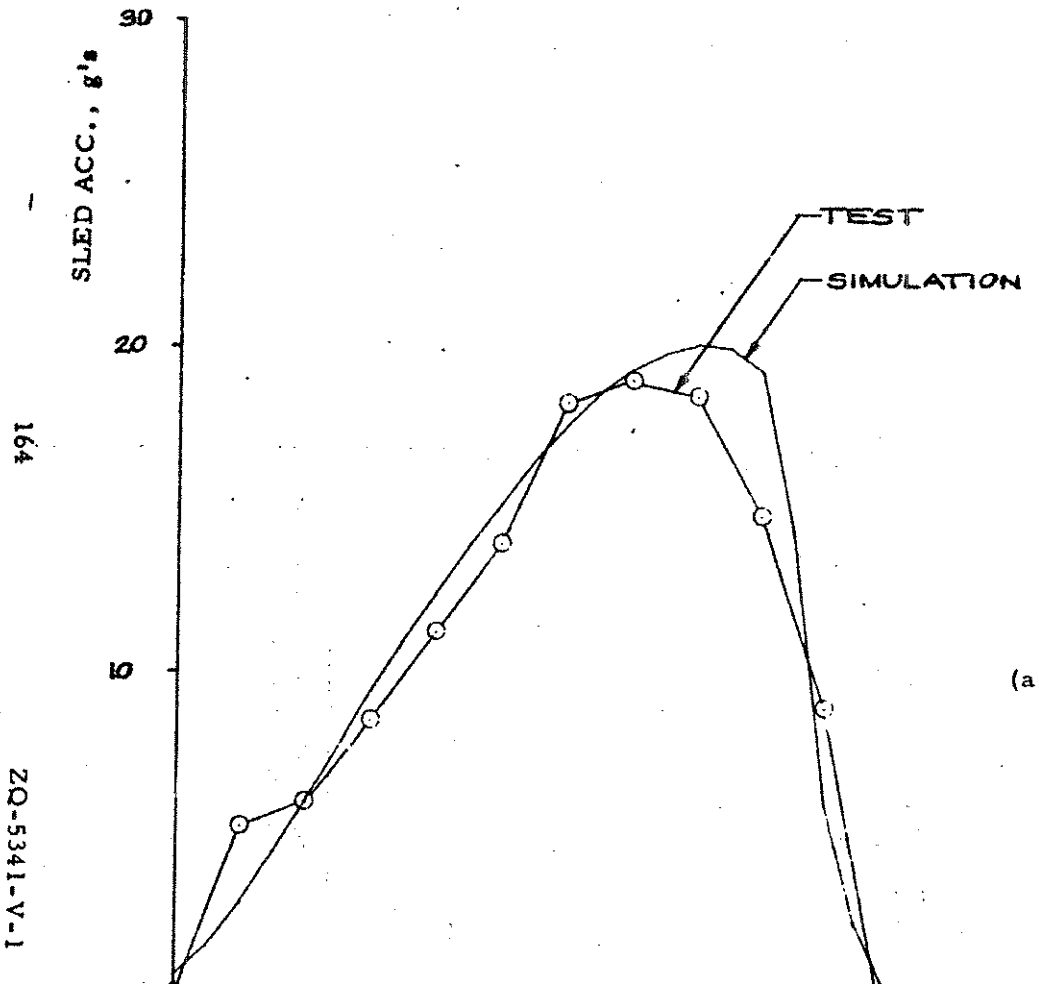

SPEED CHANGE, mph	
TEST	SIMULATION
27.5	28.2

Figure 3.5.4
CASE NO. CB00072
SLED RUN NO. 1136
(a) SLED ACCELERATION

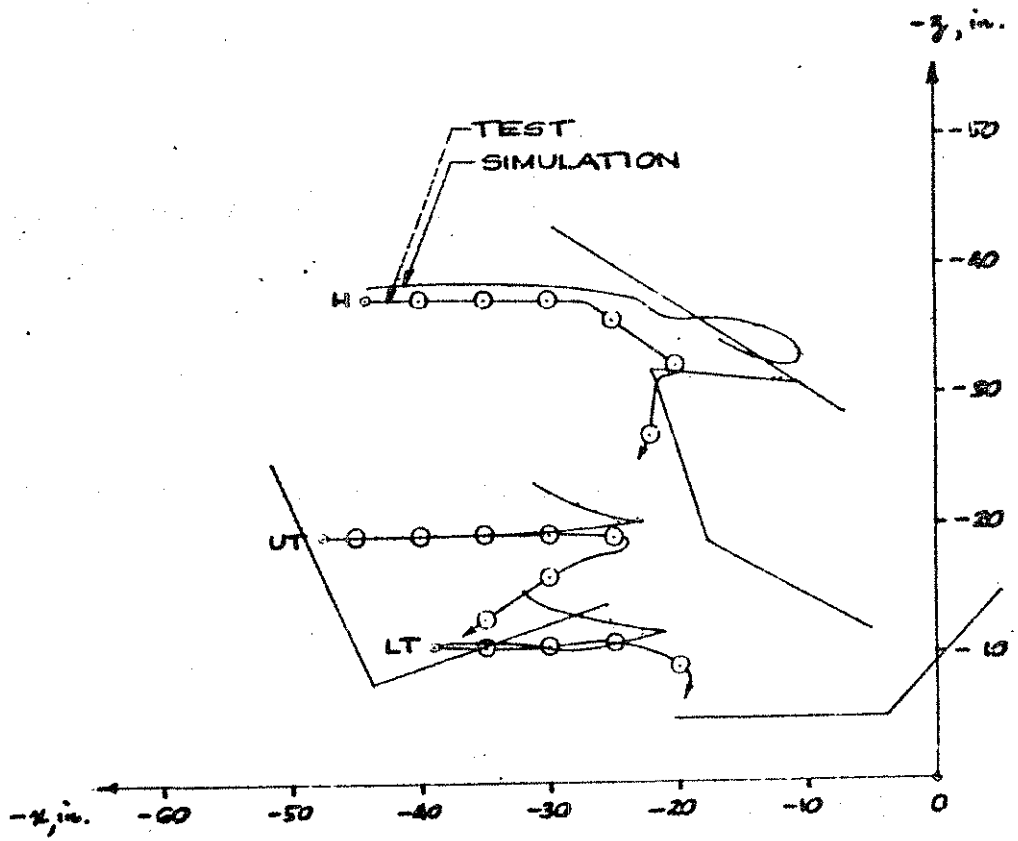

Figure 3.5.4 (cont'd)
(b) KINEMATICS

Figure 3.5.4
(c) HEAD RESULTANT ACCELERATION

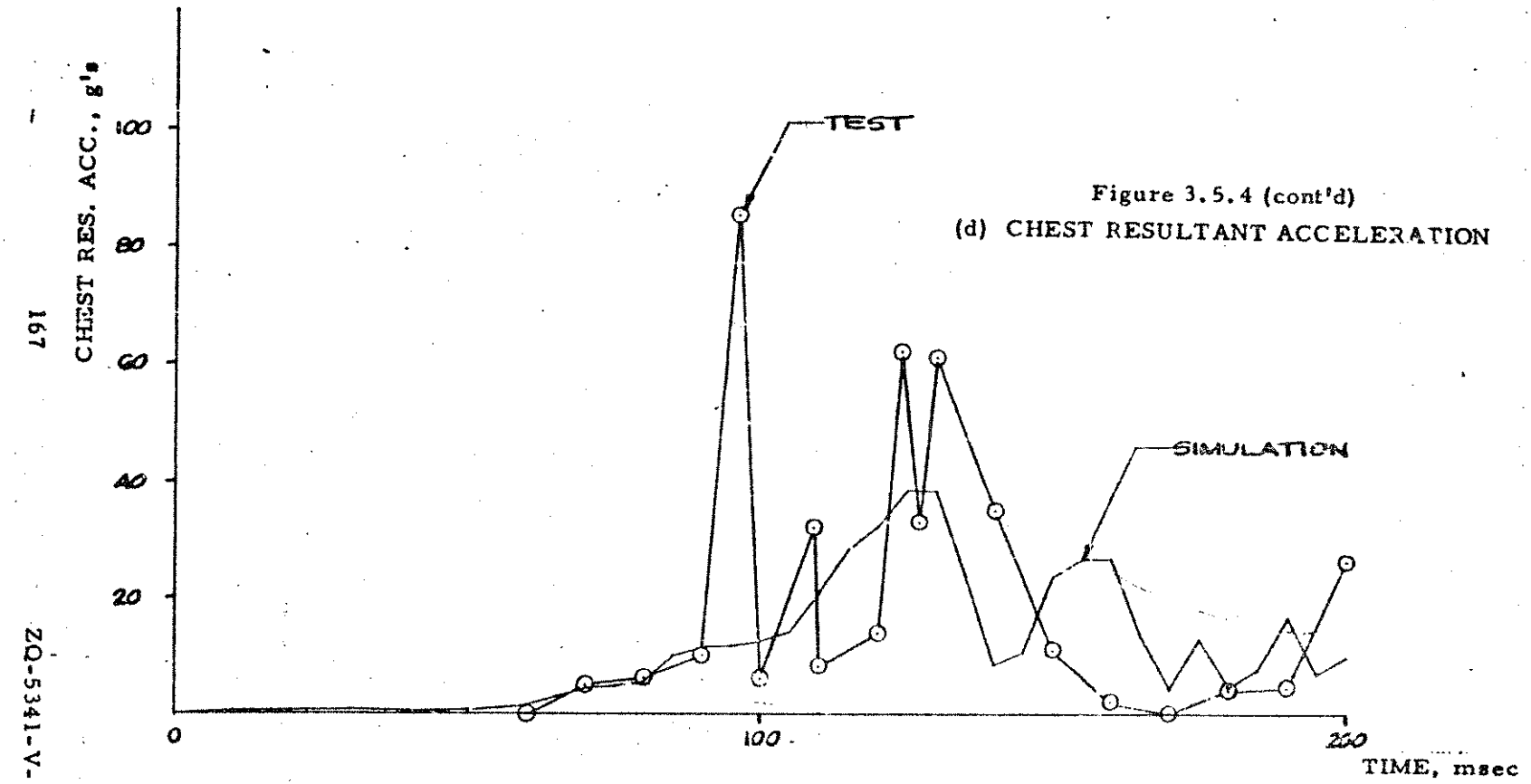

Figure 3.5.4 (cont'd)
(d) CHEST RESULTANT ACCELERATION

Case No. SW71044

Sled Run No. 1144

In this low-speed accident, the head of the right front occupant struck the windshield and broke it, as summarized in Figure 3.3.17. Similarly, the computer simulation of the accident predicted a windshield failure by head impact. In contrast, however, even though head-windshield contact occurred in the sled test, the loading did not produce cracking or failure of the windshield (see Figure 3.4.6).

This discrepancy cannot be attributed to the sled pulse, Figure 3.5.5(a). If anything, the sled pulse was too severe (13% too high speed change) compared to the predicted vehicle deceleration.

The kinematic display, Figure 3.5.5(b) suggests that the dummy head did not strike the windshield, but this is not the case, as can be seen in Figure 3.4.6*. With this factor taken into account, the predicted and measured kinematic responses agree within reason.

The head-windshield contact is best analyzed in the comparison of Figure 3.5.5(c), showing measured and predicted head resultant accelerations. In the test, the head-windshield contact occurred earlier than in the simulation, but produced about half of the peak magnitude in head resultant acceleration. This difference in measured and predicted head contact is reflected in the corresponding chest resultant accelerations, Figure 3.5.5(d).

At this low impact speed (~ 9 MPH), differences in torso slippage on the seat between test and simulation could play a major role in kinematic responses, and could account for the discrepancy in windshield failure and the lack of time correlation.

*This is caused by (1) the inaccuracy of the first-order parallax correction for small displacements and also by (2) the difference in initial dummy head position relative to the windshield compared to the simulation.

SW71044

SPEED CHANGE, mph	
TEST	SIMULATION
9.7	8.6

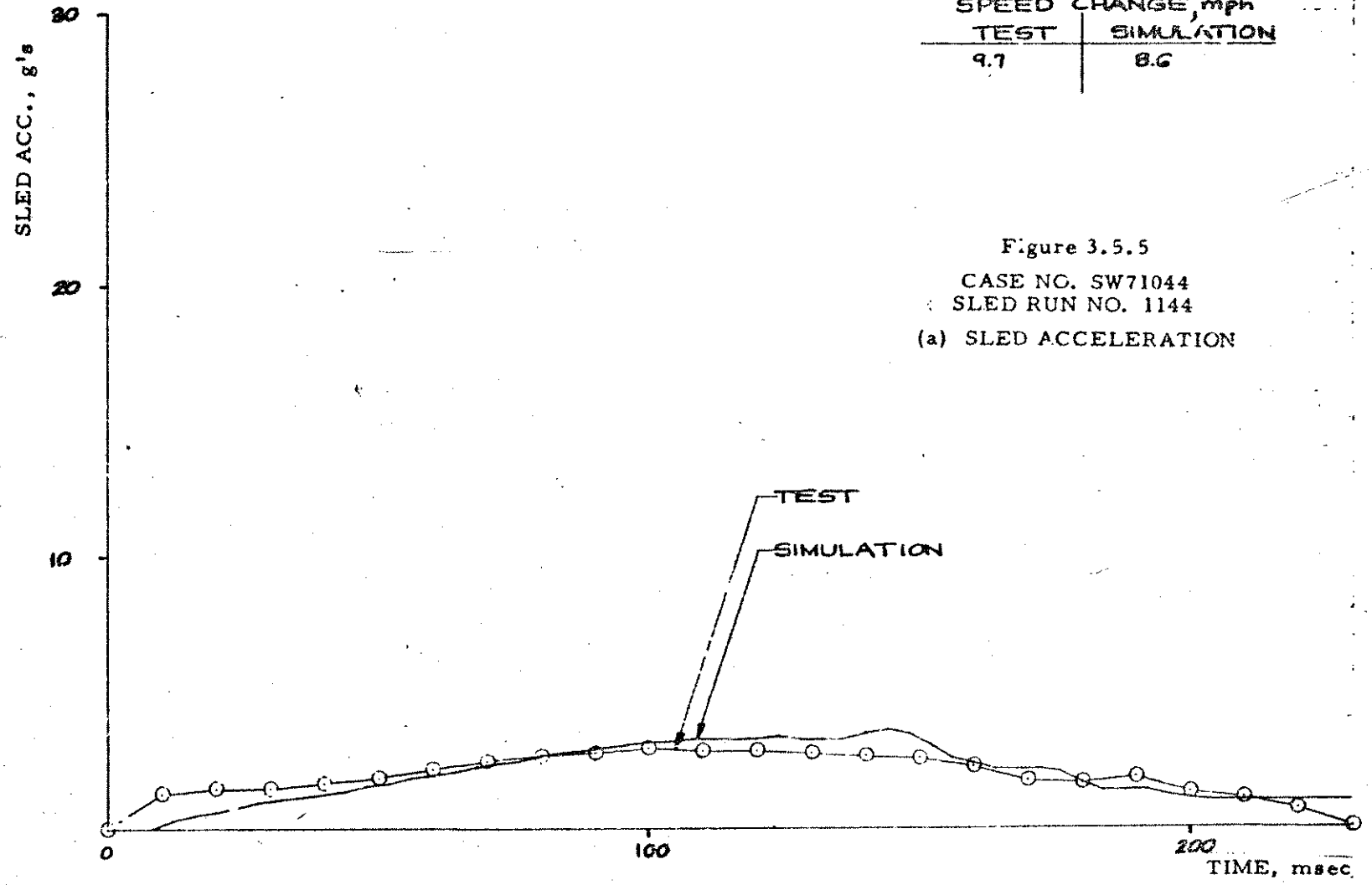

Figure 3.5.5
CASE NO. SW71044
SLED RUN NO. 1144
(a) SLED ACCELERATION

ZQ-5341-V-1

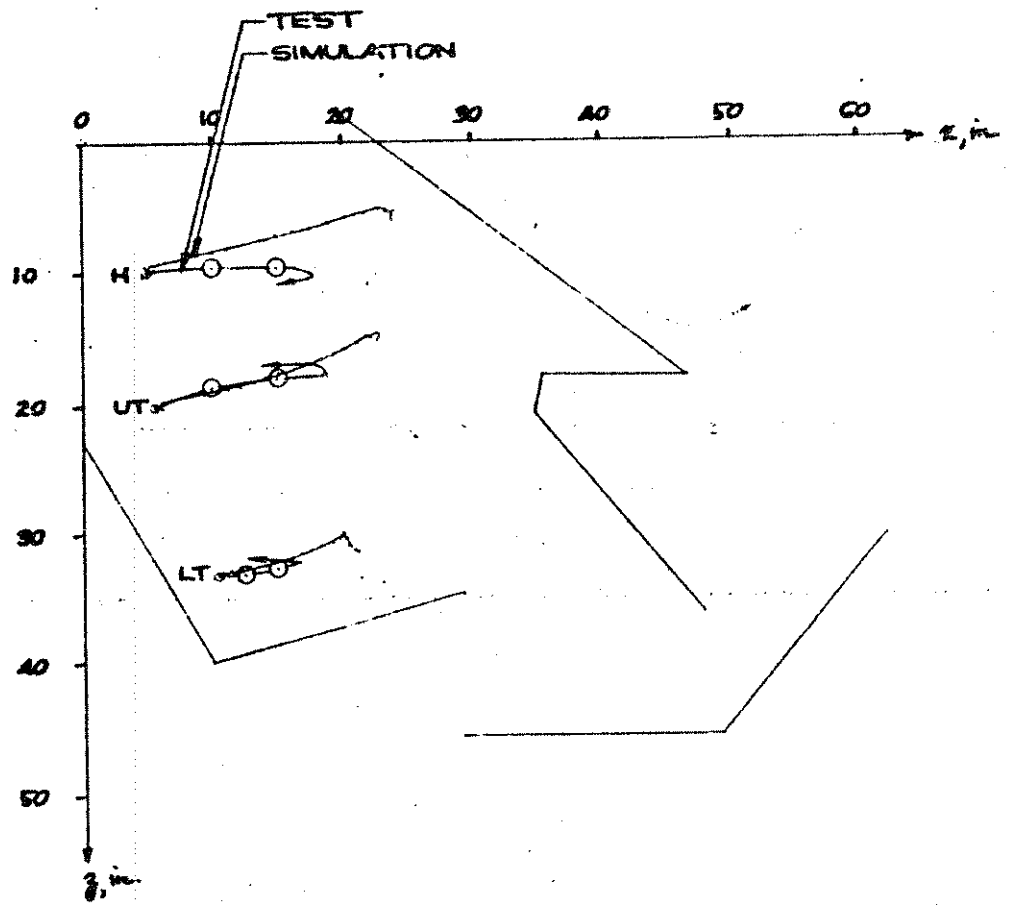

Figure 3.5.5 (cont'd)

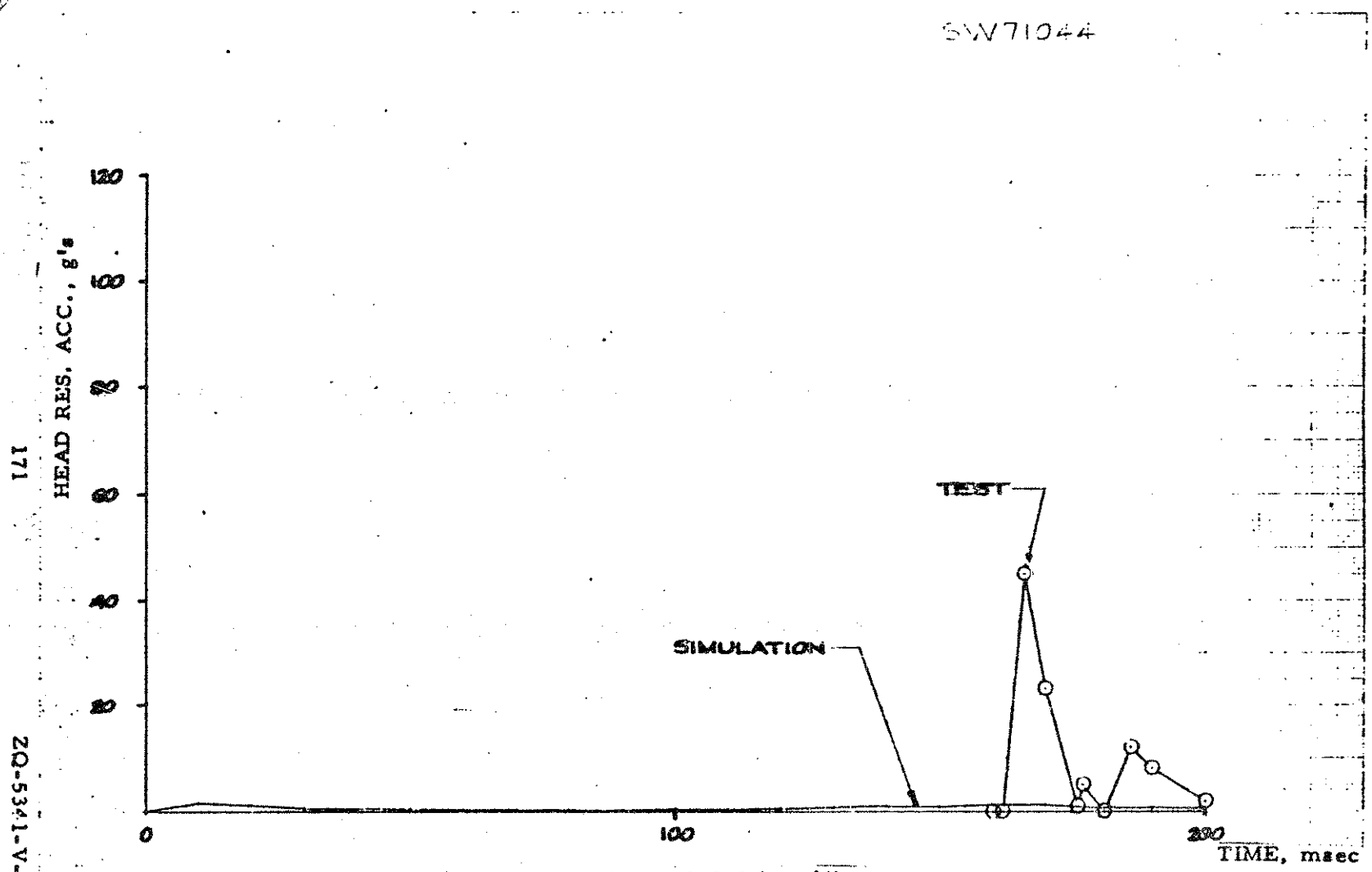

Figure 3.5.5 (cont'd)
(c) HEAD RESULTANT ACCELERATION

SW 71644 (cont'd)

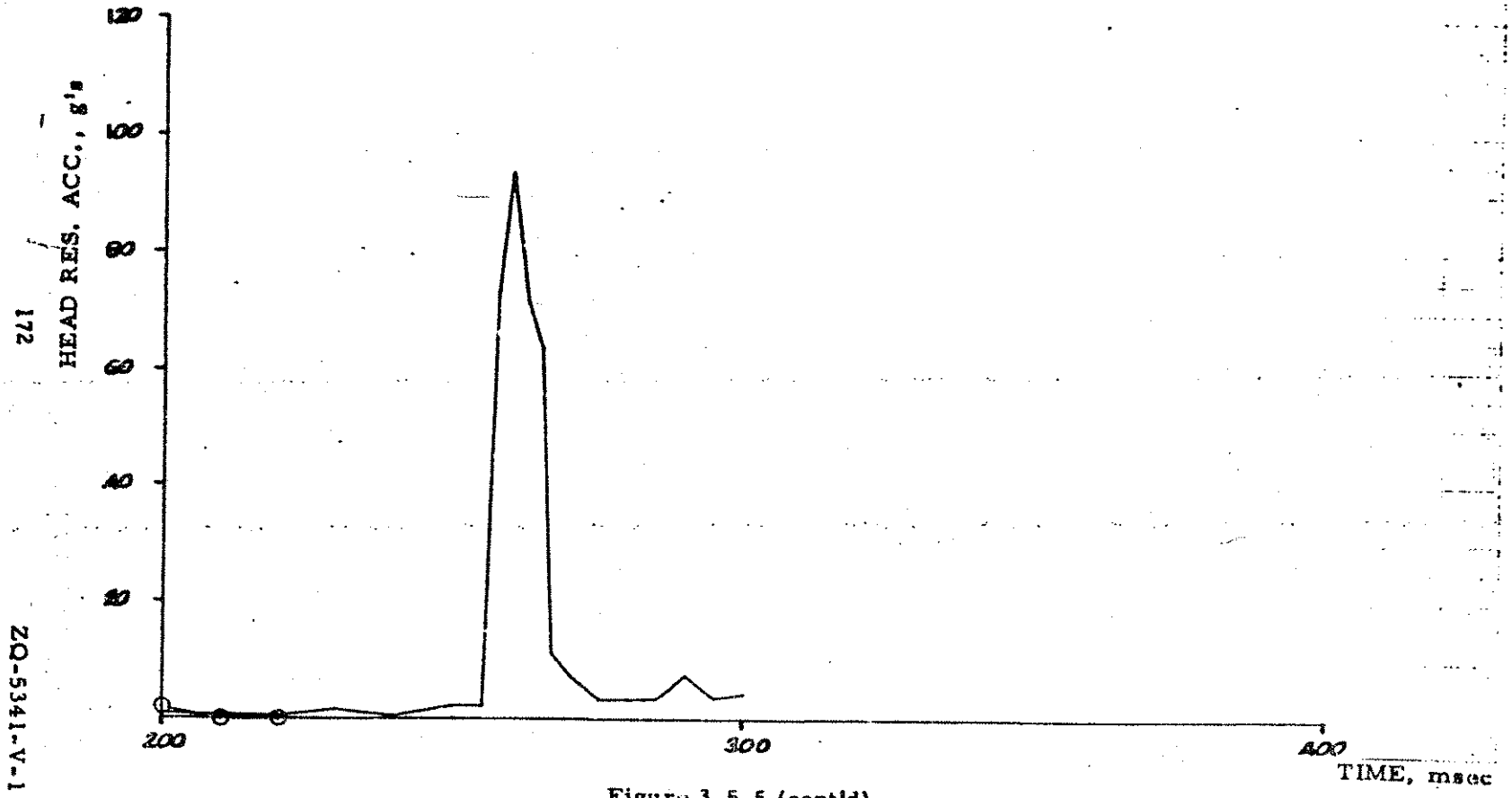

Figure 3.5.5 (cont'd)
(c) HEAD RESULTANT ACCELERATION (cont'd)

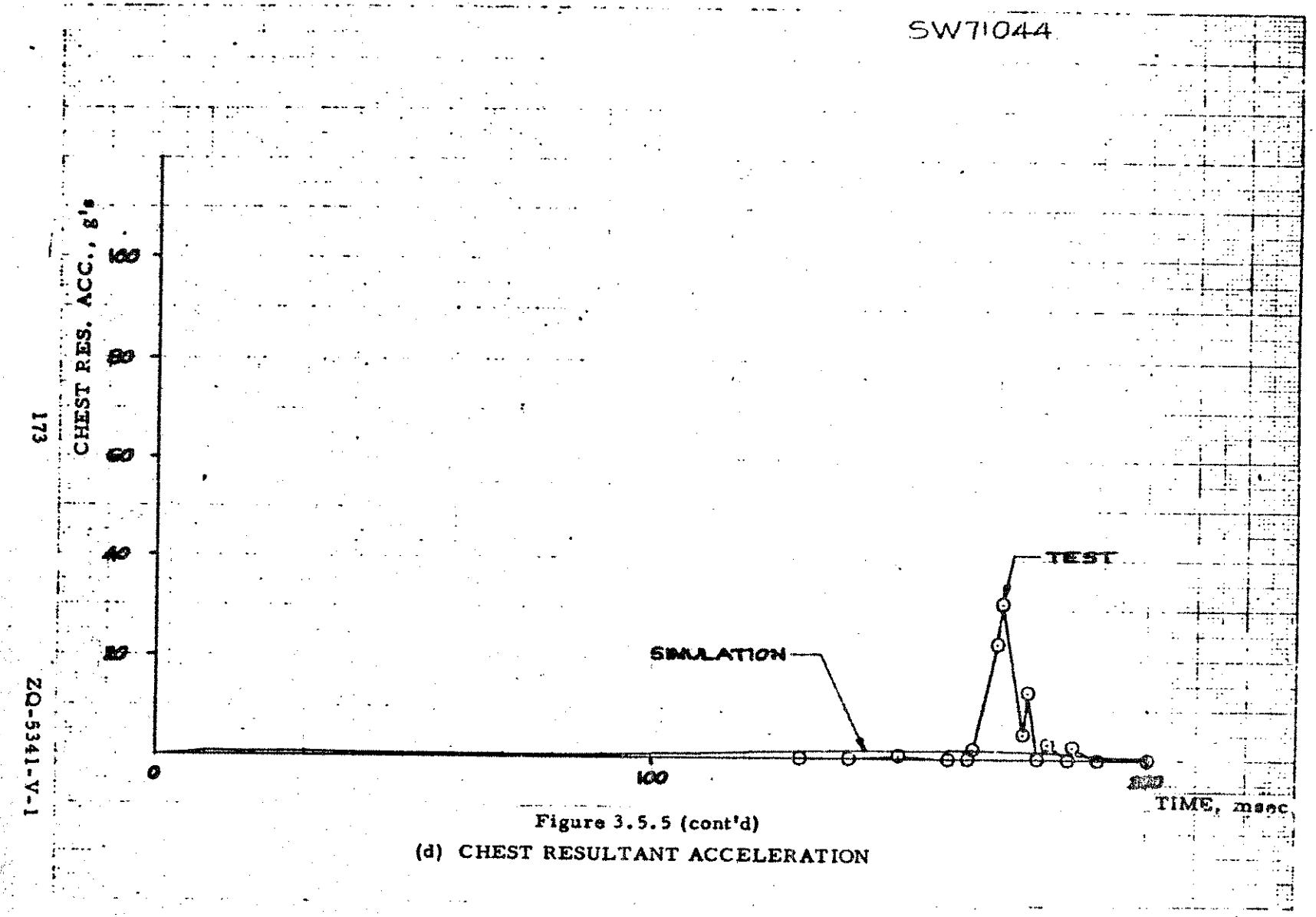

Figure 3.5.5 (cont'd)
(d) CHEST RESULTANT ACCELERATION

EW71044(cont'd)

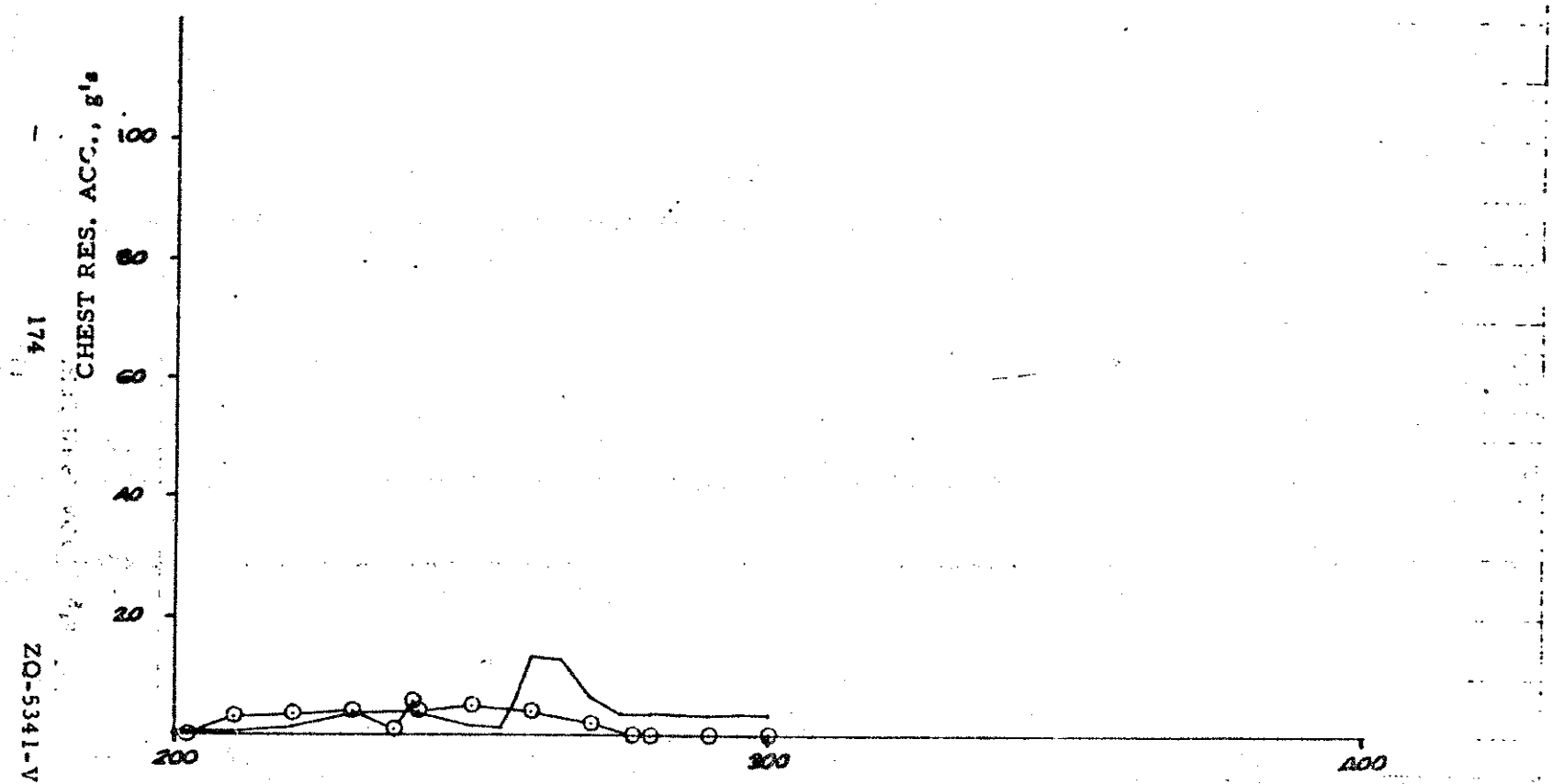

Figure 3.5.5 (cont'd)

(d) CHEST RESULTANT ACCELERATION (cont'd)

Case No. CB00053

Sled Run No. 1145

In this accident, summarized in Figure 3.3.21, the crash victim struck the windshield, resulting in severe facial abrasions and lacerations and loss of consciousness. The predicted kinematic responses of the head summarized in that figure are in good agreement with the accident case report. Similarly, the sled test reconstruction of the accident, summarized in Figure 3.4.7, produced head contact results consistent with the case report.

The sled pulse duplicated the predicted vehicle deceleration, Figure 3.5.6(a), with good accuracy, except near the end of the trace. Nevertheless, the experimental and analytically determined speed changes were within 7 percent.

The kinematic displays of Figure 3.5.6(b) illustrate that, following head contact, the simulation predicts torso rotation, in contrast to the sled test result of nonrotational torso rebound. This difference is likely caused by the use of "typical" material properties of contacting surfaces in the program input, plus the array of contacts allowed in the simulation.

Comparison of the measured and predicted head resultant accelerations, Figure 3.5.6(c), shows that the time of head-windshield contact, as evidenced by the spike in the trace, is predicted reasonably well. The measured peak, however, is significantly higher than predicted. In this sled test (No. 1145), appreciable high frequency ringing is superimposed on the base data trace, which may have contributed to the magnitude of the experimental peak.

The measured peak chest resultant acceleration, Figure 3.5.6(d), is also significantly higher than predicted, an effect considered traceable to the assumed force-deflection characteristic inputted for the chest-instrument panel contact.

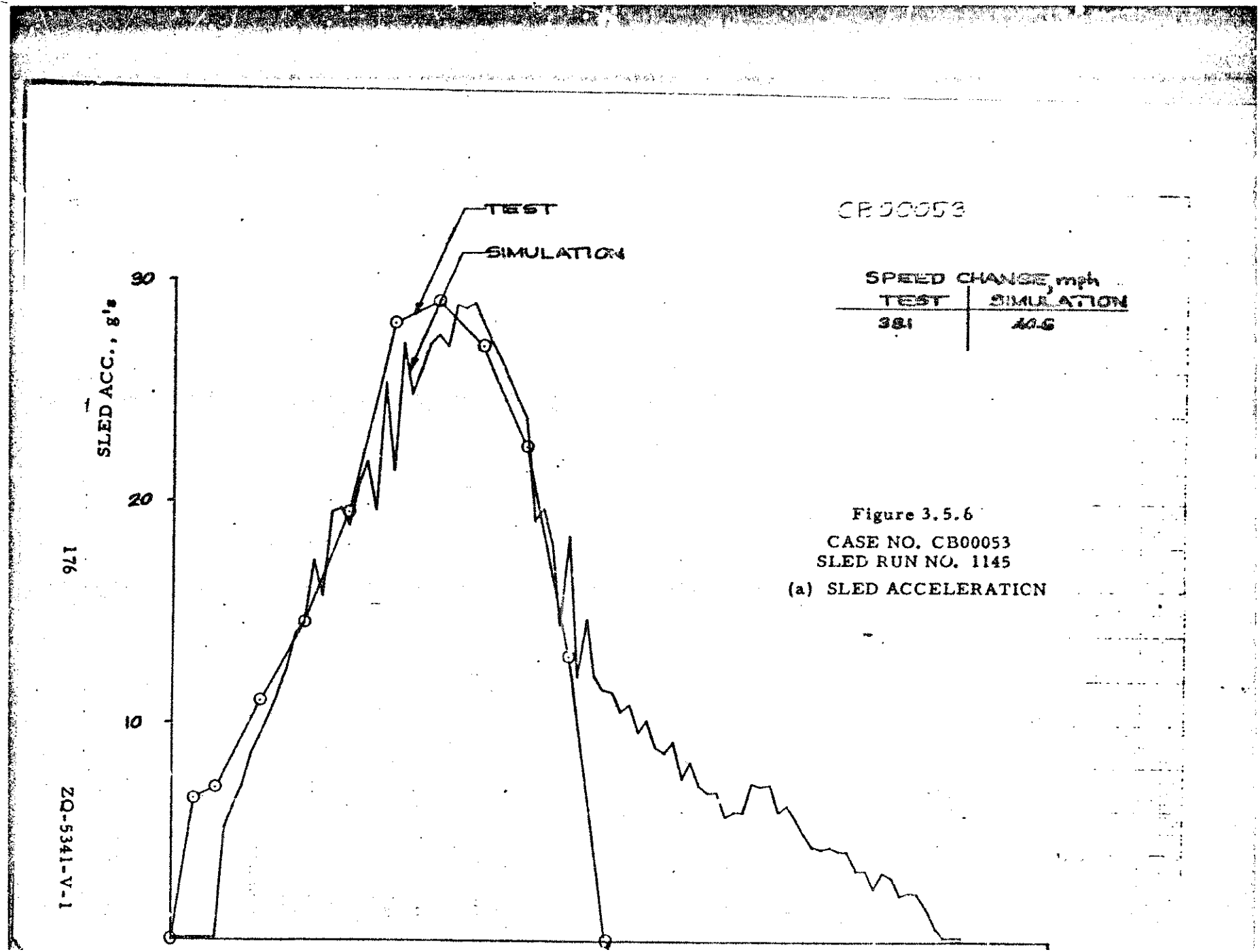

Figure 3.5.6
CASE NO. CB00053
SLED RUN NO. 1145
(a) SLED ACCELERATION

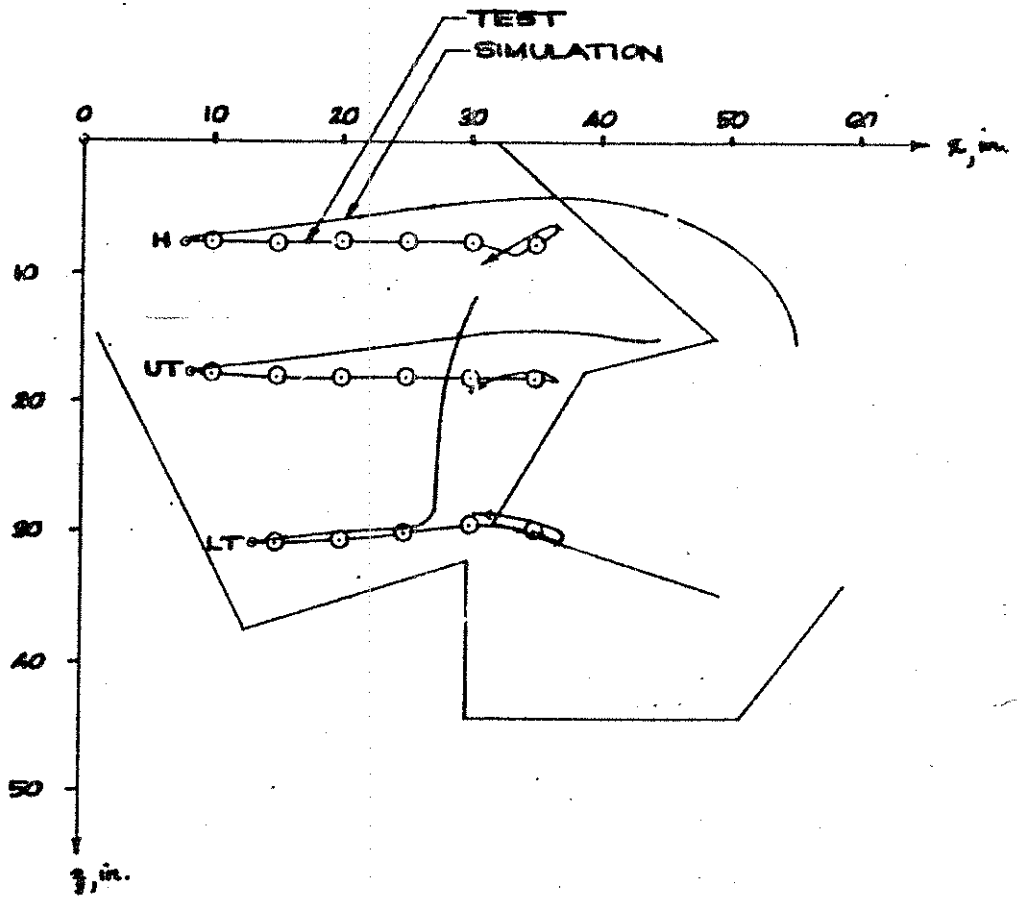

Figure 3.5.6 (cont'd)
(b) KINEMATICS

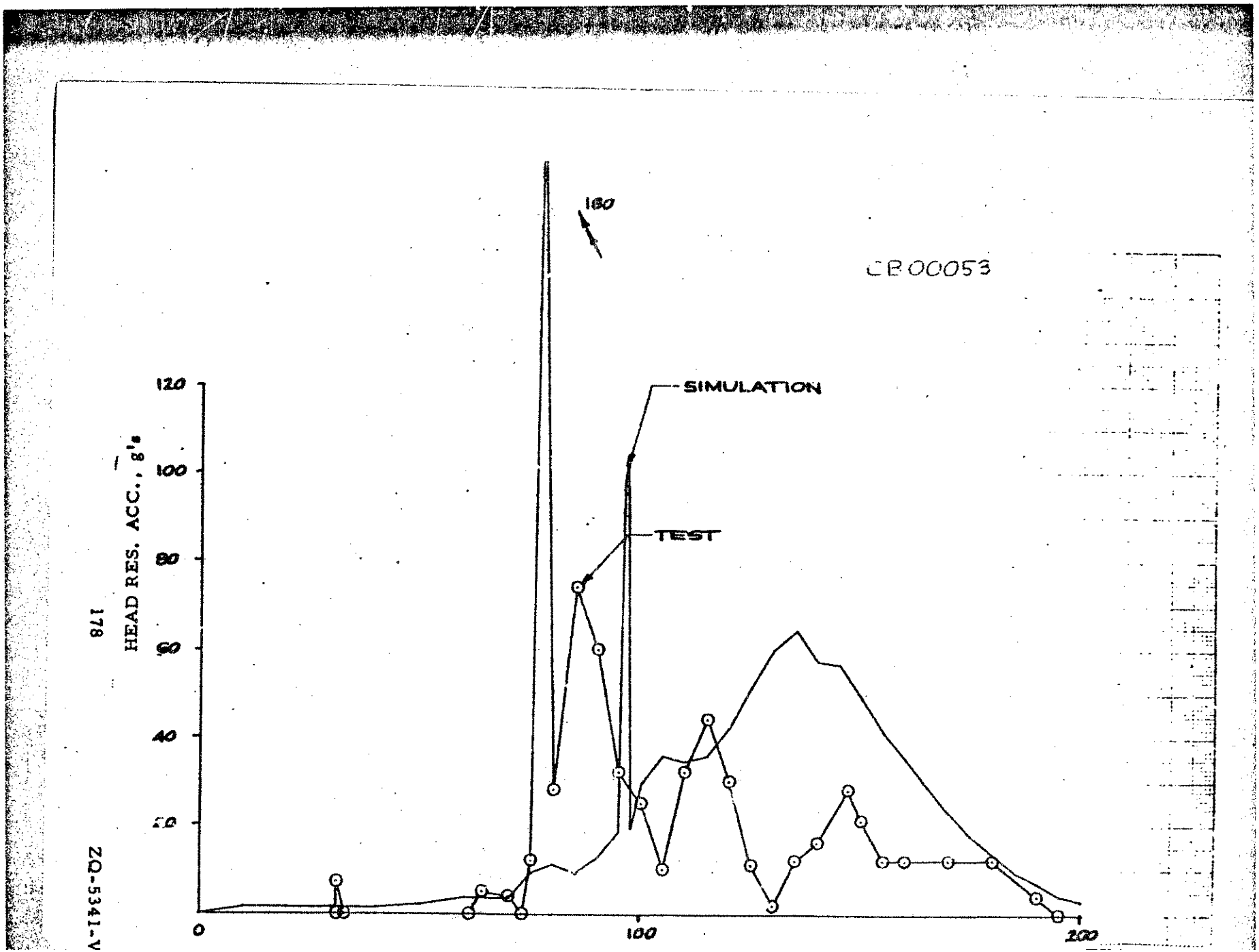
TIME, msec
180
CB00053
SIMULATION
TEST
120
100
80
60
40
20
0
100
200
HEAD RES. ACC., g's
178
ZQ-5341-V

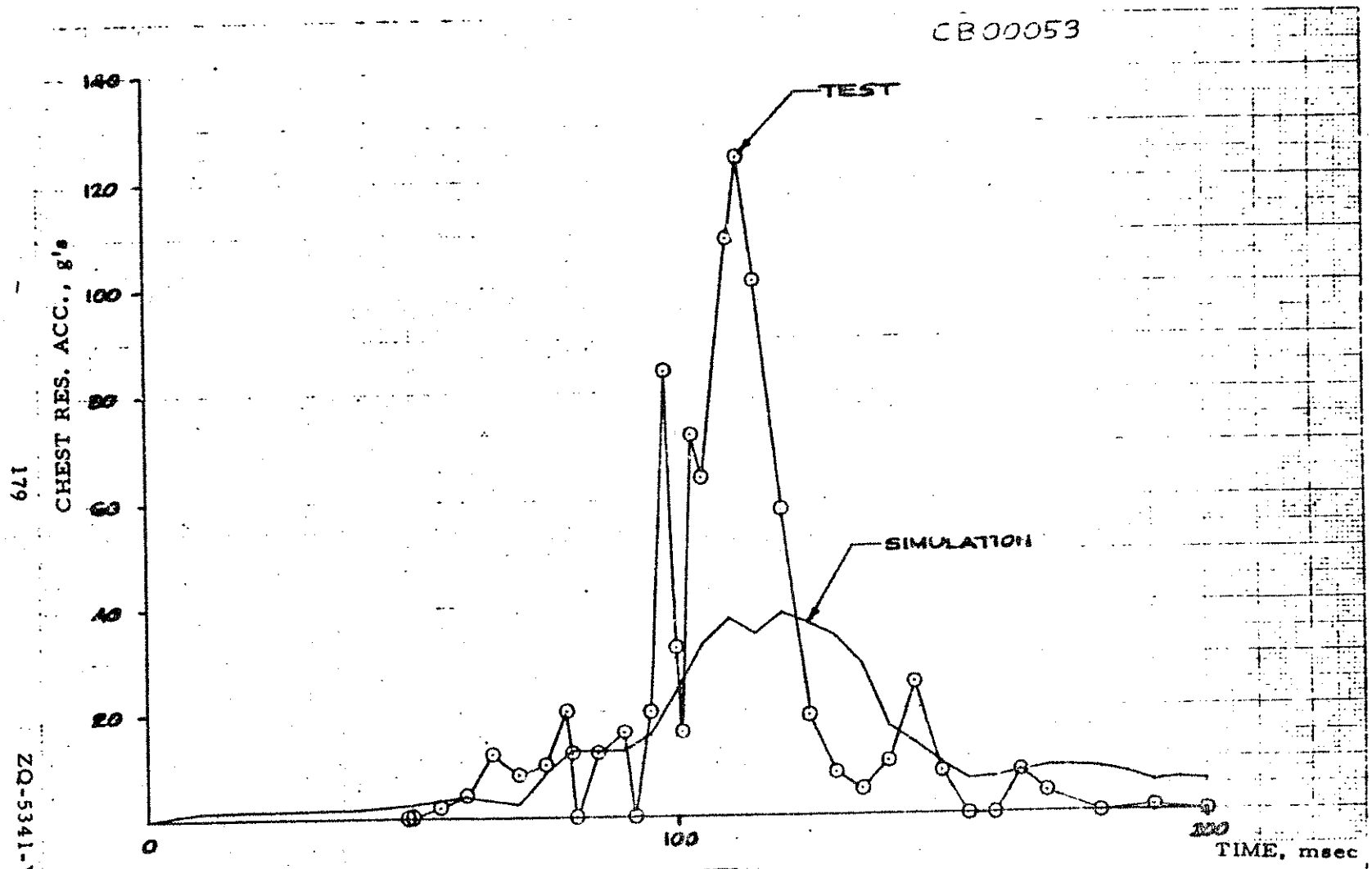

Figure 3.5.6 (cont'd)

(d) CHEST RESULTANT ACCELERATION

Case No. CB71055

Sled Runs Nos. 1134 and 1135

In this accident, the crash victim, a 60 in., 130 lb. female, suffered severe facial injuries in contacts with the rear view mirror and then the instrument panel. Because of the considerable difference between the size of the crash victim and the reference 50th percentile male size, this case was selected to study the effect of variation in occupant size.

The predicted kinematic responses of both these sizes of crash victims are summarized in Figure 3.3.25. There is little difference in kinematics due to size, and both simulated occupants strike the windshield in the general location of the rear view mirror (no rear view mirror contact was simulated). In similar manner, the sled test results for this case (sled run no. 1135 corresponding to the 50th percentile male, and sled run no. 1134 corresponding to the 5th percentile female), Figures 3.4.8 and 3.4.9, respectively, indicate a comparable contact with the windshield. In both of these sled tests, the rear view mirror, installed on the windshield for all tests, was nearly contacted by the dummy heads (within about 2-3 inches). A slight difference in initial test conditions (5° greater buck rotation angle, 2-3 inch lateral displacement of the dummy toward the center of the vehicle) would likely have caused the head-rear view mirror contact observed in the accident.

The sled acceleration pulses for both of these tests were highly repeatable, and agreed quite closely with the desired (predicted) vehicle deceleration, as shown in Figure 3.5.7(a). Note that the approximately 10-20 msec. shift in time correlation between the measured and predicted pulses has no significance for the present discussion.

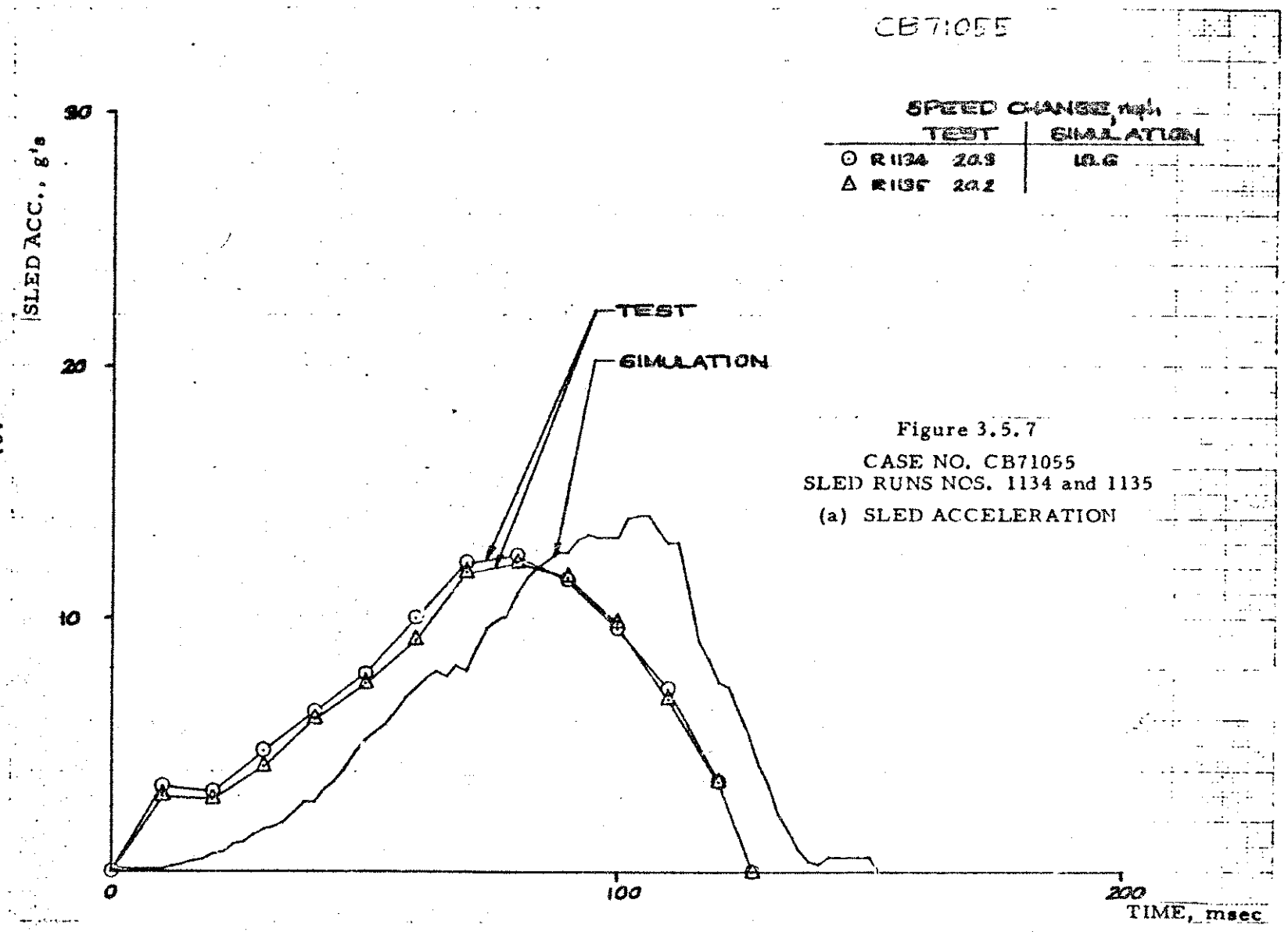

Figure 3.5.7

CASE NO. CB71055
SLED RUNS NOS. 1134 and 1135
(a) SLED ACCELERATION

The measured kinematic responses for both tests, summarized in Figure 3.5.7(b), indicate reasonable agreement with the predictions, but somewhat greater forward displacement than the simulation. This could be due to the slightly greater speed change in the tests than in the simulation (about 9 per cent).

The magnitudes, trends, and time correlation of the measured head resultant accelerations are predicted rather well, as indicated in Figure 3.5.7(c). The primary exception, the large spike of about 180 g's measured in sled run no. 1134, may be caused by the high-frequency ringing on the accelerometer traces observed in that test (see Appendix D). Note that both predictions and measurements indicate a higher peak acceleration on the less massive head of the small female compared to the 50th percentile male crash victim.

The predicted chest resultant accelerations, Figure 3.5.7(d) are notably absent of the spikes measured in both tests. The general trend and time correlation are predicted reasonably, however.

Case No. TR01161

Sled Run No. 1137

In this rather severe accident, the unrestrained right front occupant was thrown forward, resulting in his head contacting the windshield and possibly the displaced hood, and an injury rating of 3 (severe) on the ten-point scale. The predicted kinematic responses, summarized in Figure 3.3.29, are consistent with the findings of the accident investigation, as are the results from the corresponding impact sled test, presented in Figure 3.4.10.

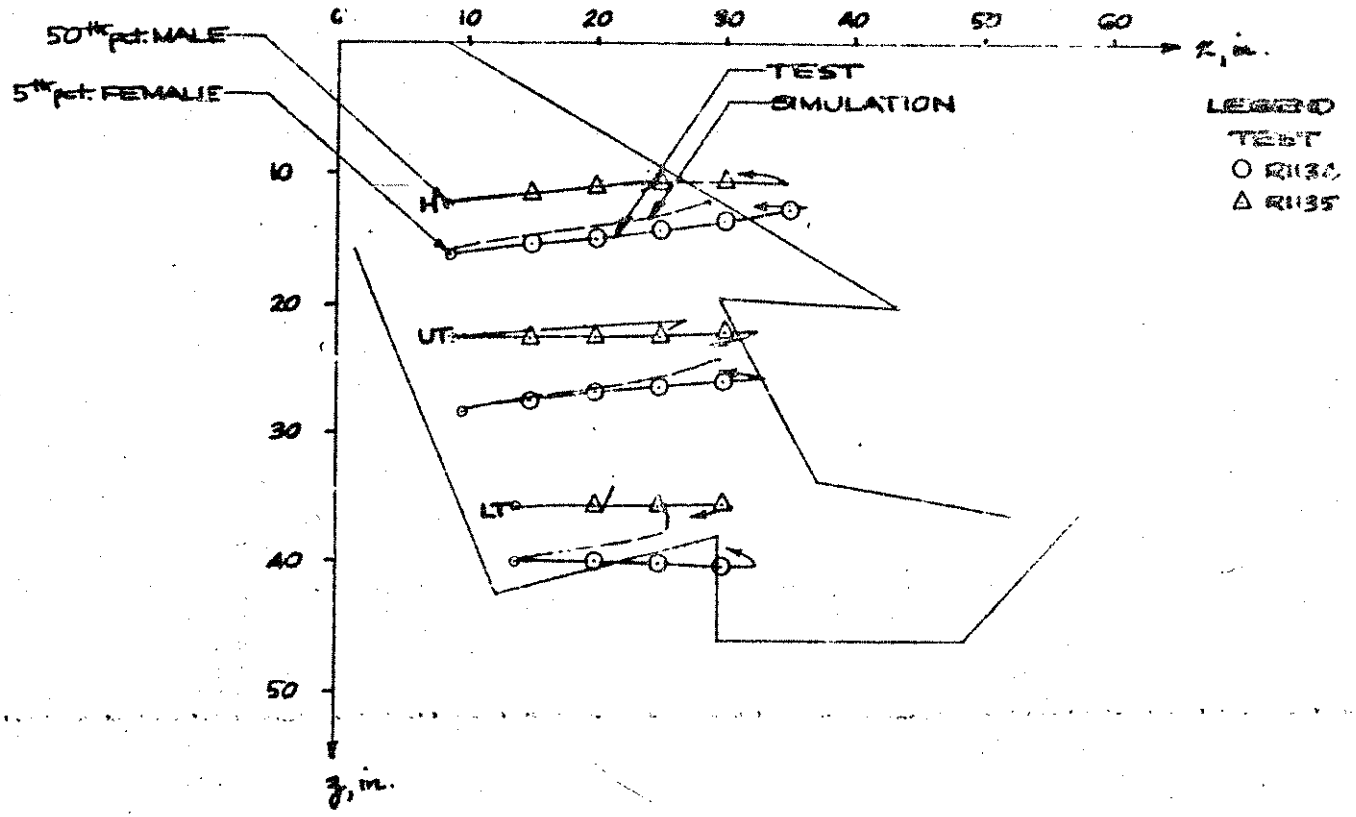

Figure 3.5.7 (cont'd)
(b) KINEMATICS

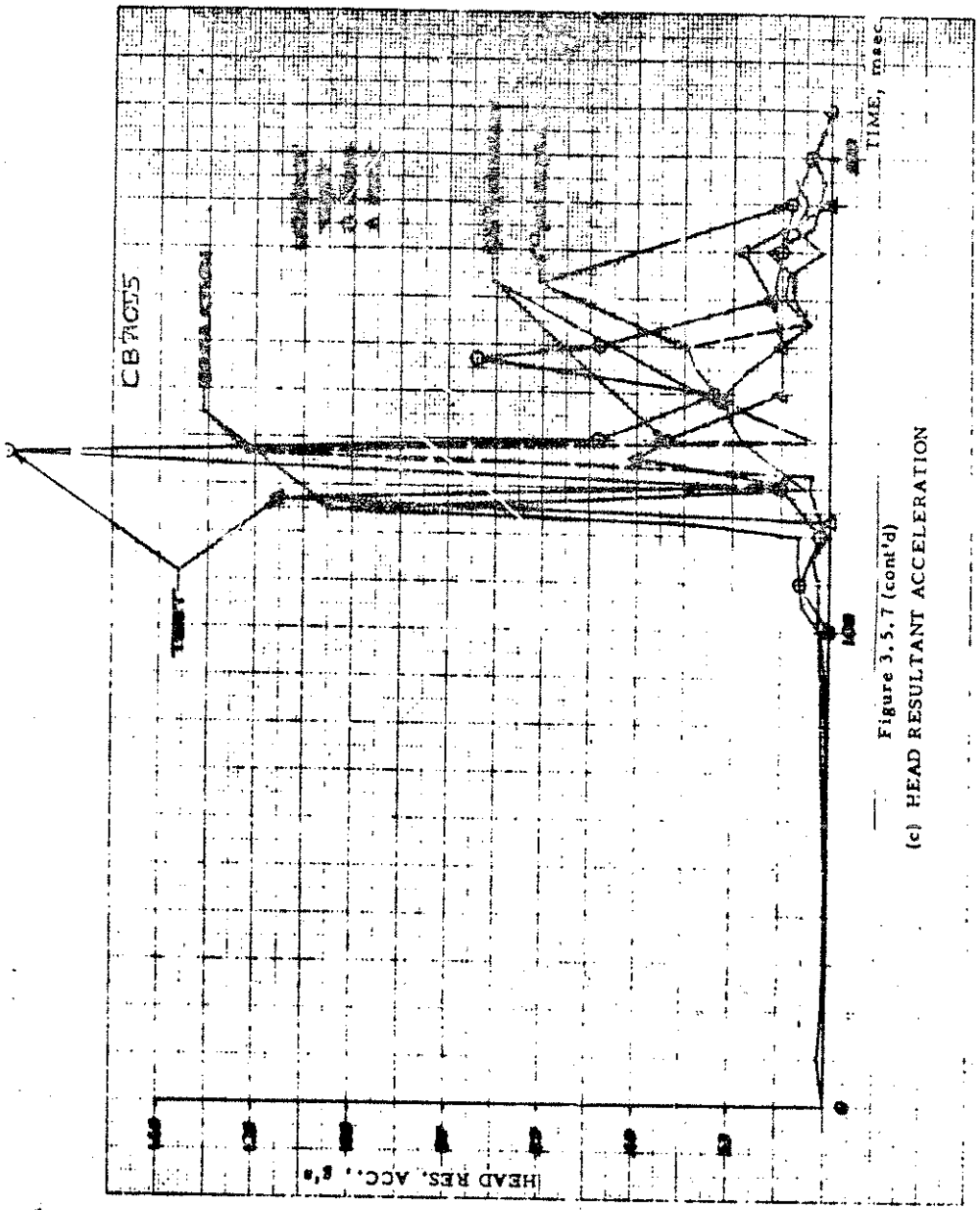

Figure 3.5.7 (cont'd)

(c) HEAD RESULTANT ACCELERATION

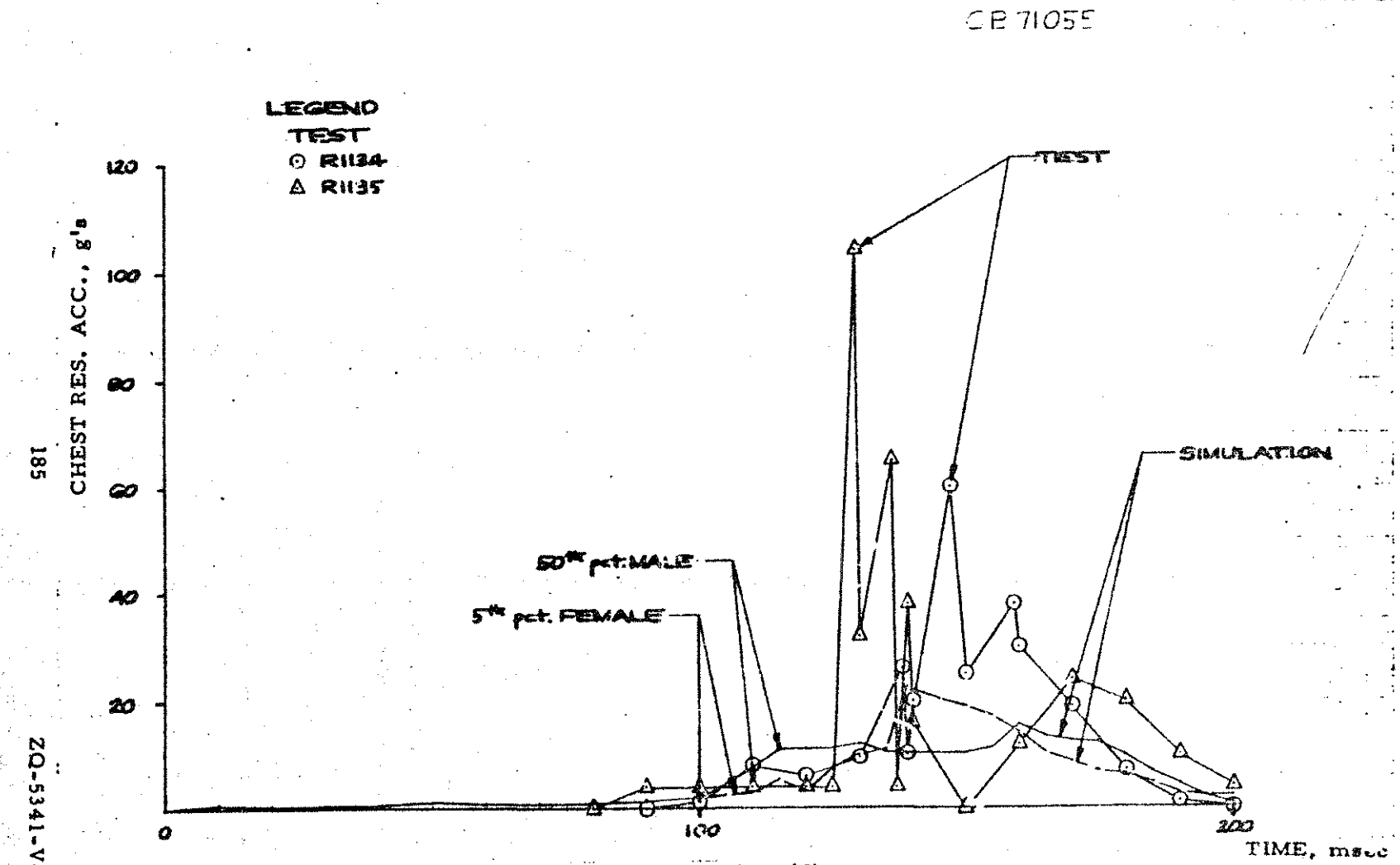

Figure 3.5.7 (cont'd)

(d) CHEST RESULTANT ACCELERATION

The desired vehicle deceleration history was reproduced reasonably well on the impact sled, as can be seen in Figure 3.5.8(a), especially when account is taken of the difference in time correlation between the two plotted pulses.

The head-windshield contact in the sled test is predicted rather well, as indicated in the kinematic displays of Figure 3.5.8(b), but the computer simulation predicts considerable torso rotation following head-windshield contact compared to the sled test result. The large forward head displacement in the simulation is consistent with the possible head-hood contact noted in the accident case report. The difference between predicted and measured kinematics is believed to be largely due to the use of "typical" material properties to represent the chest contact with the instrument panel in the computer simulation.

The measured head resultant acceleration peak, Figure 3.5.8(c), agrees reasonably with the predicted result in terms of time correlation, but the measured peak is about 80 percent higher. This may be partially caused by the high frequency ringing on the measured acceleration traces in this run (see Appendix D). However, part of this difference is undoubtedly attributable to the use of a single force-deflection function to represent the dynamic windshield failure characteristics in the simulation. It may be recalled that a single function (see Figure 3.1.2) based on measurements at 30 MPH was used in the computer program because of lack of sufficient data to define the function over a range of speeds. It is likely that the inputted function is not adequate to represent accurately the dynamic windshield failure properties at the speed change corresponding to this accident ($\sim$ 40 MPH). These preceding comments, of course, apply to the other cases in varying degrees.

The measured chest resultant acceleration, Figure 3.5.8(d), is appreciably higher than that predicted. This result is consistent with the smaller forward displacement of the dummy noted in the test, Figure 3.5.8(b). Again, the difference is considered attributable to a lack of knowledge of the instrument panel properties for computer program input.

TR01161

SPEED CHANGE, mph	
TEST	SIMULATION
36.4	38.6

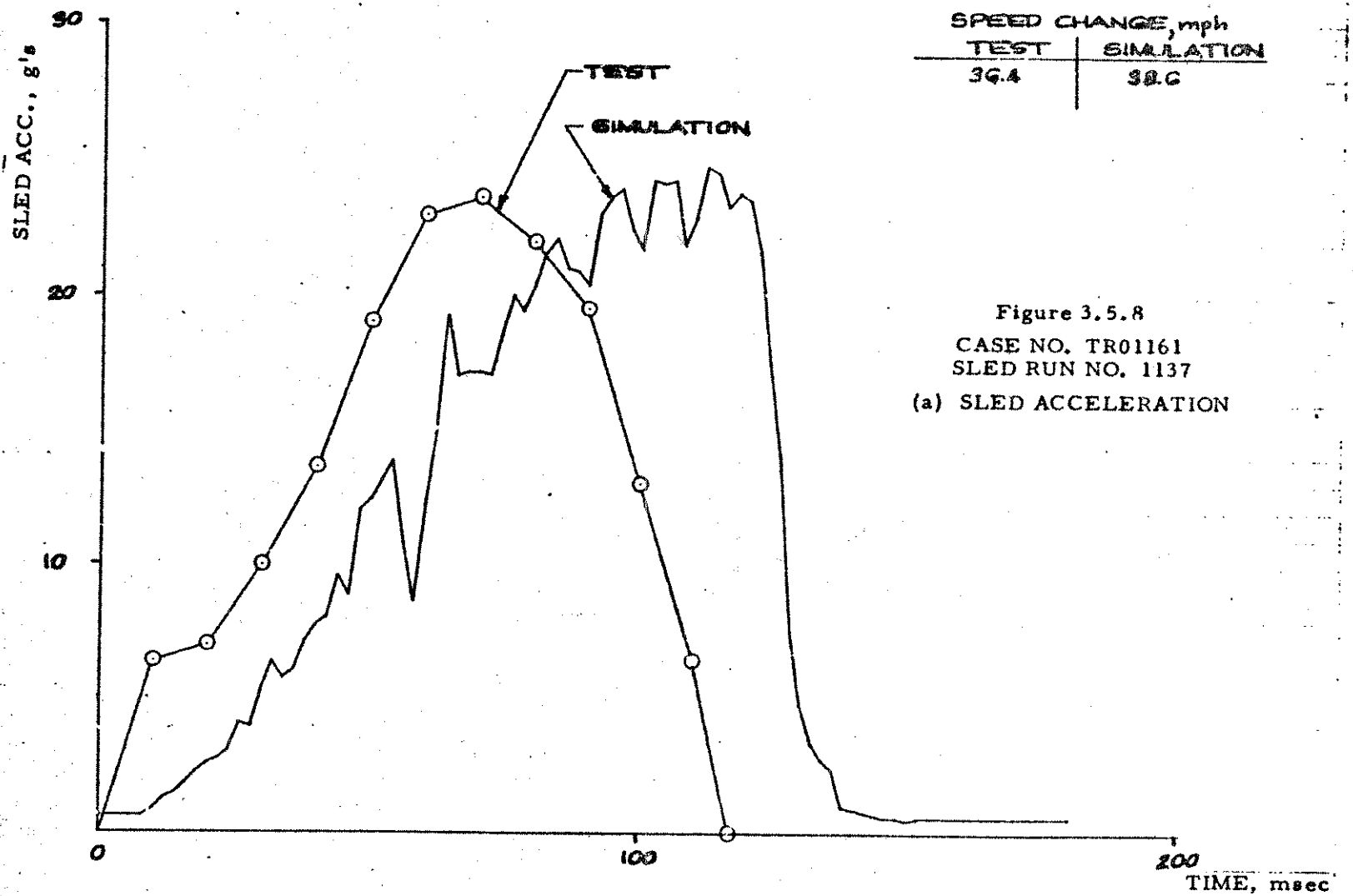

Figure 3.5.8
CASE NO. TR01161
SLED RUN NO. 1137
(a) SLED ACCELERATION

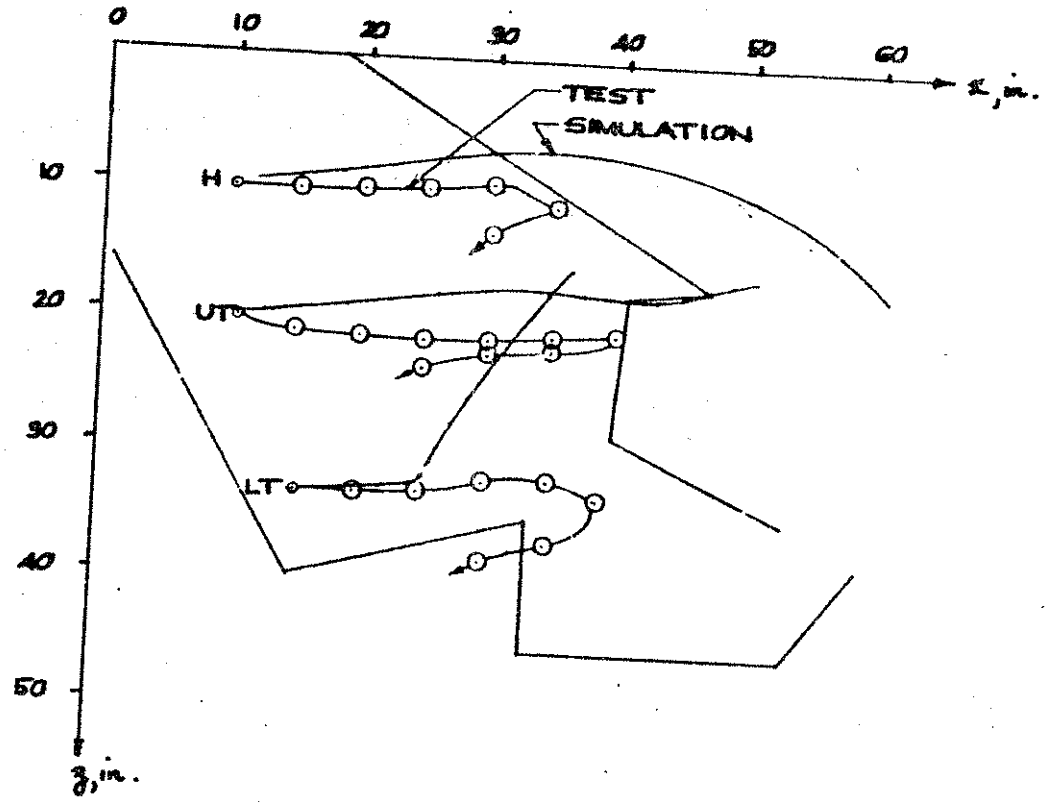

Figure 3.5.8 (cont'd)
(b) KINEMATICS

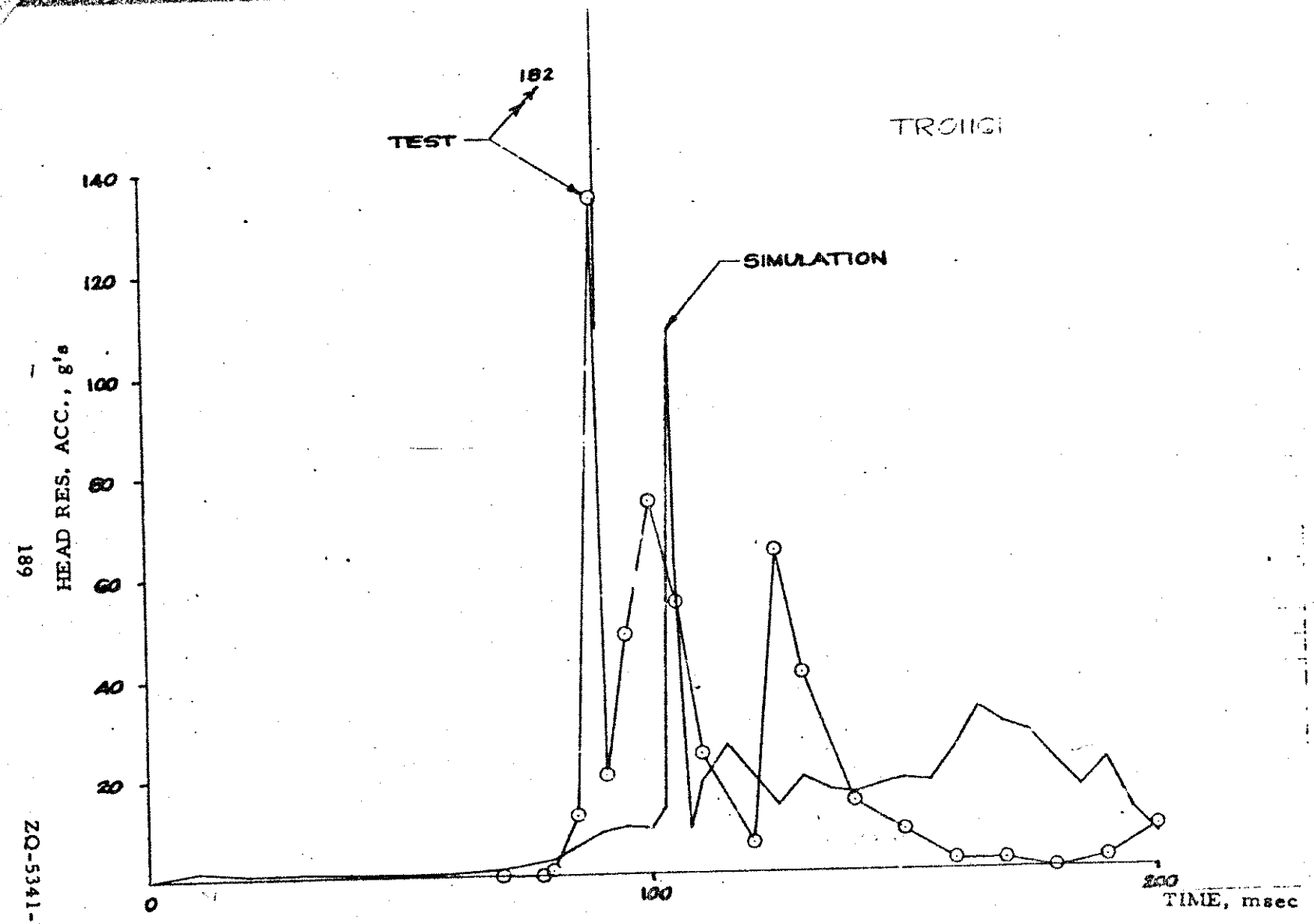

Figure 3.5.8 (con't'd)

(c) HEAD RESULTANT ACCELERATION

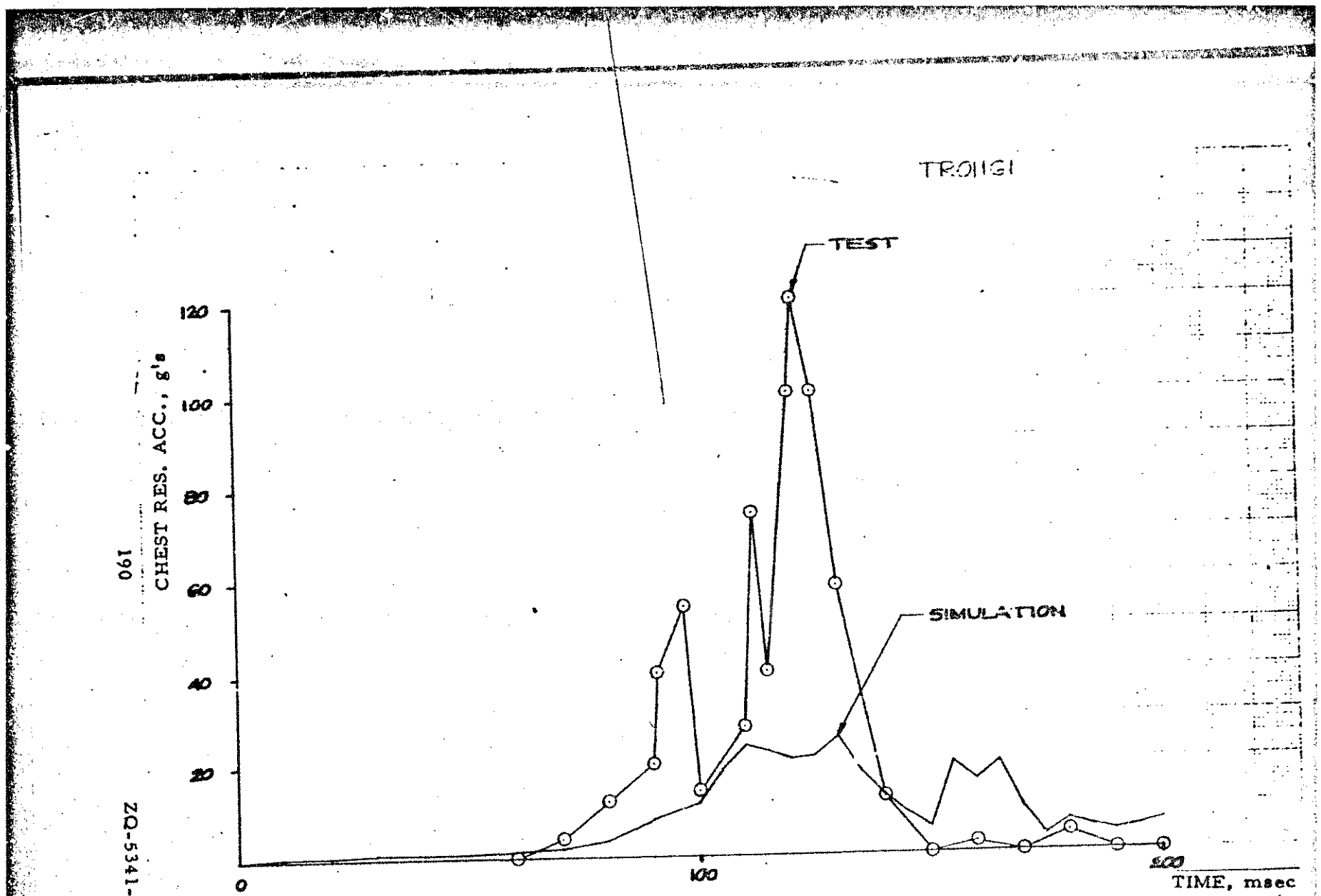

Figure 3.5.8 (cont'd)
(d) CHEST RESULTANT ACCELERATION

Case No. GI00056

Sled Runs Nos. 1142 and 1143

In this case, the head of the right front occupant struck the instrument panel, with no reported head-windshield contact, resulting in concussion and an overall injury rating of serious (4 on the ten-point Abbreviated Injury Scale).

An examination of the overall geometry for this case, illustrated by the plotter graphics display in Figure 3.3.33, suggests that head-windshield contact would probably occur in a frontal crash unless prevented by either occupant bracing or other similar response. Occupant bracing was considered in connection with Case No. AA00145, but its effect was not studied in this case. Note that head-windshield contact is in fact predicted by the computer simulation for this case, as shown in Figure 3.3.33, with no bracing response applied by the simulated occupant.

For this accident case, two sled tests were performed. The test conditions were replicate, except for the location of the seat relative to the windshield/body buck reference frame. In sled run no. 1142, the seat was placed in mid-position (corresponding to the accident), and in sled run no. 1143, the seat was moved 2 1/2 in. forward relative to that mid-position. The purpose of these two tests was to study the effect of geometrical uncertainties associated with

- crash victim size compared to size of the simulated occupant
- crash victim position and orientation compared to position and orientation of the simulated occupant
- accident vehicle interior geometry compared to the body buck interior geometry.

Examination of the summaries of sled test results, Figure 3.4.11 and 3.4.12, indicates that the geometrical variation had a rather minor effect on dummy responses and vehicle interior damage, as illustrated by the similar windshield failures in the two tests.

The sled pulse was again found to be highly repeatable, and duplicated the predicted vehicle deceleration history quite well, except for the high acceleration level near 100 msec. (see Figure 3.5.9(a)).

The measured kinematic responses were also found to be quite repeatable, as shown in Figure 3.5.9(b), and they matched the predicted head kinematics quite accurately. The predicted torso rotation, however, was not observed in the test results. Again, this is believed to be traceable to a lack of knowledge of the actual crush properties of the vehicle interior.

The measured head resultant accelerations, Figure 3.5.9(c) are likewise fairly repeatable, and agree reasonably with the corresponding prediction, except for the magnitude of the peak. High-frequency components were observed in the test results, which may be responsible for the higher measured peak values.

The general trend and time correlation of the measured chest resultant accelerations are predicted reasonably well, but not the measured spikes, as can be seen in Figure 3.5.9(d). Again, the test results are generally repeatable, with the exception of the spikes in the traces.

From these test results, the effect of variation of geometry is seen to be rather minor. However, if such geometrical variations altered the primary contacts that occurred, this conclusion would likely not be valid.

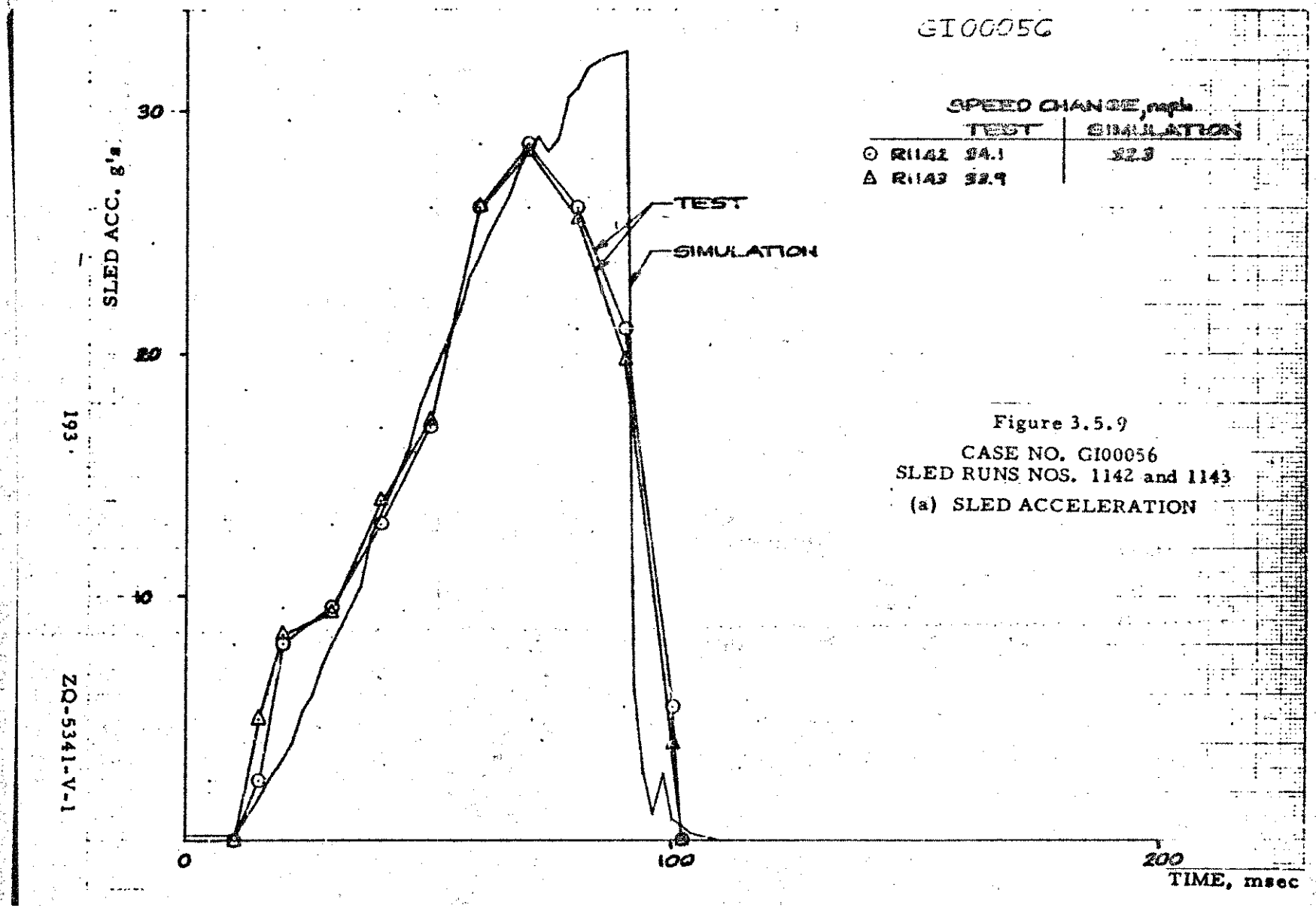

Figure 3.5.9

CASE NO. GI00056
SLED RUNS NOS. 1142 and 1143
(a) SLED ACCELERATION

GI00056

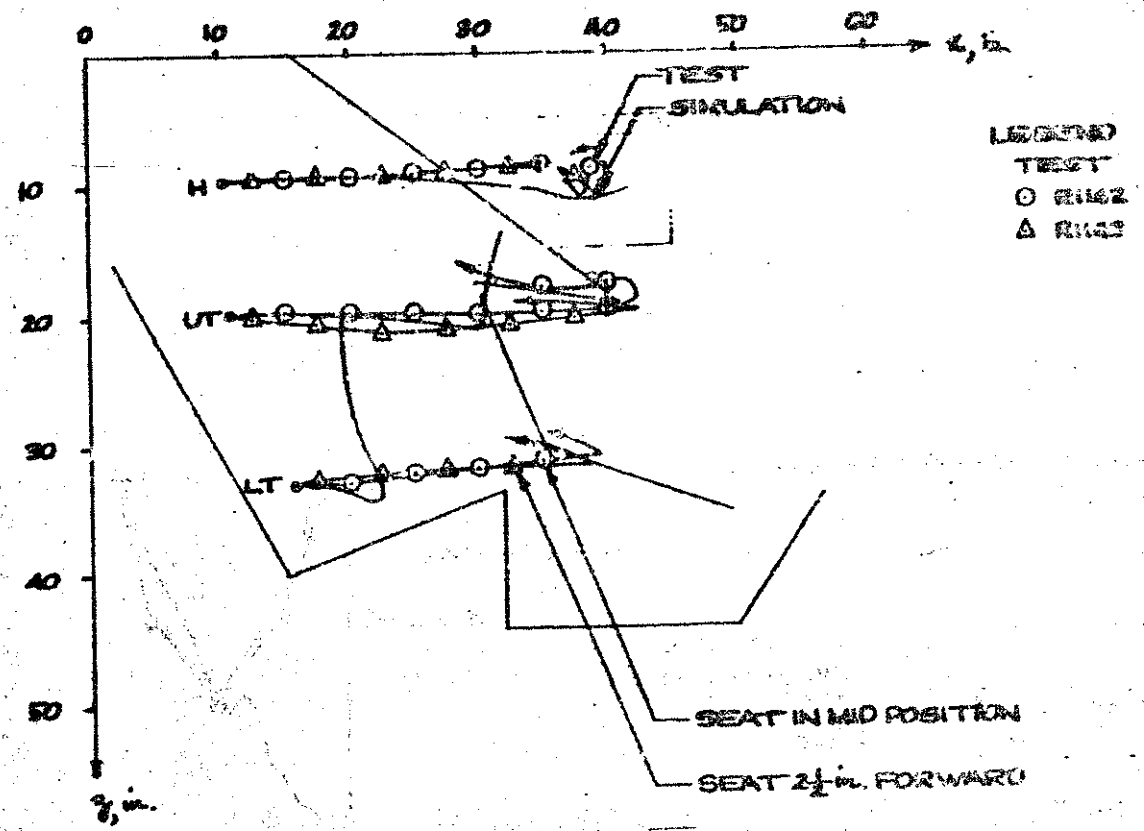

Figure 3.5.9 (cont'd)
(b) KINEMATICS

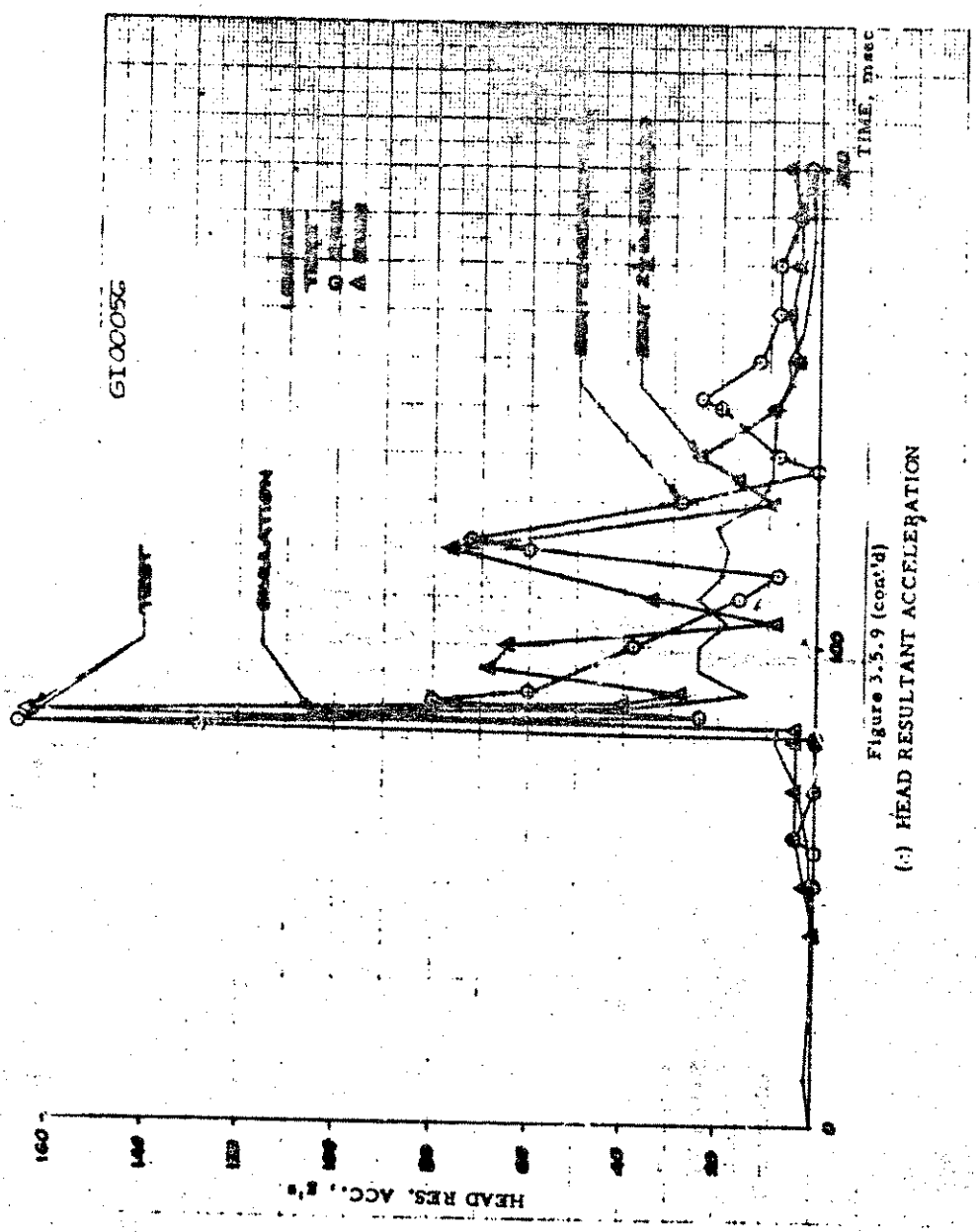

Figure 3.5.9 (cont'd)
(c) HEAD RESULTANT ACCELERATION

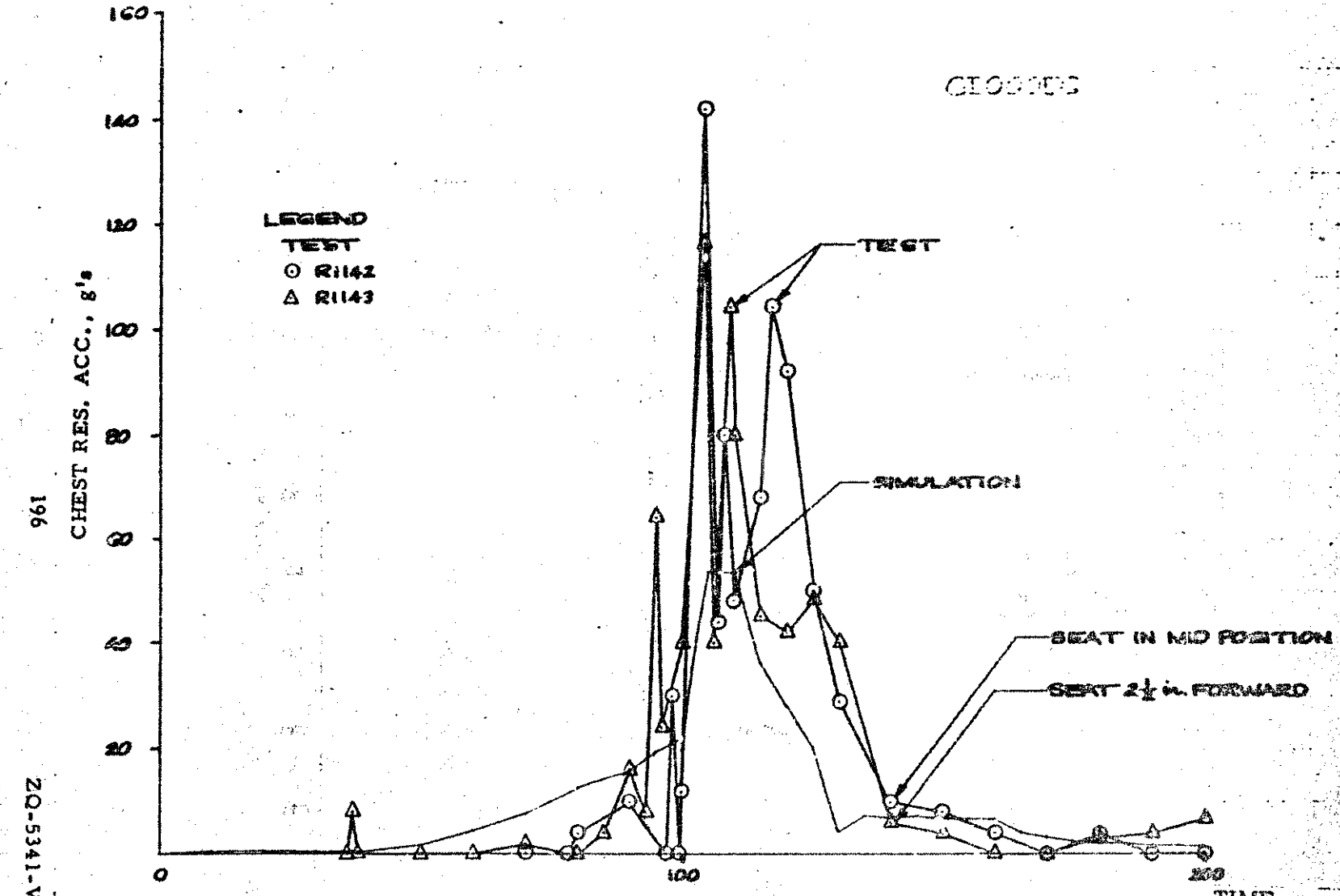

Figure 3.5.9 (cont'd)

(d) CHEST RESULTANT ACCELERATION

Case No. TR00973

Sled Run No. 1146

The subject accident victim in this case struck the windshield with his head and broke the glass and interlayer, resulting in minor facial injuries. He also sustained severe thoracic injuries, however, which resulted in fatality. The predicted kinematics for that case, summarized in Figure 3.3.37, correspond to the observed contacts in the accident report. Furthermore, the head-windshield and chest-instrument panel contacts observed in the sled test, Figure 3.4.13, are also consistent with the case report.

The desired sled pulse was obtained with reasonable accuracy on the impact sled facility, as shown in Figure 3.5.10(a). A rather notable difference in measured overall kinematic responses was found compared to the corresponding prediction, however (see Figure 3.5.10(b)). The chest-instrument panel contact in the test apparently prevented the predicted torso rotation.

The measured and predicted head resultant accelerations, Figure 3.5.10(c) agree generally both in magnitude and trend, but there is a significant difference in the time correlation. This difference in timing is at least partially the result of the faster onset of acceleration for the measured pulse compared to the corresponding predicted pulse, Figure 3.5.10(a). The difference, however, must be primarily attributed to the overall difference in predicted and measured kinematic responses, which could be the result of differences in measured and predicted torso slippage on the seat. The kinematic display, Figure 3.5.10(b), in fact, suggests this is likely. The significant overall difference in kinematics is reflected in the comparison of chest resultant acceleration, Figure 3.5.10(d), where an appreciable difference between the measured and predicted results is seen. The large measured spike at $\sim$ 90 msec. is apparently associated with the dynamic windshield failure.

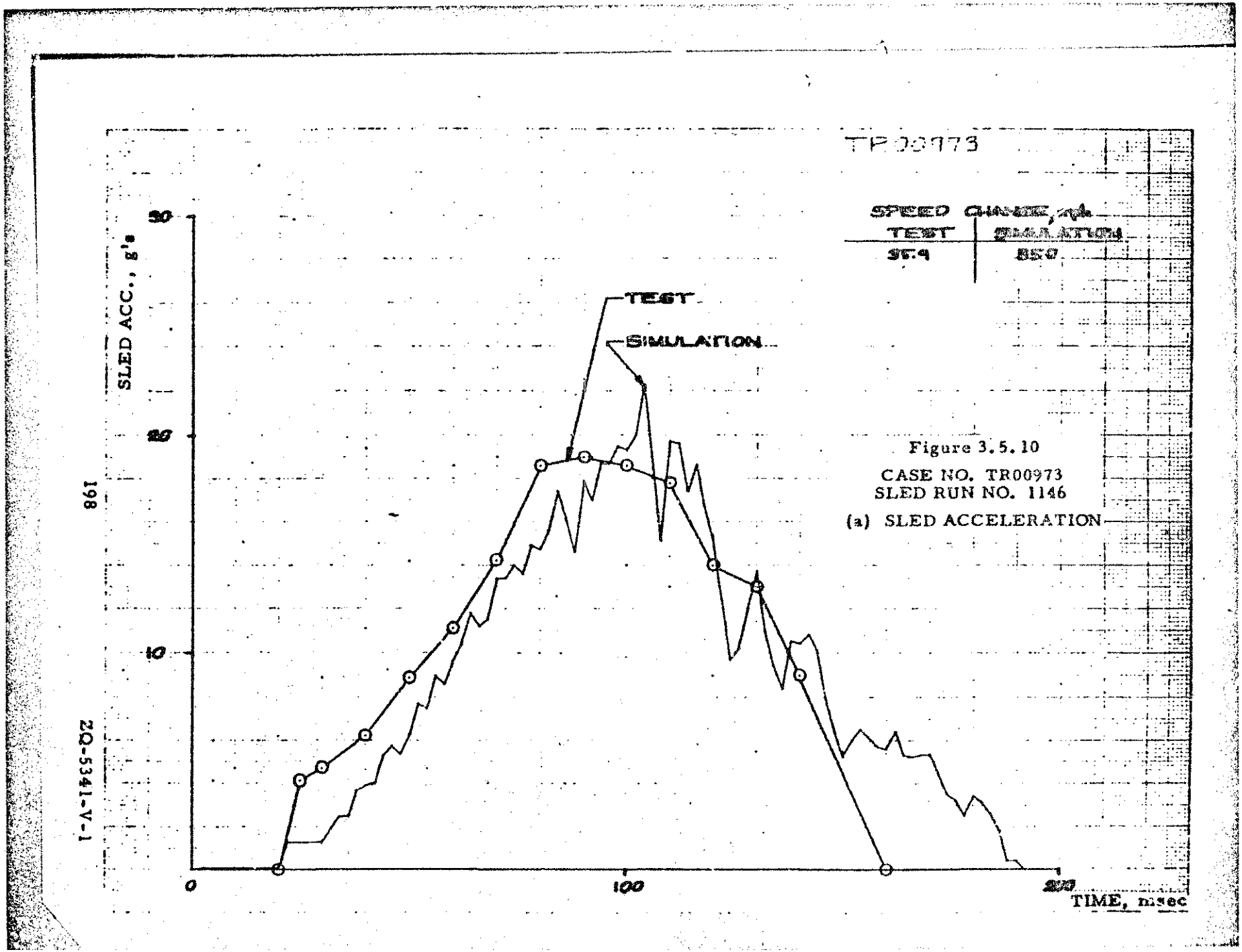

Figure 3.5.10

CASE NO. TR00973
SLED RUN NO. 1146

(a) SLED ACCELERATION

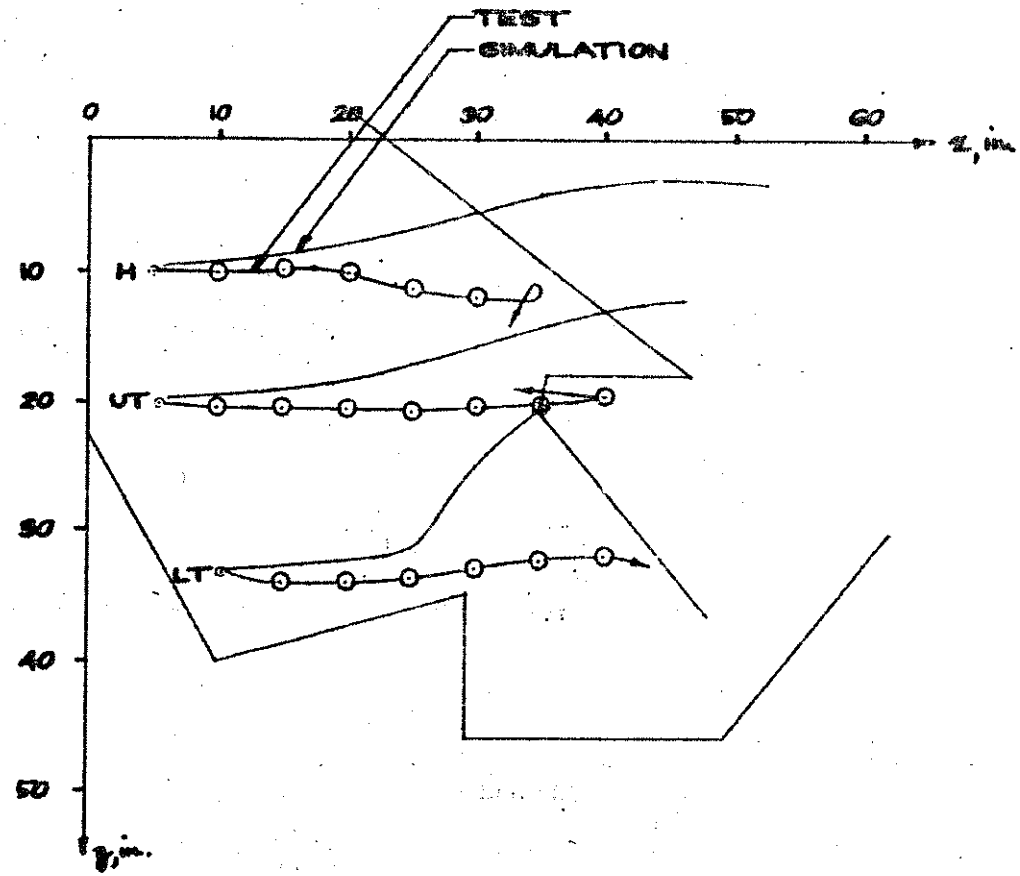

Figure 3.5.10 (cont'd)
(b) KINEMATICS

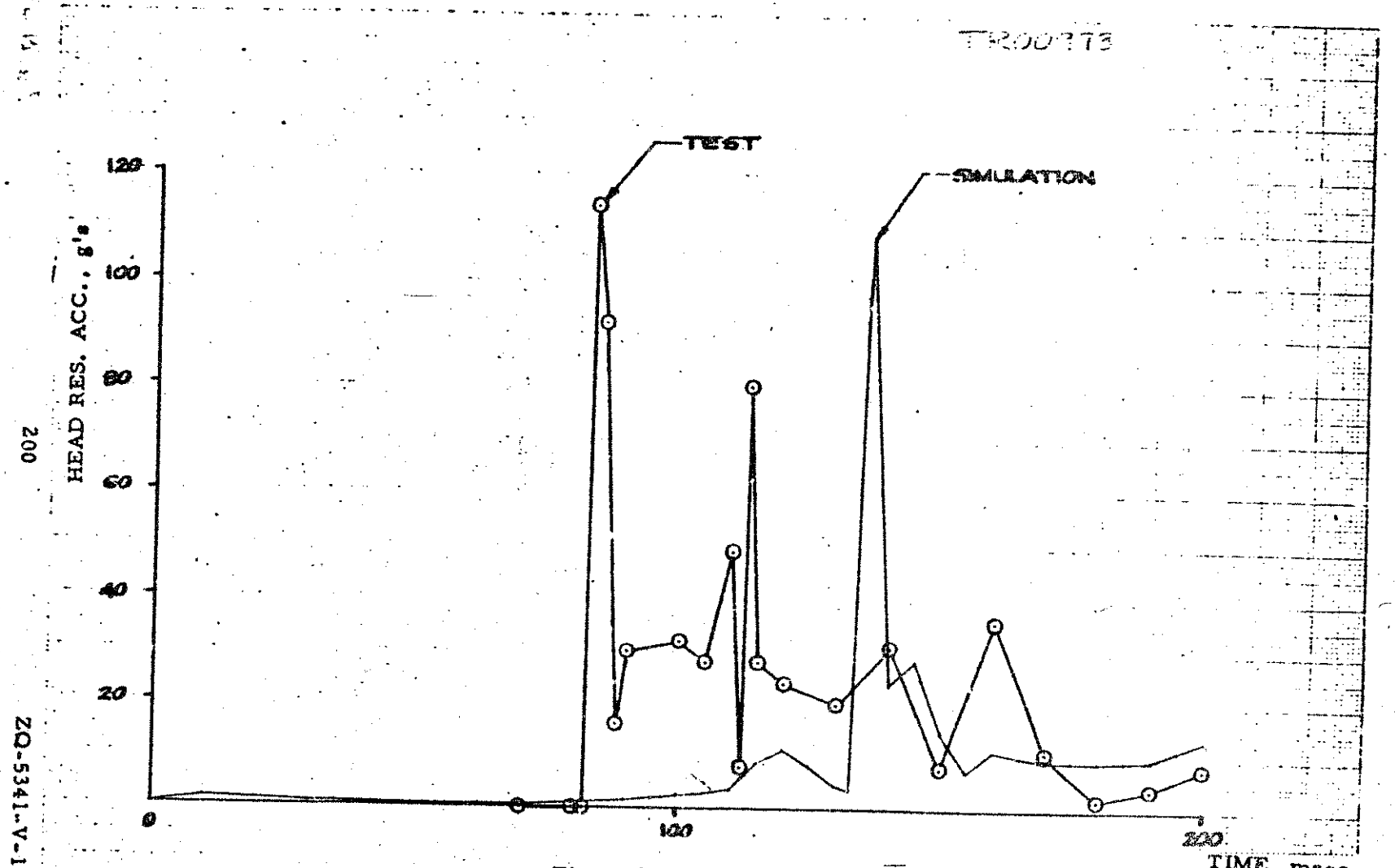

Figure 3.5.10 (cont'd)

(c) HEAD RESULTANT ACCELERATION

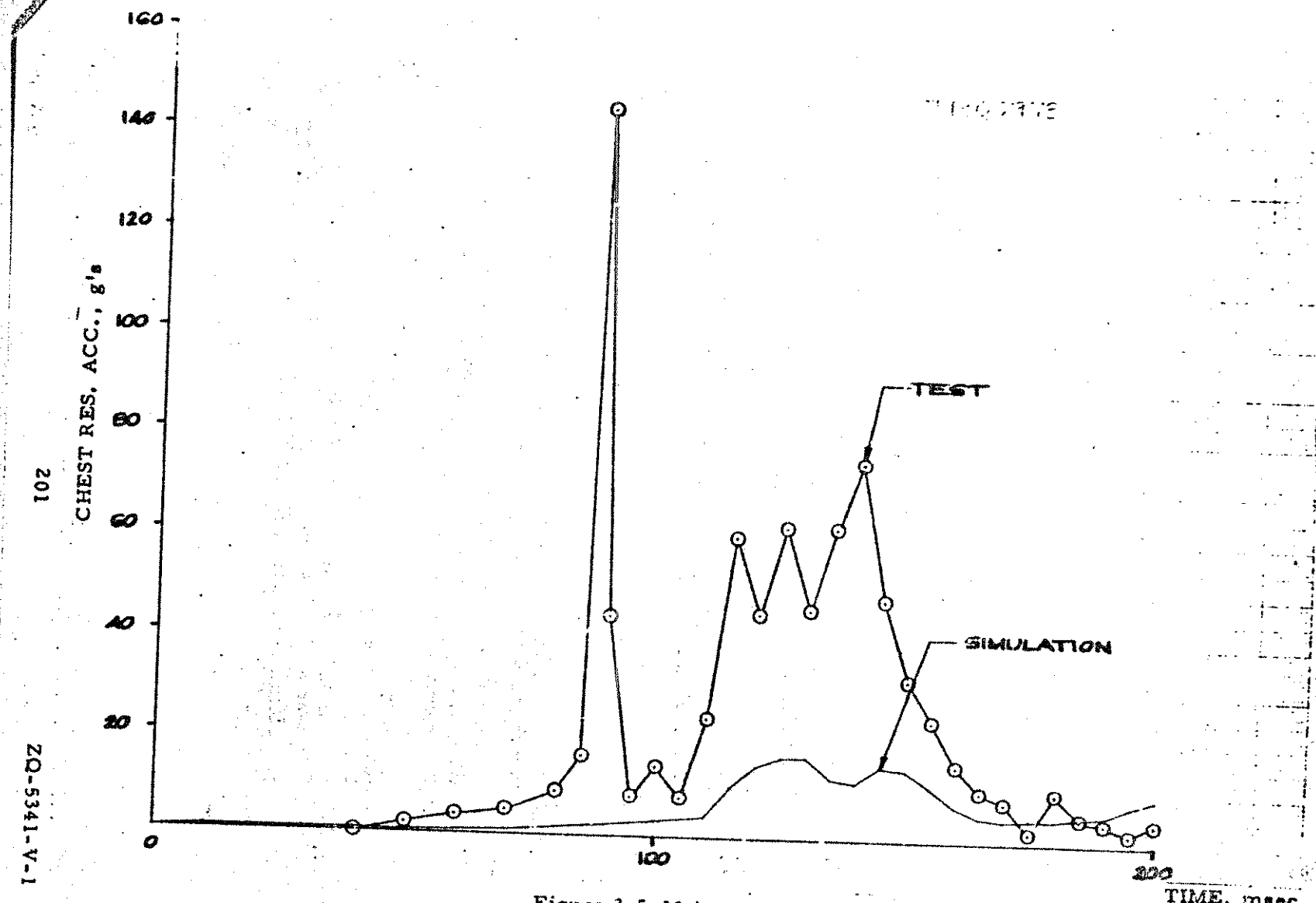

Figure 3.5.10 (cont'd)
(d) CHEST RESULTANT ACCELERATION

4.0 REFERENCES

1. McHenry, R. R., Segal, D. J., Lynch, J. P., Henderson, P. M., "Mathematical Reconstruction of Highway Accidents," Calspan Report No. ZM-5096-V-1, January 1973 (NTIS-PB-220150).

2. McHenry, R. R., "Development of a Computer Program to Aid the Investigation of Highway Accidents," CAL Report No. VJ-2979-V-1, December 1971 (NTIS - PB 208537).

3. McHenry, R. R., "A Computer Program for Reconstruction of Highway Accidents," Proceedings of the Seventeenth Stapp Car Crash Conference, Society of Automotive Engineers, New York, New York, 1973.

4. Bartz, J. A. and Butler, F. E., "A Three-Dimensional Computer Simulation of a Motor Vehicle Crash Victim - Phase 2 - Validation Study of the Model," Calspan Report No. VJ-2978-V-2, December 1972.

5. Bartz, J. A., "Development and Validation of a Computer Simulation of a Crash Victim in Three Dimensions," Sixteenth Stapp Car Crash Conference, Society of Automotive Engineers, New York, N. Y., 1972. Also, SAE Transactions, New York, N. Y., 1972.

6. Bartz, J. A., "Validation of a Three-Dimensional Mathematical Model of the Crash Victim," Proceedings of the Symposium on Human Impact Response, Plenum Press, New York, N. Y., 1973.

7. Bartz, J. A. and McHenry, R. R., "Calibration of Anthropometric Dummy Responses for Injury Interpretations - Phase 1 - Analytical Reconstruction of Three Selected Highway Accidents," Calspan Report No. ZQ-5263-V-1, March 1973 (Commercial Confidential).

8. Blizard, J. R. and Howitt, J. S., "Development of a Safer Non-lacerating Automobile Windshield," SAE No. 690484.

9. Patrick, L. M., Trosien, K. R., and DuPont, F. T., "Safety Performance Comparison of 30 Mil HPR Laminated and Monolithic Differentially Tempered Windshields," SAE No. 700427.

10. Alexander, H. M., Mattimoe, P. T., and Hofmann, J. J., "An Improved Windshield," SAE No. 700482.

11. Kay, S. E., Pickard, J., and Patrick, L. M., "Improved Laminated Windshield with Reduced Laceration Properties," Proceedings of the Seventeenth Stapp Car Crash Conference, November 1973, SAE No. 730969.

REFERENCES (continued)

12. Kramer, M., "Improved Laminated Windscreens by Energy-Controlled Breakout," Proceedings of the Seventeenth Stapp Car Crash Conference, November 1973, SAE No. 730972.

13. Hodgson, V. R., Thomas, L. M., and Brinn, J., "Concussion Levels Determined by HPR Windshield Impacts," Proceedings of the Seventeenth Stapp Car Crash Conference, November 1973, SAE No. 730970.

14. Patrick, L. M., Trosien, K. R., and DuPont, F. T., "Safety Performance of a Chemically Strengthened Windshield," SAE No. 690485.

15. Highway Safety Research Institute, "Multidisciplinary Accident Investigation Report Automation - Univariate Frequency Distributions of Multidisciplinary Accident Investigation Data - Volume 4 of 5," HSRI Report No. UM-HSRI-SA-72-1-4, October 1972.

16. Bartz, J. A. and Gianotti, C. R., "A Computer Program to Generate Input Data Sets for Crash Victim Simulations," Calspan Report No. ZQ-5167-V-1, January 1973.

17. Bartz, J. A. and Gianotti, C. R., "Computer Program to Generate Dimensional and Inertial Properties of the Human Body," Paper No. 73-WA/Bio-3, to be published in Transactions of the ASME, Journal of Fluids Engineering.

18. McHenry, R. R. and DeLeys, N. J., "Vehicle Dynamics in Single Vehicle Accidents - Validation and Extensions of a Computer Simulation," CAL Report No. VJ-2251-V-3, December 1968.

19. Rasmassen, R. E., et al, "Typical Vehicle Parameters for Dynamic Studies," General Motors Proving Ground Number A-2542, April 1970.

20. Mason, R. P. and Whitcomb, D. W., "The Estimation of Accident Impact Speed," Calspan Report No. YB-3109-V-1, August 1972.

APPENDIX A

SMAC COMPUTER PROGRAM

Table A-1

SMAC INPUT FORMAT

Card No.	Program Variable	Analysis Variable	Definition	Units
1	T0	-	Start time	Seconds
	TF	-	End time	Seconds
	DTTRAJ	-	Interval of integration at beginning and ending of run	Seconds
	DTCOLL	-	Interval of integration during collision contact	Seconds
	DTCOLT	-	Interval of integration for 100 time increments subsequent to separation	Seconds
	DTPRNO	-	Output time interval	Seconds
	UVMIN	-	Vector velocity test for stop	Inches/Sec
	PSIDMN	-	Angular velocity test for stop	Degrees/Sec
	IVEH0	-	Number of Simulated Vehicles (1.0 or 2.0)	-
2	XCP10	x'_{c10}	Vehicle 1, initial x'_c	Inches
	YCP10	y'_{c10}	Vehicle 1, initial y'_c	Inches
	PSI10	ψ_{10}	Vehicle 1, initial ψ	Degrees
	PSI1D0	$\dot{\psi}_{10}$	Vehicle 1, initial $\dot{\psi}$	Degrees/Sec
	U10	u_{10}	Vehicle 1, initial u	Inches/Sec
	V10	v_{10}	Vehicle 1, initial v	Inches/Sec
3	XCP20	x'_{c20}	Vehicle 2, initial x'_c	Inches
	YCP20	y'_{c20}	Vehicle 2, initial y'_c	Inches
	PSI20	ψ_{20}	Vehicle 2, initial ψ	Degrees
	PSI2D0	$\dot{\psi}_{20}$	Vehicle 2, initial $\dot{\psi}$	Degrees/Sec
	U20	u_{20}	Vehicle 2, initial u	Inches/Sec
	V20	v_{20}	Vehicle 2, initial v	Inches/Sec

Card No.	Program Variable	Analysis Variable	Definition	Units
4	A1	a_1	Vehicle 1, CG to F. Wheel ℄ (+)	Inches
	B1	b_1	Vehicle 1, CG to R. Wheel ℄ (+)	Inches
	TR1	T_1	Vehicle 1, Average Tread	Inches
	FIZ1	I_{Z1}	Vehicle 1, Yaw Inertia	Lb-Sec^2-In
	FMASS1	M_1	Vehicle 1, Total Mass	Lb-Sec^2/In.
	PSIR10	ψ_{R1}	Vehicle 1, Rear Axle Angle (Damage)	Degrees
	XF1	X_{F1}	Vehicle 1, CG to Front (+)	inches
	XR1	X_{R1}	Vehicle 1, CG to Rear (-)	Inches
	YS1	Y_{S1}	Vehicle 1, CG to Side (+)	Inches
5	A2	a_2	Vehicle 2, CG to F. Wheel ℄ (+)	Inches
	B2	b_2	Vehicle 2, CG to R. Wheel ℄ (+)	Inches
	TR2	T_2	Vehicle 2, Average Tread	Inches
	FIZ2	I_{Z2}	Vehicle 2, Yaw Inertia	Lb-Sec^2/In
	FMASS2	M_2	Vehicle 2, Total Mass	Lb-Sec^2/In
	PSIR20	ψ_{R2}	Vehicle 2, Rear Axle Angle (Damage)	Degrees
	XF2	X_{F2}	Vehicle 2, CG to Front (+)	Inches
	XR2	X_{R2}	Vehicle 2, CG to Rear (-)	Inches
	YS2	Y_{S2}	Vehicle 2, CG to Side (+)	Inches
6	CSTF1(1)	C_{11}	Vehicle 1, RF Tire Cornering Stiffness	Pounds/Radian
	CSTF1(2)	C_{12}	Vehicle 1, LF Tire Cornering Stiffness	Pounds/Radian
	CSTF1(3)	C_{13}	Vehicle 1, RR Tire Cornering Stiffness	Pounds/Radian
	CSTF1(4)	C_{14}	Vehicle 1, LR Tire Cornering Stiffness	Pounds/Radian

Card No.	Program Variable	Analysis Variable	Definition	Units
7	CSTF2(1)	C_{21}	Vehicle 2, RF Tire Cornering Stiffness	Pounds/Radian
	CSTF2(2)	C_{22}	Vehicle 2, LF Tire Cornering Stiffness	Pounds/Radian
	CSTF2(3)	C_{23}	Vehicle 2, RR Tire Cornering Stiffness	Pounds/Radian
	CSTF2(4)	C_{24}	Vehicle 2, LR Tire Cornering Stiffness	Pounds/Radian
8	TBTQ1	-	Initial time for torque inputs, Vehicle 1	Seconds
	TETQ1	-	Final time for torque inputs, Vehicle 1	Seconds
	TINCQ1	-	Time increment for torque inputs, Vehicle 1	Seconds
	NTBLQ1	-	If $\neq 0.0$, do not read table	-

(1) Table of Traction (+) or Braking (-) Force at RF Wheel, Vehicle 1 Card format 7F10.0, use three to two hundred and one values for each wheel. The number of entries for each wheel is computed as $\frac{TETQ1 - TBTQ1}{TINCQ1} + 1$.

Start the entries for each wheel on a new card. Seven entries per card.

(2) Table of Traction (+) or Braking (-) Force at LF Wheel, Vehicle 1

(3) Table of Traction (+) or Braking (-) Force at RR Wheel, Vehicle 1

(4) Table of Traction (+) or Braking (-) Force at LR Wheel, Vehicle 1

Card No.	Program Variable	Analysis Variable	Description	Units
9	TBTQ2	-	Initial time for torque inputs, Vehicle 2	Seconds
	TETQ2	-	Final time for torque inputs, Vehicle 2	Seconds
	TINCQ2	-	Time increment for torque inputs, Vehicle 2	Seconds
	NTBLQ2	-	If ≠ 0.0, do not read table	-
	(1) Table of Traction (+) or Braking (-) Force at RF Wheel, Vehicle 2			
	(2) Table of Traction (+) or Braking (-) Force at LF Wheel, Vehicle 2			See comments following card 8
	(3) Table of Traction (+) or Braking (-) Force at RR Wheel, Vehicle 2			
	(4) Table of Traction (+) or Braking (-) Force at LR Wheel, Vehicle 2			
10	TBPSF1	-	Initial time for steer inputs, Vehicle 1	Seconds
	TEPSF1	-	Final time for steer inputs, Vehicle 1	Seconds
	TINCP1	-	Time increments for steer inputs, Vehicle 1	Seconds
	NTBLP1	-	If ≠ 0.0, do not read table	-
	(1) Steer Table (degrees) for RF Wheel, Vehicle 1			
	(2) Steer Table (degrees) for LF Wheel, Vehicle 1			
	(See comments following card 8)			

Card No.	Program Variable	Analysis Variable	Description	Units
11	TBPSF2	-	Initial time for steer inputs, Vehicle 2	Seconds
	TEPSF2	-	Final time for steer inputs, Vehicle 2	Seconds
	TINCP2	-	Time increments for steer inputs, Vehicle 2	Seconds
	NTBLP2	-	If $\neq 0.0$, do not read table	-
	(1) Steer Table (degrees) for RF Wheel, Vehicle 2			
	(2) Steer Table (degrees) for LF Wheel, Vehicle 2			
	(See comments following card 8)			
12	XBP(1)	X'_{B1}	Points defining boundary between terrain zones	Inches
	YBP(1)	Y'_{B1}		Inches
	XBP(2)	X'_{B2}		Inches
	YBP(2)	Y'_{B2}		Inches
	XMU1	μ_1	Tire-Terrain Friction Coefficient at Zero Speed (Zone 1)	-
	XMU2	μ_2	Tire-Terrain Friction Coefficient at Zero Speed (Zone 2)	-
	CMU	C_μ	Coefficient of linear decrement of friction with tire speed	-
13	DELPS0	$\Delta\psi$	Interval between radial vectors	Degrees
	DELRØ0	$\Delta\rho$	Increment of change in radius vector	Inches
	ALAMB	λ	Acceptable error in equilibrium	Lb/Inch
	ZETAV	ζ_V	Minimum relative velocity for friction	Inches/Sec
	AKV(1)	K_{V1}	Load-deflection characteristic, Vehicle 1	Lb/In^2
	AKV(2)	K_{V2}	Load-deflection characteristic, Vehicle 2	Lb/In^2
	AMU	μ	Intervehicle friction coefficient	-

Card No.	Program Variable	Analysis Variable	Description	Units
14	C0	C_0	Coefficients of assumed parabolic variation of coefficient of restitution with deflection	-
	C1	C_1		-
	C2	C_2		-

INPUT DATA FORM

SIMULATION MODEL OF AUTOMOBILE COLLISIONS (SMAC)

RUN TITLE : _____

DATE : _____

FIELD NUMBER

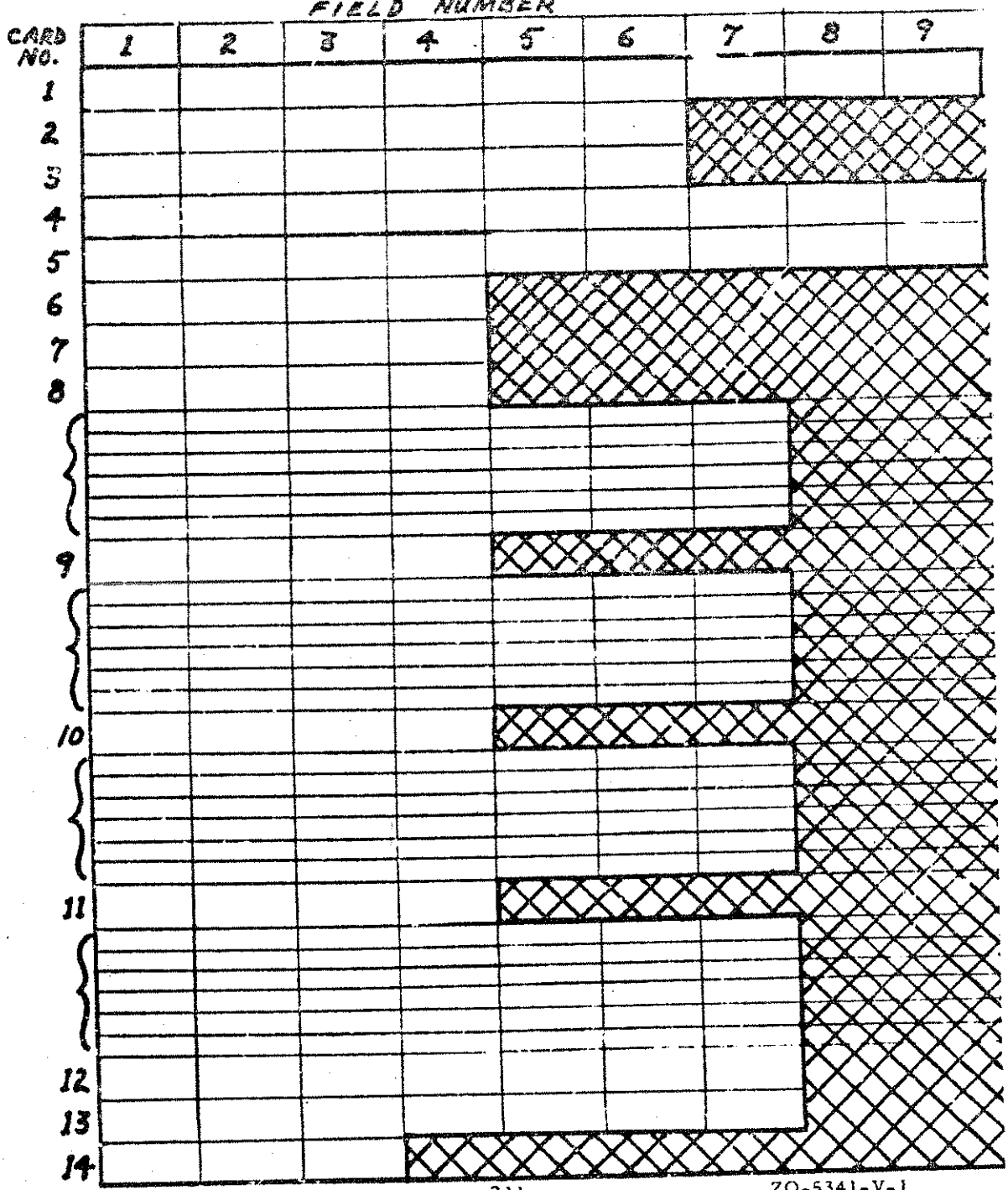

ZQ-5341-V-1

Table A-2.1

SMAC INPUTS - CASE NO. AA145

```
     MRA III     SMAC RECONSTRUCTION   COLLISION AND TRAJECTORY
  CASE NO. AA 145     MDAI  NO.  AA00145
0.0      1.1      .025      .001      .01      .001     1.20     0.50     2.0          1
228.     180.     185.      0.0       299.     0.0                                    2
-339.    127.     3.5       0.0       588.     0.0                                    3
57.3     59.7     60.       36400.    9.86     0.0      94.8     -110.8   38.4         4
50.5     52.5     57.7      19800.    7.74     0.0      87.1     -94.6    35.7         5
-10250.  -10250.  -10195.   -10195.                                                   6
-10250.  -10250.  -10195.   -10195.                                                   7
0.0      0.8      0.1       0.0                                                       8
0.0        0.0        0.0        0.0        0.0        0.0        -1200.
-1200.     -1200.
0.0        0.0        0.0        0.0        0.0        0.0        -1200.
-1200.     -1200.
0.0        0.0        0.0        0.0        0.0        0.0        0.0
0.0        0.0
0.0        0.0        0.0        0.0        0.0        0.0        0.0
0.0        0.0
0.0      3.0      1.0       0.0                                                       9
-600.      -600.      -600.      -600.
-600.      -600.      -600.      -600.
-500.      -500.      -500.      -500.
-500.      -500.      -500.      -500.
0.0      3.0      1.0       1.0                                                       10
0.0      3.0      1.0       1.0                                                       11
1.0      1.0      1.0       1.0       0.7      0.7      0.0      0.0                 12
2.0      0.2      15.0      5.0       50.      50.      .55                          13
.06423   3.5417-34.7381-5                                                           14
                                                                                    9999
```

Table A-2.2

SMAC INPUTS - CASE NO. 1316D

```
      MRA III  SMAC RECONSTRUCTION - COLLISION AND TRAJECTORY
        CASE NO. 1316 D   MDAI NO. TR01316
0.0     1.13    .025    .0005   .01     .001    5.0     1.0     2.0          1
0.0     0.0     0.0     0.0          1.-5 0.0                              2
-373.3  0.0     0.0     0.0     365.    0.0                                  3
20.     20.     15.        1.+10   1.+10 0.0    20.     -20.    7.5          4
55.5    55.5    60.     29561.  9.53    0.0     85.3    -104.1  35.2         5
-10000. -10000. -10000. -10000.                                              6
-10250. -10250. -10195. -10195.                                              7
0.0     2.0     .025    1.0                                                  8
0.0     0.4     0.1     0.0                                                  9
-1000.    -1000.    -1000.    -1000.    -1000.
-1000.    -1000.    -1000.    -1000.    -1000.
-1000.    -1000.    -1000.    -1000.    -1000.
-1000.    -1000.    -1000.    -1000.    -1000.
0.0     2.0     .025    1.0                                                  10
0.0     2.0     .025    1.0                                                  11
1.0     1.0     1.0     1.0     0.4     0.4     0.0                          12
2.0     .001    10.     5.0     10000.  100.    0.0                          13
.06423  3.5417-34.7381-5                                                     14
                                                                             9999
```

Table A-2.3

SMAC INPUTS - CASE NO. 71-31A

```
      MKA III  SMAC RECONSTRUCTION - COLLISION AND TRAJECTORY
        CASE NO. 71-31A     MDAI NO. CA71031
0.0       0.5       .025      .001      .01       .001      4.0       0.3       2.0        1
250.      100.      180.      0.0       0.0       0.0                                    2
-84.8     97.       0.0       0.0       616.      0.0                                    3
50.       50.       13.5        10.+10  10.+10    0.0       50.       -50.      13.5     4
52.9      55.1      55.7      30400.    8.76      0.0       90.2      -96.5     35.7     5
-10000.   -10000.   -10000.   -10000.                                                    6
-10250.   -10250.   -10195.   -10195.                                                    7
0.0       1.5       0.5       1.0                                                        8
0.0       0.5       .05       0.0                                                        9
0.0         0.0         0.0         0.0         0.0         0.0         0.0
-1000.      -1000.      -1000.      -1000.
0.0         0.0         0.0         0.0         0.0         0.0         0.0
-1000.      -1000.      -1000.      -1000.
0.0         0.0         0.0         0.0         0.0         0.0         0.0
0.0         0.0         0.0         0.0         0.0         0.0         0.0
0.0         0.0         0.0         0.0
0.0         0.0         0.0         0.0
0.0       1.5       0.5       1.0                                                       10
0.0       1.5       0.5       1.0                                                       11
1.0       1.0       1.0       1.0       0.2       0.3       0.0       0.0             12
2.0       .001      10.0      5.0       10000.    73.8      0.55                        13
.06423    3.5417-34.7381-5                                                            14
                                                                                      9999
```

Table A-2.4

SMAC INPUTS - CASE NO. 72

```
      MRA III  SMAC RECONSTRUCTION - COLLISION AND TRAJECTORY
      CASE NO. 72   MDAI NO. C8U0072
0.0       2.0       .025      .0005     .01       .001      12.0      1.0       2.0       1
-603.4    0.0       0.0       0.0       .50.      0.0                                     2
30.       0.0       87.5      0.0                 1.-5 0.0                                3
51.4      56.6      56.9      21506.    9.41      0.0       89.5      -98.5     37.2      4
72.       72.       60.             1.+10     1.+10 0.0     72.       -72.      30.       5
-10250.   -10250.   -10195.   -10195.                                                     6
-10000.   -10000.   -10000.   -10000.                                                     7
0.0       0.4       0.1       0.0                                                         8
-1000.    -1000.    -1000.    -1000.    -1000.
-1000.    -1000.    -1000.    -1000.    -1000.
-1000.    -1000.    -1000.    -1000.    -1000.
-1000.    -1000.    -1000.    -1000.    -1000.
0.0       1.0       .025      1.0                                                         9
0.0       1.0       .025      1.0                                                         10
0.0       1.0       .025      1.0                                                         11
0.0       204.      -504.     0.0       .55       .65       0.0                         12
2.0       .001      10.       5.0       50.       10000.    .55                         13
.06423    3.5417-34.7381-5                                                              14
                                                                                        9999
```

Table A-2.5

SMAC INPUTS - CASE NO. 7144

MRA III SMAC [illegible] AND TRAJECTORY
CASE NO. 7144 [illegible]

0.0	1.5	.025	.0031	.1	.001	[illegible]	[illegible]	2.	1
61.705	102.1[illegible]	3.5	.0	[illegible]	0.0				2
378.5	160.0	150.	0.0	0.0	0.0				3
60.5	63.	63.1	[illegible]	[illegible]	0.0	100.0	-119.5	39.0	4
60.5	63.	63.1	[illegible]	11.71	0.0	100.0	-119.5	39.0	5
-10250.	-10250.	-10195.	-10195.						6
-10250.	-10250.	-10195.	-10195.						7
0.0	1.5	.05	0.0						8
0.0	0.0	0.0	0.0	0.0	0.0	0.0			
0.0	0.0	0.0	0.0	0.0	0.0	0.0			
-1500.	-1500.	-1500.	-1500.	-1500.	-1500.	-1500.			
-1500.	-1500.	-1500.	-1500.	-1500.	-1500.	-1500.			
-1500.	-1500.	-1500.							
0.0	1.5	.05	0.0						9
0.0	0.0	0.0	0.0	0.0	0.0	0.0			
0.0	0.0	0.0	0.0	0.0	0.0	0.0			
-1500.	-1500.	-1500.	-1500.	-1500.	-1500.	-1500.			
-1500.	-1500.	-1500.	-1500.	-1500.	-1500.	-1500.			
-1500.	-1500.	-1500.							
-1200.	-1200.	-1200.	-1200.	-1200.	-1200.	-1200.			
-1200.	-1200.	-1200.	-1200.	-1200.	-1200.	-1200.			
-1200.	-1200.	-1200.	-1200.	-1200.	-1200.	-1200.			
-1200.	-1200.	-1200.	-1200.	-1200.	-1200.	-1200.			
-1200.	-1200.	-1200.							
-1200.	-1200.	-1200.	-1200.	-1200.	-1200.	-1200.			
-1200.	-1200.	-1200.	-1200.	-1200.	-1200.	-1200.			
-1200.	-1200.	-1200.	-1200.	-1200.	-1200.	-1200.			
-1200.	-1200.	-1200.	-1200.	-1200.	-1200.	-1200.			
-1200.	-1200.	-1200.							
0.0	1.5	.75	1.0						10
0.0	1.5	.75	1.0						11
1000.	0.0	1000.	100.	0.7	0.7	0.0			12
2.0	0.2	15.	5.0	30.	50.	.55	0.0		13
.06425	3.5417-34.7[illegible]1-[illegible]								14

Table A-2.6

SMAC INPUTS - CASE NO. 53

```
      MRA III  SMAC RECONSTRUCTION - COLLISION AND TRAJECTORY
       CASE NO. 53   MDAI NO. CB00053
0.0      3.0      .025     .001     .010     .01      12.0     5.0      2.0      1
-46.6    40.0     0.0      0.0      933.     0.0                                 2
471.19   25.924   183.     0.0      757.     0.0                                 3
54.5     56.5     60.0     30200.   8.75     0.0      84.3     -105.1   36.5    4
57.9     58.1     60.0     21700.   7.3      0.0      90.5     -105.5   36.0    5
-10250.  -10250.  -10195.  -10195.                                              6
-10250.  -10250.  -10195.  -10195.                                              7
0.2      1.2      0.1      0.0                                                  8
0.0        0.0        0.0        0.0        0.0        0.0        0.0
0.0        0.0        0.0        0.0
0.0        -1500.     -1500.     -1500.     -1500.     -1500.     -1500.
-1500.     -1500.     -1500.     -1500.
0.0        0.0        0.0        0.0        0.0        0.0        0.0
0.0        0.0        0.0        0.0
0.0        0.0        0.0        0.0        0.0        0.0        0.0
0.0        0.0        0.0        0.0
0.2      1.2      0.1      0.0                                                  9
0.0        -1500.     -1500.     -1500.     -1500.     -1500.     -1500.
-1500.     -1500.     -1500.     -1500.
0.0        -1500.     -1500.     -1500.     -1500.     -1500.     -1500.
-1500.     -1500.     -1500.     -1500.
0.0        0.0        0.0        0.0        0.0        0.0        0.0
0.0        0.0        0.0        0.0
0.0        0.0        0.0        0.0        0.0        0.0        0.0
0.0        0.0        0.0        0.0
0.0      0.5      0.2      1.0                                                  10
0.0      0.6      0.2      1.0                                                  11
0.0      138.     500.     138.     0.5      0.5      0.0                       12
2.0      0.2      15.0     5.0      50.0     50.0     0.55     0.0              13
.06423   3.5417-34.7381-5                                                      14
                                                                               9999
```

2.7

ZQ-5341-V-1

Table A-2.7

SMAC INPUTS - CASE NO. 71-55B

```
      MKA III  SMAC RECONSTRUCTION  COLLISION AND TRAJECTORY
        CASE NO. 71-55B   MDAI NO. CB71055
0.0     2.0     .025    .001    .01     .02     6.0     1.0     2.0          1
330.77  337.54  -37.    0.0     247.596 0.0                                  2
637.    227.    180.    0.0     440.    0.0                                  3
57.3    59.7    60.     34200.  9.36    0.0     97.2    -109.   38.4         4
53.4    55.6    57.7    25600.  7.98    0.0     93.4    -96.1   35.7         5
-10250. -10250. -10195. -10195.                                              6
-10250. -10250. -10195. -10195.                                              7
0.0     2.0     1.0     0.0                                                  8
-1200.    -1200.    -1200.    -1200.
-1200.    -1200.    -1200.    -1200.
-1200.    -1200.    -1200.    -1200.
-1200.    -1200.    -1200.    -1200.
0.2     0.5     0.1     0.0                                                  9
0.0       0.0       0.0       0.0
0.0       -1000.    -1000.    -1000.
0.0       0.0       0.0       0.0
0.0       -1000.    -1000.    -1000.
0.0     2.0     1.0     1.0                                                 10
0.0     2.0     1.0     1.0                                                 11
1.0     1.0     1.0     1.0     0.7     0.7     0.0     0.0                 12
2.0     0.2     15.     5.0     50.     50.     .55                         13
.06423  3.5417-34.7381-5                                                    14
                                                                          9999
```

Table A-2.8

SMAC INPUTS - CASE NO. 1161D

```
      MRA III  SMAC RECONSTRUCTION  COLLISION AND TRAJECTORY
        CASE NO. 1161 D  MDAI NO. TR01161
0.0       1.25      .025      .0005     .010      .001      24.       2.        2.0       1
559.6     220.      210.      0.0       0.0       0.0                                     2
246.14    208.17    -6.0      0.0       750.37    0.0                                     3
24.       24.       24.         10.+10  10.+10    0.0       64.       -40.      24.       4
47.5      49.5      57.7      30400.    8.8       0.0       87.5      -89.5     35.7      5
-10000.   -10000.   -10000.   -10000.                                                     6
-10250.   -10250.   -10195.   -10195.                                                     7
0.0       1.5       0.5       1.0                                                         8
0.0       1.5       0.5       0.0                                                         9
-1000.      -1000.      -1000.      -1000.
-1000.      -1000.      -1000.      -1000.
-1000.      -1000.      -1000.      -1000.
-1000.      -1000.      -1000.      -1000.
0.0       1.5       0.5       1.0                                                        10
0.0       1.5       0.5       1.0                                                        11
1.0       1.0       1.0       1.0       0.6       0.6       0.0       0.0              12
2.0       .001      10.0      5.0       10000.    50.       0.55                       13
                                                                                        14
.06423    3.5417-34.7361-5                                                            9999
```

Table A-2.9

SMAC INPUTS - CASE NO. 56

```
MRA III  SMAC RECONSTRUCTION - COLLISION AND TRAJECTORY
 CASE NO. 56    MDAI NO. G100056
0.0      0.5      .025     .001     .01      .001     3.0      0.25     2.0                    1
250.     149.     180.     0.0      0.0      0.0                                              2
-68.9    150.     0.0      0.0      5o3.     0.0                                              3
50.      50.      10.      10.+10   10.+10   0.0      50.      -50.     10.                    4
56.8     59.2     60.      28200.   8.51     0.0      94.8     -110.8   33.                    5
-10000.  -10000.  -10000.  -10000.                                                            6
-10250.  -10250.  -10195.  -10195.                                                            7
0.0      1.5      0.5      1.0                                                                 8
0.0      1.5      0.5      1.0                                                                 9
0.0      1.5      0.5      1.0                                                                 10
0.0      1.5      0.5      1.0                                                                 11
1.9      1.0      1.0      1.0      0.7      0.7      0.0      0.0                            12
2.0      .001     10.0     5.0      10000.   95.      .55                                      13
.06423   3.5417-34.7381-5                                                                    14
                                                                                             9999
```

Table A-2.10

SMAC INPUTS - CASE NO. 973D

```
     MRA III   SMAC RECONSTRUCTION   COLLISION AND TRAJECTORY
          CASE NO. 973D      MOAT NO. TR00973
0.0       2.2       .025      .001      .01       .0.1      2.0       1.0       .0
245.61    72.369    183.      0.0       650.      0.0
-238.8    97.       0.0       0.0       600.      0.0
60.5      63.       63.1      41000.    10.74     0.0       100.5     -119.6    55.0
60.5      63.       63.1      46000.    11.45     0.0       100.5     -119.6    55.0
-10250.   -10250.   -10195.   -10195.
-10250.   -10250.   -10195.   -10195.
0.2       2.2       0.1       0.0

0.0       -1100.    -1100.    -1100.    -1100.    -1100.    -1100.
-1100.    -1100.    -1100.    -1100.    -1100.    -1100.    -1100.
-1100.    -1100.    -1100.    -1100.    -1100.    -1100.    -1100.

0.2       2.2       0.1       0.0

0.0       -1200.    -1200.    -1200.    -1200.    -1200.    -1200.
-1200.    -1200.    -1200.    -1200.    -1200.    -1200.    -1200.
-1200.    -1200.    -1200.    -1200.    -1200.    -1200.    -1200.

0.0       2.0       1.0       1.0
0.0       2.0       1.0       1.0
100.      1000.     -100.     1000.     .6        .6        0.
2.0       .2        15.       5.        50.       50.       .55       0.0
.06423    3.5417-34.7361-5
```

APPENDIX B

3-D CRASH VICTIM SIMULATION COMPUTER PROGRAM

Table B-1

PROGRAM INPUTS -- THREE-DIMENSIONAL CRASH VICTIM SIMULATION

CALSPAN 3-D CRASH VICTIM SIMULATION PROGRAM

SEP. 7, 1973

CARD: A

W11203 ACCIDENT RECONSTRUCTION 3-D RUN NO. 3
CASE NO. 1 SW71046 1965 FORD SEDAN 160 LB.-71 IN. MALE NO RESTRAINTS

NOINT = 4 NSTEPS = 70 DT =0.005000 HO =0.000500 HMAX =0.002500

NPRT ARRAY

1	2	3	4	5	6	7	8	9	10	11	12	13	14	15	16	17	18	19	20	21	22	23	24	25	26	27	28	29	30	31	32	33	34	35	36	37	38	39	40
1	0	0	0	1	1	0	0	0	0	0	0	0	0	0	0	0	0	0	0	0	0	0	0	0	0	0	0	0	0	0	0	0	0	0	0	0	0	0	0

SEGMENT I	SYM	PLOT	WEIGHT (LBS.)	SEGMENT MOMENT OF INERTIA (LB-SEC**2-IN) X	Y	Z	SEGMENT CONTACT ELLIPSOID SEMIAXES (IN) X	Y	Z	CENTER (IN) X	Y	
1	LT	>	35.750	1.76000	1.14000	1.71000	4.94	6.94	7.60	0.0	0.0	0.0
2	CT	4	9.260	0.32100	0.31400	0.14900	4.91	6.35	7.00	0.0	0.0	-2.00
3	UT	3	31.750	2.32000	1.65000	1.33000	4.41	6.78	4.94	0.0	0.0	0.0
4	N	2	3.130	0.04000	0.04000	0.00660	2.07	2.28	3.28	0.0	0.0	0.0
5	M	1	10.130	0.25900	0.31100	-0.20000	3.49	3.10	4.55	0.0	0.0	0.0
6	NUL	6	17.440	0.72700	0.70300	0.15400	2.99	3.74	12.40	0.0	0.0	-2.60
7	RLL	7	6.970	0.44000	0.44200	0.01900	2.36	2.23	9.07	0.0	0.0	-0.45
8	RF	8	2.750	0.03830	0.04340	0.01320	1.52	1.80	5.22	0.0	0.0	0.95
9	LUL	9	17.440	0.72700	0.70300	0.15400	2.99	3.74	12.40	0.0	0.0	-2.60
10	LLL	A	6.970	0.44000	0.44200	0.01900	2.36	2.23	9.07	0.0	0.0	-0.45
11	LF	B	2.750	0.03830	0.04340	0.01320	1.52	1.80	5.22	0.0	0.0	0.95
12	AUA	C	5.260	0.16400	0.16600	0.01410	2.07	1.64	6.88	0.0	0.0	0.0
13	ALA	D	4.790	0.25900	0.25900	0.01150	1.30	1.31	8.38	0.0	0.0	0.0
14	LUA	E	5.260	0.16400	0.16600	0.01410	2.07	1.64	6.88	0.0	0.0	0.0
15	LLA	F	4.790	0.25500	0.25900	0.01150	1.30	1.31	8.38	0.0	0.0	0.0

CASE# 6.3

JOINT J	SYM	PLOT	JNT	PIN	LOCATION(IN) - SEG(JNT) X	Y	Z	LOCATION(IN) - SEG(J+1) X	Y	Z	CENTER OF SYMMETRY (DEG) YAW	PITCH	ROLL
1	P	P	1	0	-1.80	0.0	-2.50	-1.50	0.0	2.50	0.0	0.0	0.0
2	N	O	2	0	-1.50	0.0	-2.30	-1.50	0.0	4.80	0.0	0.0	0.0
3	MP	N	3	0	-0.90	0.0	-2.20	0.0	0.0	3.80	0.0	0.0	0.0
4	MP	M	4	0	0.0	0.0	-1.20	-1.10	0.0	3.34	0.0	0.0	0.0
5	RM	Q	1	0	2.10	4.45	2.50	0.0	0.0	-7.35	0.0	45.50	-5.22
6	RK	R	6	1	0.0	0.0	6.79	0.0	0.0	-7.68	0.0	-52.80	0.0
7	RA	S	7	0	0.0	0.0	8.69	1.54	0.0	-1.28	0.0	83.00	0.0
8	LM	T	1	0	2.10	-4.45	2.50	0.0	0.0	-7.31	0.0	46.50	5.22
9	LK	U	9	1	0.0	0.0	6.79	0.0	0.0	-7.68	0.0	-52.80	0.0
10	LA	V	10	0	0.0	0.0	8.69	1.54	0.0	-1.28	0.0	83.00	0.0
11	AS	W	3	0	-0.80	7.80	-1.60	0.0	0.0	-5.25	0.0	42.50	-10.29
12	AR	X	12	1	0.0	0.0	5.45	0.0	0.0	-6.59	0.0	64.30	0.0
13	AS	Y	3	0	-0.80	-7.80	-1.60	0.0	0.0	-5.25	0.0	52.50	10.29
14	AR	Z	14	1	0.0	0.0	5.45	0.0	0.0	-6.59	0.0	86.30	0.0

JOINT TORQUE CHARACTERISTICS

CARDS 5.4

FLEXURAL SPRING CHARACTERISTICS

JOINT	SPRING COEF. (IN LB/DEG**J) LINEAR (J=1)	QUADRATIC (J=2)	CUBIC (J=3)	ENERGY DISSIPATION COEF.	JOINT STOP (DEG)
1 P	209.440	609.230	0.0	1.000	5.000
2 W	20.944	60.923	0.0	1.000	35.000
3 NP	17.174	60.923	0.0	1.000	25.000
4 HP	21.293	60.923	0.0	1.000	25.000
5 RH	0.0	609.230	0.0	1.000	85.500
6 RK	0.0	16.754	0.0	1.000	58.300
7 RA	0.0	627.510	0.0	1.000	37.000
8 LH	0.0	609.230	0.0	1.000	85.500
9 LK	0.0	16.754	0.0	1.000	58.300
10 LA	0.0	627.510	0.0	1.000	37.000
11 RS	0.0	609.230	0.0	1.000	122.500
12 RE	0.0	11.697	0.0	1.000	65.300
13 LS	0.0	609.230	0.0	1.000	122.500
14 LE	0.0	11.697	0.0	1.000	65.300

TORSIONAL SPRING CHARACTERISTICS

SPRING COEF. (IN LB/DEG**J) LINEAR (J=1)	QUADRATIC (J=2)	CUBIC (J=3)	ENERGY DISSIPATION COEF.	JOINT STOP (DEG)
343.830	609.230	0.0	1.000	5.000
34.383	60.923	0.0	1.000	35.000
8.011	60.923	0.0	1.000	35.000
8.011	60.923	0.0	1.000	35.000
0.0	609.230	0.0	1.000	55.500
0.0	0.0	0.0	0.0	0.0
0.0	94.431	0.0	1.000	20.700
0.0	609.230	0.0	1.000	55.500
0.0	0.0	0.0	0.0	0.0
0.0	94.431	0.0	1.000	20.700
0.0	609.230	0.0	1.000	180.000
0.0	0.0	0.0	0.0	0.0
0.0	609.230	0.0	1.000	180.000
0.0	0.0	0.0	0.0	0.0

FLEXURAL VISCOUS CHARACTERISTICS

CARDS 5.5

JOINT	VISCOUS COEFFICIENT (IN LB SEC/DEG)	COULOMB FRICTION COEF. (IN LB)	FULL FRICTION ANGULAR VELOCITY (DEG/SEC)		
1 P	104.720	600.00	30.00	0.0	0.0
2 W	10.472	60.00	30.00	0.0	0.0
3 NP	1.745	10.00	30.00	0.0	0.0
4 HP	1.745	10.00	30.00	0.0	0.0
5 RH	3.997	229.00	30.00	0.0	0.0
6 RK	3.456	198.00	30.00	0.0	0.0
7 RA	0.436	25.00	30.00	0.0	0.0
8 LH	3.997	229.00	30.00	0.0	0.0
9 LK	3.456	198.00	30.00	0.0	0.0
10 LA	0.436	25.00	30.00	0.0	0.0
11 RS	3.229	185.00	30.00	0.0	0.0
12 RE	1.292	74.00	30.00	0.0	0.0
13 LS	3.229	185.00	30.00	0.0	0.0
14 LE	1.292	74.00	30.00	0.0	0.0

TORSIONAL VISCOUS CHARACTERISTICS

VISCOUS COEFFICIENT (IN LB SEC/DEG)	COULOMB FRICTION COEF. (IN LB)	FULL FRICTION ANGULAR VELOCITY (DEG/SEC)		
130.900	750.00	30.00	0.0	0.0
13.090	75.00	30.00	0.0	0.0
5.236	30.00	30.00	0.0	0.0
5.236	30.00	30.00	0.0	0.0
4.887	280.00	30.00	0.0	0.0
0.0	0.0	30.00	0.0	0.0
0.105	6.00	30.00	0.0	0.0
4.887	280.00	30.00	0.0	0.0
0.0	0.0	30.00	0.0	0.0
0.105	6.00	30.00	0.0	0.0
0.733	42.00	30.00	0.0	0.0
0.0	0.0	30.00	0.0	0.0
0.733	42.00	30.00	0.0	0.0
0.0	0.0	30.00	0.0	0.0

VEHICLE DECELERATION INPUTS

CARD C

REVISED VEHICLE DECELERATION INPUT FROM SMAC PROGRAM

C1

YAW	PITCH	ROLL	VMPH	VTIME	XU(X)	XU(Y)	XU(Z)	MATAB	AYO	AYD
5.000	0.0	0.0	12.500	0.0	0.0	0.0	0.0	68	0.0	0.004000

UNIDIRECTIONAL VEHICLE POSITION TABLES

TIME (MILLESEC)	ACC (G)	VELOCITY (IN/SEC)	POSITION (IN)	TIME (MILLESEC)	ACC (G)	VELOCITY (IN/SEC)	POSITION (IN)
0.0	0.0	220.0000	0.0	200.00	1.10	54.4043	29.71256
4.00	0.0	220.0000	0.88000	204.00	1.00	52.7956	29.92694
8.00	0.0	220.0000	1.76000	208.00	1.00	51.2641	30.13503
12.00	0.26	219.7915	2.63970	212.00	1.00	49.7197	30.33700
16.00	0.46	219.2278	3.51786	216.00	1.00	48.1754	30.53276
20.00	0.62	218.3977	4.39320	220.00	1.00	46.6314	30.72240
24.00	0.81	217.2974	5.26468	224.00	1.00	45.0867	30.90584
28.00	0.96	215.9075	6.13116	228.00	1.00	43.5423	31.08309
32.00	1.09	214.3013	6.99165	232.00	1.00	41.9980	31.25417
36.00	1.21	212.5249	7.84536	236.00	1.00	40.4536	31.41906
40.00	1.32	210.5692	8.69161	240.00	1.00	38.9093	31.57780
44.00	1.41	208.4778	9.52978	244.00	1.00	37.3649	31.73035
48.00	1.63	206.1472	10.35911	248.00	1.00	35.8206	31.87672
52.00	1.74	203.5475	11.17856	252.00	1.00	34.2762	32.01692
56.00	1.87	200.7625	11.98724	256.00	1.00	32.7319	32.15093
60.00	1.98	197.7856	12.78439	260.00	1.00	31.1875	32.27877
64.00	2.06	194.6623	13.56933	264.00	1.00	29.6432	32.40043
68.00	2.29	191.2905	14.34133	268.00	1.00	28.0988	32.51592
72.00	2.42	187.6407	15.09929	272.00	1.00	26.5545	32.62522
76.00	2.53	183.8236	15.84228	276.00	1.00	25.0101	32.72835
80.00	2.66	179.8057	16.56961	280.00	1.00	23.4658	32.82530
84.00	2.81	175.5600	17.28039	284.00	1.00	21.9214	32.91606
88.00	2.89	171.1521	17.97387	288.00	1.00	20.3771	33.00068
92.00	3.01	166.5937	18.64942	292.00	1.00	18.8327	33.07909
96.00	3.11	161.8654	19.30640	296.00	1.00	17.2884	33.15134
100.00	3.20	156.9853	19.94413	300.00	1.00	15.7440	33.21740
104.00	3.23	152.0125	20.56215	304.00	1.00	14.1997	33.27729
108.00	3.29	146.9576	21.15012	308.00	1.00	12.6553	33.33100
112.00	3.27	141.8918	21.73785	312.00	1.00	11.1109	33.37855
116.00	3.29	136.8362	22.29532	316.00	1.00	9.5666	33.41989
120.00	3.34	131.7145	22.83242	320.00	1.00	8.0222	33.45506
124.00	3.40	126.4856	23.34881	324.00	1.00	6.4779	33.48406
128.00	3.27	121.3106	23.84438	328.00	1.00	4.9335	33.50689
132.00	3.29	116.2414	24.31949	332.00	1.00	3.3892	33.52353
136.00	3.28	111.1644	24.77430	336.00	1.00	1.8448	33.53400
140.00	3.50	105.9174	25.20856	340.00	1.00	0.3005	33.53829
144.00	3.63	100.4002	25.62128	344.00	1.00	-1.2439	33.53640
148.00	3.50	94.6547	26.01164	348.00	1.00	-2.9169	33.52783
152.00	3.06	89.7494	26.38071	352.00	0.0	-3.8178	33.51410
156.00	2.62	85.3917	26.73062				
160.00	2.40	81.5437	27.06452				
164.00	2.21	78.0073	27.38357				
168.00	2.20	74.6250	27.68878				
172.00	2.19	71.2351	27.98046				
176.00	2.10	67.9245	28.25877				
180.00	1.72	64.9118	28.52440				
184.00	1.41	62.5734	28.77933				
188.00	1.40	60.4054	29.02329				
192.00	1.40	58.2440	29.26256				
196.00	1.24	56.2086	29.49141				

PLANE INPUTS

PLANE NO. 1 SEAT CUSHION

	X	Y	Z
POINT 1	10.0000	-50.0000	40.0000
POINT 2	10.0000	50.0000	40.0000
POINT 3	29.3000	-50.0000	34.6000

PLANE NO. 2 SEAT BACK

	X	Y	Z
POINT 1	10.0000	-50.0000	40.0000
POINT 2	0.0	-50.0000	22.7000
POINT 3	10.0000	50.0000	40.0000

PLANE NO. 3 FLOORBOARD

	X	Y	Z
POINT 1	29.3000	-50.0000	45.8000
POINT 2	29.3000	50.0000	45.8000
POINT 3	49.3000	-50.0000	45.8000

PLANE NO. 4 TOEBOARD

	X	Y	Z
POINT 1	49.3000	-50.0000	45.8000
POINT 2	49.3000	50.0000	45.8000
POINT 3	62.1000	-50.0000	30.2000

PLANE NO. 5 LOWER INSTR. PANEL

	X	Y	Z
POINT 1	47.9000	-50.0000	36.2000
POINT 2	47.9000	50.0000	36.2000
POINT 3	35.0000	-50.0000	20.9000

PLANE NO. 6 MIDDLE INSTR. PANEL

	X	Y	Z
POINT 1	42.1000	-50.0000	29.3000
POINT 2	42.1000	50.0000	29.3000
POINT 3	35.0000	-50.0000	20.9000

PLANE NO. 7 UPPER INSTR. PANEL

	X	Y	Z
POINT 1	35.5000	-50.0000	17.9000
POINT 2	35.5000	50.0000	17.9000
POINT 3	46.6000	-50.0000	17.9000

PLANE NO. 8 WINDSHIELD

	X	Y	Z
POINT 1	46.6000	-50.0000	17.9000
POINT 2	46.6000	50.0000	17.9000
POINT 3	20.0000	-50.0000	-2.1000

CARDS 5-7

FUNCTION NO. 1 SEAT CUSHION FOR

CARDS E

D0	D1	D2	D3	D4
0.0	-6.9400	0.0	0.0	0.0

FIRST PART OF FUNCTION - 12 TABULAR POINTS

U	F(U)
0.0	0.0
0.394000	46.4000
0.767000	88.0000
1.160000	110.0000
1.370000	154.0000
1.970000	198.0000
2.240000	242.0000
2.760000	292.0000
3.150000	336.0000
3.450000	383.0000
3.940000	440.0000
6.440000	2810.0000

FUNCTION NO. 2 SEAT R

CARDS E

D0	D1	D2	D3	D4
0.0	0.0	0.6520	0.0	0.0

FUNCTION IS CONSTANT 0.652000

FUNCTION NO. 3 SEAT G

CARDS E

D0	D1	D2	D3	D4
0.0	0.0	0.0	0.0	0.0

FUNCTION IS CONSTANT 0.0

FUNCTION NO. 4 SEAT CF

CARDS E

D0	D1	D2	D3	D4
0.0	-3.9400	0.0	0.0	0.0

FIRST PART OF FUNCTION - 6 TABULAR POINTS

U	F(U)
0.0	1.0000
0.276000	1.0000
0.511000	0.7100
0.825000	0.5600
1.160000	0.5400
3.940000	0.5400

FUNCTION NO. 5 SEAT BACK PDF CARDS F

D0	D1	D2	D3	D4
0.0	-4.3200	0.0	0.0	0.0

FIRST PART OF FUNCTION - 15 TABULAR POINTS

D	F(D)
0.0	0.0
0.394000	6.8000
0.787000	15.4000
1.180000	35.2000
1.570000	54.4000
1.970000	83.6000
2.340000	102.3000
2.760000	141.0000
3.150000	167.2000
3.540000	220.0000
3.740000	255.0000
3.940000	363.6000
4.320000	572.0000

FUNCTION NO. 6 STIFF SURFACE PDF CARDS F

D0	D1	D2	D3	D4
0.0	-4.0000	0.0	0.0	0.0

FIRST PART OF FUNCTION - 5 TABULAR POINTS

D	F(D)
0.0	0.0
1.000000	860.0000
2.000000	1690.0000
3.000000	2270.0000
4.000000	2380.0000

FUNCTION NO. 7 COMP. S.N. R CARDS F

D0	D1	D2	D3	D4
0.0	0.0	0.1000	0.0	0.0

FUNCTION IS CONSTANT 0.100000

FUNCTION NO. 8 COMP. S.N. G CARDS F

D0	D1	D2	D3	D4
0.0	0.0	0.8800	0.0	0.0

FUNCTION IS CONSTANT 0.880000

FUNCTION NO. 9 COMP. S.M. CF

D0	D1	D2	D3	D4
0.0	0.0	0.5000	0.0	0.0

FUNCTION IS CONSTANT 0.500000

FUNCTION NO. 10 BELT FRI

D0	D1	D2	D3	D4
0.0	-0.4326	0.0	0.0	0.0

FIRST PART OF FUNCTION - 16 TABULAR POINTS

G	FRI
0.0	0.0
0.066000	200.0000
0.141200	400.0000
0.196100	600.0000
0.244900	800.0000
0.288800	1000.0000
0.322300	1200.0000
0.346400	1400.0000
0.363300	1600.0000
0.376300	1800.0000
0.389800	2000.0000
0.397800	2200.0000
0.406800	2400.0000
0.415300	2600.0000
0.424300	2800.0000
0.432800	3000.0000

FUNCTION NO. 11 BELT R

D0	D1	D2	D3	D4
0.0	0.0	0.4050	0.0	0.0

FUNCTION IS CONSTANT 0.405000

FUNCTION NO. 12 BELT G

D0	D1	D2	D3	D4
0.0	0.0	0.2e10	0.0	0.0

FUNCTION IS CONSTANT 0.2E1000

FUNCTION NO. 13 CONSTANT F=1.0

D0	D1	D2	D3	D4
0.0	0.0	1.0000	0.0	0.0

FUNCTION IS CONSTANT 1.000000

FUNCTION NO. 14 AVERAGE SURFACE PDF

D0	D1	D2	D3	D4
0.0	-5.0000	0.0	0.0	0.0

FIRST PART OF FUNCTION - 6 TABULAR POINTS

D	F(D)
0.0	0.0
1.000000	470.0000
2.000000	890.0000
3.000000	1220.0000
4.000000	1470.0000
5.000000	1560.0000

FUNCTION NO. 15 SOFT SURFACE PDF

D0	D1	D2	D3	D4
0.0	-5.0000	0.0	0.0	0.0

FIRST PART OF FUNCTION - 6 TABULAR POINTS

D	F(D)
0.0	0.0
1.000000	300.0000
2.000000	560.0000
3.000000	880.0000
4.000000	1040.0000
5.000000	1110.0000

FUNCTION NO. 16 WINDSHIELD PDF

D0	D1	D2	D3	D4
0.0	8.0000	0.0	0.0	0.0

FIRST PART OF FUNCTION - 5TH DEGREE POLYNOMIAL

A0	A1	A2	A3	A4	A5
0.0	109.950000	50.356900	-16.025200	1.005800	0.0

FUNCTION NO. 17 WINDSHIELD R

CARDS E

D0	D1	D2	D3	D4
0.0	-8.0000	0.0	0.0	0.0

FIRST PART OF FUNCTION - 4 TABULAR POINTS

U	F(U)
0.	1.0000
0.[illegible]0000	1.0000
0.[illegible]0000	0.0500
0.[illegible]0000	0.0500

FUNCTION NO. 18 WINDSHIELD G

CARDS E

D0	D1	D2	D3	D4
0.0	-6.0000	0.0	0.0	0.0

FIRST PART OF FUNCTION - 4 TABULAR POINTS

U	F(U)
0.0	0.0
0.500000	0.0
0.800000	0.9500
0.000000	0.9500

FUNCTION NO. 19 WINDSHIELD CF

CARDS E

D0	D1	D2	D3	D4
0.0	0.0	0.6700	0.0	0.0

FUNCTION IS CONSTANT 0.670000

FUNCTION NO. 20 WINDSHIELD I. S.

CARDS E

D0	D1	D2	D3	D4
0.0	1.0000	0.0	0.5000	0.0

FIRST PART OF FUNCTION - 5TH DEGREE POLYNOMIAL

A0	A1	A2	A3	A4	A5
0.0	3090.100000	510.400000	-7187.400000	3587.280000	0.0

ALLOWED CONTACTS AND ASSOCIATED FUNCTIONS

PLANE	SEGMENT	FENCE DEFLECTION	INERTIAL SPIKE	R FACTOR	G FACTOR	FRICTION COEF.
1 SEAT CUSHION	1 LT	1 SEAT CUSHION FDF	0	SEAT R	SEAT G	SEAT CF
1 SEAT CUSHION	2 RUL	1 SEAT CUSHION FDF	0	SEAT R	SEAT G	SEAT CF
1 SEAT CUSHION	4 LUL	1 SEAT CUSHION FDF	0	SEAT R	SEAT G	SEAT CF
2 SEAT BACK	1 LT	5 SEAT BACK FDF	0	SEAT R	SEAT G	SEAT CF
2 SEAT BACK	2 CT	5 SEAT BACK FDF	0	SEAT R	SEAT G	SEAT CF
2 SEAT BACK	3 UT	5 SEAT BACK FDF	0	SEAT R	SEAT G	SEAT CF
3 FLOORBOARD	8 RF	6 STIFF SURFACE FDF	0	COMP. S.M. R	COMP. S.M. G	COMP. S.M. CF
3 FLOORBOARD	11 LF	6 STIFF SURFACE FDF	0	COMP. S.M. R	COMP. S.M. G	COMP. S.M. CF
4 TOEBOARD	8 RF	6 STIFF SURFACE FDF	0	COMP. S.M. R	COMP. S.M. G	COMP. S.M. CF
4 TOEBOARD	11 LF	6 STIFF SURFACE FDF	0	COMP. S.M. R	COMP. S.M. G	COMP. S.M. CF
5 LOWER INSTR. PANEL	7 RLL	14 AVERAGE SURFACE FDF	0	COMP. S.M. R	COMP. S.M. G	COMP. S.M. CF
5 LOWER INSTR. PANEL	10 LLL	14 AVERAGE SURFACE FDF	0	COMP. S.M. R	COMP. S.M. G	COMP. S.M. CF
6 MIDDLE INSTR. PANEL	6 RUL	14 AVERAGE SURFACE FDF	0	COMP. S.M. R	COMP. S.M. G	COMP. S.M. CF
6 MIDDLE INSTR. PANEL	9 LUL	14 AVERAGE SURFACE FDF	0	COMP. S.M. R	COMP. S.M. G	COMP. S.M. CF
7 UPPER INSTR. PANEL	5 M	15 SOFT SURFACE FDF	0	COMP. S.M. R	COMP. S.M. G	COMP. S.M. CF
7 UPPER INSTR. PANEL	5 UT	15 SOFT SURFACE FDF	0	COMP. S.M. R	COMP. S.M. G	COMP. S.M. CF
5 WINDSHIELD	5 M	16 WINDSHIELD FDF	20 WINDSHIELD I. S.	17 WINDSHIELD R	17 WINDSHIELD G	17 WINDSHIELD CF

INITIAL BODY POSITIONS

SEGMENT NO.	SYM	INITIAL POSITION (IN) X	Y	Z	YAW (DEG)	PITCH (DEG)	ROLL (DEG)
1	LT	10.400	0.0	33.300	0.0	20.000	0.0
2	CT	6.596	0.0	28.630	0.0	20.000	0.0
3	UT	5.464	0.0	20.085	0.0	20.000	0.0
4	N	3.885	0.0	14.525	0.0	0.0	0.0
5	H	4.985	0.0	10.025	0.0	0.0	0.0
6	RUL	20.534	4.450	34.676	0.0	92.000	0.0
7	RLL	33.662	4.450	36.065	0.0	61.000	0.0
8	RF	43.430	4.450	41.905	0.0	151.000	0.0
9	LUL	20.534	-4.450	34.676	0.0	92.000	0.0
10	LLL	33.662	-4.450	36.065	0.0	61.000	0.0
11	LF	43.430	-4.450	41.905	0.0	151.000	0.0
12	RUA	8.024	7.600	22.435	0.0	47.000	0.0
13	RLA	18.232	7.600	28.294	0.0	71.000	0.0
14	LUA	8.024	-7.600	22.435	0.0	47.000	0.0
15	LLA	18.232	-7.600	28.294	0.0	71.000	0.0

CARDS G

APPENDIX C

VEHICLE STIFFNESS FOR NARROW OBSTACLES

In Reference 20, a compilation of known values of maximum crush distances versus initial impact velocity for frontal impacts with rigid poles is given. These data are summarized in Figure C-1. By fitting a straight line through these points (via a least-squares regression) a relationship between crush and impact velocity can be obtained in the form of:

$$V_o = \mathcal{L} C,$$

where V_o is in MPH, the crush distance, C, is in inches and $\mathcal{L}$ is a slope determined from the fit.

Assuming a linear rate, the longitudinal displacement of a vehicle is given by:

$$x = \dot{x}_o \sqrt{\frac{m}{k}} \sin \sqrt{\frac{k}{m}}\, t$$

and the maximum displacement is:

$$x_{max} = C = \dot{x}_o \sqrt{\frac{m}{k}}$$

Converting the initial velocity to MPH,

$$C = 17.6\, V_o \sqrt{\frac{m}{k}}$$

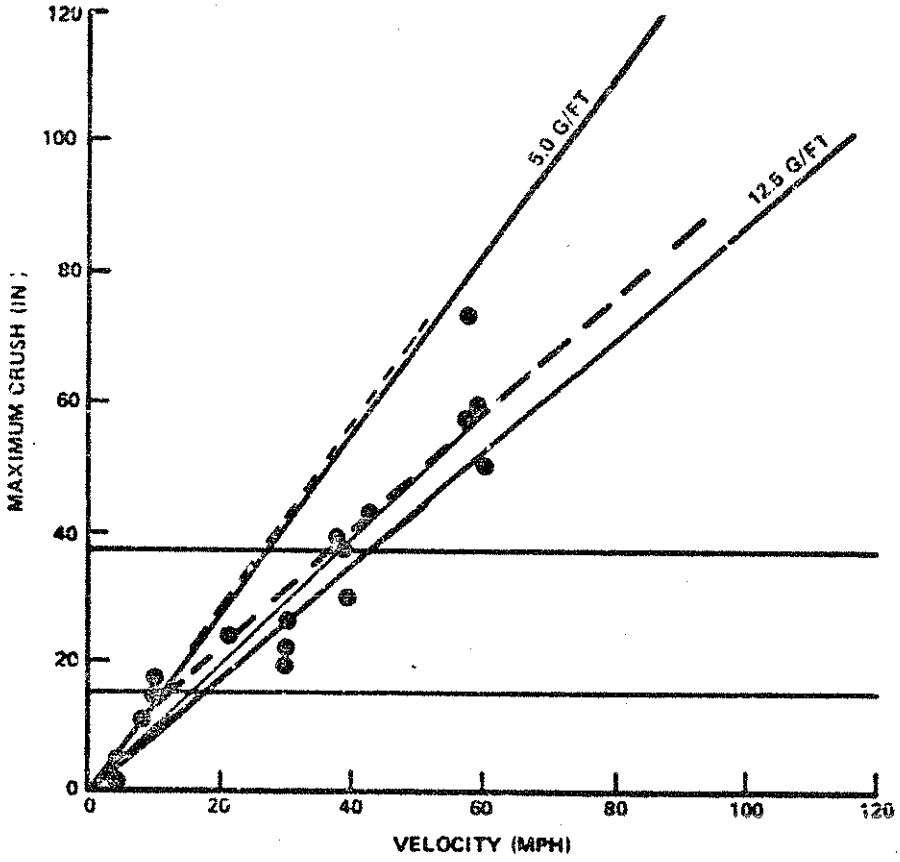

Figure C-1 FRONT IMPACTS WITH RIGID POLES (DATA POINTS FROM REF. 20)

Therefore

$$\sqrt{\frac{k}{m}} = 17.6\left(\frac{V_o}{C}\right)$$

$$k = (17.6)^2 m\left(\frac{V_o}{C}\right)^2 = (17.6)^2 \frac{W}{386.4}\left(\frac{V_o}{C}\right)^2$$

$$\frac{k}{W} = \frac{(17.6)^2}{386.4}\left(\frac{V_o}{C}\right)^2 \qquad g/in.$$

or

$$K = \frac{k}{W}(12) = \frac{12(17.6)^2}{386.4}\left(\frac{V_o}{C}\right)^2 \qquad g/ft$$

$$K = 9.62\left(\frac{V_o}{C}\right)^2 \qquad g/ft$$

Linear fits to the data shown in Figure C-1 were made in the following crush ranges: 0 to 15 inches, 0 to 39 inches, and 0 to 73 inches. The resulting straight line equations are:

Crush Range	
0-15"	$C = -0.255 + 1.443\ V_o$
0-39"	$C = 1.04 + 0.8553 V_o$
0-73"	$C = 0.245 + 0.975\ V_o$

Ignoring the intercept, the following stiffness factors can be calculated.

Crush Range in	$\frac{V_o}{C}$ mph/in	K g/ft
0-15"	0.693	4.63
0-39"	0.8553	7.04
0-73"	1.026	10.14

From these values of K for impacts with narrow, rigid obstacles, a value for the equivalent structural stiffness parameter required in the SMAC program can be obtained.

$$\frac{12\,k\,b}{W} = K$$

where: k is the SMAC structural stiffness parameter, $\frac{lb}{in^2}$

b is the width of contact, in.

W is the weight of the vehicle, lbs.

Therefore,

$$k = \frac{K\,W}{12\,b} \quad \frac{lb}{in^2}$$

As an example, Case No. 71-31A involves an impact between a 3400 lb. vehicle and a 27 inch diameter tree, with a maximum penetration of 37.7 inches. For this case,

$$k = \frac{(7.04)(3400)}{12(27)} = 73.8 \quad \frac{lb}{in^2}$$

APPENDIX D

IMPACT SLED TESTS

This section contains the following data from the thirteen impact sled tests:

Time histories of

- sled acceleration
- head resultant acceleration
- head severity index
- chest resultant acceleration,

with the corresponding time scale, as plotted by a direct-writing (Brush) recorder from the analog test data stored on magnetic tape.

Table D-1

Impact Sled Data Summary

Figure	Case No.	Sled Run No.	Remarks
D-1	AA00145	1139	
D-2	AA00145	1140	dummy braced against instrument panel
D-3	TR01316	1141	
D-4	CA71031	1138	
D-5	CB00072	1136	
D-6	SW71044	1144	
D-7	CBJ0053	1145	
D-8	CB71055	1135	
D-9	CB71055	1134	5th percentile female dummy
D-10	TR01161	1137	
D-11	GI00056	1142	
D-12	GI00036	1143	
D-13	TR00973	1146	seat moved forward

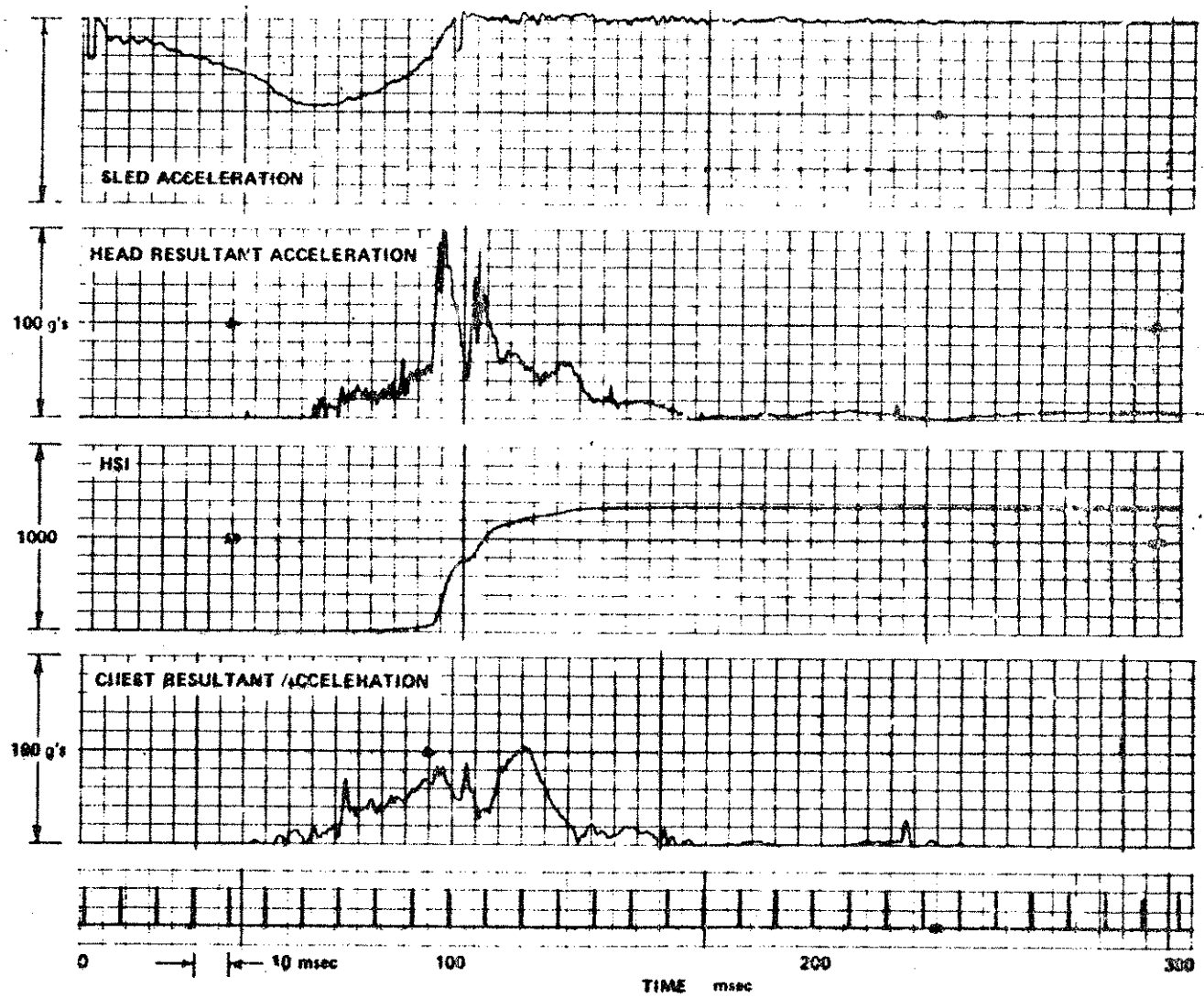

Figure D-1 DATA TRACES
CASE NO. AA00145
SLED RUN NO. 1139

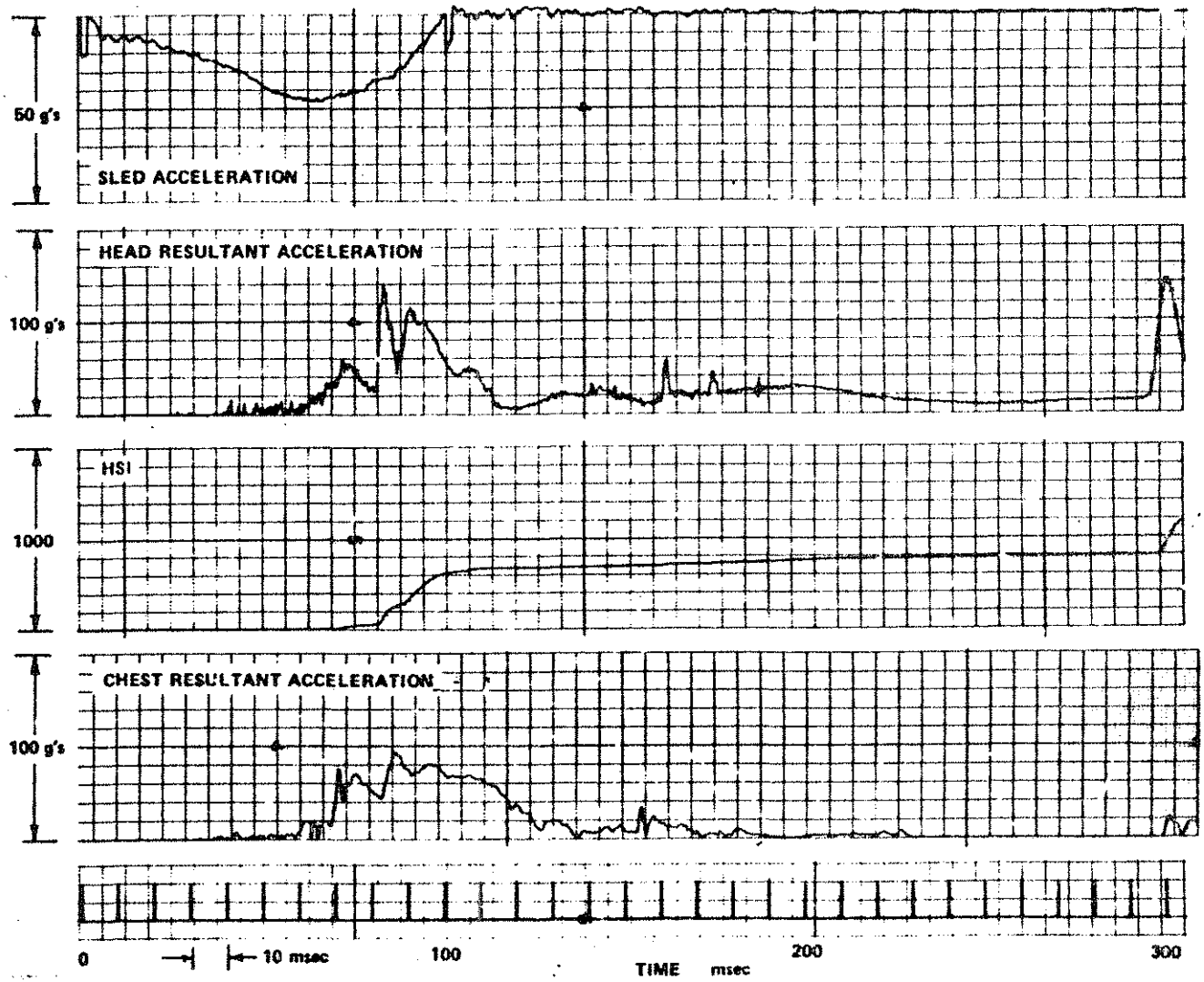

Figure D-2 DATA TRACES
CASE NO. AA00145
SLED RUN NO. 1140

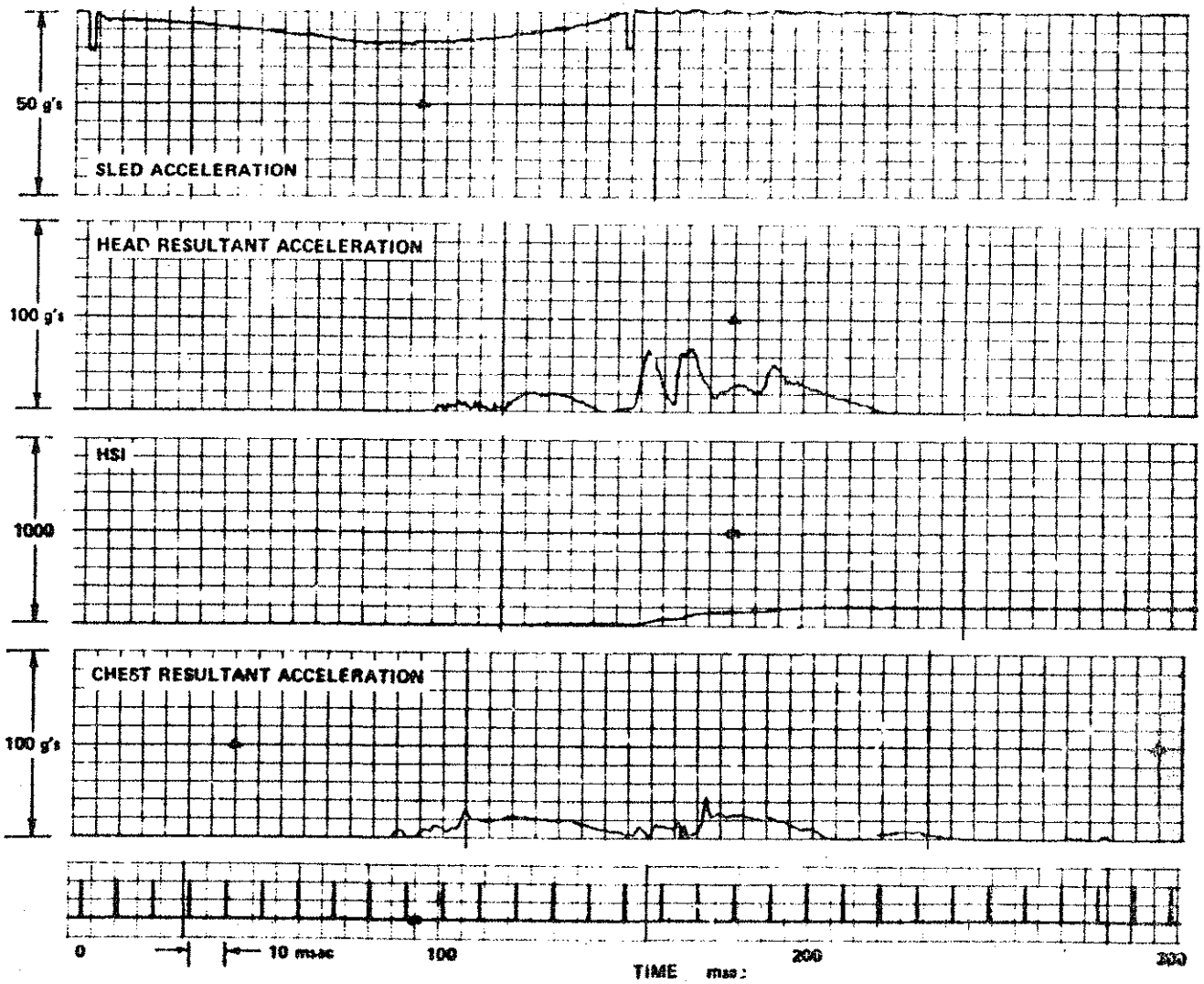

Figure D-3 DATA TRACES
CASE NO. TR01316
SLED RUN NO. 1141

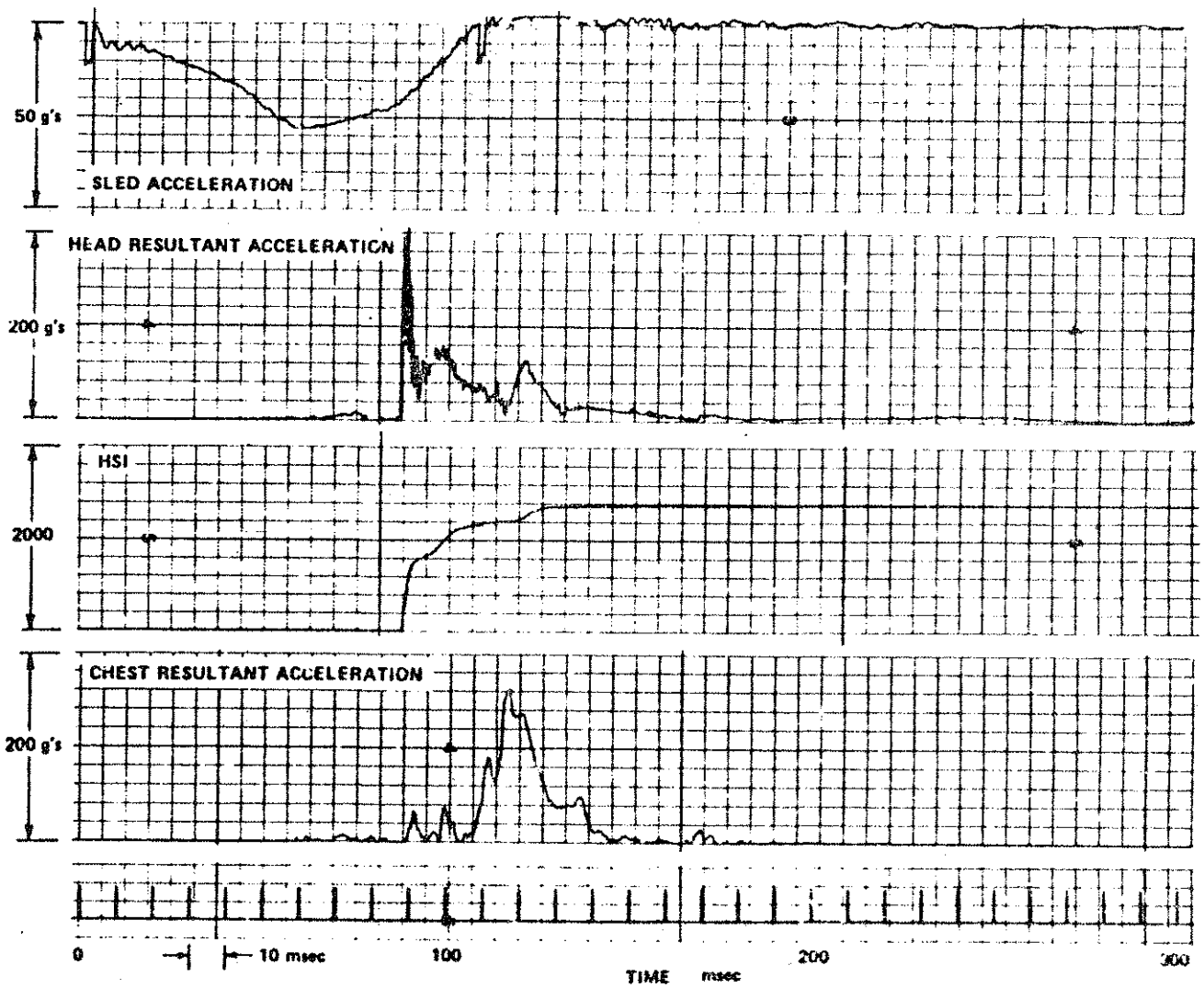

Figure D-4 DATA TRACES
CASE NO. CA71031
SLED RUN NO. 1138

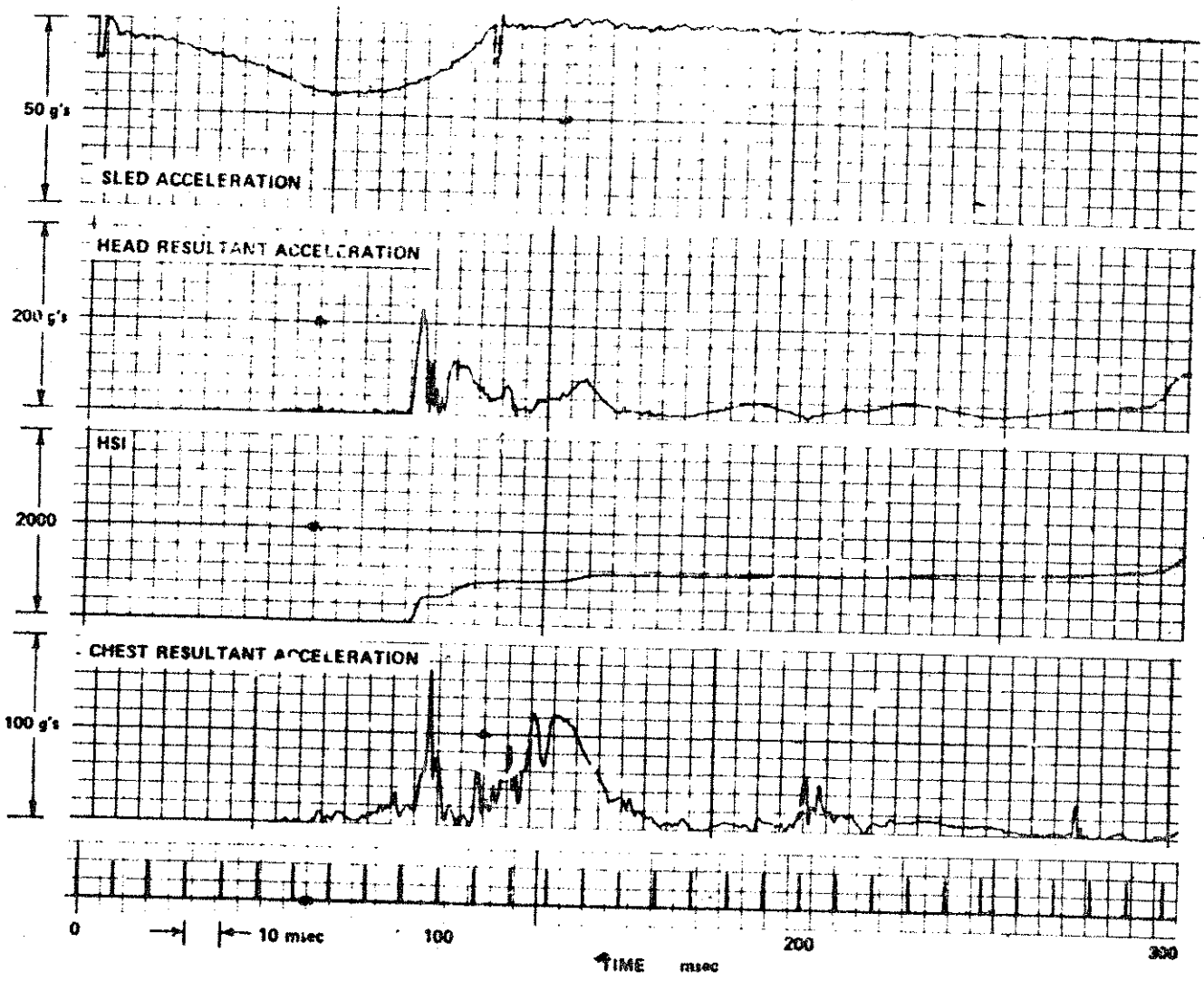

Figure D-5 DATA TRACES
CASE NO. CB09072
SLED RUN NO. 1136

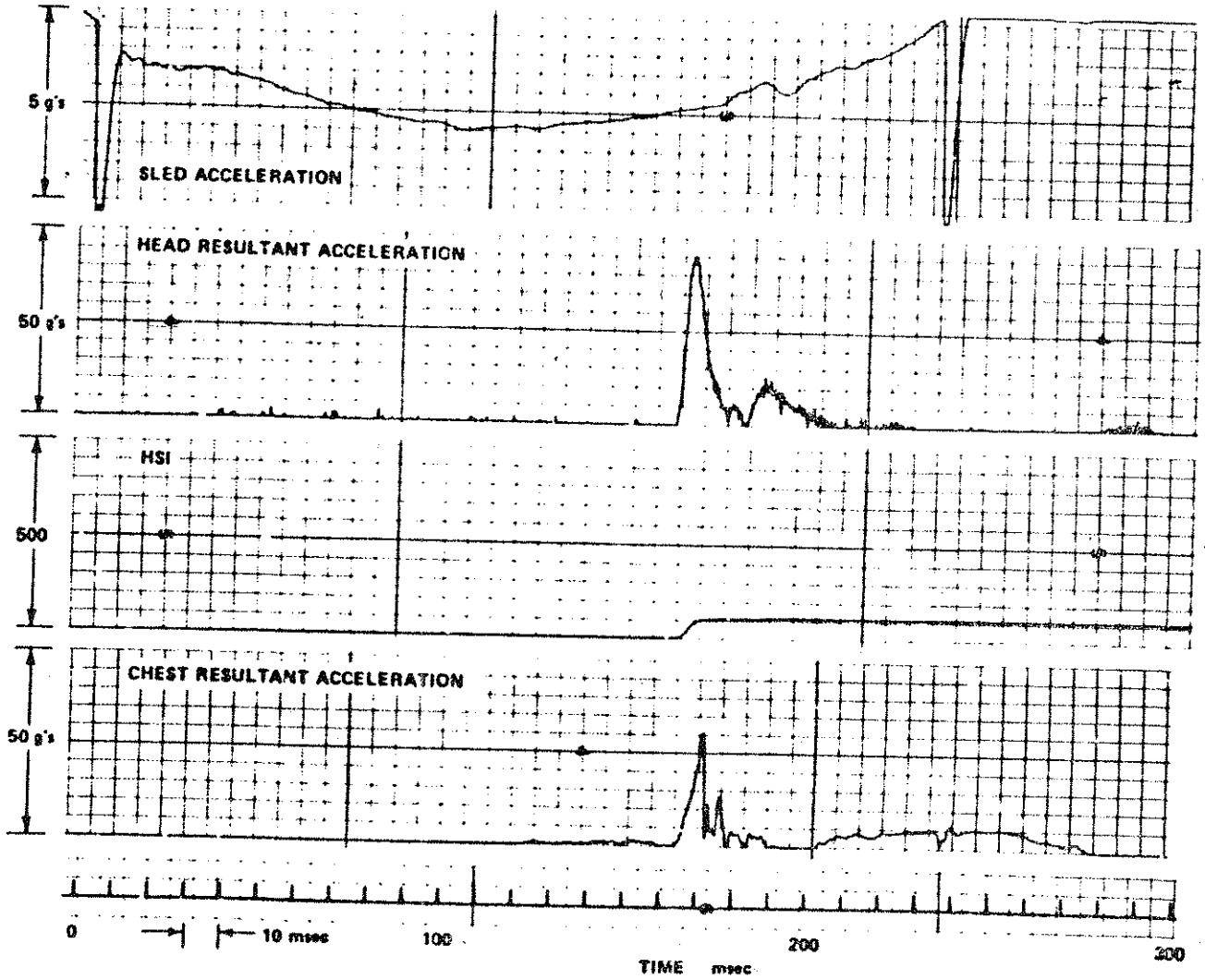

Figure D-6 DATA TRACES
CASE NO. SW71044

SLED RUN NO. 1145

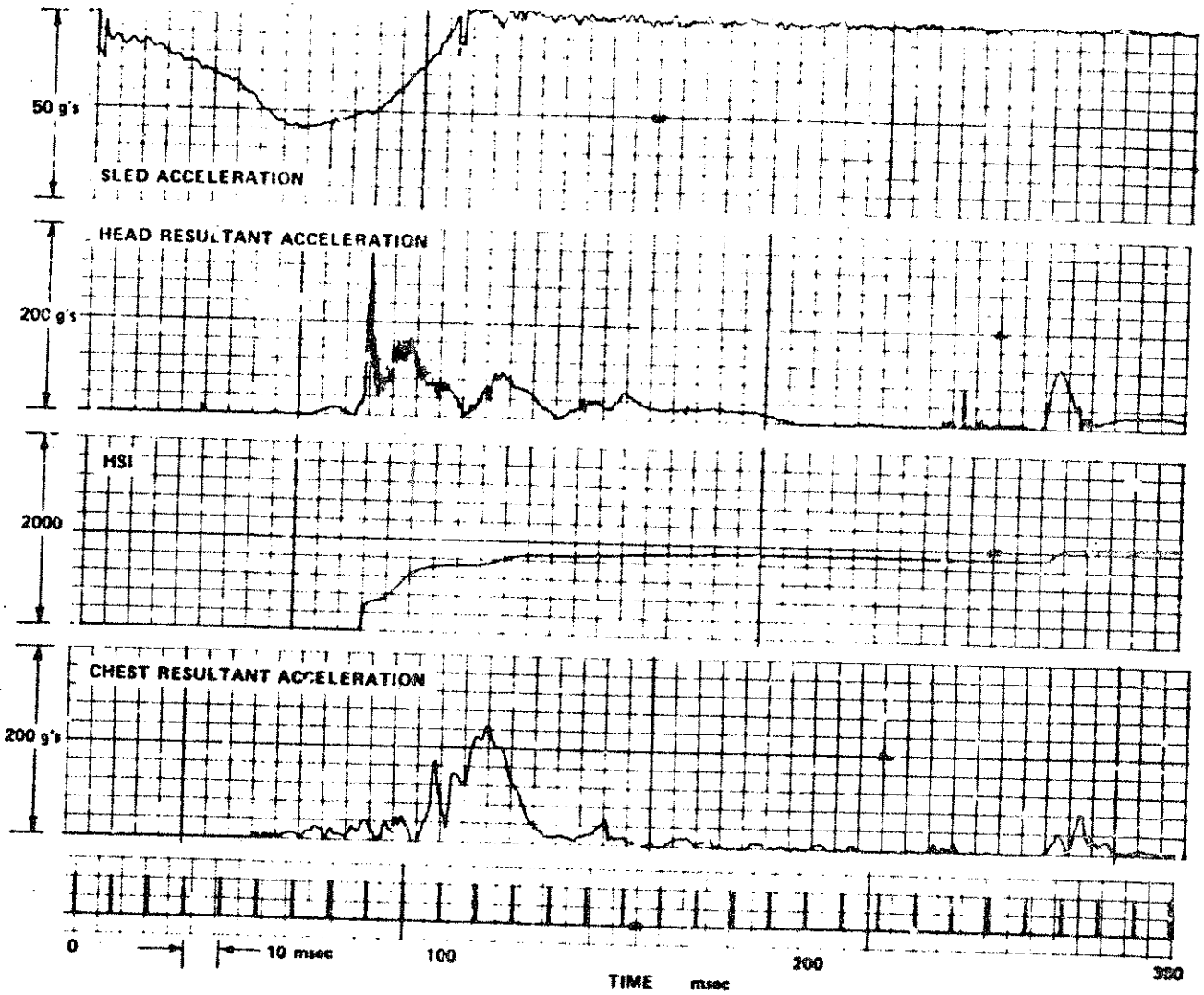

Figure 5-7 DATA TRACES
CASE NO. CB00053

ZQ-5341-V.1

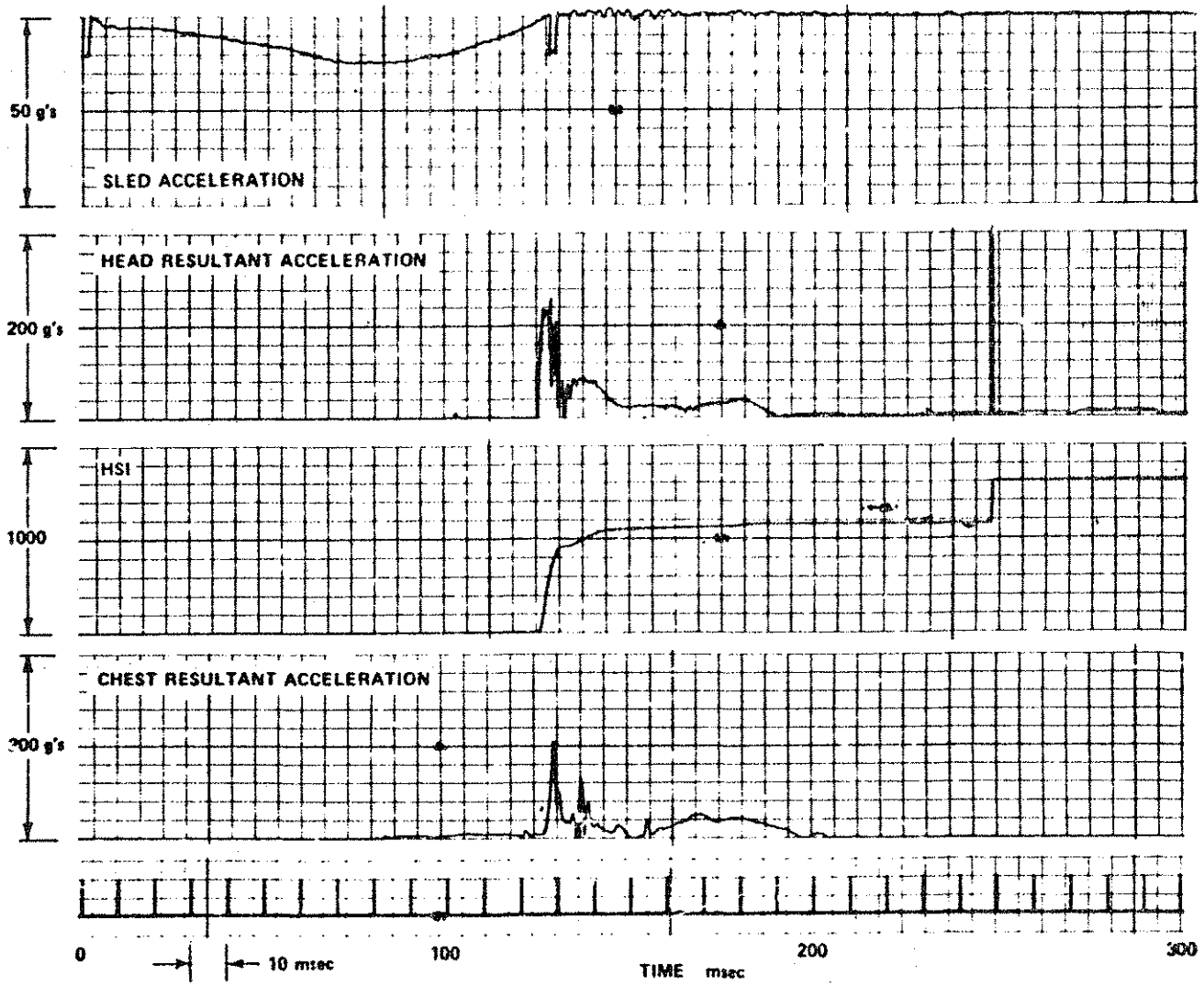

Figure D-8 DATA TRACES
CASE NO. CB71055
SLED RUN NO. 1135

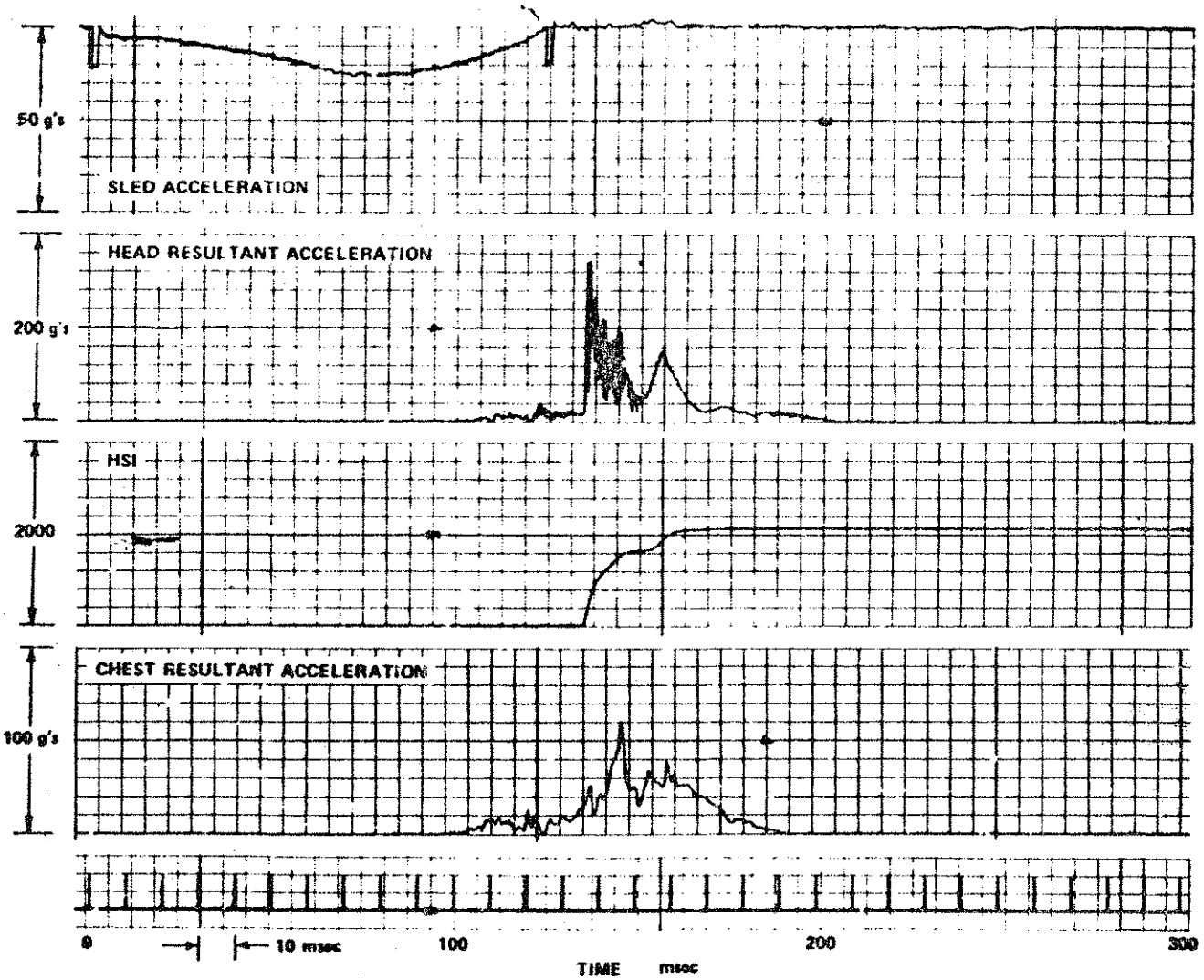

Figure D 9 DATA TRACES
CASE NO. CB71055

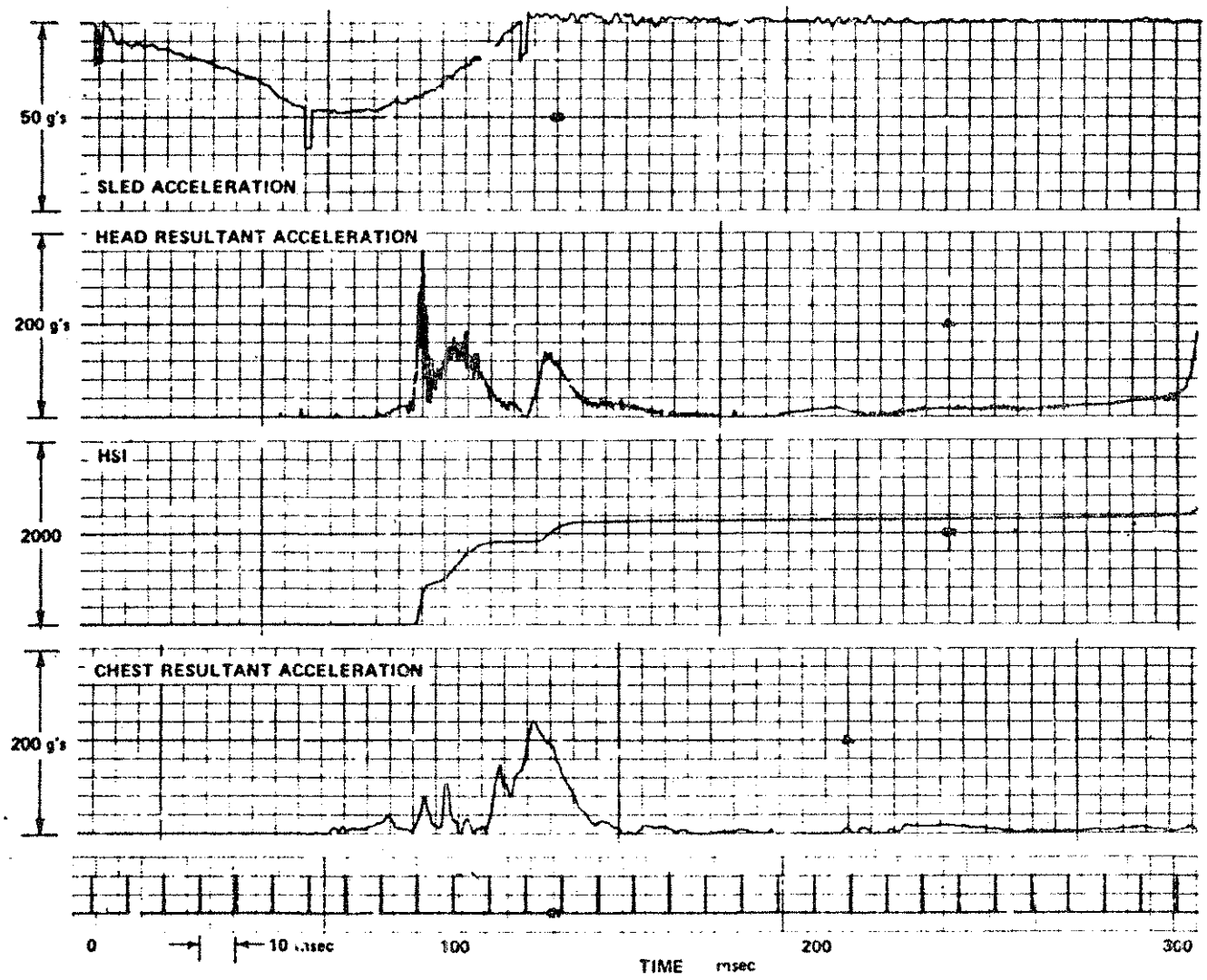

Figure D-10 DATA TRACES
CASE NO. TR01161
SLED RUN NO. 1137

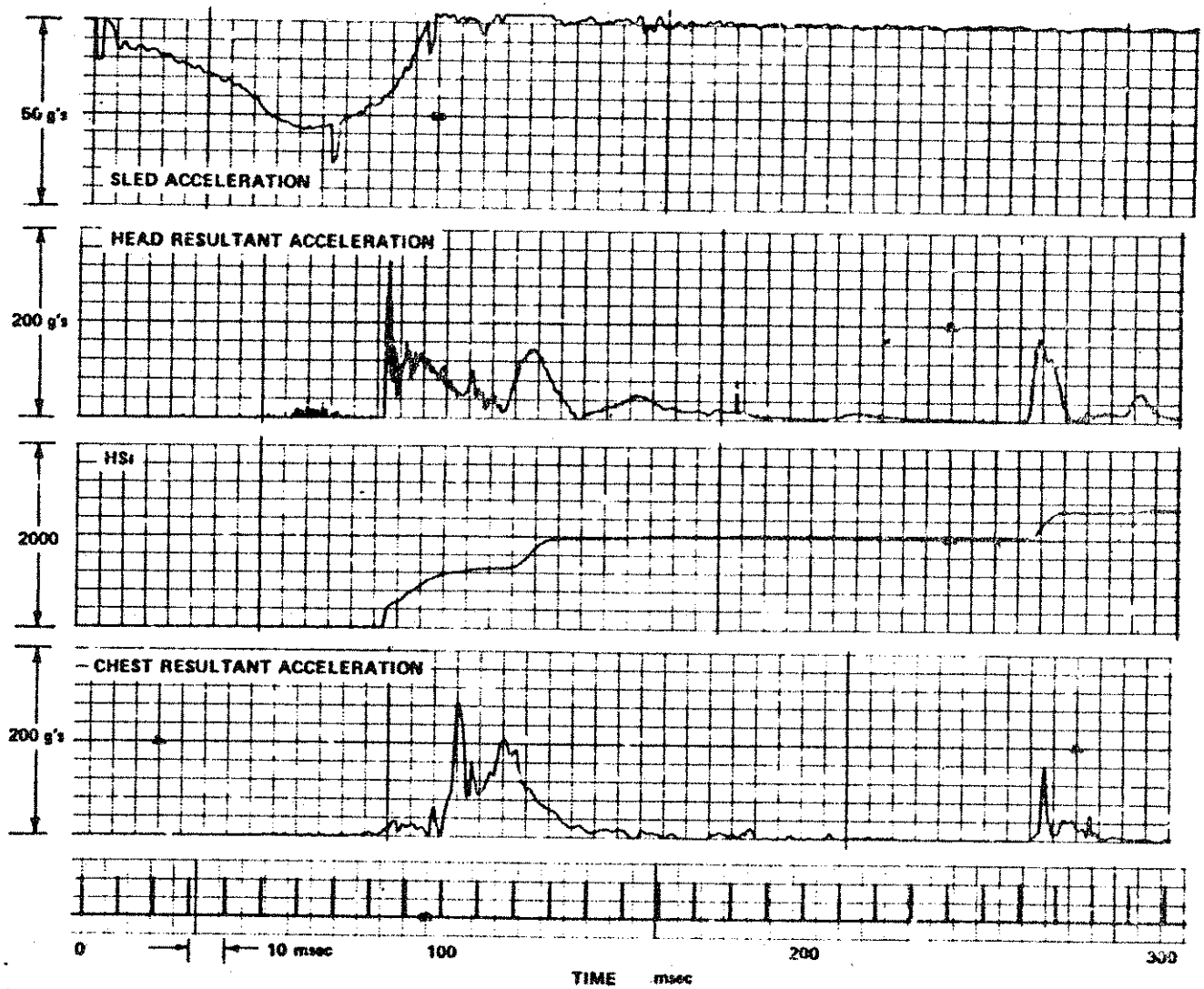

Figure D-11 DATA TRACES
CASE NO. GI00056
SLED RUN NO. 1142

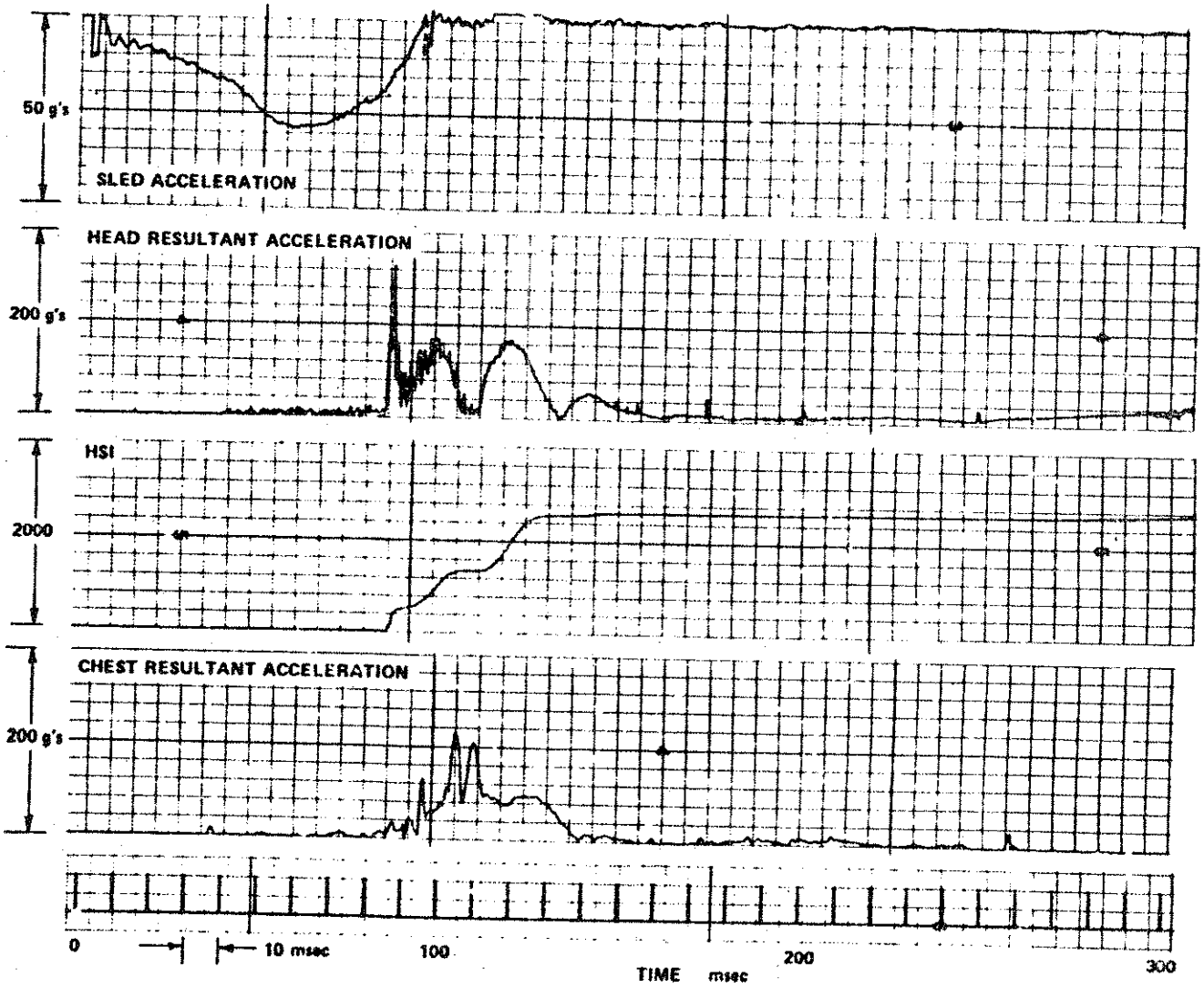

Figure D-12 DATA TRACES
CASE NO. GI00056
SLED RUN NO. 1143

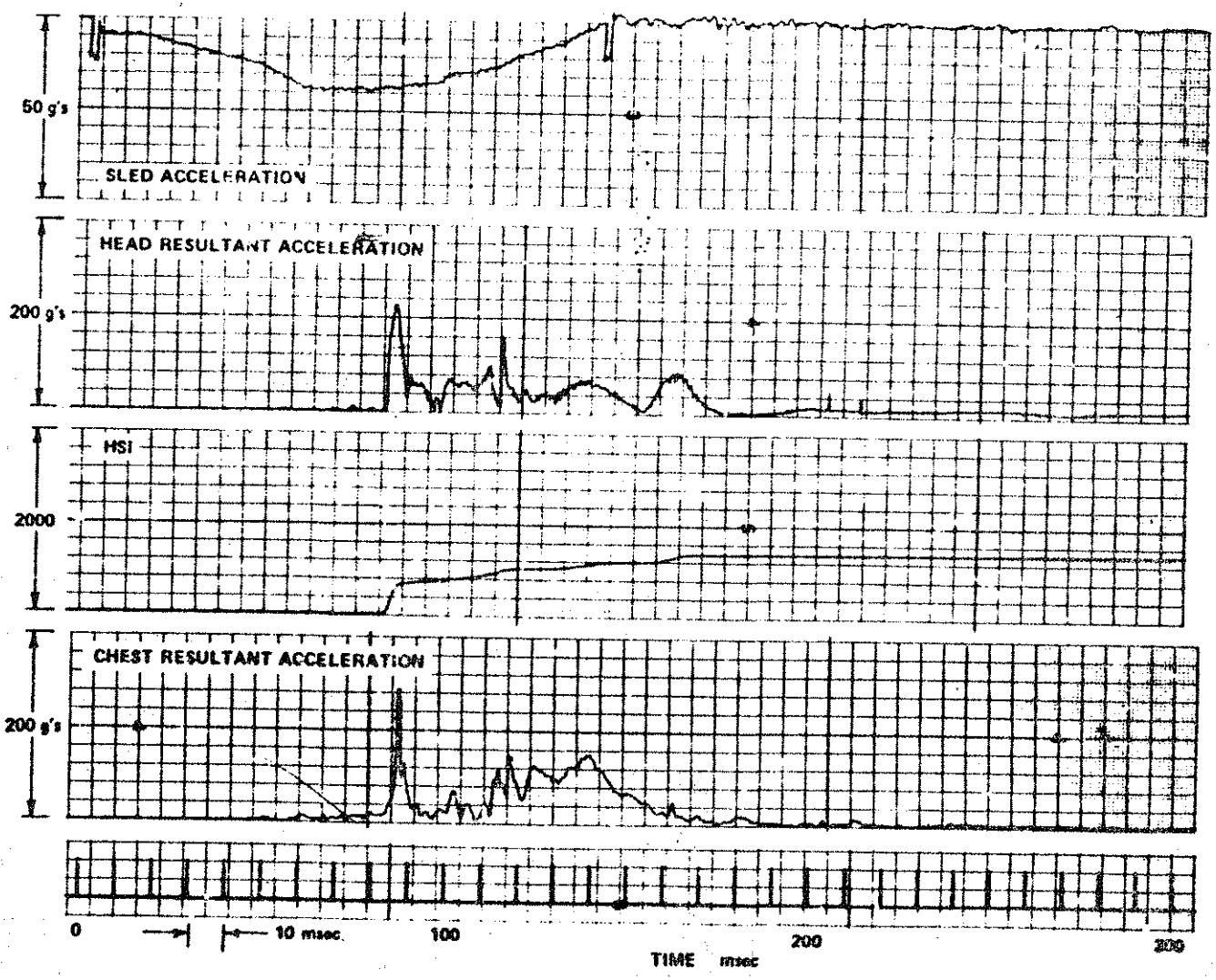

Figure D-13 DATA TRACES
CASE NO. TR00973
SLED RUN NO. 1146